THE PATHWAYS INVOLVED IN CYTOCHROME P450

REGULATION DURING LPS-INDUCED CENTRAL NERVOUS

SYSTEM AND PERIPHERAL INFLAMMATION

by

Dalya Abdulla

Submitted in partial fulfillment of the requirements

for the degree of Doctor of Philosophy

at

Dalhousie University

Halifax, Nova Scotia

November 2005

Canada

DALHOUSIE UNIVERSITY

This thesis is dedicated to my wonderful family and husband who have constantly provided me with support

Table of Contents

List of Tables

List of Figures

Abstract

The cytochromes P450 represent a superfamily of heme-containing drug metabolizing enzymes found in the liver and in other tissues. The regulation of these enzymes is altered during conditions of infection and inflammation however the mechanisms leading to such changes remain largely unknown, with cytokines believed to play a role in this regulation. The objectives of this thesis were to examine potential mechanisms that protect against the downregulation of cytochrome P450 (P450) and to determine the mechanisms of P450 regulation during conditions of lipopolysaccharide (LPS)-induced inflammation. Based on the fact that norepinephrine has many anti-inflammatory properties, we chose to examine the potential effects of beta-adrenergic stimulation on CYP1A levels using an *in vitro* model of central nervous system (CNS) inflammation induced by incubating primary astrocytes with LPS. Our results demonstrate that the co-administration of beta-adrenergic receptor agonists with LPS to cultured astrocytes prevents the LPS-mediated reduction in CYP1A activity in part due to a reduction in TNFα. To outline the mechanisms by which LPS regulates P450 *in vivo*, we administered LPS either intracerebroventricularly or intraperitoneally and examined the mRNA expression of CYP1A1/2, CYP2B1/2, CYP2D5, and CYP2E1. We show that during CNS inflammation, LPS is detected in the serum as early as 15 minutes following its i.c.v. administration. The results indicate that various transcription factors such Nuclear Factor kappa B (NF-κB) play an important role in the regulation of P450 during LPS-induced inflammatory models. In addition, we show that the regulation of CYP2E1 during conditions of LPS-induced inflammation occur predominantly at a post-transcriptional level.

List of Abbreviations and Symbols Used

βAR	β-adrenergic receptors
AC	Adenylyl cyclase
AD	Alzheimer's disease
AD	Actinomycin-D
ADX	Adrenalectomy
AhR	Aryl hydrocarbon receptor
ANOVA	Analysis of variance
AP-1	Activator protein-1
ARNT	AhR nuclear translocator
AUC	Area under the curve
BBB	Blood brain barrier
C/EBP	CCAAT/enhancer binding protein
cAMP	cyclic AMP
CAR	Constitutive androstane receptor
CHX	Cycloheximide
Clen	Clenbuterol
clone1	pCYP2D5–NF-κB–Luc
CNS	Central nervous system
COX2	Cyclooxygenase-2
CREB	cAMP response element binding protein
CSF	Cerebrospinal fluid
C_T	Threshold cycle

CYP; P450; cyt P450	Cytochrome P450
CZX	Chlorzoxazone
DBA	Dibenz[a,h]anthracene
DMEM	Dulbecco's modified essential medium
DMSO	Dimethylsulfoxide
DTT	Dithiothreitol
EMSA	Electromobility (electrophoretic) mobility shift assay
EROD	7-ethoxyresorufin O-dealkylase
FBS	Fetal bovine serum
For	Forskolin
FXR	Farnesoid X receptor
GABPα	GA binding protein alpha
GABPβ	GA binding protein beta
HNF1α	Hepatocyte nuclear factor 1-alpha
HPA	Hypothalamic pituitary adrenal
HPLC	High performance liquid chromatography
i.c.v.	Intracerebroventricular
i.p.	Intraperitoneal
i.v.	Intravenous
IFNα	Interferon alpha
IFNβ	Interferon beta
IFNγ	Interferon gamma
IκB	Inhibitor of κB

IKK	Inhibitor of κB kinase
IL-1	Interleukin-1
IL-10	Interleukin-10
IL-6	Interleukin-6
IRAK	IL-1 receptor associated kinase
Iso	Isoproterenol
JAK	Janus kinase
LBP	LPS binding protein
LIF	Leukemia-inhibitory factor
LPS	Lipopolysaccharide
MAPKK	Mitogen associated protein kinase kinase
MKK	Mitogen associated protein kinase kinase
MPP+	1-methyl-4-phenylpyridinium
MS	Multiple Sclerosis
MTT	3-(4,5-dimethylthiazol-2-yl)-2,5-diphenyltetrazolium
mut7	pCYP2D5–mutNF-κB–Luc
MyD88	Myeloid differentiation factor 88
NADPH	nicotinamide adenine dinucleotide
NE	Norepinephrine
NF-κB	Nuclear factor κB
NO	Nitric oxide
PAMP	Pathogen associated molecular patterns
PBS	Phosphate buffer saline

PCR	Polymerase chain reaction
PKA	Protein kinase A
PMSF	phenylmethylsulfonyl fluoride
PPARγ	Peroxisome proliferator activated receptor gamma
PROD	Pentoxyresorufin O-dealkylase
Prop	Propranolol
PXR	Pregnane X receptor
RLU	Relative light units
RXR	Retinoic X receptor
STAT	Signal transducers and activators of transcription
TIR	Toll/IL-1 receptor
TLR	Toll-like receptor
TNFα	Tumor necrosis factor alpha
TNFβ	Tumor necrosis factor beta
TNFR1	Tumor necrosis factor receptor 1
TNFR2	Tumor necrosis factor receptor 2
XRE	Xenobiotic response element

Acknowledgements

CHAPTER 1

INTRODUCTION

1.1 The inflammatory response

Immunity defines the ability of the host to respond to tissue injury or infectious diseases [1]. Immunity comprises both a non-specific (innate immunity) and a specific component (adaptive immunity). Innate immunity refers to the acute response that allows pathogen elimination and tissue repair. The inflammatory response is considered as one part of the innate immune response (illustrated in Figure 1.1), and the events it comprises include vasodilation, an increase in capillary permeability to cause tissue swelling, and the influx of phagocytes from the capillaries into the affected tissues [2]. Adaptive immunity refers to the antigen specific response to foreign antigen [1].

An effective inflammatory response depends on the complex interaction between various cell types such as lymphoid cells, inflammatory cells, and hematopoietic cells, which interact among each other with the aid of a group of proteins known as cytokines [2]. Cytokines are low-molecular weight proteins or glycoproteins secreted by white blood cells in response to various stimuli and mediate cell-to-cell interaction of the immune system [2]. Table 1.1 (adapted from [2]) shows some of the important cytokines that will be discussed throughout this thesis and Figure 1.2 shows some of the ways by which cytokines act to cause their effects [2]. Some of the signal transduction mechanisms by which cytokines cause their intracellular effects will be discussed later in this section.

1.1.1 Lipopolysaccharide (LPS)

LPS is a large complex molecule found in the outer layer of gram-negative bacteria. The outer layer of the gram-negative bacteria is more complex than that of the gram-positive

2

Table 1.1 – The biological function of selected cytokines (adapted from [2]).

Cytokine	Major Functions
Interleukin-1 (IL-1α and IL-1β)	1- Enhances the activity of natural killer cells 2- Chemotactically attracts macrophages and neutrophils 3- Induces the synthesis of acute phase proteins from hepatocytes 4- Induces fever
Interleukin-6 (IL-6)	1. Induces the synthesis of acute phase proteins from hepatocytes 2. Stimulates antibody release from plasma cells
Interleukin-10 (IL-10)	1. Suppresses cytokine production from macrophages 2. Anti-inflammatory cytokine
Interferon alpha (IFNα)	1. Inhibits viral replication in uninfected cells
Interferon beta (IFNβ)	1. Inhibits viral replication in uninfected cells
Interferon gamma (IFNγ)	1. Enhances the activity of macrophages 2. Inhibits viral replication in uninfected cells
Leukemia-inhibitory factor (LIF)	1. Induces the synthesis of acute-phase proteins from hepatocytes
Tumor necrosis factor alpha (TNFα)	1. Has a cytotoxic effect on tumor cells 2. Induces cytokine secretion from inflammatory cells 3. Responsible for extensive weight loss (cachexia) resulting from chronic inflammation
Tumor necrosis factor beta (TNFβ)	1. Has similar activities to TNFα 2. Has a cytotoxic effect on tumor cells 3. Enhances the phagocytic activity of macrophages and neutrophils
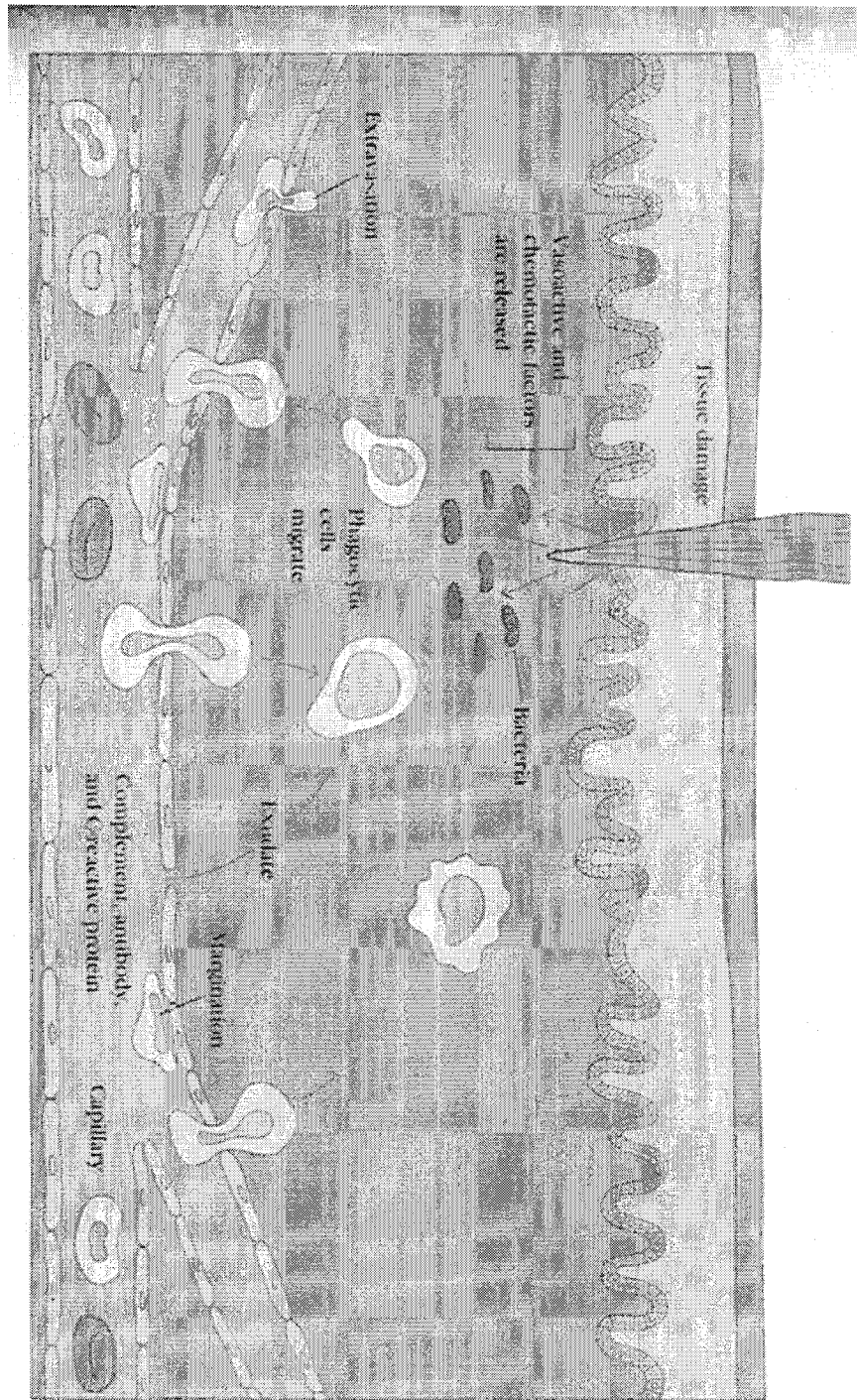
Figure 1.1 – A depiction of some of the events that occur during the inflammatory response as part of the innate immune system. These events include vasodilation, an increase in capillary permeability to cause tissue swelling, and the influx of phagocytes from the capillaries into the affected tissues. Figure taken from [2].

4
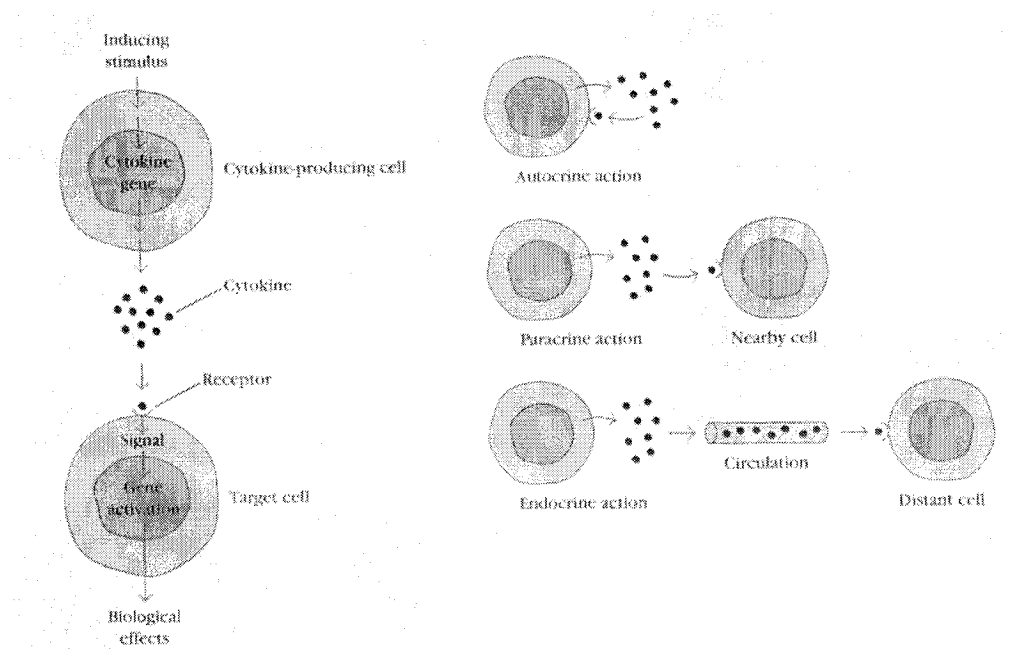
Figure 1.2 – A depiction of some of the general mechanisms by which cytokines cause their effects. Cytokines can either act on the same cell that released them (autocrine fashion), or on neighbouring cells (paracrine fashion). Cytokines may also be relased into the systemic circulation and travel to act on distant cells (endocrine fashion). Figure taken from [2]

bacteria; the latter consists only of a single layer of peptidoglycan adjacent to the plasma membrane [3, 4]. In a gram-negative bacteria, there are two outer layers adjacent to the plasma membrane, with the inner part composed of a thin layer of peptidoglycan and the outer segment consisting of LPS (outlined in Figure 1.3 A and B) [3]. LPS contains both lipid and carbohydrate components and consists of three parts (outlined in Figure 1.4): lipid A, core polysaccharide, and the O side chain [4]. Due to its toxic properties, the presence of the lipid A component causes LPS to be considered as an endotoxin [4]. Lipid A is also the only portion of LPS recognized by the innate immune system [3, 5].

Infection by *E. coli* (a gram negative bacteria) in humans leads to a condition known as gram-negative sepsis, a term that describes the often fatal response of the immune system against microbial pathogens and which leads to an annual 200,000 deaths in the United States alone [3, 5, 6]. The presence of bacterial pathogens in the CNS can cause bacterial meningitis, which is also associated with a high morbidity and mortality rate despite effective anti-microbial treatments [7, 8]. Some of the general mechanisms by which LPS can cause sepsis and multiple organ failure are shown in Figure 1.5.

1.1.2 Toll-like receptor signal transduction

Most of the intracellular cytoplasmic signals observed following LPS are caused by activation of a receptor known as Toll-Like receptor 4 (TLR4) [5]. These receptors were first identified in *Drosophila* where they were found to be involved in dorsal-ventral patterning in embryos and in the induction of an antifungal response [5]. Different Toll-like receptors can identify different pathogen-associated molecular patterns (PAMPs) (outlined in Figure 1.6) [9]. TLR2 recognizes lipoteichoic acid and peptidoglycans, TLR9 is activated by bacterial DNA motifs, and both TLR3 and TLR7 are involved in the

(A)

(B)
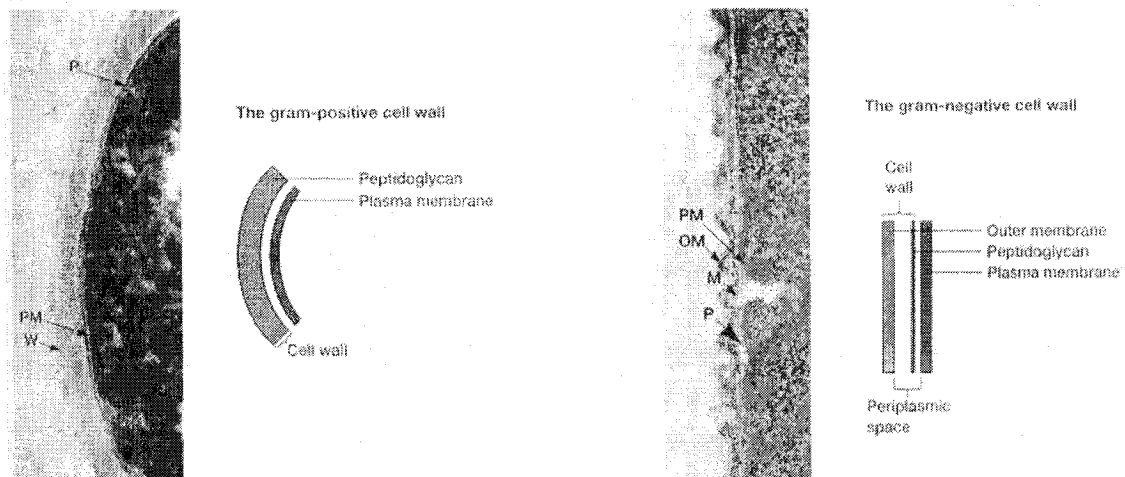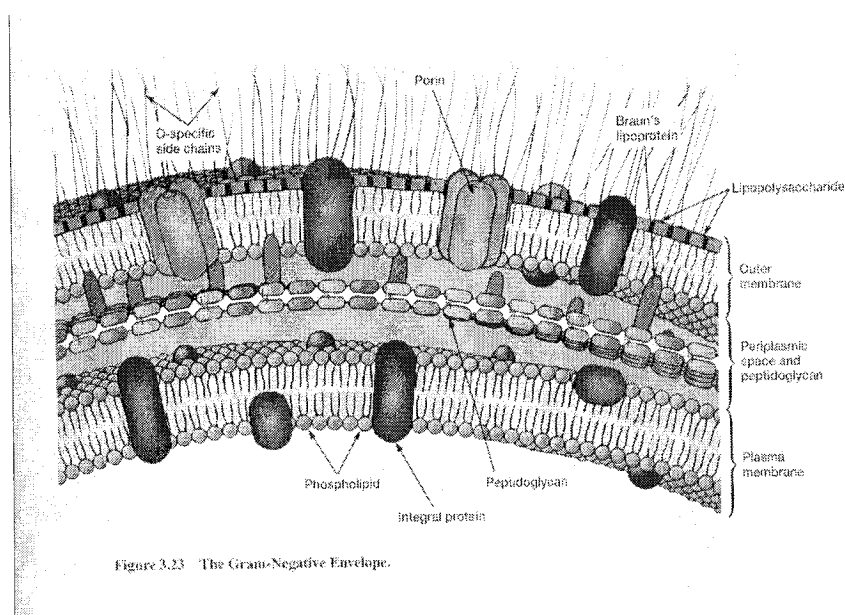
Figure 1.3 – Outer layer structure of gram negative and positive bacteria. Panel A depicts the difference in structure between the outer layers of gram-positive and negative bacteria. Panel B shows the components of a gram-negative bacterial outer layer, with a perspective on the location of LPS. Both panels taken from [4]

7
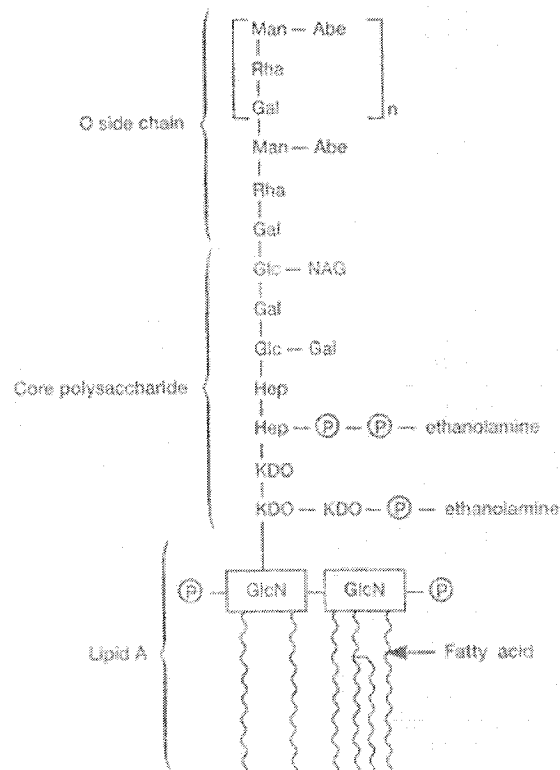
Figure 1.4 – The structure of LPS. LPS consists of a core polysaccharide with a lipid A and an O side chain. It is the Lipid A component that is recognized by the innate immune system and causes the stimulation of an inflammatory response. Figure taken from [4].
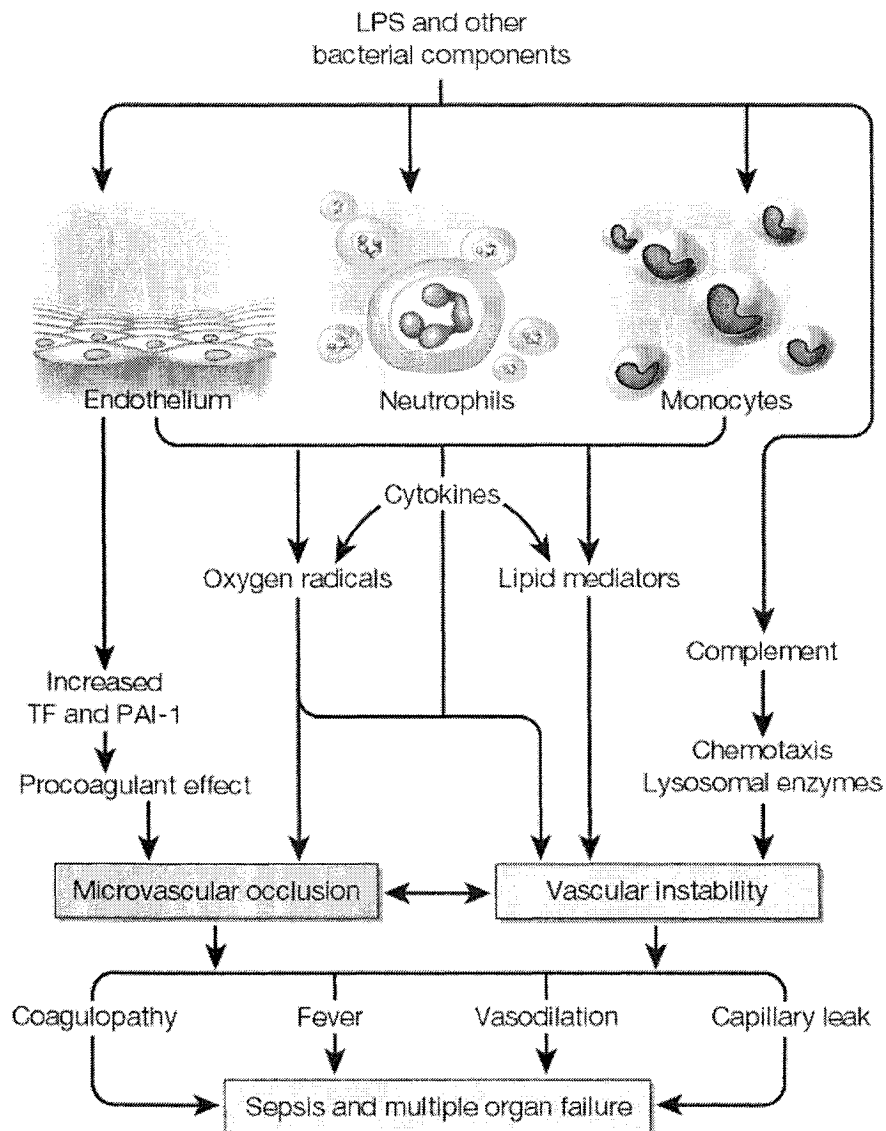
Figure 1.5 – Mechanisms by which LPS causes sepsis and multiple organ failure in the host. It is thought that LPS or other bacterial products activate various cells types to lead to the production of cytokines and other mediators, eventually leading to sepsis and multiple organ failure. TF refers to transcription factor and PAI-1 refers to plasminogen-activator inhibitor type-1. Figure taken from [10].
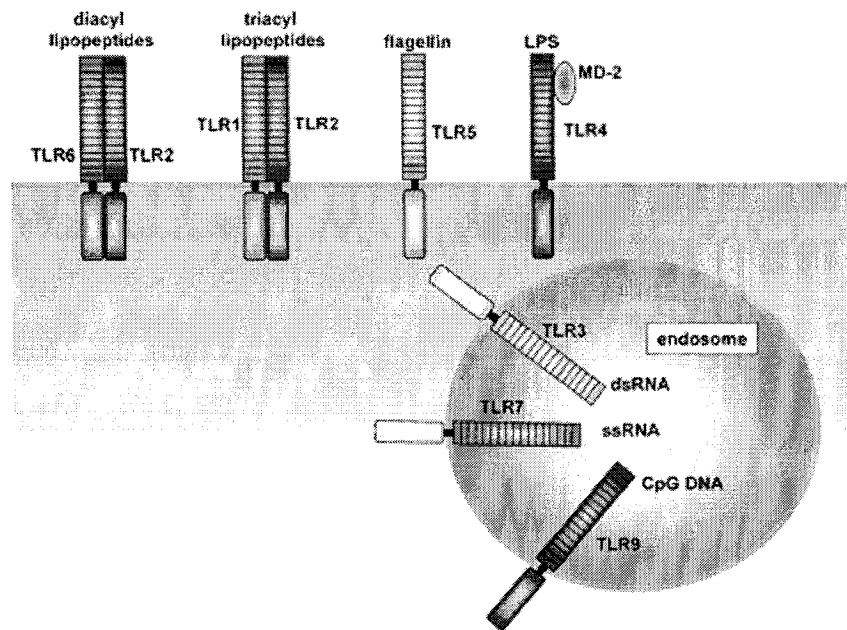
Figure 1.6 – The different types of toll-like receptors. This figure shows the anchorage of several types of TLR and the ligands they respond to. TLR1, TLR2, TLR4, and TLR5 are considered as cell surface receptors, whereas TLR3, TLR7, TLR9, and TLR8 are present in intracellular compartments such as the endosome. Some TLR act separately (such as TLR4) whilst others act in heterodimeric form (such as TLR2/TLR6 and TLR2/TLR1). Figure taken from [11]

immune response against viral infections [12]. More than 10 TLR are thought to exist in rodents and humans [13].

It is believed that when LPS is present in the serum, it binds to a protein known as LPS-binding protein (LBP) [14]. The LPS-LBP complex then engages to the GPI-linked glycoprotein CD14 (Figure 1.7) [13, 14]. CD14 exists in two forms: soluble CD14 (sCD14) found on endothelial cells and membrane-bound CD14 (mCD14) present on the surface of myeloid cells [14]. Since CD14 is not a transmembrane receptor, it cannot transduce the cytoplasmic signals elicited by LPS [5]. The LPS-LBP complex is then brought into direct contact with TLR4 and another glycoprotein known as MD-2 (Figure 1.7) [13]. All of the Toll-like receptors have a Toll/IL-1 receptor (TIR) domain responsible for signal transduction [9]. Signal transduction through TLR4 involves the sequential recruitment of myeloid differentiation factor 88 (MyD88) and IL-1 receptor associated kinase (IRAK) [15, 16]. One of the main intracellular signaling pathways activated by LPS through TLR4 stimulation is Nuclear Factor kappa B (NFκB) activation, which leads to the synthesis of both anti-inflammatory (IL-10) and pro-inflammatory cytokines (TNFα, IL-1, and IL-6) (Figure 1.8) [5]. Using MyD88 knockout mice, it has been shown that LPS is able to stimulate NF-κB activation, albeit with slower kinetics and the expression of only a target subset of genes [16]. The pathway for TLR signal transduction (including LPS signaling through TLR4) is outlined in Figure 1.9. For comparision, signal transduction through the cytokine receptors IL-6, IL-1, and TNFα is shown in Figure 1.10 A and B.

11
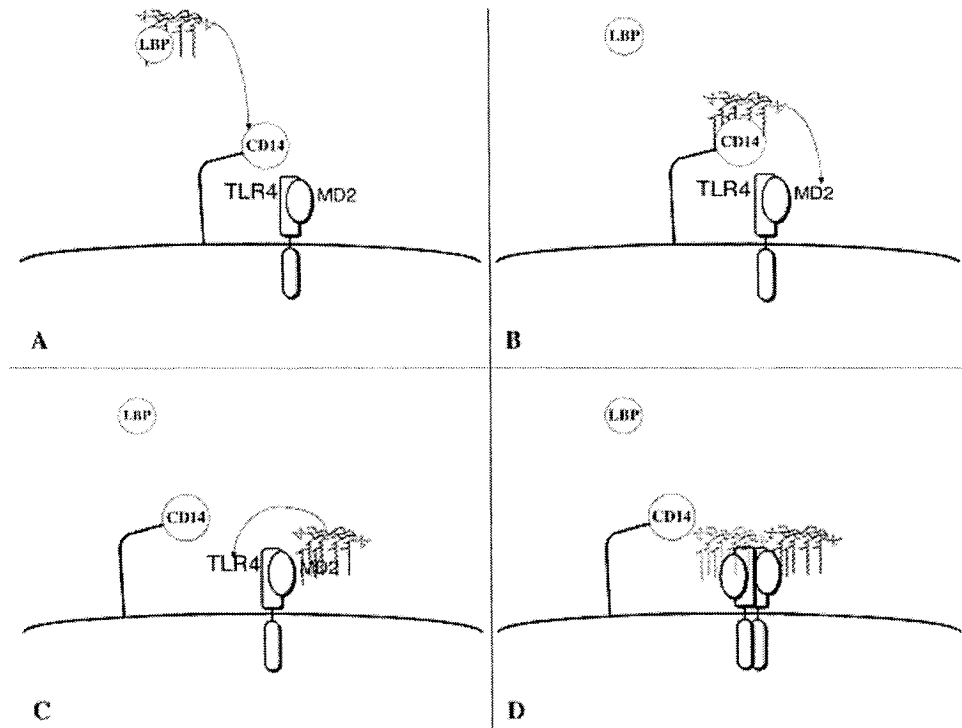
Figure 1.7 – Interaction between LPS and LBP and anchorage to TLR4 through CD14 interaction. Schematic depicts the proposed mechanism by which LPS is anchored to TLR4 to cause its effects. See text for details. Figure taken from [17]

12
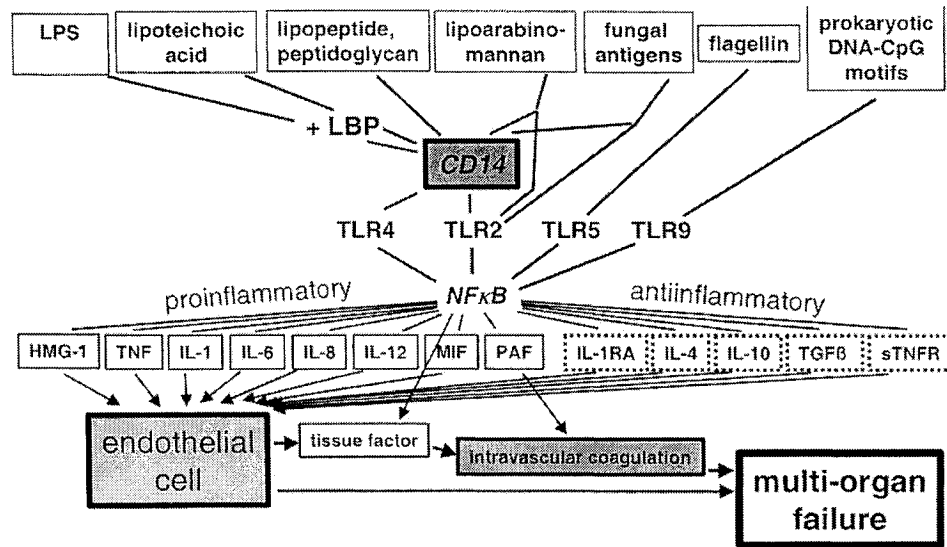
Figure 1.8 – Some of the pro-inflammatory and anti-inflammatory cytokines activated by TLR stimulation. Figure shows that NF-κB can be considered as an almost universal signal transduction mechanism for TLR activation, however some pathways occur independent of this transcription factor (not shown in Figure). Both pro-inflammatory and anti-inflammatory cytokines are released from TLR stimulation. Figure taken from [18]
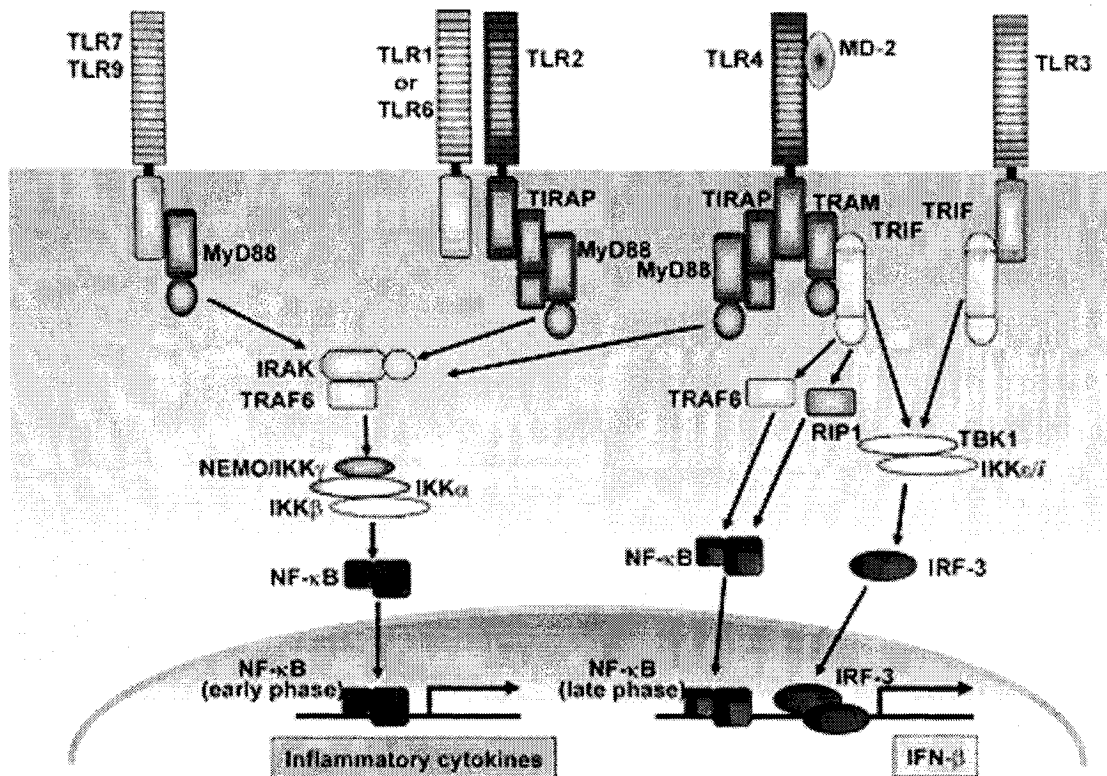
Figure 1.9 – Intracellular signal transduction through TLR. This figures illustrates some of the intracellular mechanisms by which TLR signal intracellularly. NF-κB is depicted as the key transcription factor activated by these signal transduction mechanisms. See text for details for an explanation of the other molecules involved in these signal transduction processes. Figure taken from [11]

14

(A)

(B)
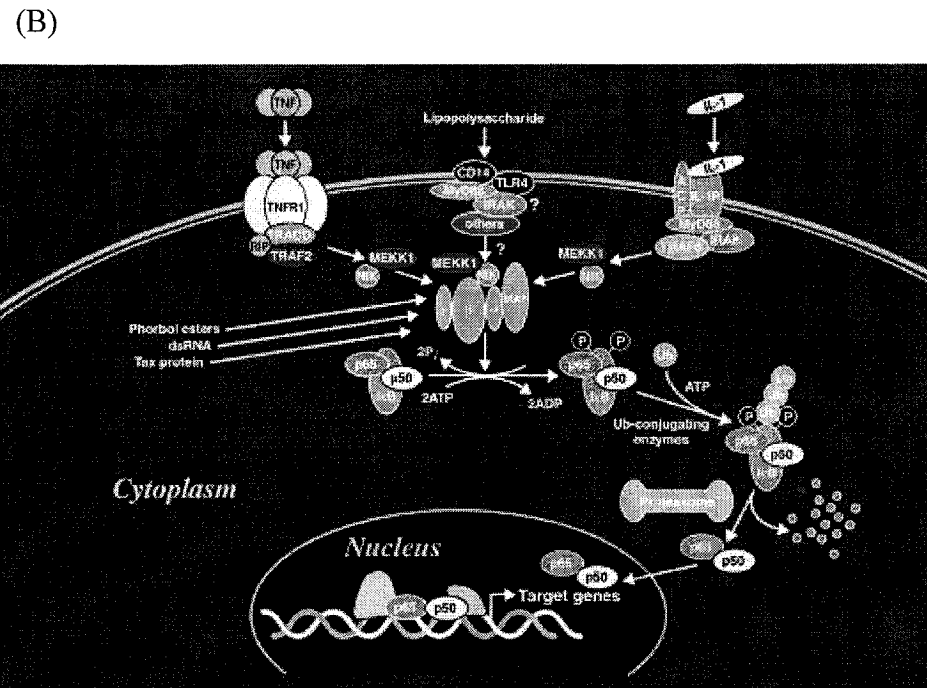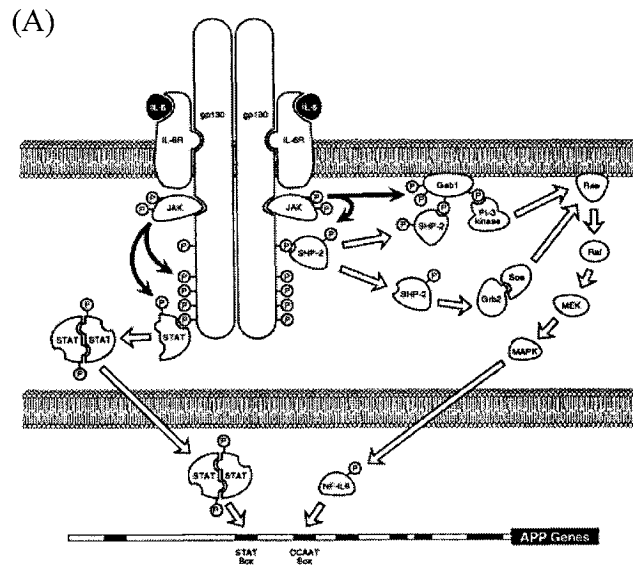
Figure 1.10 – Signal transduction pathways elicited by stimulation of IL-6, IL-1, TNFα, and TLR. Schematics showing the differences and similarities in signal transduction between three of the major pro-inflammatory cytokines and TLR stimulation. Both panels taken from [19].

1.1.3 Nuclear factor-κB

Stimulation of many cells types by LPS and TNFα causes the activation of NF-κB, which is considered as a common pathway for many inflammatory signaling pathways. The NF-κB family of proteins consists of five members: p65 (RelA), RelB, c-Rel, p50/p105 (NF-κB1), and p52/p100 (NF-κB2) [16]. In un-activated states, NF-κB proteins exist in a homodimeric or heterodimeric form in the cytoplasm [20]. Following stimulation by an extracellular signal, the inhibitor protein of IκB kinase (IKK) is activated and causes the phosphorylation of two specific serine residues on IκB proteins (IκBα and IκBβ) [20]. Phosphorylation of the IκB proteins signals them for ubiquitination, which allows the free NF-κB to be available for translocation into the nucleus [20]. After nuclear translocation, NF-κB can bind to the promoters of target genes and activate the production of more cytokines and inflammatory mediators [20]. One of the main genes upregulated by NF-κB is IκBα, which serves as a negative feedback loop to control the activity of NF-κB [16]. NF-κB activation may occur through either the classical or alternative pathway, where the main differences between the two pathways is the IKK subtype required to activate translocation of NF-κB into the nucleus and the stimulus for NF-κB activation (both pathways outlined in Figure 1.11) [16]. Upon nuclear translocation, NF-κB binds to promoter regions containing the following consensus sequence: GGGRNNYYCC (N = any base, R = purine, and Y = pyrimidine) [16].

1.2 Blood-brain barrier

The blood-brain barrier (BBB) and the blood-cerebrospinal fluid (CSF) barrier are considered as the primary interfaces between the central nervous system (CNS) and the peripheral circulation (illustrated in Figure 1.12 A) [21]. The existence of the BBB has
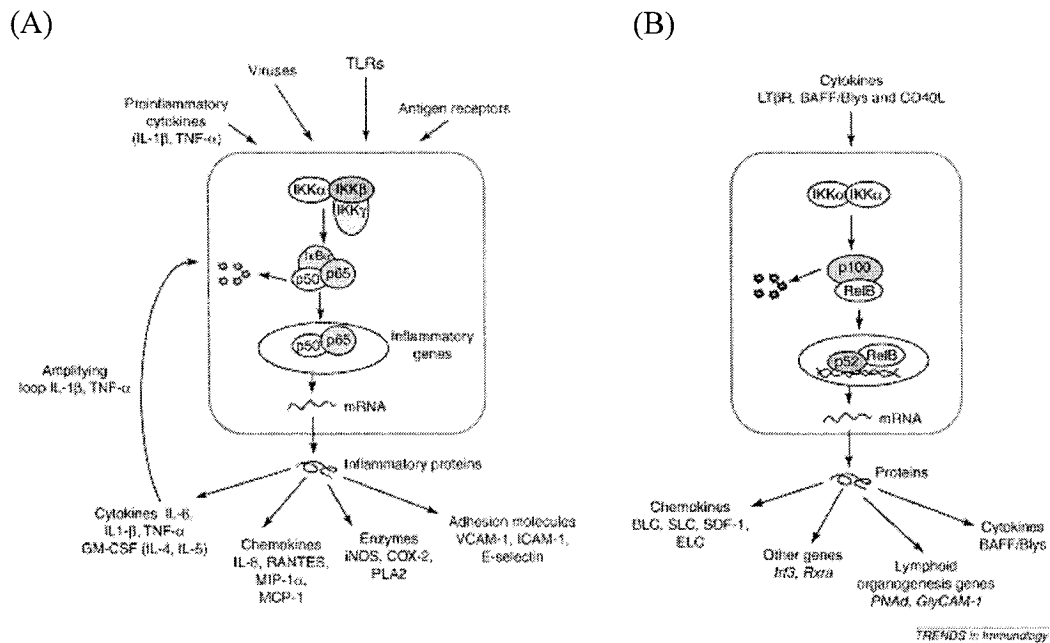
Figure 1.11 – The two pathways of NF-κB activation. NF-κB activation may occur through either the classical (panel A) or alternative pathway (panel B), where the main differences between the two pathways is the subtype of IKK required to activate NF-κB translocation into the nucleus and the stimulus for NF-κB activation Figure taken from [22].

(A)

(B)
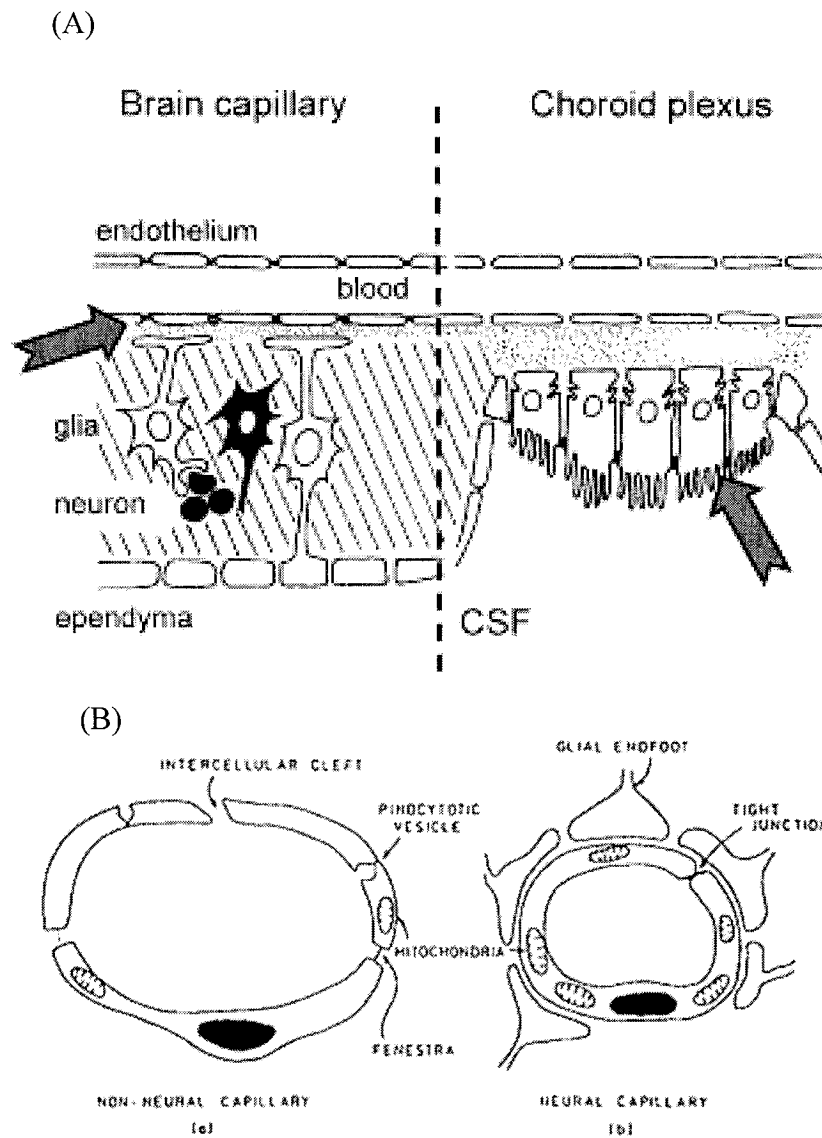
Figure 1.12 – A schematic outlining the differences between the BBB and the blood-CSF barrier and the differences between neuronal and non-neuronal capillaries. Panel A depicts the BBB and the blood-CSF barrier, where the BBB is located at the cerebral capillary endothelium and the blood-CSF barried is located at the choroid plexus epithelium and arachnoid membranes. The block arrows indicate the location of the tight junctions, which are tight in the BBB but slightly leaky at the blood-CSF barrier. Panel B highlights some of the differences between neuronal and non-neuronal capillaries. The main differences include the presence of tight junctions in neuronal capillaries, the absence of fenestra, and the presence of a higher amount of mitochondria. Panel A taken from from [23] and panel B taken from [24].

been known for over 100 years, and was first demonstrated by the German microbiologist

Ehrlich [25]. The barrier between the blood and the brain extracellular fluid is located at

the cerebral capillary endothelium, whereas the barrier between the blood and CSF is

located at the choroid plexus epithelium and arachnoid membrane [26]. The presence of

both barriers is essential in allowing the CNS to function in an environment where the

accumulation and maintenance of substrates is highly controlled, thereby limiting the

uptake and penetration of many circulating macromolecules into the brain and CSF [21,

26]. Due to the fact that the BBB has a much larger surface area than the blood-CSF

barrier, it is considered as essential in maintaining the stability of the CNS environment

[21]. The only areas in the CNS that completely lack a barrier are the circumventricular

organs [27].

The BBB is made up of cerebral endothelial cells that are thought to possess

various metabolic enzymes (such as cytochrome P450 enzymes and glutathione

transferases) and energy-dependent efflux transporters (such as p-glycoprotein and

multidrug-resistance proteins) [21]. Cerebral endothelial cells have few plasmalemmal

vesicles and do not generally demonstrate pinocytosis [27]. In addition, theses cells lack

fenestrations and possess tight-junctions with high electrical resistance [21, 27]. All these

characteristics of cerebral endothelial cells allow the BBB to prevent the accumulation of

substrates in the CNS [21, 27]. A comparison between endothelial capillaries of the BBB

and non-neuronal capillaries is outlined in Figure 1.12 B. Another cell type part of the

architecture of the BBB are astrocytes, which are in close contact with the BBB and play

an essential role in the phenotype of the BBB by providing it with protection against

hypoxia and aglycemia (Figure 1.13) [28, 29].
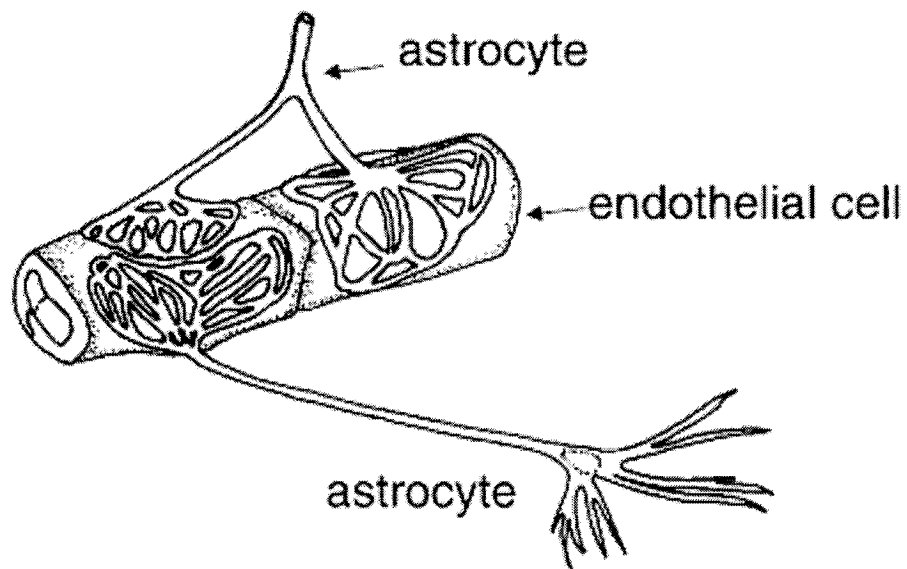
Figure 1.13 – Location of astrocytes on the endothelial cells in the BBB. Astrocytes
are also considered as being part of the architecture of the BBB. Astrocytic end-feet
structures are found on the endothelial cell surface. Figure taken from [30].

Only small and lipophilic molecules can easily cross the BBB from the blood to CNS [25]. The large polypeptide insulin plays an important role in the regulation of brain glycogen and neuronal maturation and coupling, thereby making it essential for the CNS to be able to transport it across the BBB [31]. This necessitates the presence of specific membrane transporters at the BBB to allow essential nutrients such as glucose and certain amino acids passage into the CNS. Since BBB permeability is usually difficult to study in the whole animal, many *in vitro* cell culture models have been developed to aid in the understanding mechanisms of transport across the BBB [32].

1.2.1 Effects of inflammation on the CNS and BBB permeability

The BBB was once thought to act as a selective barrier to the entry of cytokines into the CNS, thereby causing the brain to be considered as an immunologically privileged organ [28, 33]. It is now widely acknowledged that the BBB is a dynamic structure that is capable of rapid modulation [29]. It is now known that many pathophysiological conditions such as peripherally induced inflammation, stroke, multiple sclerosis, and Alzheimer's disease can regulate the permeability of the BBB [25, 29]. During Alzheimer's disease, β-amyloid causes an increase in cytokine release and monocyte migration across the BBB [29]. Similarly, it is generally accepted that disruption of the BBB occurs following cerebral ischemia, however the timing and causes of this disruption have still not been determined [25].

TNFα can be transported across the BBB via the the the two TNFα receptors, TNFR1 and TNFR2 [33, 34]. The intravenous administration of various cytokines and cytokine inducers causes an increase in prostaglandin E_2 accumulation in the CSF with a peak at 90 minutes following administration [35]. Similarly, using cultured bovine brain

microvessel endothelial cells, it was shown that the administration of TNFα caused permeability changes in these cells in part due to an induction in cyclooxygenase-2 (COX2) [36]. It it thought that BBB breakdown occurs 3 – 7 days following the injection of LPS into either the ventricles or the parenchyma [37].

The inflammatory response has the potential to cause major damage to the CNS [38]. Microglia are the resident macrophages of the CNS and are located within the brain parenchyma behind the BBB [39]. Under normal conditions they function as glial cells, however they take on an activated phenotype in response to inflammatory stimuli manifested by an increase in their branches and an upregulation in the expression of their cell surface antigen molecules [39, 40]. Astrocytes are also considered as CNS immune effector cells and can participate in the inflammatory response in the CNS [28]. Peripherally generated immune cell mediators such as lymphocytes and macrophages have also been shown to be able to cross the BBB in pathological conditions [7, 25]. Some of the effects of these cells are shown in Figure 1.14.

The injection of LPS and other inflammatory mediators directly into the ventricular system of the CNS has been used as a model to understand the pathophysiology of bacterial meningitis [8]. Various areas of the CNS express the TLR4 and CD14 mRNA required for a response to LPS [14]. Most of the *in vivo* studies conducted to date have demonstrated the presence of TLR exclusively in glial cells in the CNS [12, 41], however *in vitro* studies using cultured primary astrocytes have shown the expression of TLR2, TLR4, TLR5, and TLR9 [42].
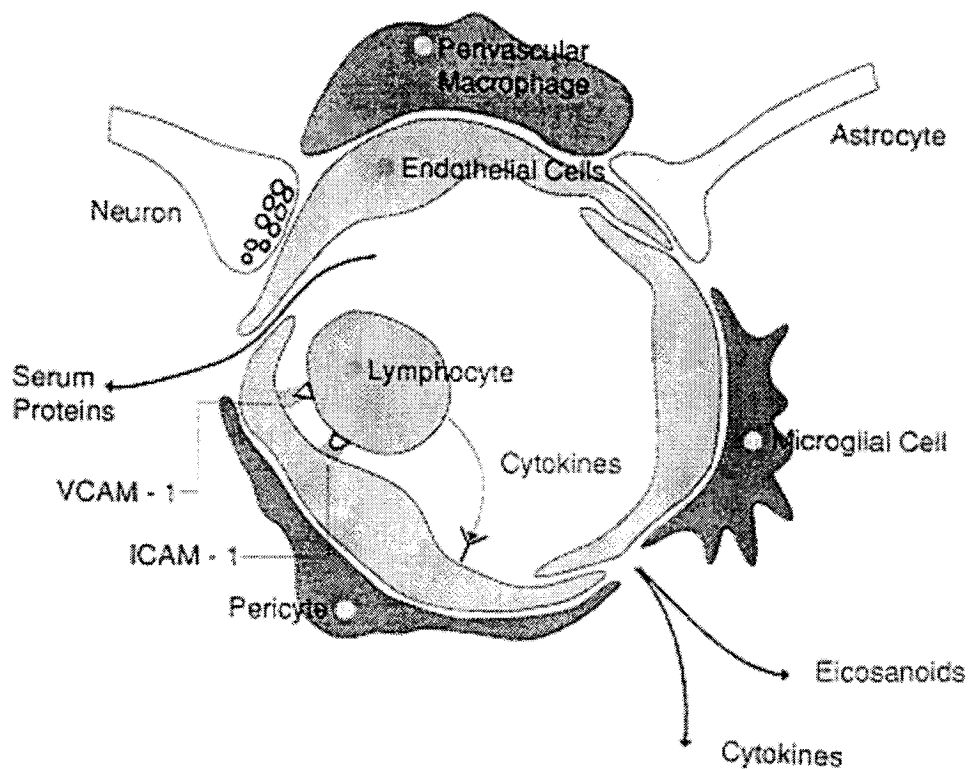
Figure 1.14 – Hypothetical schematic outlining the characteristics of BBB endothelial cells during conditions of CNS inflammation. BBB endothelial cells, in addition to microglial and astrocytes, can release cytokines during conditions of CNS inflammation. In addition, it is thought that the expression of adhesion molecules during neurological diseases such as multiple sclerosis leads to the entry of leukocytes into the CNS. Figure taken from [24]

1.3 Cytochrome P450

The cytochrome P450 (P450) family represents a large group of heme-containing enzymes thought to have existed for more than 3.5 billion years and present in plants, mammals, and bacteria [43, 44]. The enzymes were first discovered through the demonstration of mixed-function oxidation activity for the metabolism of drugs and carcinogens and currently encompasses over 2000 members [43, 45]. These enzymes are named cytochrome P450 because they have a spectrophotometric absorption peak at or near 450 nm when bound to carbon monoxide and the iron is reduced [44].

The chemical reactions catalyzed by the P450 enzymes vary substantially, and their substrates range from physiologically important endogenous substances to xenobiotics [46]. Some P450 substrates include steroids, eicosanoids, fatty acids, lipid hydroperoxides, retinoids, drugs, alcohols, procarcinogens, antioxidants, organic solvents, anesthetics, dyes, pesticides, odorants, and flavorants [46]. P450 enzymes are responsible for the metabolism and elimination of xenobiotics through biotransformation of the parent drug into a more polar metabolite which is then excreted by the kidneys [47]. Physiologically, P450 enzymes are involved in the biosynthesis and/or degradation of steroid hormones, cholesterol, and fatty acids [44]. P450 also play a role in the synthesis of bile acids from cholesterol and in the metabolism of arachidonic acids [44].

1.3.1 P450 intracellular localization

P450 enzymes are hydrophobic membrane proteins that are tightly associated with intracellular membranes [48]. The mammalian P450 enzymes can be divided into two major classes based on their intracellular localization, where a minority of the enzymes are located in the mitochondria and the majority in the endoplasmic reticulum membrane

[48]. The mitochondrial enzymes are found in the mitochondria of steroid producing cells

(the adrenal cortex, ovary, testes) and are involved in steroid biosynthesis [48]. The

types, amounts, and activity of P450 isoforms within a given tissue are regulated by

numerous factors such as age, gender, dexposure to certain chemical inducers, smoking,

alcohol consumption, disease states and nutrition [47, 49].

1.3.2 P450 nomenclature

With the identification of a multitude of P450 enzymes, a need arose to determine a

specific nomenclature for the different isoforms. Original nomenclature of the P450

enzymes was based on sources used for identification, spectral properties, electrophoretic

mobility, substrates, or inducers [46]. In some cases, the number was assigned arbitrarily

in series [46]. P450 proteins are named based on alignments in their amino acid

sequences, not nucleotide sequences [50]. Currently, P450 protein members sharing 40%

or more sequence homology are included in the same family designated by an Arabic

number, and those with 55% or more sequence homology are included in the same

subfamily designated by a capital letter [44, 46]. Individual gene products are then

assigned arbitrary numbers [44, 46]. The schematic below illustrates P450 nomenclature,

which will be used throughout this thesis:

Subfamily
number

Family
number

CYP2D6 ← gene

Cytochrome
P450

25
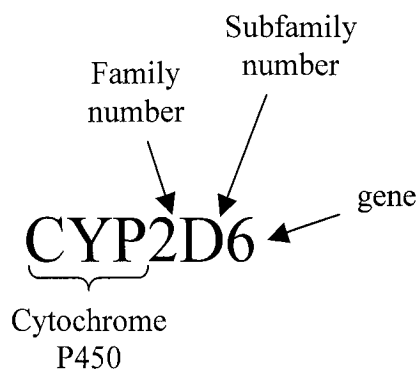
The next sections will describe some selected P450 isoforms that will be studied in this thesis, followed by a general description of a typical P450 catalytic cycle reaction.

CYP1A: CYP1A1 and CYP1A2 are known to play a role in the metabolism of many procarcinogenic substrates [51, 52]. Some of the substrates for CYP1A2 include caffeine, clozapine, haloperidol, and theophylline [47]. The expression of the *cyp1a* genes is highly regulated by many factors such as development, tissue-specific factors, hormonal influences, xenobiotics, and pathophysiological mechanisms [51]. CYP1A1 is present both in the liver and extrahepatically [53].

The aryl hydrocarbon receptor (AhR) plays an essential role in the regulation of CYP1A (Figure 1.15 A) [52]. Some of the ligands for the transcription factor AhR include polycyclic aromatic hydrocarbons (such as 3-methylcholanthrene, benzo(a)pyrene), polyhalogenated aromatic hydrocarbons (such as 2,3,7,8-tetrachlorodibenzo-*p*-dioxin), and certain polyhalogenated biphenyls [51]. AhR normally resides in the cytoplasm associated with heat shock protein 90 (hsp90), but translocates to the nucleus upon ligand binding and binds to another protein known as the AhR nuclear translocator (ARNT) [51, 52]. The heterodimeric protein complex then binds to xenobiotic response elements (XRE) present on the promoter regions of the genes being regulated [51]. It is also thought that the glucocorticoid receptor, the estrogen receptor, and retinoid receptors may also play a role in the regulation of CYP1A genes with a possible role for cross talk between these receptors and AhR [52].

CYP2B, CYP2E1, and CYP2D: The CYP2 family is fairly large and encompasses 2A, 2B, 2C, 2D and 2E subfamilies [44]. Members of this family are highly inducible by

many xenobiotics [54]. Of importance to this work are CYP2B, CYP2E1, and CYP2D isoforms, which will be discussed throughout this thesis.

There are many members in the CYP2B subfamily and they play a role in the metabolism of various xenobiotics and steroids [52]. What distinguishes the members of the CYP2B subfamily is the ability of a wide variety of chemicals to induce them through the action of nuclear receptors [52]. Phenobarbital, a known inducer of CYP2B subfamily members, is thought to cause its effects through the nuclear constitutive androstane receptor (CAR) (Figure 1.15 B) [52]. Human CYP2B6 (CYP2B1 is the rat equivalent) plays a limited role in human liver drug metabolism [44, 55]. CYP2E1 is the only existing gene in the CYP2E subfamily, and has an important toxicological role [44]. Chronic ethanol consumption and starvation cause an induction in the enzyme [44, 56]. The predominant mechanism of regulation of this isoform is thought to occur at the protein level [57].

The human CYP2D6 gene is a highly polymorphic gene responsible for the metabolism of over 100 drugs to which humans are exposed [58]. Some of the agents metabolized by CYP2D6 include β-adrenergic blocking agents, antiarrhythmics, antidepressants, and analgesics [58]. The selective serotonin reuptake inhibitors bind tightly to the enzyme and inhibit its activity [44]. Only one isoform (CYP2D6) is present in this family in humans, however several polymorphic variants of this isoform exist in humans [59]. CYP2D6 is localized in the liver, kidney, brain, breast, and lung [60]. In contrast, at least 6 isoforms (CYP2D1, CYP2D2, CYP2D3, CYP2D4, CYP2D5, and CYP2D18) have been identified in rats, with each isoform having a specific tissue

distribution [60]. There is a marked species difference in CYP2D substrates making it difficult to use animal models to study the activity of CYP2D6 [58].

CYP3A: The CYP3A enzymes are very active in the metabolism of steroids, bile acids, and a multitude of xenobiotics [52]. They are expressed in the liver and gut and are considered as critical drug metabolizing enzymes for a number of important therapeutic agents [52, 53]. Human CYP3A4 (CYP3A11 in mouse and CYP3A1/2 in rat) plays a role in the metabolism of a large number of structurally diverse drugs in clinical use [61]. Some of the substrates for CYP3A isoforms include carbamazepine and quinidine [47]. Compounds such as ketoconazole, erythromycin, and grapefruit juice inhibit members of the CYP3A subfamily [44], making it an important aspect to consider in the determination of drug-drug interactions. The transcriptional activation of CYP3A4 is under the control of several nuclear receptors, with the pregnane X receptor (PXR) and CAR playing prominent roles (Figure 1.15 C) [53, 61].

1.3.3 P450 catalytic activity cycle

The iron atom present in the heme group of P450 enzymes is essential for the enzyme's drug transformation ability. The iron atom takes electrons and uses them to charge oxygen atoms, thereby making the oxygen atom reactive and able to cause changes to various toxic molecules [62]. Mitochondrial P450 enzymes receive their electron source from the iron sulfur protein adrenodoxin via the NADPH-adrenodoxin oxidoreductase while the microsomal P450 enzymes receive their electrons through the flavoprotein NADPH-P450 oxidoreductase [48]. The substrate binding region of P450 enzymes is specific to each isoform, however some aspects that are common to all P450 enzymes

(A)
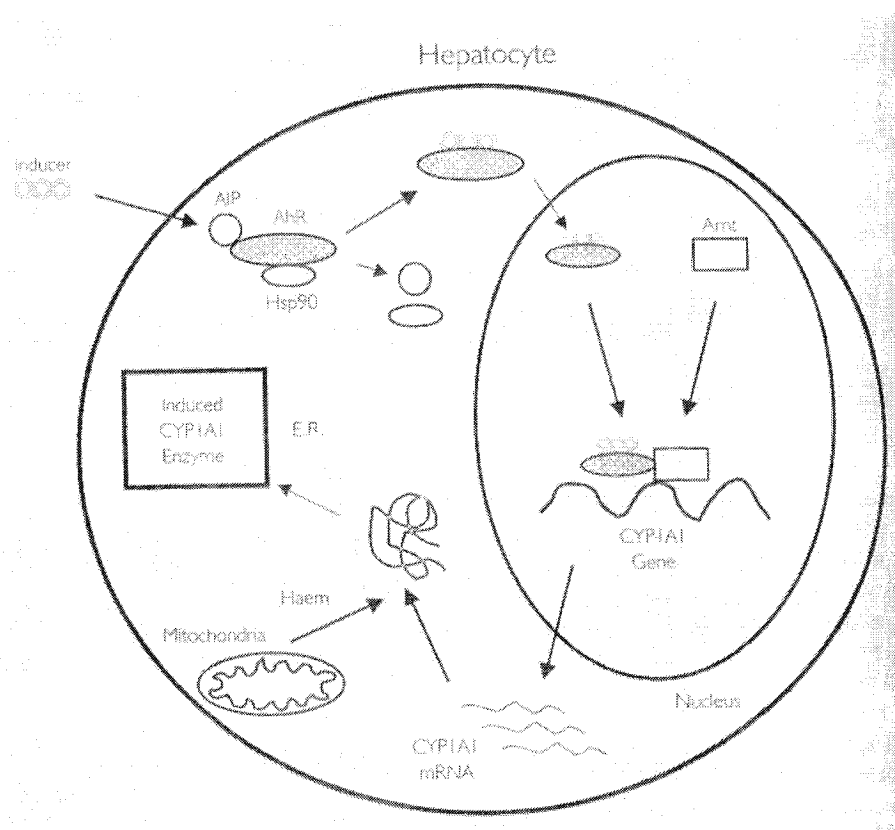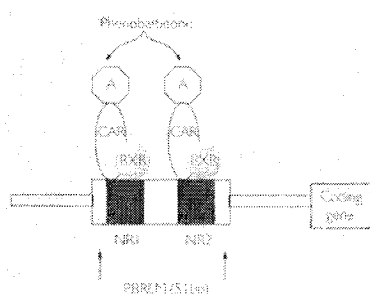
(B)   (C)
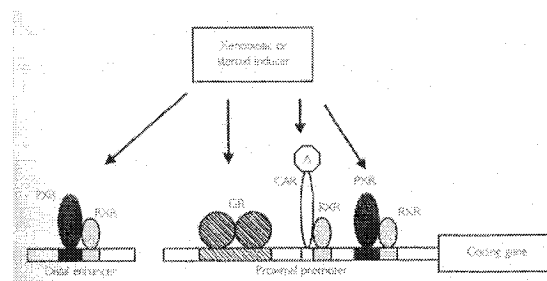
Figure 1.15 – Induction of CYP1A, CYP2B, and CYP3A isoforms. Panel A is a schematic of the mechanism by which AhR-mediated induction of CYP1A1 occurs. Panel B depicts how phenobarbitone acts through the nuclear receptor CAR to cause the induction of human CYP2B6. Finally, panel C indicates some of the nuclear receptors involved in the induction of CYP3A4 by various xenobiotics. All panels were taken from [59].

include a membrane-binding domain that anchors the P450 to the endoplasmic reticulum and the use of NADPH cytochrome P450 reductase and cytochrome b_5 to catalyze their reactions [49].

A typical P450 catalytic cycle is outlined in Figure 1.16 [59]. The cycle is initiated by the binding of the substrate (RH). The following step is the reduction of the heme iron by the addition of an electron from the electron source NADPH (nicotinamide adenine dinucleotide phosphate) and the binding of molecular oxygen [63]. It is believed that a metabolite is then formed whereby a second electron is added to reduce the bound oxygen to the level of a peroxide [63]. Breakage of the peroxide bond gives rise to another peroxide compound that has the ability to eventually hydroxylate the original substrate [63]. A typical reaction catalyzed by P450 can be summarized as follows [44]:

$$NADPH + H^+ + O_2 + RH \rightarrow NADP^+ + H_2O + ROH$$
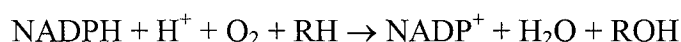
1.4 Effects of inflammation on cytochrome P450

Infectious and inflammatory conditions are known to change P450 regulation in the liver, intestines, brain, and kidney [64-66]. The suppression of cytochrome P450 enzymes during infectious and inflammatory conditions may result in many untoward clinical consequences such as toxicities from drugs with narrow therapeutic windows or a reduced therapeutic effect from drugs that need to be converted into their active metabolites via cytochrome P450 in both animals and humans [64]. The administration of LPS is a commonly utilized model to examine the effects of inflammation on cytochrome P450 [65]. Using both primary and established hepatocyte cultures, it has been shown *in vitro* that LPS can downregulate a wide variety of P450 isoforms [65]. LPS
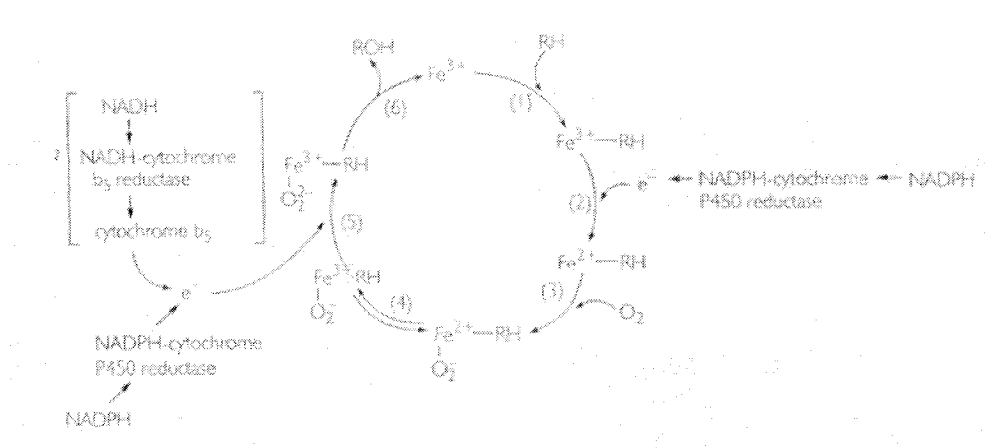
Figure 1.16 – A typical P450 catalytic cycle. A typical cycle by which P450 catalyzes the formation of a polar metabolite (denoted by ROH) from a non-polar drug (RH). See text for reaction details. Figure taken from [59].

administration also causes a downregulation in human and rodent P450 enzyme drug

metabolism [65, 67, 68]. Cytochrome P450 can be downregulated by both transcriptional

(changes at the level of the gene or mRNA) and post-transcriptional mechanisms

(changes at the level of the protein) in response to inflammatory stimuli (see sections

1.4.1 and 1.4.2 in this thesis) [69].

The administration of LPS intracerebroventricularly (i.c.v.) is known to cause an

inflammatory model in the brain characterized by microglial activation and production of

pro-inflammatory cytokines both in the CNS and the periphery [37, 66, 70-74]. The i.c.v.

administration of LPS causes a reduction in P450 both in the brain and in liver [71-73,

75]. We have shown a reduction in CYP1A1/2 expression and activity in the brain in both

in vitro and *in vivo* models of LPS-induced inflammation [66, 76-78]. A reduction in

hepatic CYP1A, CYP2B, CYP2C, CYP2E, CYP2D, and CYP3A isoforms is also

observed following the i.c.v. administration of LPS [71-73, 75, 79].

The mechanism(s) underlying the downregulation in P450 following infectious

and inflammatory conditions remains largely unknown [64]. The mechanisms underlying

the regulation of P450 during CNS inflammation will be discussed in the individual

chapters of this thesis. Since different cytochrome P450s are regulated by different

mechanisms and inflammatory stimuli, it is likely that changes to P450 regulation during

inflammation is not a non-specific event [64]. It is also possible that P450

downregulation during infectious and inflammatory conditions is occurring as an

adaptive or homeostatic response and as a need for the liver to devote its transcriptional

machinery to the formation of acute-phase proteins essential during such conditions [64].

1.4.1 Transcriptional regulation of cytochrome P450 during inflammation

LPS is known to enhance the hepatic expression of many inflammatory and acute-phase

proteins [80]. It has been shown that the administration of LPS intraperitoneally causes

the suppression of the nuclear receptors retinoic X receptor (RXR), PXR, farnesoid X

receptor (FXR), and CAR [80]. These transcription factors along with the hepatocyte

nuclear factor (HNF)1α, HNF4α, and CCAAT/enhancer-binding protein (C/EBP) are

known to play a role in the regulation of hepatic P450 [81].

It is believed that the regulation of most P450 isoforms in response to cytokines

occurs at the level of the gene [66]. The effects of cytokines on cytochrome P450

enzymes *in vitro* has been examined extensively using cultured hepatocytes [64]. Many

liver-enriched transcription factors are upregulated in the liver during an acute phase

response in response to blood-borne pro-inflammatory cytokines [82]. CYP1A1 has been

shown to be downregulated by cytokines and LPS *in vitro* through an NFκB pathway

[51]. Similarly, it has been observed that IL-1 regulated CYP2C11 by NFκB both *in vitro*

and *in vivo* [83]. IL-6 has also been shown to downregulate CYP3A4 through the

JAK/STAT (Janus kinase/signal transducer and activators of transcription) transcription

factors [84].

1.4.2 Post-transcriptional regulation of cytochrome P450 during inflammation

Post-transcriptonal regulation of P450 during inflammatory and infectious conditions is

thought to only account for a small proportion of the changes of regulation of these

enzymes [65]. LPS administration can cause the induction of reactive oxygen and

nitrogen species that lead to the downregulation in cytochrome P450 through protein

oxidation and nitration reactions [64]. It has been shown that the administration of high

concentrations of LPS to rat hepatocytes causes a rapid degradation in phenobarbital

induced CYP2B1 protein [69]. The regulation of CYP2E1 is also thought to occur mainly at the protein level, where substrates are known to bind to the heme group of the enzyme and prevent its proteosomal degradation [57].

CHAPTER 2

THE ROLE OF BETA-ADRENERGIC RECEPTOR SIGNALING IN THE

REGULATION OF CYP1A1 IN A CELL CULTURE MODEL OF CNS

INFLAMMATION

Portions of this chapter appeared in the following publication:

2.1 Abstract

CYP1A1 and 1A2, two important P450 isoforms in the brain that metabolize many endogenous and exogenous substrates, are downregulated during central nervous system (CNS) inflammation. The stimulation of beta-adrenergic receptors has been demonstrated to be anti-inflammatory in many cell types, leading us to hypothesize that stimulation of beta-adrenergic receptors could prevent the downregulation in CYP1A1 and 1A2 activity in an *in vitro* model of CNS inflammation. Isoproterenol, a general β_1/β_2 receptor agonist, and clenbuterol, a specific β_2 receptor agonist, were both able to prevent the LPS-induced downregulation in CYP1A1/2 activity in astrocytes. The involvement of β-adrenergic receptors was confirmed using the general β_1/β_2 receptor antagonist propranolol, which was able to abrogate the protection conferred by isoproterenol and clenbuterol in astrocytes treated with LPS. The isoproterenol and clenbuterol mediated protective effect on the LPS-induced downregulation in CYP1A activity was a cyclic AMP (cAMP) dependent process, since forskolin was able to mimic the protective effect. Isoproterenol and clenbuterol may also prevent the LPS-induced downregulation in CYP1A activity through changes in TNFα expression. Despite a slight reduction in the LPS-induced nuclear translocation of the p65 subunit of NF-κB, isoproterenol and clenbuterol had no effect on the DNA binding ability of this transcription factor, indicating that the β-adrenergic protective effects on CYP1A activity occurred independent of changes in NF-κB activity. The results presented in this paper reveal that beta-adrenergic receptor stimulation can modulate cytochrome P450 activity in an *in vitro* model of CNS inflammation by a cAMP mediated pathway.

2.2 Introduction

Cytochrome P450 (cyt P450) constitutes a superfamily of heme containing enzymes responsible for the metabolism and elimination of exogenous and endogenous substances [44, 66]. The majority of the cyt P450 isoforms are located in the liver, however other extra-hepatic sites of cyt P450 localization include the central nervous system (CNS), gastrointestinal tract, kidney, lungs, and adrenal glands [85]. In the CNS, cyt P450 isoforms are thought to play a role in neurosteroid synthesis and drug metabolism [86]. In particular, members of the CYP1A family, whose roles in carcinogen detoxification and activation are well established, are thought to play a role in metabolism of eicosanoids and estrogen in the brain [87, 88]. Additional substrates for the CYP1A family of cyt P450s include a diverse group of endogenous and exogenous compounds such as polyaromatic hydrocarbons, arylamines, nitrosamines, and heterocyclic amines [88, 89].

Various immunostimulants cause an inflammatory response in the brain that is highly regulated and characterized by the production of cytokines, immune cell infiltration, and tissue damage [66, 76, 77, 90, 91]. Many inflammatory mediators, such as cytokines, can cause differential regulation of cyt P450 expression and activity in the brain [56, 64, 66, 69, 75-77, 92]. Activity of CYP1A1 and CYP1A2 isoforms has been shown to be downregulated in response to LPS administered directly into the lateral cerebral ventricle in rat brain [66, 75-77, 86]. Similarly, in dibenz[a,h]anthracene (DBA) treated astrocytes, LPS causes the downregulation of CYP1A1 and CYP1A2 activity in a dose-dependent manner [76]. Previously, our lab has shown that inflammatory conditions of the CNS lead to changes in the ability of the brain to metabolize endogenous and

38

exogenous substrates and may exacerbate susceptibility to neurotoxic environmental

agents, such as 1-methyl-4-phenylpyridinium (MPP+) induced neurotoxicity [93].

2.2.1 Signal transduction through the beta-adrenergic receptor

G-protein coupled receptors refer to a group of seven-transmembrane-spanning receptors

that signal through activation of heterotrimeric (α-, β-, and γ-subunit) guanine nucleotide-

binding proteins [94]. They represent the largest family of cell-surface receptors [95]. G

proteins can belong to one of several groups, with the Gs (stimulatory) causing the

activation of adenylyl cyclase (AC) resulting in an increase in cyclic AMP (cAMP) and

Gi (inhibitory) causing a decrease in cAMP through the inhibition of AC [95]. On the

other hand, Gq proteins cause changes in intracellular calcium [95]. The adrenergic

receptors, which are G protein coupled receptors, can be divided into two categories: the

alpha-adrenergic and the beta-adrenergic receptors [96]. The beta-adrenergic receptor is

coupled to the Gα stimulatory (Gαs) protein and activates AC [96]. The activation of AC

through Gαs causes an increase in the intracellular second messenger cAMP, ultimately

stimulating protein kinase A (PKA) [96].

2.2.2 Anti-inflammatory role of the adrenergic agents

The idea that norepinephrine (NE), one of the major catecholaminergic neurotransmitters,

is neuroprotective and anti-inflammatory is not an old one. CNS diseases with an

inflammatory component, such as Alzheimer's disease (AD) and multiple sclerosis (MS),

involve NE depletion and/or perturbations in the NE signaling system [90]. Many studies

support the notion that the increase in plasma levels of catecholamines seen during LPS-

induced inflammation is an event that can be beneficial to the host response during

endotoxemia [97]. Beta-adrenergic receptor (βAR) ligands have been shown to modulate

the release of pro-inflammatory mediators such as cytokines and cyclooxygenase-2 (COX2) from various immune cells when given concurrently with LPS in both *in vivo* and *in vitro* models of inflammation [90, 98-103]. Szabó and coworkers have demonstrated that isoproterenol can protect endotoxemic mice from hypotension and causes a reduction in the amount of plasma tumor necrosis factor (TNFα) in these mice [100, 103]. Clenbuterol was observed to be a potent inhibitor of the release of several LPS induced cytokines both *in vivo* and *in vitro* [104]. Norepinephrine and isoproterenol were both shown to increase the protein and mRNA levels of IκBα, a protein that binds to the transcription factor nuclear factor κB (NF-κB) and prevents its translocation into the nucleus [90].

2.2.3 Objective

Given the anti-inflammatory role of norepinephrine in astrocytes, we chose to examine the effects of beta-adrenergic receptor stimulation on CYP1A activity in an *in vitro* model of CNS inflammation. We hypothesize that beta-adrenergic receptor stimulation would prevent the downregulation in CYP1A1/2 activity in astrocytes treated with LPS. Preventing the loss of P450 activity in the brain during conditions of CNS inflammation would protect the capacity of the brain to metabolize endogenous and exogenous agents.

2.3 Materials and methods

2.3.1 Materials.

All reagents were purchased from Sigma-Aldrich Chemical Co. with the exception of fetal bovine serum (FBS), which was obtained from CanSera. Other exceptions are noted below. E. coli lipopolysaccharide (LPS) of sereotype 0127:B8 was utilized in experiments as outlined below. Several sereotypes of LPS exist, with each sereotype possessing a certain potency. The dose of LPS was chosen based on previously observed reductions in CYP1A1/2 activity seen in our laboratory [77].

2.3.2 Isolation and treatment of astrocytes.

Astrocyte cultures were obtained using one-day old Sprague-Dawley rats (Charles River Labs) as previously described [77]. Briefly, one-day old rat pups were stunned in ice and decapitated and the brain was washed in ice-cold PBS once and placed in ice-cold 10% FBS Dulbecco's Modified Essential Medium (DMEM). The brains were broken up mechanically using a 10 mL serological pipette and the homogenate was sequentially filtered through a 75 μm and a 25 μm mesh bag. The cellular filtrate was then vortexed and centrifuged for 5 minutes at 3000 rpm. The cellular pellet was then re-suspended in DMEM supplemented with 10 % FBS and 1% antibiotic/antimycotic (100 units penicillin, 0.1 mg streptomycin, and 0.25 μg amphotericin B) and seeded on either 6- or 12-well plates. Cell cultures were grown for 10 – 14 days in DMEM containing 10% FBS and 1% antibiotic/antimycotic until cells reached a 90-95% confluency. We have previously shown that 14 days following the cell isolation, cell cultures consisted predominantly of astrocytes (> 97% of the cells stained positive for the astrocyte marker

glial fibrillary acid protein), with a minor contribution of oligodendrocytes and microglia [76, 77].

On the day of drug treatment, fresh 10% FBS DMEM containing 1% antibiotic and antimycotic was added to the cells. Cell monolayers were treated with 50 nM DBA and either 10 or 50 μl drug of interest (10 μg mL^{-1} LPS, 50 μg mL^{-1} LPS, 10 nM isoproterenol, 10 nM clenbuterol, 10 nM propranolol, 1 μM forskolin, or 10 μM forskolin) administered concurrently. We have previously shown that EROD activity is not detectable in astrocytes that have not been induced with DBA [77]. Following the addition of drugs, cells were incubated for 24 hours prior to measuring enzymatic activity.

2.3.3 7-Ethoxyresorufin O-dealkylase (EROD) activity and protein determination. CYP1A1/2 activity in astrocyte cultures was determined by measuring the rate of formation of resorufin from the CYP1A1/2 substrate ethoxyresorufin using a modification of a previously described procedure [77]. Briefly, cells were incubated with the specified drugs as usual in either 12 well or 6 well plates, after which the media was removed and 3 mL of new media containing 0.6 μM of the substrate ethoxyresorufin was added to the cells and allowed to incubate for 2 hours at 37°C. Following this, the amount of resorufin in 2 mL of media was detected using a fluorescence spectrophotometer (Varian, Cary Eclipse) with the excitation wavelength set at 510 nm and the emission wavelength set at 586 nm. The values obtained were subtracted from blank wells determined by measuring the amount of fluorescence in wells containing ethoxyresorufin without the cells. CYP1A activity is expressed as the amount (pmoles) of resorufin formed per mg protein per minute.

Following determination of EROD activity in astrocytes, the remaining cell medium was aspirated and 1 mL of fresh phosphate buffered saline (PBS) was added to each well. The astrocytes were scraped into the PBS then sonicated to lyse the cells. Protein concentrations in cell lysates were determined using a modification of the method described by Lowry *et al.* [105]. Briefly, the media was removed and 1 mL of ice-cold PBS was added to the cells. The cells were scraped into the PBS and lysed by sonication for a period of 3 minutes. The homogenates were then spun at 13,000 rpm to pellet the debris and the amount of protein was then determined using 1:3 dilution of the lysate. The diluted lysate was incubated with a 5× volume of Mix A (0.97% $NaCO_3$ containing 0.1M NaOH, 0.02% sodium potassium tartarate, and 0.01% $CuSO_4$) for 10 minutes at room temperature. Following this incubation, a 0.5× volume of phenol mixture (1:1 dilution with water) was added to the samples, which were then allowed to incubate for a further 30 minutes. The sample absorbances were determined in a 96-well plate format at 700 nm using a plate reader (BioTek Instruments) and protein amounts were determined based on a protein bovine serum albumin (BSA) standard curve. For all experiments, EROD activity was normalized to the amount of protein present in the sample.

2.3.4 Nuclear extract preparations

Nuclear extracts from treated astrocytes were prepared according to a modified Dignam protocol [106]. Briefly, cell monolayers were scraped in a total of 1mL of phosphate buffered saline, and spun at 13000 rpm for 10 minutes to collect the cellular pellet. The pellet was then lysed using Lysis Buffer (10 mM Hepes buffer pH 7.9, 10 mM KCl, 2 mM $MgCl_2$, 0.5 mM dithiothreitol (DTT), 0.5 mM phenylmethylsulfonyl fluoride (PMSF), 5 μg mL^{-1} aprotonin, 5 μg mL^{-1} pepstatin A, and 5 μg mL^{-1} leupeptin)

containing 0.1% Nonidet P-40 and incubated for a period of 15 minutes on ice to ensure

complete lysis. Following 10 homogenization strokes with a Dounce homogenizer, the

suspension was spun at 7500 rpm for 10 minutes to pellet the nuclei. The supernatants

were stored at -80°C until usage. The nuclear pellet was suspended in Nuclear Lysis

Buffer (20 mM Hepes buffer pH 7.9, 0.25% glycerol, 0.42 M NaCl, 1.5 mM MgCl$_2$, 0.2

mM EDTA, 0.5 mM DTT, 0.5 mM PMSF, 5 μg mL^{-1} aprotonin, 5 μg mL^{-1} pepstatin A,

and 5 μg mL^{-1} leupeptin) and incubated on ice for a period of 60 minutes to ensure lysis

of the pellet. Nuclear proteins were collected following a spin at 10000 rpm and stored at

-80°C until usage.

2.3.5 NF-κB p65 subunit immunoblotting

4μg of nuclear protein was separated by electrophoresis on 7.5% gels and transferred

onto an Immobilon-P membrane (Millipore Corporation) using a wet transfer apparatus

(Bio-Rad, Ontario, Canada) running over night at 22 V. The p65 subunit of NF-κB was

detected using a polyclonal antibody that detects non-phosphorylated murine p65 subunit

(Santa Cruz) coupled with an anti-rabbit secondary antibody conjugated to peroxidase

(1/4000 dilution). Band visualization was performed using enhanced

chemiluminescence+ (ECL$^+$) substrate (Amersham Biosciences). Band densities were

detected using a phosphor imager (Amersham) and quantified using ImageQuant^{TM} 5.2

software.

2.3.6 Electrophoretic mobility shift assay (EMSA)

A double stranded oligonucleotide with high affinity for NF-κB binding (Santa Cruz,

USA) with a κB site (5'-GGG GAC TTT CCC-3') was utilized. A total of 2 μg of the NF-

κB oligonucleotide was end labelled using γ-[^{32}P]-ATP (Perkin and Elmer) using PNK

kinase (Fermentas). Binding reactions were performed in a 20 μL volume and were pre-incubated for a period of 15 – 20 minutes with the non-specific DNA competitor poly(dI-dC) prior to the addition of the specified oligonucleotides. Binding reactions contained 10 μg of nuclear extracts, 4 μL of 5× Binding Buffer (50 mM Tris, pH 7.6, containing 5 mM MgCl$_2$, 2.5 mM EDTA, 2.5 mM DTT, 250 mM NaCl, and 20% glycerol), 2 μg of poly(dI-dC), and 50000 cpm of the [^{32}P] labelled NF-κB oligonucleotide. Following a 30 minute incubation at room temperature, 2 μL of a 10× Loading Dye (250 mM Tris, pH 7.6, containing 0.2% bromophenol blue and 40% glycerol) was added to each reaction and the samples were then loaded onto a 5% – 0.4× TBE non-denaturing polyacrylamide gel (pre-run at 100V for an hour) in 0.4× TBE, pH 8.0, for ~ 2 hours. In cases of competition, a 20× in excess non-radioactive oligonucleotide was utilized (NF-κB for the specific competitions and AP-1 for the non-specific competitions) and was included in the reaction mixture. Gels were dried using a Bio-Rad gel dryer (Bio-Rad) and exposed to a phosphor storage screen for a period of 16 – 24 hours. Band densities were detected using a phosphor imager (Amersham) and quantified using ImageQuant™ 5.2 software.

2.3.7 RNA isolation and Northern blotting

Total RNA from confluent astrocyte cultures for the indicated treatments was isolated using the TriZol® method, and quality was determined using 260/280 nm ratios. 2.5 μg of total RNA was separated by electrophoresis on a 1.1% formaldehyde gel and transferred onto an immobolin–NY+ membrane (Millipore Corporation) overnight and fixed to the membrane by UV cross linking and heating for 1 hour at 65°C. Blots were prehybridized for 1 hour in 10mL of Sigma Perfecthyb™ Plus (Sigma-Aldrich Chemical Co.) after which the α-[^{32}P]-CTP (Perkin and Elmer) labelled probes (RmT Random Primer

45

Labelling kit, Stratagene) were added to a specific activity of 1×10^7 cpm. Blots were

exposed to a storage phosphor screen (Amersham Biosciences) for 16 hours and scanned

using a phospher imager (Amersham Biosciences). Bands were quantified using

ImageQuant 5.2™ software (Amersham Biosciences). Probes specific for rat IκBα and

TNFα were made using a TOPO TA Cloning® kit (Invitrogen) according to

manufacturer's instructions and based on the following primers: IκBα FWD 5′ CAT

GAA GAG AAG ACA CTG ACC ATG GAA 3′, IκBα REV 5′ TGG ATA GAG GCT

AAG TGT AGA CAC G 3′ [90], TNFα FWD 5′ TAC TGA ACT TCG GGG TGA TTG

GTC C 3′, and TNF α REV 5′ CAG CCT TGT CCC TTG AAG AGA ACC 3′ [107]. A

human GAPDH probe (obtained from Dr. C.J. Sinal, Dalhousie University) that cross-

reacts with rat GAPDH was utilized to determine equal loading.

2.3.8 MTT assay

Mitochondrial respiration, an indicator of cell viability, was assessed in astrocytes using

an MTT assay. The basis of this assay is to determine the mitochondrial dependent

reduction of 3-(4,5-dimethylthiazol-2-yl)-2,5-diphenyltetrazolium bromide

(MTT) into formazan, which can then be quantified colorimetrically [108]. Astrocytes

were grown in 96-well plates for one week in 10% FBS supplemented DMEM containing

1% antibiotic and antimycotic. On the day of the experiment, cells were incubated with

0.83 μg mL^{-1} of MTT for 2 hours at 37°C and 5% CO_2. Following the incubation period,

the culture medium was removed by blotting the 96-well plate on blotting paper and the

cells were solubilized with 100 μL of dimethylsulfoxide (DMSO). The amount of

formazan formed from MTT was quantified colorimetrically at a wavelength of 492 nm.

2.3.9 Statistical analysis

All data are reported as the mean ± the standard error of the mean. Multiple comparisons were made using the one-way or two-way analysis of variance (ANOVA) with statistical significance set at $p<0.05$ and assessed by the Bonferroni post-hoc analysis test.

2.4 Results

2.4.1 Isoproterenol and Clenbuterol prevent the LPS-induced downregulation of EROD activity

The incubation of astrocytes with LPS for a period of 24 hours caused a decrease in EROD activity (Figure 2.1). To examine the effects of beta adrenoceptor activation on EROD activity, astrocytes were incubated with 50 μg mL^{-1} LPS and either isoproterenol (a β_1/β_2 agonist) or clenbuterol (a specific β_2 agonist) (Figure 2.1). A 70% decrease in EROD activity was observed in cells treated with LPS compared to those treated with media. When either isoproterenol or clenbuterol were co-incubated with 50 μg mL^{-1} LPS, the loss in EROD activity in response to LPS was prevented. Incubation of astrocytes with isoproterenol alone caused a 20% increase in EROD activity while incubation with clenbuterol alone had no effect on EROD activity. The protective effects of isoproterenol and clenbuterol occurred independent of cell viability, since astrocytes treated with 50 μg mL^{-1} of LPS experienced a 21.9% ($\pm$ 3.0%) decrease in cell viability and the addition of isoproterenol or clenbuterol (10 nM) caused no further change in cell viability (18 $\pm$ 4.4% and 16 $\pm$ 8.0%, respectively). Both isoproterenol and clenbuterol alone had no effects on cell viability (4% increase ($\pm$ 10.8%) and 5% decrease ($\pm$ 10.6%), respectively). Similar effects were obtained with cells that were incubated with 10 μg mL^{-1} of LPS (Figure 2.2).

2.4.2 The isoproterenol and clenbuterol mediated protection of the LPS-induced downregulation in EROD activity is a β-adrenoceptor mediated process

The effect of 10nM propranolol on the isoproterenol and clenbuterol mediated protection in EROD activity in the presence of either 10 μg mL^{-1} or 50 μg mL^{-1} of LPS is shown in Figure 2.3. LPS (10 μg mL^{-1} or 50 μg mL^{-1}) reduced EROD activity by 50% and 70%,

(A)
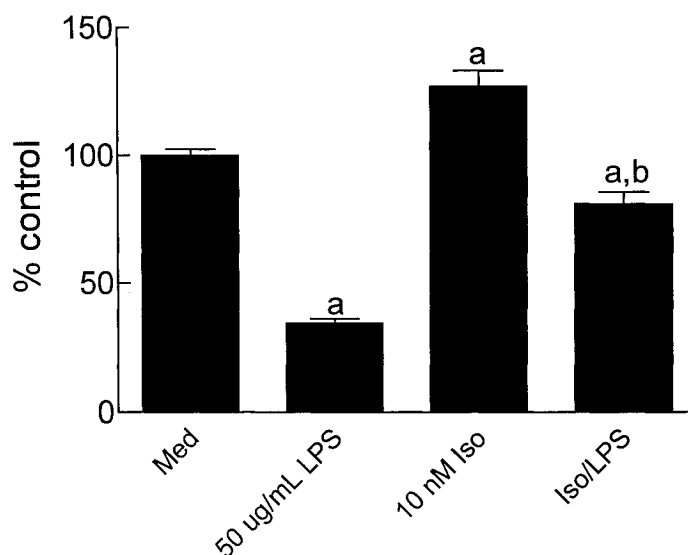
(B)
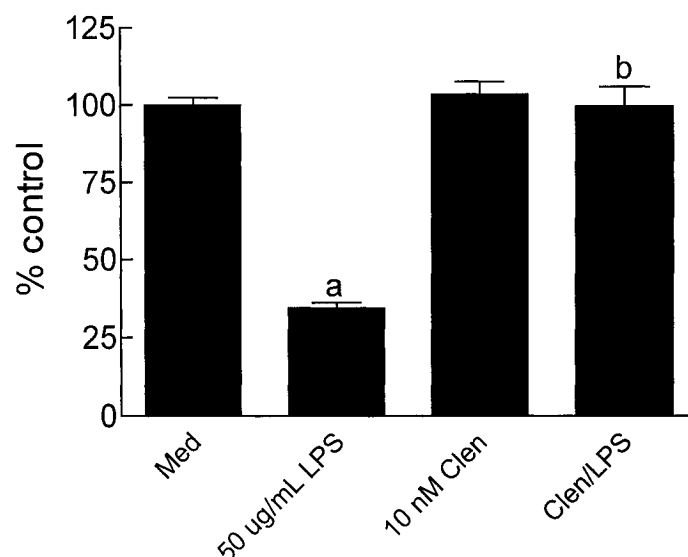
Figure 2.1. Isoproterenol and clenbuterol protect against the LPS-induced downregulation in CYP1A1/2 activity in astrocytes. Astrocytes were incubated with 50 μg mL^{-1} of LPS with or without 10 nM isoproterenol (Iso) (A) or 10 nM clenbuterol (Clen) (B). Following incubation, the media was removed and the cells were incubated with 0.6 μM ethoxyresorufin and activity was measured 2 hours later. Results are presented as % control of media only (med) treated samples and represent the averages of six separate experiments. Average EROD activity for media treated cells was 2.84 pmoles of resorufin per mg protein per minute, which was normalized to 100%. "a" statistically different compared to media treated cells (p < 0.05). "b" statistically different compared to LPS treated cells (p < 0.05).

(A)

(B)
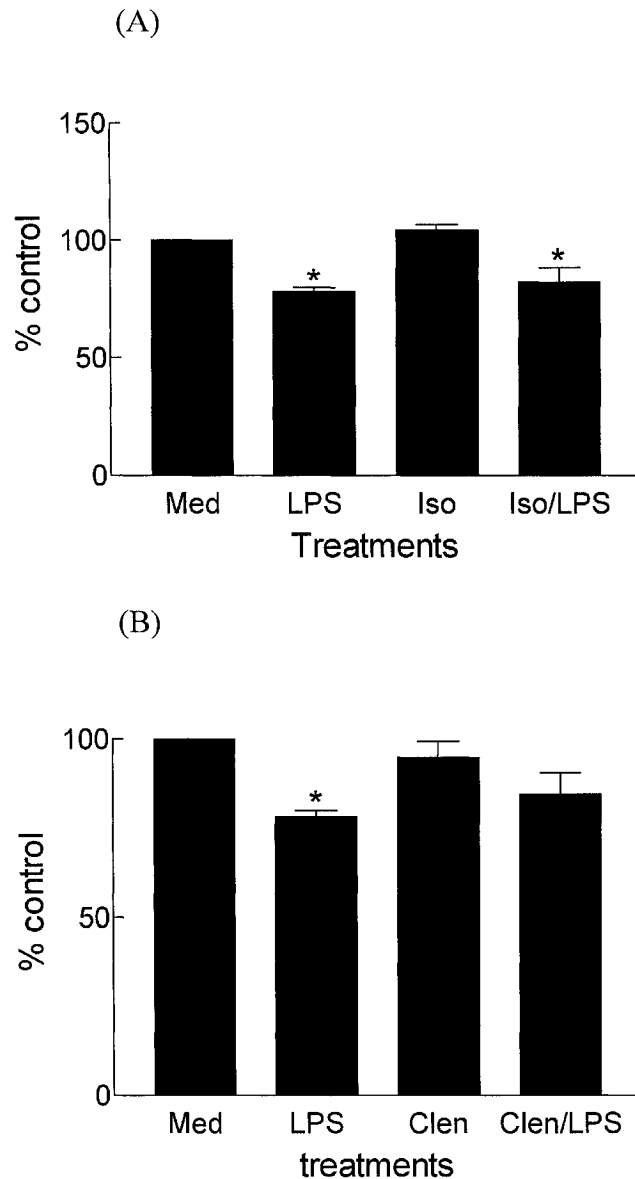
Figure 2.2. The isoproterenol and clenbuterol mediated protection against the LPS-induced downregulation in CYP1A1/2 activity in astrocytes occurs independent of cell viability. Astrocytes were incubated with 10 μg mL^{-1} of LPS with or without 10 nM isoproterenol (Iso) (A) or 10 nM clenbuterol (Clen) (B). Following incubation, the media was removed an MTT was performed as indicated in the methods section. Results are presented as % control of media only (med) treated samples and represent the averages of six separate experiments. "*" statistically different compared to media treated cells (p < 0.05).

50

respectively, compared to media treated cells. Both isoproterenol and clenbuterol abrogated the loss in EROD activity in astrocytes treated with 10 µg mL^{-1} or 50 µg mL^{-1} of LPS. Propranolol, a general beta adrenoceptor antagonist, was able to restore the ability of 10 µg mL^{-1} and 50 µg mL^{-1} of LPS to depress CYP1A activity in isoproterenol and clenbuterol treated cells. Propranolol alone had no effect on EROD activity.

2.4.3 The isoproterenol and clenbuterol mediated protection of EROD activity is a cAMP dependent process

To examine the effects of cAMP elevation on EROD activity, cells were treated with 50 µg mL^{-1} LPS concurrently with either 1 µM or 10 µM of forskolin. These doses of forskolin were previously shown to cause an elevation in cAMP levels in astrocytes [109]. EROD activity was reduced by 80% with the 50 µg mL^{-1} dose of LPS when compared to media treated cells (Figure 2.4). At a dose of 10 µM, forskolin caused a significant increase in EROD activity, however the 1 µM dose had no effect on EROD activity. In cells treated with either dose of forskolin, LPS was unable to depress EROD activity. Similar results were obtained when astrocytes were treated with 10 µg mL^{-1} of LPS and 10 µM of forskolin (Figure 2.4).

2.4.4 Isoproterenol and clenbuterol prevent the LPS-induced upregulation in TNFα expression

The expression levels of TNFα were significantly increased in astrocytes 3 hours following the treatment with 50 µg mL^{-1} of LPS (Figure 2.5). When astrocytes were administered either isoproterenol or clenbuterol alone, TNFα expression levels were unchanged compared to media treated cells. The expression levels of TNFα in astrocytes treated with isoproterenol and LPS were significantly lower compared to LPS only
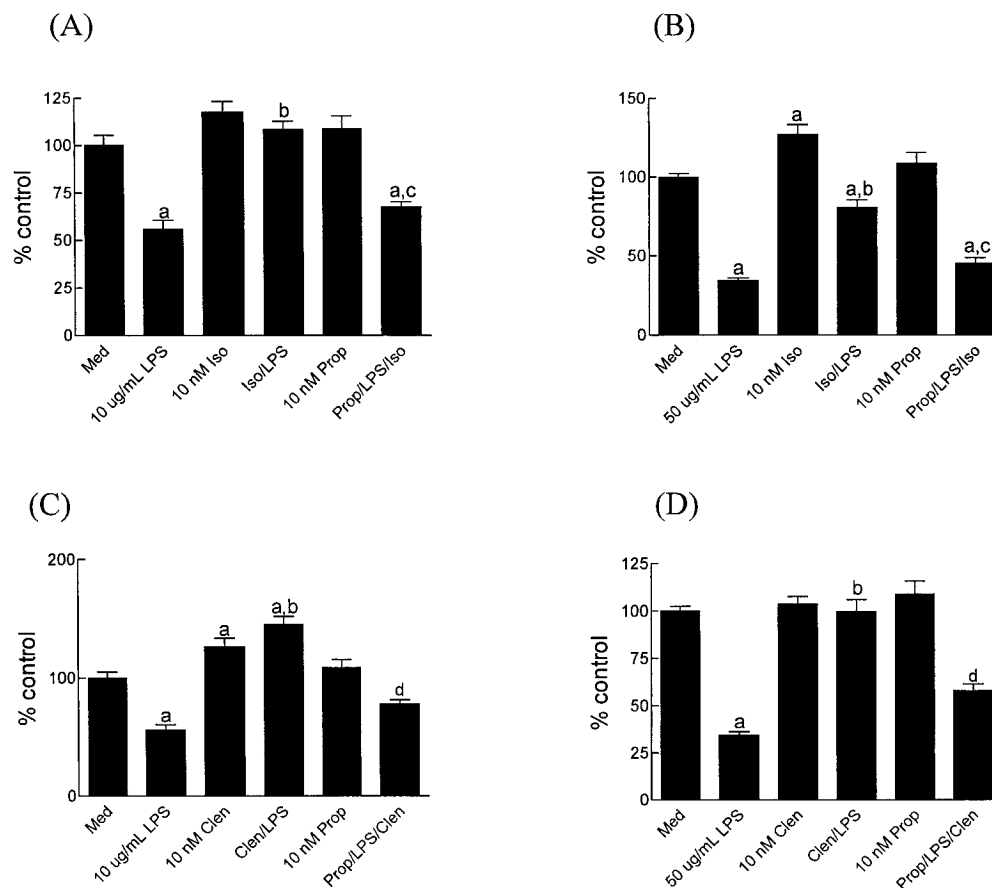
Figure 2.3. The protection in the LPS-induced downregulation in CYP1A1/2 activity by isoproterenol and clenbuterol in astrocytes is a beta-adrenergic receptor mediated effect. Astrocytes were incubated with 10nM of propranolol (Prop) and treated with (A) 10 nM isoproterenol (Iso) and 10 μg mL^{-1} LPS, (B) 10 nM isoproterenol and 50 μg mL^{-1} LPS, (C) 10 nM clenbuterol (Clen) and 10 μg mL^{-1} LPS, and (D) 10 nM clenbuterol and 50 μg mL^{-1} LPS. CYP1A1/2 activity was measured 24 hours later as described in materials and methods and results are presented as % control of media only (med) treated cells (average EROD activity was 6.109 pmoles of resorufin per mg protein per minute). "a" is statistically different compared to media treated cells ($p < 0.05$). "b" is statistically different compared to LPS treated cells ($p < 0.05$). "c" is statistically different compared to isoproterenol and LPS treated cells ($p < 0.05$). "d" is statistically different when compared to clenbuterol and LPS treated cells ($p < 0.05$).
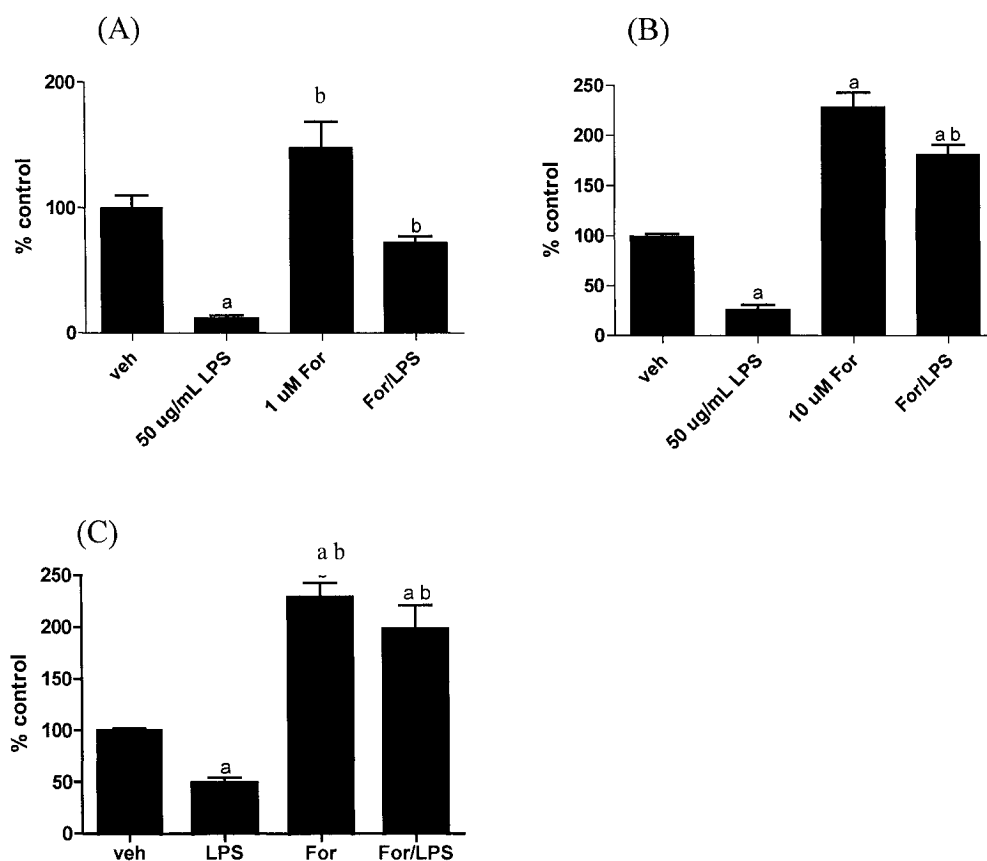
Figure 2.4. The isoproterenol and clenbuterol mediated protection in CYP1A1/2
activity following LPS stimulation in astrocytes occurs through increases in cAMP.
Astrocytes were incubated with 50 μg mL^{-1} of LPS and either 1 μM (A) or 10 μM (B)
forskolin (For) for a period of 24 hours. For panel (C), astrocytes were incubated with 10
μg mL^{-1} of LPS and 10 μM forskolin (For). EROD activity was then measured as
described in the materials and methods section. The mean values from three separate
experiments are shown for each treatment and are presented as % control of media (med)
treated cells only. The average EROD activity for media treated cells was 8.38 pmoles of
resorufin per mg protein per minute. "a" is statistically different compared to media
treated cells ($p < 0.05$). "b" is statistically different compared to LPS treated cells ($p <
0.05$).

53
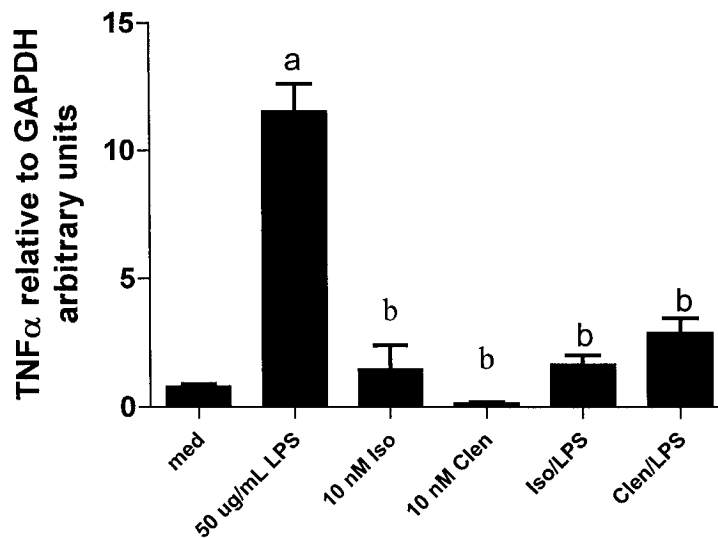
Figure 2.5. Isoproterenol and clenbuterol abrogate the LPS-induced upregulation in TNFα expression. Astrocytes were incubated with 50μg mL^{-1} of LPS and either 10 nM isoproterenol (Iso) or clenbuterol (Clen) for 3 hours. Total RNA was isolated using TriZol Reagent as described in the materials and methods section and 2.5 μg of RNA was electrophoresed and probed using both a TNFα and GAPDH probe. Blot quantification was performed as described in the Methods section, and the results represent the pooled data of 3 separate experiments performed 3 hours following drug addition. "a" is statistically different compared to media treated cells (p < 0.05). "b" is statistically different compared to LPS treated cells (p < 0.05).

treated cells (Figure 2.5). Similarly, the expression levels of TNFα in astrocytes treated

with clenbuterol and LPS were significantly lower compared to LPS only treated cells

(Figure 2.5).

2.4.5 Isoproterenol and clenbuterol do not exert their protective effect on the LPS-induced downregulation in EROD activity through direct changes in NF-κB activity

The effects of LPS on the translocation of the p65 NF-κB subunit was examined using a

specific p65 NF-κB subunit antibody. The levels of nuclear p65 appeared to be increased

by 74% and 51% at 1 hour and 2 hours, respectively, following the addition of LPS to

media (Figure 2.6). Incubating cells with isoproterenol or clenbuterol appeared to reduce

the LPS-mediated nuclear translocation of the p65 NF-κB subunit at 1 and 2 hours.

Isoproterenol (10 nM) and clenbuterol (10 nM) alone had a modest or no effect on

nuclear p65 translocation.

The effect of LPS on the DNA binding ability of NF-κB was assessed using

electromobility shift assays and changes in IκBα mRNA. Up to a 6-fold increase in NF-κB binding was observed in astrocytes incubated with 50 μg mL^{-1} LPS for a period of 1

hour compared to media treated cells. Isoproterenol and clenbuterol alone had no effects

on NF-κB binding. When given in combination with LPS, neither isoproterenol nor

clenbuterol were able to abrogate the LPS-induced upregulation in NF-κB binding

(Figure 2.7). IκBα mRNA levels were significantly increased (over 5 fold) 1 hour

following the addition of 50 μg mL^{-1} LPS to astrocytes (Figure 2.8A and C), but were not

affected by treatment with either isoproterenol or clenbuterol. The levels of IκBα mRNA

expression remained elevated 24 hours following the administration of 50 μg mL^{-1} LPS,

and were not affected by isoproterenol or clenbuterol (Figure 2.8B and D).

(A)

| 100% | 174% ± 56 | 132% ± 45 | 121% ± 48 | 122% ± 37 | 115% ± 46 |

+ve Ctrl   Med   LPS   Iso   Clen   Iso/LPS   Clen/LPS

(B)

| 100% | 151% ± 29 | 81% ± 38 | 84% ± 37 | 99% ± 22 | 108% ± 23 |

+ve Ctrl   Med   LPS   Iso   Clen   Iso/LPS   Clen/LPS
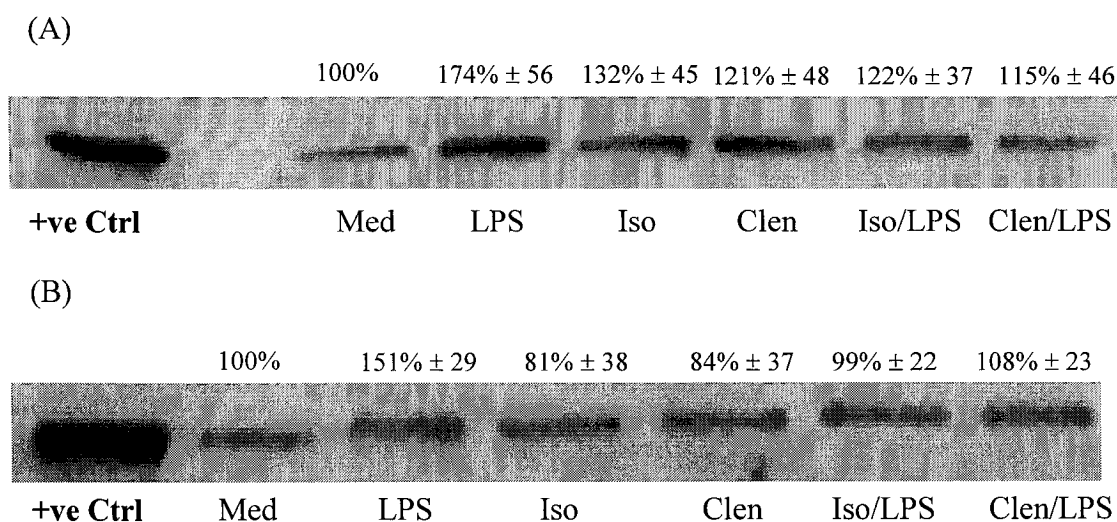
Figure 2.6. The protective effects of isoproterenol and clenbuterol on the LPS-induced downregulation in CYP1A1/2 activity occurs independent of changes in p65 translocation. Astrocytes were incubated with 50µg mL^{-1} of LPS and either 10 nM isoproterenol (Iso) or 10 nM clenbuterol (Clen) for either 1 or 2 hours. Nuclear and cytoplasmic fractions were prepared as described in the materials and methods section, electrophoresed and the p65 subunit determined using a specific antibody. The cytoplasmic fraction containing NF-κB was used as a positive control (+ve Ctrl). Representative blots for 1 hour samples (A) and 2 hour samples (B) are shown. The mean values from three separate experiments are shown for each treatment. Amido black staining was performed to ascertain equal protein loading. No treatments were statistically significant.

Figure 2.7. Isoproterenol and clenbuterol have no effect on the LPS-induced upregulation in NF-κB binding in astrocytes. Astrocytes were incubated with 50μg mL^{-1} of LPS and either (B) 10 nM isoproterenol (Iso) or (C) clenbuterol (Clen) for a period of 1 hour, following which nuclear fractions were prepared and binding reactions were performed as described in the materials and methods section. A representative blot is shown in (A), where solid line indicates specific binding and the dashed line indicates a non-specific binding. Specific comp and non-specific comp indicate competitions performed with excess non-radioactive NF-κB oligonucleotide and non-radioactive AP-1 oligonucleotide, respectively, as described in the materials and methods section. Lane 1 indicates probe only, lanes 2 and 3 refer to nuclear fractions obtained from media and LPS treated cells, respectively. Lanes 4 and 5 refer to nuclear samples obtained from isoproterenol and clenbuterol treated cells, respectively. Lanes 6 and 7 refer to nuclear fractions obtained from isoproterenol/LPS and clenbuterol/LPS treated samples. Finally, lane 8 refers to specific competition while lane 9 refers to the nonspecific competition. The plotted results in (B) and (C) represent the pooled data from 3 separate experiments.

(A)

(B)   (C)

Figure 2.7.

(A)   (B)

(C)

(D)
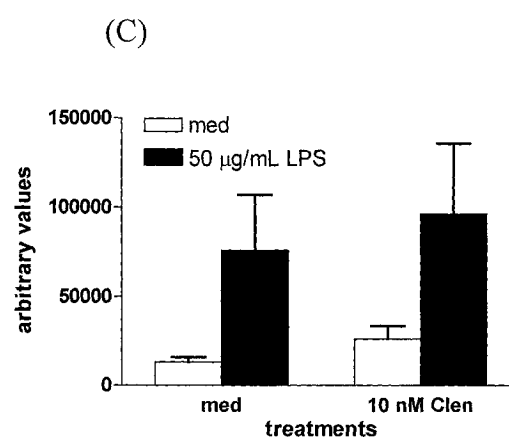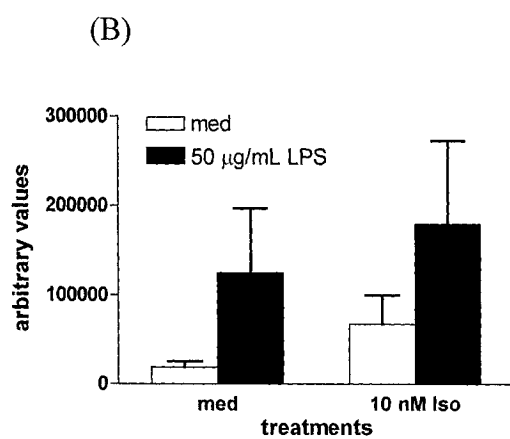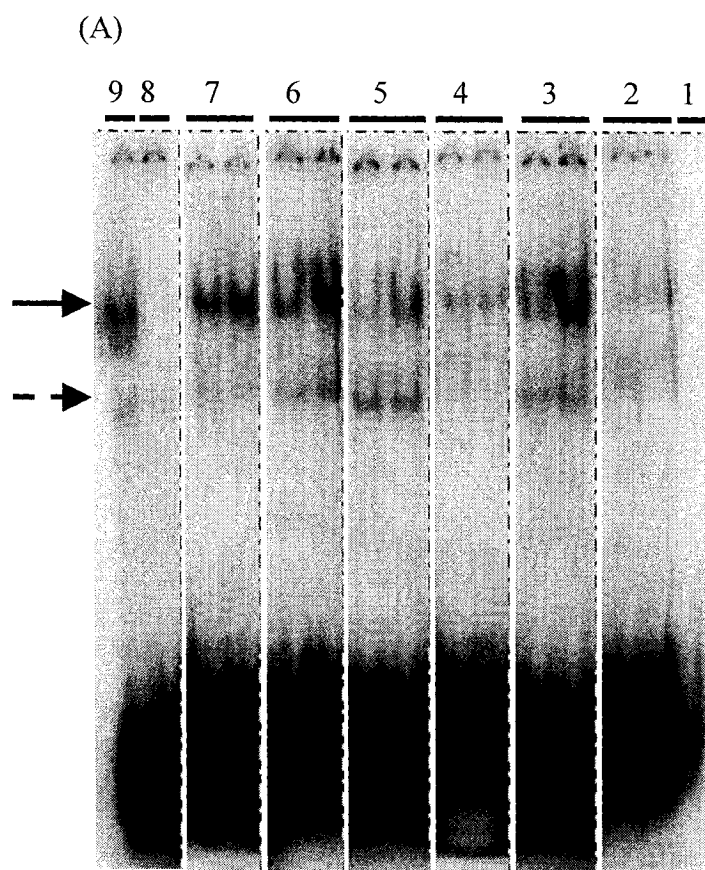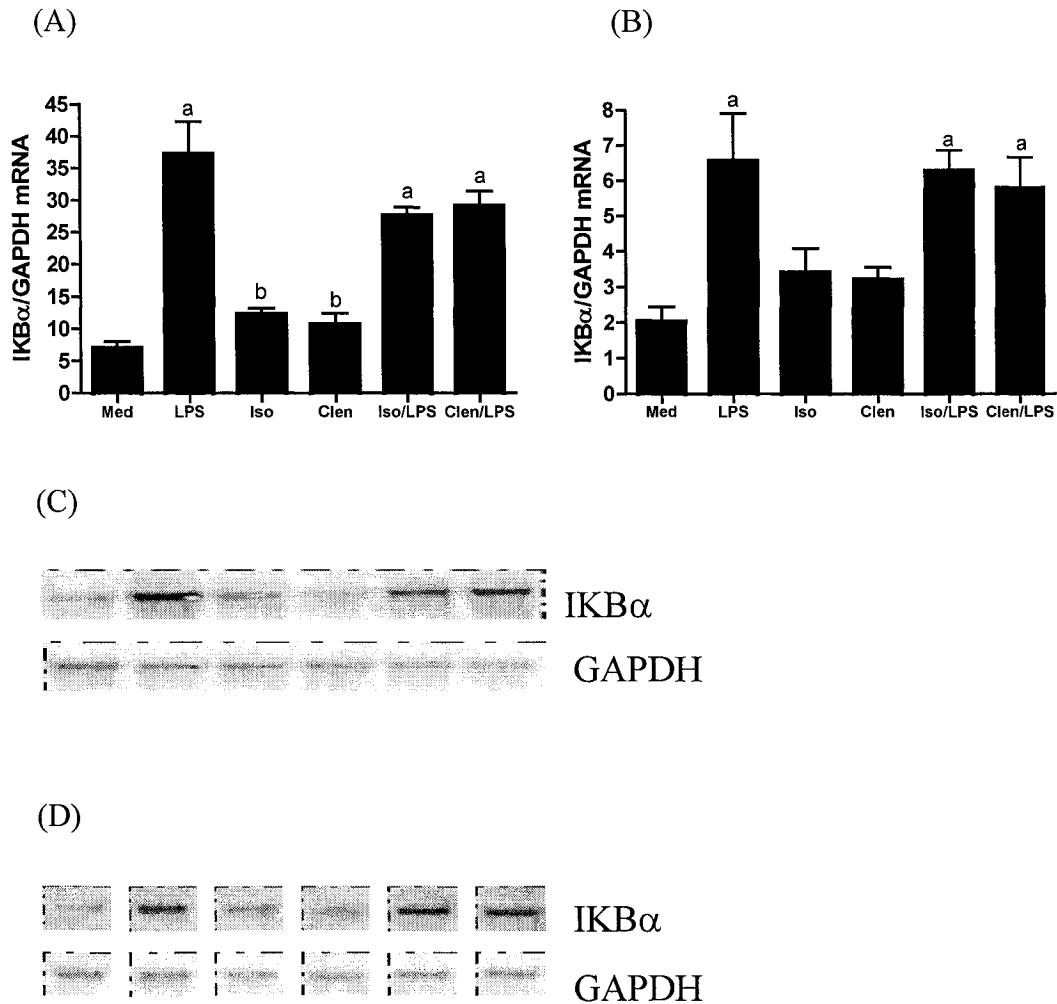
Figure 2.8. The effects of isoproterenol and clenbuterol on the LPS-induced upregulation of IκBα expression in astrocytes. Astrocytes were incubated with 50μg mL^{-1} of LPS and either 10 nM isoproterenol (Iso) or clenbuterol (Clen) for either 1 or 24 hours. Total RNA was isolated using TriZol Reagent as described in the materials and methods section and 2.5 μg of RNA was electrophoresed and probed using both an IκBα and GAPDH probe. Representative blots for the 1 hour samples (C) and the 24 hour samples (D) are shown. Blot quantification was performed as described in the Methods section, where (A) and (B) represent the pooled data of 3 separate experiments performed at 1 and 24 hours, respectively, following drug addition. "a" is statistically different compared to media treated cells (p < 0.05). "b" is statistically different compared to LPS treated cells (p < 0.05).

59

2.5 Discussion

During CNS inflammation, a wide variety of inflammatory mediators such as cytokines, prostaglandins, nitric oxide, and reactive oxygen species are released from activated microglia, the resident macrophages of the CNS [91]. Astrocytes are the major glial cells in the CNS and have an important physiological role in integrating neuronal inputs, neurotransmitter release, and the protection and repair of nervous tissue after damage [110]. We have previously shown that stimulation of astrocytes with lipopolysaccharide (LPS) causes a loss in cyt P450 activity that is accompanied by the production of an inflammatory response characterized by increased levels of cytokines and NO production [76, 77]. Pro-inflammatory cytokines such as TNFα, interleukin-1β (IL-1β), and interleukin-6 (IL-6), participate in the downregulation of several cyt P450 isoforms at the activity, protein, and mRNA levels in both peripheral and CNS models of inflammation [51, 64, 76, 87]. Previous work in our laboratory has provided evidence that TNFα, IL-1β, and interferon-γ (IFNγ) are capable of downregulating CYP1A activity in astrocytes [76].

In the present study, we show that the administration of the beta-adrenergic agonists isoproterenol and clenbuterol prevents the LPS-induced downregulation of CYP1A1/2 activity in astrocytes. Since the protective effect of these beta-adrenergic agonists was blocked by propranolol (a general β1/β2 antagonist), we conclude that beta-adrenergic receptor stimulation protects against the loss of CYP1A1/2 activity. To our knowledge, this is the first time an observation has been made linking CYP activity regulation through beta-adrenergic receptor stimulation during inflammatory conditions. Norepinephrine has been reported to be neuroprotective in astrocytes (which express both

β_1 and β_2 receptors) in various models of inflammation and neurotoxicity [102, 111]. The protection provided by beta-adrenergic receptor stimulation during the LPS-induced downregulation of CYP1A activity did not occur by the prevention of cell death, since MTT assays revealed a slight decrease in cell viability with 50 $\mu g\ mL^{-1}$ LPS that was not altered by either isoproterenol or clenbuterol.

The beta-adrenergic receptor is a seven-transmembrane protein coupled to a stimulatory G protein. Upon ligand binding, the $G\alpha$ subunit dissociates and activates adenylyl cyclase (AC), eventually leading to increases in intracellular cyclic AMP (cAMP) concentrations. The second messenger cAMP activates protein kinase A (PKA), leading to a multitude of effects such as the release of intracellular Ca^{2+} stores and phosphorylation of cAMP response element binding (CREB) protein [112]. To examine the effects of cAMP elevation on the LPS-induced downregulation in CYP1A activity, we co-incubated astrocytes with forskolin and LPS. Forskolin was able to completely prevent the LPS-induced downregulation in CYP1A activity. It has been shown that the phosphodiesterase (an enzyme involved in cAMP degradation) inhibitor, pentoxifylline, can protect against the LPS-induced downregulation in cyt P450 during models of systemic inflammation [113]. These observations, coupled with the fact that forskolin was able to abrogate the LPS-induced downregulation in CYP1A activity, indicate that the isoproterenol and clenbuterol mediated protection in CYP1A activity observed in this study is likely occurring through increases in intracellular cAMP.

The administration of LPS to astrocytes causes an increase in the release of pro-inflammatory cytokines such as TNFα and IL-1β [114] . We have previously shown that TNFα and IL-1β cause a downregulation in EROD activity in astrocytes [114]. Beta-

receptor agonists have been shown to modulate the LPS-induced release of these

cytokines from various immune cells [103], and therefore to examine whether the

isoproterenol and clenbuterol mediated effects observed in this study were mediated

through changes in TNFα, we examined the effects of these agents on the LPS induced

upregulation in the expression of this cytokine. Our results reveal that both isoproterenol

and clenbuterol were able to abrogate the LPS-induced increases in TNFα expression,

indicating a possible mechanism for the protective role of these two agents on CYP1A

activity in astrocytes. Norepinephrine has been shown to upregulate the expression of

PPARγ (peroxisome proliferator-activated receptor gamma), a nuclear hormone receptor

present in the CNS and adipose tissue [115]. Several PPARγ agonists have demonstrated

anti-inflammatory effects in immune cells and diseases [116, 117], and therefore it is

possible that the beta-adrenergic agonist mediated abrogation of the LPS-induced

upregulation in TNFα expression in astrocytes is occurring through an upregulation in

PPARγ.

We sought to examine the role of NF-κB in the beta-adrenergic mediated

protection observed in this study, since the anti-inflammatory effects of isoproterenol and

clenbuterol have been attributed to changes in NF-κB signalling [90]. NF-κB is a major

transcription factor responsible for the induction of pro-inflammatory genes and is

present in the cytoplasm as a dimer of different components of the Rel family of proteins

bound to and inhibited by IκBα [118]. There is a continuous shuttling of NF-κB bound to

IκBα between the cytoplasm and nucleus, however upon stimulation by LPS and TNFα,

proteosome-mediated degradation of IκBα occurs which allows the translocation of

NFκB into the nucleus to induce the transcription of numerous pro-inflammatory genes

[119]. LPS was only able to cause a slight upregulation in p65 translocation compared to media treated cells, since the antibody utilized in these experiments identifies non-active and non-phosphorylated p65. The incubation of astrocytes with isoproterenol or clenbuterol was not able to completely prevent this slight upregulation in p65 translocation that occurs one hour following the treatment of astrocytes with LPS. In order to ascertain the role of NF-κB on the β-adrenergic mediated protection in CYP1A activity, we performed electromobility shift assays (EMSAs) and northern blot analyses to examine the DNA binding capacity of NF-κB and changes in IκBα mRNA, respectively. The EMSAs indicated that the LPS-mediated increase in NF-κB binding was not altered by isoproterenol or clenbuterol. We observed an increase in IκBα mRNA, and since it is known that the IκBα promoter contains several κB response elements [120], this result strengthens our observations of increased nuclear NF-κB translocation following LPS stimulation. Both β-adrenergic receptor agonists were not able to abrogate the LPS-induced increase in IκBα mRNA levels, however both agents had a tendancy to reduce the LPS-induced upregulation in IκBα mRNA 1 hour following treatment. The LPS-induced upregulation in TNFα expression at 3 hours observed in this study could still lead to an upregulation in NF-κB. Therefore the ability of isoproterenol and clenbuterol to abrogate the LPS-induced upregulation in TNFα expression could indicate that the beta-adrenergic receptor mediated protection in CYP1A activity observed in this study could still be occurring through changes in NF-κB activity at later time points.

In conclusion, we have shown that the loss of CYP1A1/2 activity in astrocytes can be minimized by beta-adrenergic receptor stimulation in an *in vitro* model of CNS inflammation. We also provide evidence that increases in intracellular levels of cAMP

63

and changes in TNFα expression likely play a role in mediating this beta-adrenergic

effect. In addition, we provide evidence that this β-adrenergic effect occurs independent

of direct changes in NF-κB activity induced by LPS. The results of this study support the

idea that beta-adrenoceptor stimulation during conditions of CNS inflammation may be

protective against a reduction in the drug-metabolizing capacity of the brain.

CHAPTER 3

THE PATHWAYS INVOLVED IN CYTOCHROME P450 REGULATION IN THE LIVER DURING LPS-INDUCED CNS INFLAMMATION

Sections not done by PhD candidate:

Figure 3.9 panels B and D and Figure 3.10 panels B and D were taken from experimental results performed by Elena Garcia Del Busto, who was a research assistant in Kenneth W. Renton's laboratory for the period 2000 – 2002.

Portions of this chapter appeared in the following publication:

Abdulla D, Goralski KB, Garcia Del Busto Cano E, Renton KW. (2005) *The signal transduction pathways involved in hepatic cytochrome P450 regulation in the rat during an LPS-induced model of CNS inflammation*. Drug Metabolism and Disposition. 33 (10): 1521-31. Epub 2005 Jul 8.

3.1 Abstract

It is well known that inflammatory and infectious conditions of the central nervous system (CNS) differentially regulate hepatic drug metabolism through changes in cytochrome P450 (CYP), however the pathways leading to this regulation remain unknown. We provide evidence delineating a signal transduction pathway for hepatic CYP gene expression downregulation in an established rat model of CNS inflammation using lipopolysaccharide (LPS) injected directly into the lateral cerebral ventricle (i.c.v.). Brain cytokine levels were elevated and the expression of TNFα and IκBα were increased in the liver following the i.c.v. administration of LPS, indicating the presence of an inflammatory response in the brain and liver. The expression of CYP2D1/5, CYP2B1/2, and CYP1A1 was downregulated following CNS inflammation. The binding of several transcription factors (NF-κB, AP-1, CREB, C/EBP) to responsive elements on CYP promoter regions was examined using electromobility shift assays. Binding of both NF-κB and C/EBP to the promoter regions of CYP2D5 and CYP2B1, respectively, was increased, indicating that they play an important role in the regulation of these two isoforms during inflammatory responses. Evidence is also provided suggesting that the rapid transfer of LPS from the CNS into the periphery likely accounts for the downregulation of CYPs in the liver.

3.2 Introduction

Cytochrome P450 constitutes a superfamily of heme containing enzymes that are well known for their role in the metabolism and elimination of various exogenous and endogenous substances [44, 66]. In addition to metabolism, CYP isoforms play a major role in many biochemical and physiological pathways such as the biosynthesis and/or degradation of steroid hormones and fatty acids [44]. Changes in the levels of CYP isoforms may contribute to the development of cancer, Parkinson's disease, and adrenal hyperplasia [44]. The majority of the CYP isoforms are found in the liver, however other extra-hepatic sites of CYP localization include the CNS, gastrointestinal tract, kidney, lungs, and adrenal glands [85].

3.2.1 Effects of inflammation on cytochrome P450

The effects of host defence and immune stimulation on CYP isoforms have been well documented [66, 69]. Both viral and bacterial inflammatory conditions can lead to differential regulation of hepatic CYP isoforms [75, 114]. Cytokines are known to play a dominant role in this regulation; IFNγ, IL-1β, IL-6, and TNFα have been shown to downregulate hepatic CYP1A1, CYP1A2, CYP2B1/2, and CYP3A1/2 in rat models of systemic inflammation when given alone or in combination [64, 66, 69, 76, 87, 121, 122]. The injection of immunostimulants directly into the CNS produces a highly regulated inflammatory response characterized by the production of cytokines, immune cell infiltration, and tissue damage [66, 76, 77, 90, 91]. We have previously demonstrated that the catalytic activity of both hepatic and CNS CYP isoforms are downregulated in rat models of CNS inflammation/infection [75, 114, 123]. A reduction in brain CYP metabolism may exacerbate susceptibility to neurotoxic agents such as 1-methyl-4-

phenylpyridinium [93]. A loss or reduction in hepatic CYP levels has direct

consequences for reduced metabolism of therapeutic agents [44, 66]. The pathways

directly causing the downregulation of CYP isoforms following conditions of CNS

inflammation are not completely understood, however multiple mechanisms are

implicated.

3.2.2 Objective

Our objective was to determine the signal transduction mechanisms that contribute to

hepatic CYP regulation in a rat model of LPS-induced CNS inflammation. To perform

that, we examined the regulation of hepatic CYP gene expression following the

intracerebroventricular (i.c.v.) administration of LPS, a well known and utilized model of

CNS inflammation/infection [72, 75, 124]. Our major findings are that several hepatic

transcription factors play a vital role in CYP gene regulation during conditions of CNS

inflammation and that LPS is rapidly transferred from the CNS into the periphery where

it likely contributes to the effects observed in this rodent model of CNS inflammation.

3.3 Methods

3.3.1 Reagents

All laboratory reagents were purchased from Sigma (St. Louis, MO) with the exceptions noted in the text. Gel purified *Escherichia coli* lipopolysaccharide (LPS) of sereotype 0127:B8 (Sigma, St Lois, USA) was utilized in the experiments as outlined below.

3.3.2 Animals and treatments

Male Sprague-Dawley rats (125 – 150 grams) were obtained from Charles River Laboratories (Quebec, Canada) and were housed on corncob bedding for a period of 5 days on a 12-hour light/dark cycle. All animal procedures were performed according to the Dalhousie University Committee on Laboratory Animals following the guidelines established by the Canadian Council on Animal Care. Rats were allowed *ad-libitum* access to food and water prior to and following the experimental procedure. On the day of the experiment, rats were anaesthetized using enflurane and maintained on a 4% level of the anaesthetic during the surgery. Intracerebroventricular (i.c.v.) injections into the lateral ventricle were performed using a KOPF sterotaxic instrument. The coordinates utilized relative to bregma were 1.7 mm lateral and 4.7 mm below the skull surface. A dose of 25 μg LPS was dissolved in pyrogen-free saline and injected in a volume of 5 μL. In a separate set of experiments, rats were injected intravenously (i.v.) through the tail vein with 25 μg LPS dissolved in 100 μL of saline and tissue samples obtained at either 3, 6, or 24 hours following injection. Some experiments required intraperitoneal injection of rats with 25 μg LPS dissolved in 100 μL of saline. All experiments utilized 4 – 6 male rats per treatment. For the cytokine experiments, animals received a cytokine cocktail containing 100 ng TNFα, 50 ng IL-1β, 45 ng IL-1α, 50 ng IL-6, and 50 ng IFNγ (all

cytokines obtained from CedarLane Laboratories Ltd, Ontario, Canada) made in 0.1 %

sterile filtered BSA. For the cytokine inhibitor experiments, rats received 25 µg of LPS

i.c.v. in combination with one of the following treatments: the TNFα soluble antibody

etanercept (Enbrel™, Immunex, Wyeth-Ayerst, Canada) administered either i.p. (25 mg

kg^{-1}) or i.c.v. (40 µg) or the IL-1 inhibitor YVAD (Alexis Biochemicals, California,

USA) administered i.c.v. (0.63 µg). Doses for the cytokine cocktail and the cytokine

inhibitor experiments were selected based on results from previous dose response curves

(data not shown).

3.3.3 Tissue isolation, microsomal fraction preparation, and microsomal metabolism assays

At 2, 4, 6, and 9 hours following the i.c.v. injection of either saline or LPS, rats were

anaesthetized with enflurane, decapitated, and liver (~100 mg) for RNA isolation was

obtained, serum collected, and whole brain homogenates for cytokine measurement was

obtained. For the i.v. experiments, total liver RNA was isolated at 3 and 6 hours

following treatment. Liver microsomal fractions were obtained at 24 hours following

either the i.v. or i.c.v. injection of LPS as described previously [75]. Briefly, whole rat

livers were rinsed in ice-cold 1.15% KCl and homogenized using a motor driven polytron

homogenizer in 20 mL of ice-cold 1.15% KCl. The homogenate was then centrifuged at a

speed of 9000 rpm for 10 min at 4°C, and the supernatant was centrifuged at a speed of

40,000 rpm also at 4°C to obtain the microsomal fraction. Liver microsomes were

suspended in a glycerol-phosphate buffer (50 mM KH_2PO_4 buffer, pH 7.4, containing

20% glycerol and 0.4% KCl) and were aliquoted and stored at −80°C until usage. Total

protein concentrations were determined according to a modified Lowry protocol [105].

Microsomal samples were diluted 1:100 and a 5× volume of Mix A (0.97% $NaCO_3$ in 0.1 M NaOH, 0.02% sodium potassium tartarate, and 0.01% $CuSO_4$) was added to the samples, which were then incubated at room temperature for 10 minutes. Following this incubation, a 0.5× volume of phenol mixture (1:1 dilution with water) was added to the samples and the incubation was carried on for a further 30 minutes. Sample absorbances were then determined at 700 nm using a plate reader (BioTek Instruments) and protein amounts were determined based on a protein bovine serum albumin (BSA) standard curve. The activity of CYP1A1/2 and CYP2B1/2 were determined using the 7-Ethoxyresorufin O-dealkylase (EROD) assay and the Pentoxyresorufin O-dealkylase (PROD) assay, respectively, as described by Burke *et al* [125]. A total of 1 mg of microsomal protein was incubated in 0.1 M KH_2PO_4 (pH 7.4) with 0.5 µM of either ethoxyresorufin or pentoxyresorufin at 37°C for 2 minutes for CYP1A and CYP2B assays, respectively. In both incubations, the reaction was initiated by the addition of 10 µL of 25 µM NADPH and the amount of fluorescent resorufin forming was monitored every 30 seconds over a 3-minute time period. The excitation and emission wavelengths for the CYP1A assay were 510 and 586 nm, respectively. For the CYP2B assay, the excitation and emission wavelengths were 530 and 586 nm, respectively. Total P450 values were determined according to the method of Omura and Sato [126]. Liver microsomes were diluted to a final concentration of 1 mg mL^{-1} using 1.15 % KCl and 1 mL of 1 M KH_2PO_4 buffer and reduced using sodium dithionite. The absorbance spectrum was measured before and after the bubbling of the samples with CO (for ~25 seconds) and the absorbance difference spectrum (450/490 nm) was quantified using a Beckman DU-70 spectrometer. P450 content is reported as nmoles/mg protein.

3.3.4 RNA extraction and northern blot analysis

Total liver RNA was extracted using the TriZol® method according to manufacturer's instructions and quality was determined using 260/280 nm ratios. 10 μg of total RNA was electrophoresed on a 1.1% formaldehyde gel and transferred onto an immobolin–NY+ membrane (Millipore Corporation, MA, USA) overnight and fixed to the membrane by UV cross linking and heating for 1 hour at 65°C. Blots were prehybridized for 1 hour in 10 mL of Sigma Perfecthyb™ Plus (Sigma, St Lois, MS) after which the $[^{32}P]dCTP$ (Perkin and Elmer, Canada) labelled probes (RmT Random Primer Labelling kit, Stratagene, USA) were added to a specific activity of 1×10^7 cpm. Blots were exposed to a storage phosphor screen (Amersham Biosciences, NJ, USA) for 16 – 24 hours and scanned using a phospher imager (Amersham Biosciences, NJ, USA). Bands were quantified using ImageQuant 5.2™ software (Amersham Biosciences, NJ, USA). CYP2D1/5 [127], TNFα [107], and IκBα [90] probes were constructed from forward and reverse primers (CYP2D1/5 FWD 5′ ATC GCT GGA CTT CTC GCT AC 3′, CYP2D1/5 REV 5′ GTC TTC TGA CCT TGG AAG AC 3′, TNFα FWD 5′ TAC TGA ACT TCG GGG TGA TTG GTC C 3′, TNFα REV 5′ CAG CCT TGT CCC TTG AAG AGA ACC 3′, IκBα FWD 5′ CAT GAA GAG AAG ACA CTG ACC ATG GAA 3′, IκBα REV 5′ TGG ATA GAG GCT AAG TGT AGA CAC G 3′) using a TOPO TA Cloning® kit (Invitrogen, Ontario, Canada) according to manufacturer's instructions. CYP2B1/2, MAPKK, and GAPDH probes were a generous gift from Dr. C. J. Sinal (Dalhousie University, Canada).

3.3.5 Real-time quantitative PCR

A total of 5 μg of liver RNA was reverse transcribed in a 25 μL reaction containing 62.5 nM random primers, 20 Units of RNaseOUT (Invitrogen, Ontario, Canada), 1× StrataScript® RT-buffer and 12.5 Units of StrataScript® Reverse Transcriptase (both Stratagene, California, USA) according to the instructions provided with the Reverse Transcriptase enzyme. Real-time quantitative PCR was performed using an MX3000P™ instrument (Stratagene, California, USA) in a total volume of 20 μL. Reactions contained 10 μL of 2× Brilliant® SYBR® Green QPCR mix (Stratagene, California, USA), 62.5 ng of both forward and reverse primers, and 25 nM of reference dye. Cycle parameters consisted of an initial 10 minute denaturation step at 95°C followed by either 35 cycles for GAPDH or 45 cycles for CYP1A1 as follows: 30 second denaturation at 95°C, 18 seconds annealing at 60°C, and 30 seconds extension at 72°C. Dissociation curves were also performed to verify the amplicon being amplified. Primers specific for CYP1A1 and GAPDH were specifically designed using the published sequence for rat CYP1A1 (Accession number X00469) and rat GAPDH (Accession number X02231) as follows: CYP1A1 FWD 5′ GGA GCT GGG TTT GAC ACA AT 3′, CYP1A1 REV 5′ GAT AGG GCA GCT GAG GTC TG 3′ (amplicon size 157 bp), GAPDH FWD 5′ AGA CAG CCG CAT CTT CTT GT 3′, GAPDH REV 5′ CTT GCC GTG GGT AGA GTC AT 3′ (amplicon size 207 bp). Data was analysed using the $2^{-\Delta\Delta C_T}$ method [128], where the cycle threshold (C_T) values for CYP1A1 and GAPDH were ~ 32 and ~19, respectively.

3.3.6 Cytokine measurements

Whole brain was obtained following the i.c.v. injection of LPS at 2, 4, 6, and 9 hours and homogenized in 2 mL of phosphate buffer saline, pH 7.4. The homogenates were spun at

13,000 rpm for 10 minutes at 4°C and the supernatant was stored at –80°C until used for cytokine measurements. Protein levels in the brain homogenates were determined using a modified Lowry method [105]. Levels of TNFα and IL-1β in the brain were measured using a sandwich ELISA (R&D systems, Minneapolis, USA) and results are reported as pg of cytokine per mg of protein present in the brain homogenate. The limits of detection for both TNFα and IL-1β cytokine ELISA assays was 5 pg mL^{-1}.

3.3.7 Nitrite measurement

The total amount of NO in plasma was indirectly determined by measuring total nitrites and nitrates (end products of NO oxidation) using a NO assay kit (Cayman Chemical, Ann Arbour, Michigan, USA) according to manufacturer's instructions. The kit involved converting nitrates into nitrites and then measuring the converted products using Griess Reagent. Nitrite accumulation was determined in a 96-well plate format with the absorbances determined at 540nm. The limit of detection for this assay was 2.5 μM.

3.3.8 Determination of endotoxin levels

LPS concentrations were determined in serum at 15 minutes, 30 minutes, 2 hours, 4 hours, 6 hours, 15 hours, and 24 hours following the administration of LPS by either the i.c.v. or i.p. route. Rats were injected with 25 μg of LPS either i.c.v (in 5 μL of pyrogen-free saline) or i.p. (in 100 μL of pyrogen-free saline). Following decapitation, trunk blood was collected and allowed to clot for 1 hour at room temperature and 1 hour on ice, and serum was obtained following a 10-minute spin at 3000 rpm, and stored at –80°C until usage. All groups were compared to non-injected rats. LPS levels were determined per manufacturer's instructions from a commercially available kinetic assay kit based on ChromoLAL as a substrate (Associates of Cape Cod, MA, USA). The assay was linear

from 0.0395 pg mL^{-1} to 100 ng mL^{-1} of LPS. The levels of endotoxin in the saline used to resuspend LPS were below the limit of detection of the assay, indicating that samples preparation was sufficiently aseptic for endotoxin detection.

3.3.9 Liver nuclear fraction isolation

Liver nuclear fractions were isolated from rats 1 and 3 hours following the i.c.v. injection of LPS according to a previously described method [129]. Briefly, animals were decapitated and livers were homogenized in 20 mL of Homogenization Buffer (100 mM HEPES, pH 7.4, containing 25 mM KCl, 0.15 mM spermine, 0.5 mM spermidine, 1 mM EDTA, 2 M sucrose, 10% glycerol, 5 μg mL^{-1} pepstatin A, and 5 μg mL^{-1} leupeptin) and centrifuged at 17,000 rpm for a period of 20 minutes at 4°C. The nuclear pellet was resuspended in 10 mL of Nuclear Lysis Buffer (100 mM HEPES, pH 7.4, containing 100 mM KCl, 3 mM MgCl$_2$, 0.1 mM EDTA, 1 mM DTT, 0.1 mM PMSF, 10% glycerol, 5 μg mL^{-1} pepstatin A, and 5 μg mL^{-1} leupeptin) and homogenized using a Dounce homogenizer. The extraction was initialized by the addition of (NH$_4$)$_2$SO$_4$ to the nuclear lysate in drop-wise fashion to a final concentration of 0.4 M. The viscous lysates were incubated for period of 30 minutes on ice with constant shaking, after which they were ultra-centrifuged at 35,000 rpm for a period of 60 minutes at 4°C. Solid (NH$_4$)$_2$SO$_4$ was added to the supernatants at a concentration of 0.3 g mL^{-1}. The solutions were inverted several times and incubated on ice for a period of 20 minutes until all the (NH$_4$)$_2$SO$_4$ had dissolved. The solutions were then further centrifuged at 35,000 rpm for a period of 25 minutes at 4°C and the pellets were re-suspended in Suspension Buffer (25 mM HEPES, pH 7.6, containing 40 mM KCl, 0.1 mM EDTA, 1 mM DTT, 10% glycerol, 5 μg mL^{-1}

75

pepstatin A, and 5 μg mL^{-1} leupeptin) and stored at −80°C until usage. Total protein

concentrations were determined according to a modified Lowry protocol [105].

3.3.10 Electromobility shift assays

Reactions were carried out in a total volume of 20 μL and contained 5 μg of protein,

50000 cpm of [^{32}P]-labeled probes, Binding Buffer (50 mM Tris-HcL, pH 7.9 containing

5 mM MgCl2, 2.5 mM EDTA, 2.5 mM DTT, 250 mM NaCl, and 20% glycerol), and 2

μg of polydIdC. Reactions were pre-incubated with the polydIdC for a period of 15

minutes after which the radiolabeled probe was added to initiate the reaction. In cases of

specific competitions, a 20× excess amount of non-radioactive self oligonucleotide was

utilized and was included in the reaction mixture. Reactions were incubated at room

temperature for a period of 30 minutes and run on a 5% TBE-acrylamide gel at a voltage

of 170 V. In the case of non-specific competitions, a 20× excess amount of non-

radioactive non-self oligonucleotide was utilized in the reaction mixture. For supershift

reactions, the reaction mixture was incubated with either a p65 antibody (Santa Cruz,

California, USA) or a C/EBPα antibody (generous gift from Dr. M. W. Nachtigal) for a

30-minute period following the addition of the radioactive specific probe. The gels were

then dried using a Bio-Rad gel dryer (Bio-Rad, Ontario, Canada) operating under vacuum

and set at 80°C for 105 minutes. Gels were then exposed to a phospher-storage screen for

a period of 16 – 24 hours and scanned using a phospher imager (Amersham Biosciences,

NJ, USA). Bands were quantified using ImageQuant 5.2™ software (Amersham

Biosciences, NJ, USA). The probes (described in Table 1) were either obtained

commercially from Santa Cruz or as single-stranded oligonucleotides from Sigma

Genosys (Sigma-Aldrich, Ontario, Canada) and annealed according to a standard

protocol. Briefly, 300 pmoles of each oligonucleotide were incubated in Annealing

Buffer (100 mM Tris, pH 7.9 and 50 mM $MgCl_2$) for 10 minutes at 95°C and allowed to

gradually cool down to 25°C.

3.3.11 Statistical analysis

All data are reported as the mean ± the standard error of the mean. Each time point

constituted a separate experiment in which LPS treatment was compared to saline and

was carried out on a different day, and therefore an unpaired t-test was utilized to

compare saline versus LPS groups, where $p < 0.05$ determined statistical significance.

Data is presented in one graph for all time points for convenience in illustrating the data.

Table 3.1 – List of EMSA oligonucleotides utilised

The underlined portion of each oligonucleotide in the last four rows refers to the response element for the transcription factor being observed.

Description	Oligonucleotide	Source
NF-κB	5' AGT TGA GGG GAC TTT CCC AGG 3'	Santa Cruz
AP-1	5' CGC TTG ATG ACT CAG CCG GAA 3'	Santa Cruz
CREB	5' AGA GAT TGC CTG ACG TCA GAG AGC TAG 3'	Santa Cruz
CYP2D5 NF-κB	–654 5' CCA ACG T<u>AG GGA CTT</u> <u>CCC A</u>AG ATC CT 3' –680	Single Stranded oligonucleotides annealed according to standard procedure
CYP1A1 NF-κB	–746 5'GC<u>G AGA GGA ATC TCC</u> <u>C</u>AG GC 3' –726	Single Stranded oligonucleotides annealed according to standard procedure
CYP2B1 NF-κB	–888 5'CCA GGG GT<u>G GAA TTT</u> <u>CCC</u> ACA GT 3' –879	Single Stranded oligonucleotides annealed according to standard procedure
CYP2B1 C/EBP	–67 5' ACA TGT <u>GAA GTT GCA</u> <u>TAA</u> CTG AGT 3' –45	Single Stranded oligonucleotides annealed according to standard procedure

78

3.4 Results

3.4.1 The intracerebroventricular injection of LPS initiates an inflammatory response in the brain and liver

Levels of TNFα and IL-1β proteins were increased in the brains of animals at 2, 4, and 6 hours following the i.c.v. administration of LPS as compared to saline control rats (Figure 3.1A and B). These data indicate that a CNS inflammatory response occurs in response to the i.c.v administration of LPS.

The liver is considered as the major target organ of the acute phase response [81] and therefore we measured the expression of various important acute phase proteins in that organ. IκBα expression levels in the liver were increased at 2, 4, 6, and 9 hours following the induction of CNS inflammation (Figure 3.2A). MAPKK expression levels in livers of rats treated with LPS i.c.v. were significantly increased by 3.4 fold and 3.7 fold at 4 and 6 hours, respectively, following the i.c.v. administration of LPS (Figure 3.2B). The expression of TNFα in the liver was significantly increased following LPS i.c.v. at 2, and 6 hours compared to saline i.c.v. administration (Figure 3.2C). These results indicate the activation of hepatic acute phase signalling proteins in this rat model of LPS-induced CNS inflammation.

We have previously reported increased amounts of cytokines in the serum of rats treated with LPS i.c.v. compared to saline-injected controls [114]. Since the elevation of nitrites/nitrates is also associated with inflammation, we examined nitric oxide levels in the plasma of animals treated with LPS i.c.v. compared to saline. The levels of total nitrates and nitrites increased at 4, 6, and 9 hours and were 19 fold higher than saline treated rats 15 hours following LPS administration (Figure 3.3).

(A)

(B)
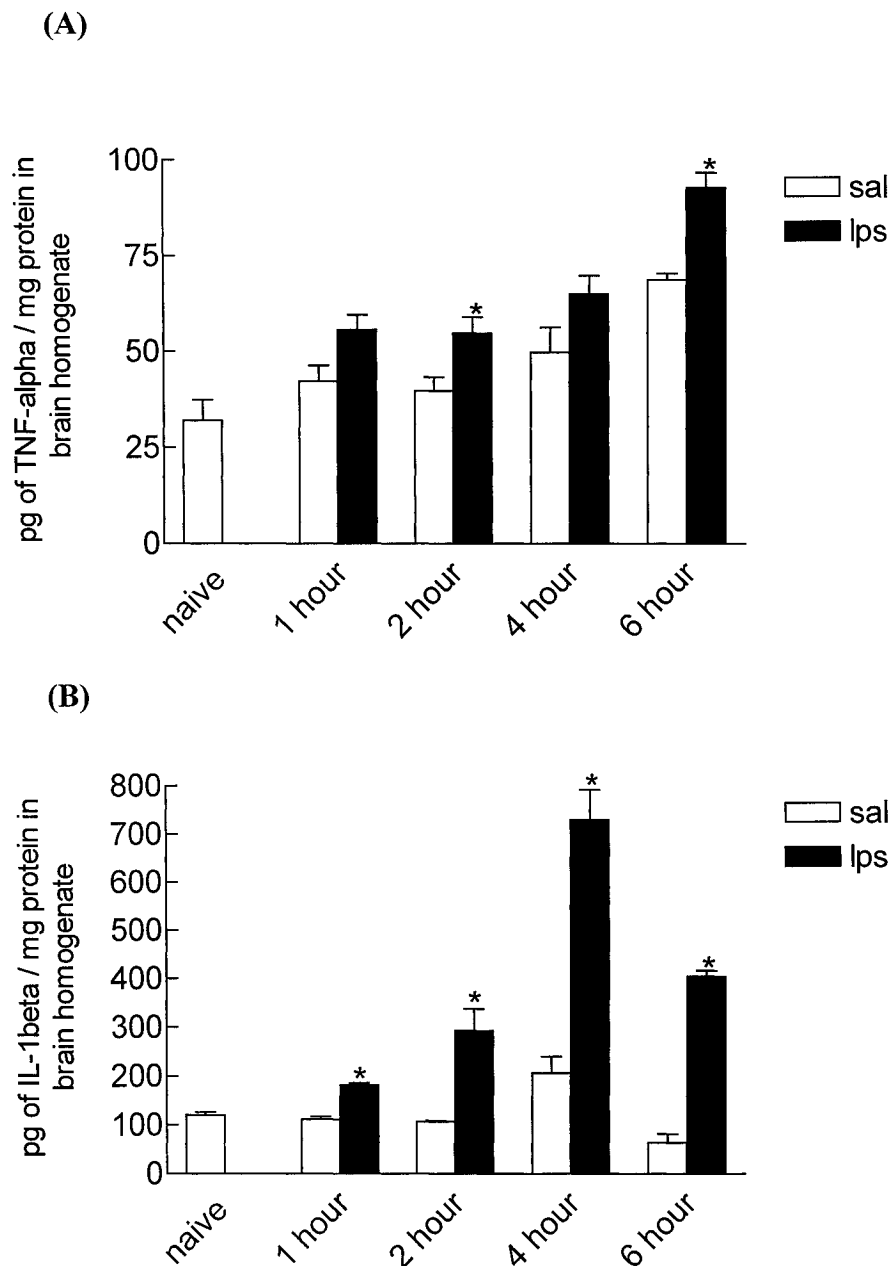
Figure 3.1. The upregulation of TNFα and IL-1β levels in the brain following the administration of LPS into the lateral cerebral. Rats were injected i.c.v. with either 25 μg LPS or saline and brain homogenates were obtained 1 – 6 hours later. Levels of TNFα (A) and IL-1β (B) are shown as pg of cytokine per mg of protein present in the brain homogenates. The levels of these two cytokines in naïve rats that have not received any i.c.v. treatment are shown in each panel. Each bar represents the mean ± S.E.M. from 4 rats. * Cytokine level is higher compared to the respective saline treatment using an un-paired t-test ($p < 0.05$).

Figure 3.2. The induction of an inflammatory response in the liver in response to the administration of LPS into the lateral cerebral. Rats were injected i.c.v. with either 25 µg LPS or saline, and liver RNA was isolated to be used for northern blot analysis at various time points following treatment. The ratio of the intensity of each band to its respective GAPDH was obtained by densitometry, and the results are plotted as % control of each respective saline group for IκBα (A) and MAPKK (B). The average absolute value for IκBα expression (with respect to GAPDH) was 0.29 for the 2 hour saline samples, 0.67 for the 4 hour saline samples, 0.64 for the 6 hour saline samples, and 0.50 for the 9 hour saline samples. The average absolute value for MAPKK expression (with respect to GAPDH) was 0.66 for the 2 hour saline samples, 0.55 for the 4 hour saline samples, 0.79 for the 6 hour saline samples, and 0.71 for the 9 hour saline samples. Each bar represents the mean ± S.E.M. mRNA expression from 4 rats. Representative blots for TNFα (C) relative to GAPDH are shown for the 2, 4, 6, and 9 hour time points following the induction of CNS inflammation. * mRNA expression is higher compared to corresponding saline treated rats using an un-paired t-test ($p < 0.05$).

(A)

(B)

(C)
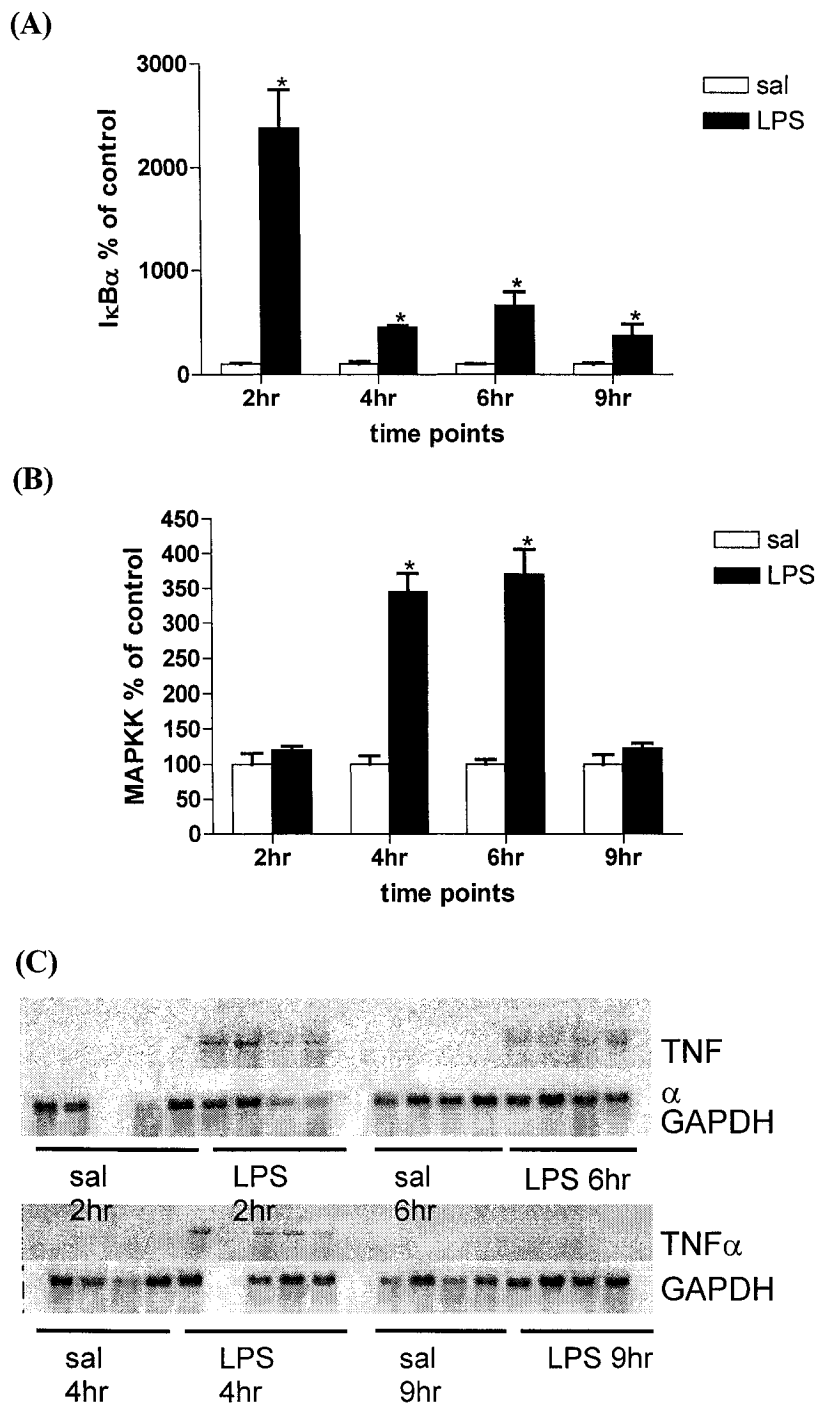
Figure 3.2.

Figure 3.3. An increase in nitrite levels in plasma of rats occurs in response to the administration of LPS into the lateral cerebral ventricle. Rats were injected with 25 μg LPS i.c.v. and 2 – 15 hours later rats were sacrificed and plasma was obtained. Nitrite levels in the plasma were detected using a commercially available kit that converts total nitrates into nitrites (both end products of nitric oxide). Each bar represents the mean ± S.E.M.total nitrite level from 4 rats. * Nitrite level is higher compared to corresponding saline treated animals using an un-paired t-test (p < 0.05).

3.4.2 The effects of CNS inflammation on mRNA expression of CYP isoforms

Based on the observed changes in TNFα, IκBα, and MAPKK in the liver following the i.c.v. administration of LPS, we examined the expression of CYPs in the liver at these time points. The expression level of CYP2D1/5 was unchanged at 2 and 4 hours but was significantly reduced by 45% and 58% at 6 and 9 hours, respectively, following the i.c.v. administration of LPS (Figure 3.4A). The expression levels of CYP2B1/2 were significantly downregulated (by 45%) only at 6 hours following the induction of CNS inflammation, and were unchanged at 2, 4, and 9 hours following LPS administration (Figure 3.4B). The levels of hepatic CYP1A1 expression began to decline between 2 and 4 hours following CNS inflammation and were significantly reduced by 90 % at 6 hours following the i.c.v. administration of LPS (Figure 3.4C). At 9 hours following the i.c.v. administration of LPS, CYP1A1 expression levels in the liver had returned to normal in the LPS treated rats compared to saline. These results indicate that the changes in the expression of these CYP isoforms correlates with the increased expression of hepatic acute phase signalling molecules.

3.4.3 The involvement of hepatic transcription factors in the regulation of CYPs during LPS-induced CNS inflammation

The importance of several transcription factors in the regulation of CYP expression during CNS inflammation was observed using EMSA assays. NF-κB, activator protein-1 (AP-1), CCAAT-enhancer binding protein (C/EBP), and cAMP response element binding protein (CREB) are important down-stream transcription factors that are activated by the acute phase response and are responsible for gene regulation in the liver during conditions of inflammation [81, 130]. At 3 hours following the administration of LPS

84

Figure 3.4. Rapid changes in the expression of CYP2D1/5, CYP2B1/2, and CYP1A1 occur following the administration of LPS into the lateral cerebral ventricle to induce CNS inflammation. Animals were administered either 25 μg of LPS or 5 μL of saline, and liver RNA was isolated. Specific probes for CYP2D1/5 and CYP2B1/2 were utilized for northern blot analyses (A and B). Specific primers for CYP1A1 were utilized for the quantitative PCR in (C). LPS treated animals were compared to the respective group of saline treated animals at each time point, with each bar showing the mean results from 4 rats. For CYP2D1/5 (A) and CYP2B1/2 (B), the ratio of the intensity of each band to its respective GAPDH was obtained, and the results are plotted as % control of the respective saline groups. The $2^{-\Delta\Delta C_T}$ method was used to obtain the fold decrease of CYP1A1 (C) at each time point compared to its respective saline treated group. The average absolute value for CYP2D1/5 expression (with respect to GAPDH) was 1.53 for the 2 hour saline samples, 0.78 for the 4 hour saline samples, 2.23 for the 6 hour saline samples, and 1.83 for the 9 hour saline samples. The average absolute value for CYP2B1/2 expression (with respect to GAPDH) was 0.48 for the 2 hour saline samples, 0.23 for the 4 hour saline samples, 0.57 for the 6 hour saline samples, and 0.36 for the 9 hour saline samples.* CYP expression is lower compared to respective saline treated animals using an un-paired t-test ($p < 0.05$).

85

(A)

(B)

(C)

Figure 3.4.

86
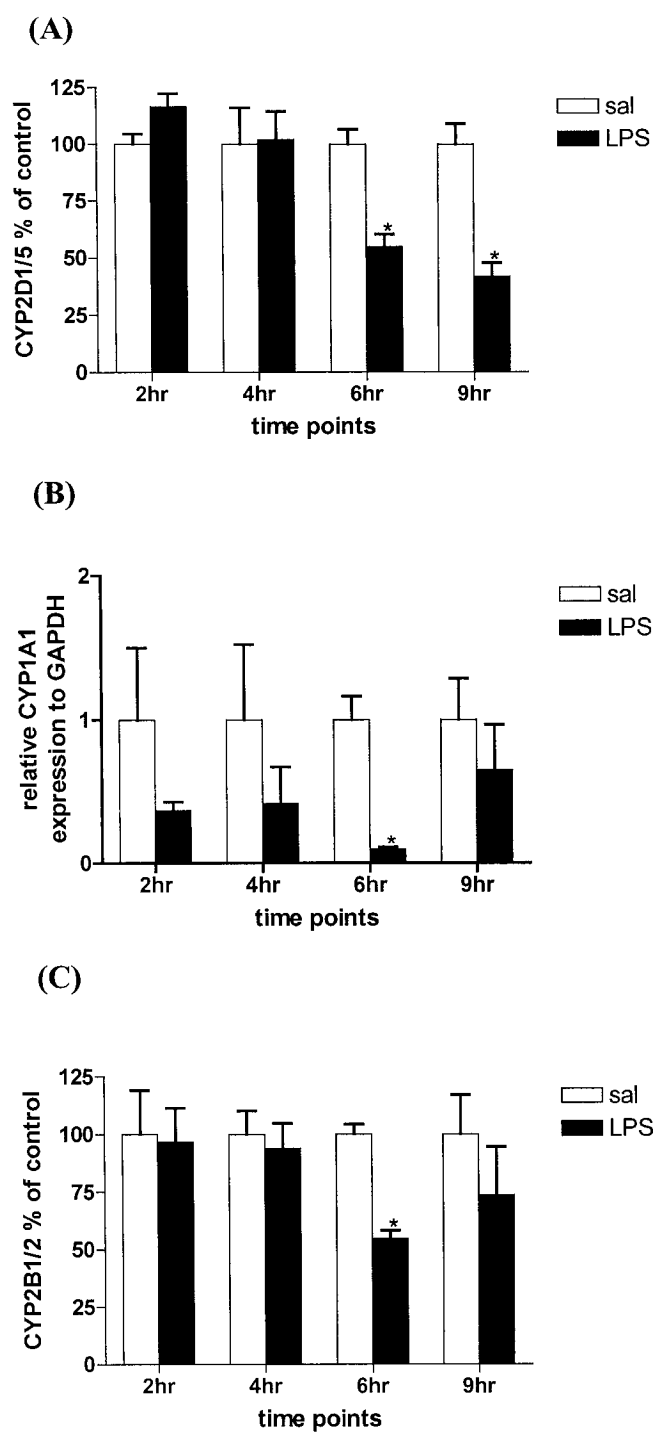
i.c.v., a significant upregulation in the binding of P^{32}-labeled NF-κB, AP-1, and CREB

oligonucleotides to response elements in liver nuclear fractions isolated from LPS treated

animals compared to saline treated animals was observed (Figure 3.5A, B, and C). One

hour following the induction of CNS inflammation, the binding of AP-1 in liver nuclear

fractions obtained from LPS treated animals was also significantly upregulated (data not

shown). These data indicate that NF-κB, AP-1, and CREB proteins are elevated in

hepatic nuclear fractions prior to the loss of CYP mRNA expression.

The binding of transcription factors to the promoter regions of specific CYP

isoforms is illustrated in Figures 3.6 and 3.7. An upregulation in the binding of an NF-κB

response element (identified using MacVector®) on the CYP2D5 promoter occurred in

liver nuclear fractions isolated 3 hours following the treatment of rats with LPS i.c.v.

(Figure 3.6A). The binding of NF-κB to this response element on CYP2D5 was

confirmed using specific and non-specific competitions and was supershifted using a p65

antibody. NF-κB and C/EBP response elements have been identified on the CYP2B1

promoter [131, 132]. An increased binding of NF-κB and C/EBP response elements

occurred in hepatic nuclear fractions 3 hours following the administration of LPS i.c.v.

(Figure 3.6B and Figure 3.7A). The binding of both proteins was confirmed using

specific and non-specific competitions and was supershifted using a p65 and a C/EBPα

antibody. Finally, an upregulation in the binding of an NF-κB response element

(identified using MacVector®) on the CYP1A1 promoter was observed in liver nuclear

fractions isolated 3 hours following the treatment of rats with LPS i.c.v. (Figure 3.7B).

The binding was confirmed using specific and non-specific competitions. No binding was

Figure 3.5. The binding of specific transcription factors in the liver is increased in response to the administration of LPS into the lateral cerebral ventricle. Rats were injected with either 25 µg of LPS or 5 µl of saline i.c.v., and liver nuclear fractions were isolated 3 hours later and were used in electromobility shift assays using commercially obtained oligonucleotides (Table 3.1). Representative blots for NF-κB (A), CREB (B), and AP-1 (C) are shown, where the solid arrow indicates specific binding. Specific competitions (Spec comp) and non-specific competitions (Non-spec comp) indicate competitions performed with excess non-radioactive specific oligonucleotide and non-radioactive non-specific oligonucleotide, respectively. Each blot shows the results from 4 saline and 4 LPS treated rats. Lane 1 refers to probe only, while lanes 2 – 5 and 6 – 9 represent nuclear fractions obtained from saline and LPS treated animals, respectively. Lanes 10 and 11 represent specific and non-specific competition, respectively.

(A) NF-κB

11 10 9 8 7 6 5 4 3 2 1

(B) CREB

11 10 9 8 7 6 5 4 3 2 1

(C) AP-1

9 8 7 6 5 4 3 2 1

Figure 3.5.

89
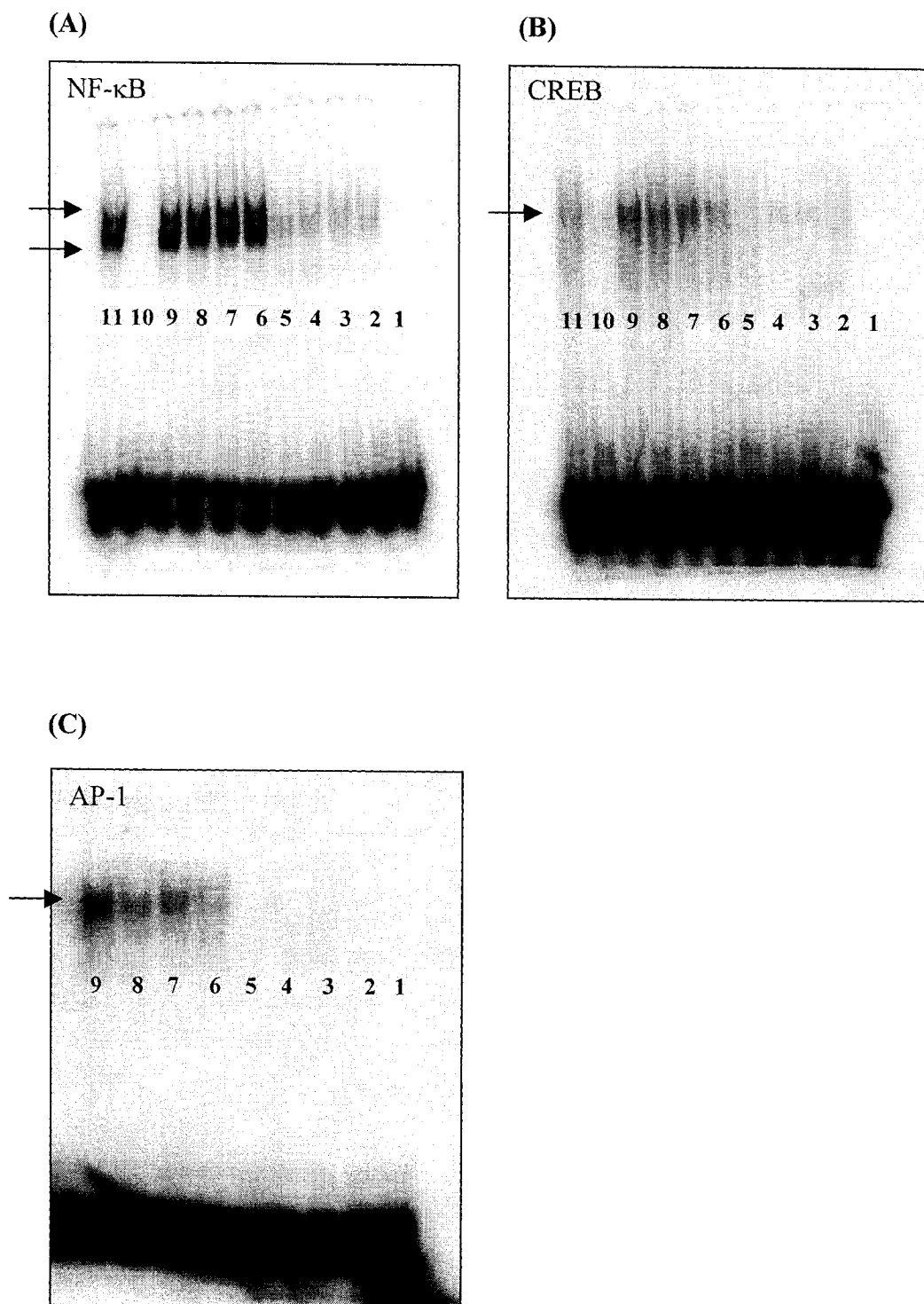
Figure 3.6. NF-κB plays a vital role in the regulation of CYP isoforms. Rats were injected with either 25 μg LPS or 5 μl saline i.c.v., and liver nuclear fractions were isolated 3 hours later and were used in electromobility shift assays using commercially obtained oligonucleotides (Table 3.1). EMSA binding reactions were performed using single stranded oligonucleotides (Table 3.1) that were annealed according to a standard annealing procedure as outlined in the Methods section. An upregulation in NF-κB binding to an NF-κB responsive region on the promoter of CYP2D5 (A) and CYP2B1 (B) is shown, where the solid arrow indicates specific binding, and the dashed arrow indicates non-specific binding. Specific competitions (Spec comp) and non-specific competitions (Non-spec comp) indicate competitions performed with excess non-radioactive specific oligonucleotide and non-radioactive non-specific oligonucleotide, respectively. The binding of NF-κB was confirmed using supershift assays, where (C) and (D) show a super shift (indicated by the diamond head arrow) in binding to the CYP2D5 NF-κB region and the CYP2B1 NF-κB region, respectively, observed following incubation with a p65 antibody. Each blot shows the results from 4 saline and 4 LPS treated rats. Lane 1 refers to probe only, while lanes 2 – 5 and 6 – 9 represent nuclear fractions obtained from saline and LPS treated animals, respectively. Lanes 10 and 11 represent specific and non-specific competition, respectively. Lanes 12 and 13 refers to an LPS sample and a super-shifted sample, respectively.

(A) CYP2D5 NF-κB

11 10 9 8 7 6 5 4 3 2 1

(B) CYP2B1 NF-κB

11 10 9 8 7 6 5 4 3 2 1

(C)

12 13

(D)

12 13
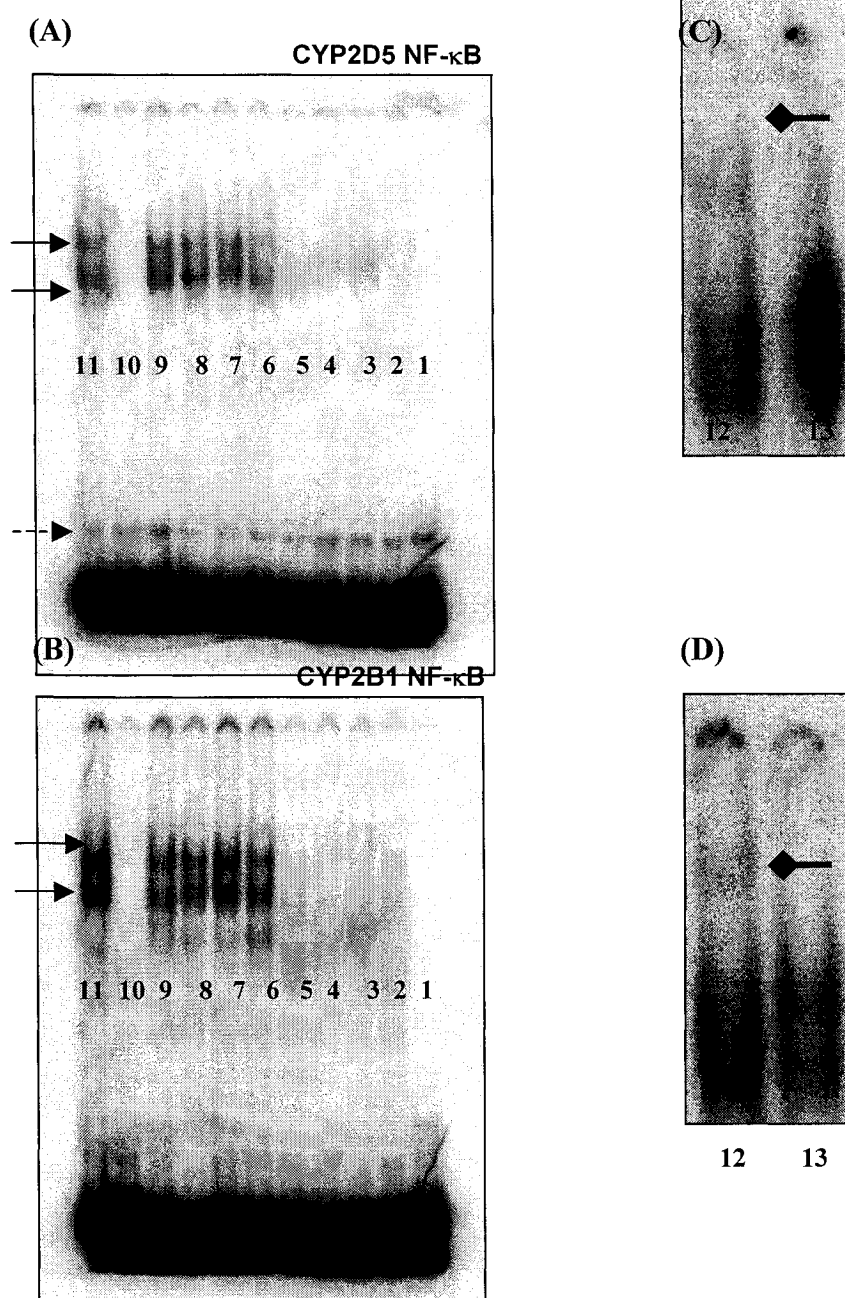
Figure 3.6.

Figure 3.7. The roles of C/EBP and NF-κB in the regulation of CYP2B1 and CYP1A1. Rats were injected with either 25 μg of LPS or 5 μl of saline i.c.v., and liver nuclear fractions were isolated 3 hours later. EMSA binding reactions were performed using single stranded oligonucleotides (Table 3.1) that were annealed according to a standard annealing procedure. The binding of C/EBP to a C/EBP responsive region on the promoter of CYP2B1 (A) and NF-κB to an NF-κB response element on the promoter region of CYP1A1 (B) is shown, where the solid line indicates specific binding. Specific competitions (Spec comp) and non-specific competitions (Non-spec comp) indicate competitions performed with excess non-radioactive specific oligonucleotide and non-radioactive non-specific oligonucleotide, respectively, as described in the Methods section. The binding of C/EBPα to the CYP2B1 C/EBP region was confirmed using a supershift assay as shown in (C), where the diamond head arrow indicates the shift following incubation with a C/EBPα antibody. Each blot shows the results from 4 saline and 4 LPS treated rats. Lane 1 refers to probe only, while lanes 2 – 5 and 6 – 9 represent nuclear fractions obtained from saline and LPS treated animals, respectively. Lanes 10 and 11 represent specific and non-specific competition, respectively. Lanes 12 and 13 refers to an LPS sample and a super-shifted sample, respectively.

(A) CYP2B1 C/EBP

11 10 9 8 7 6 5 4 3 2 1

(B) CYP1A1 NF-κB

9 8 7 6 5 4 3 2 1

10 11

(C)

12 13
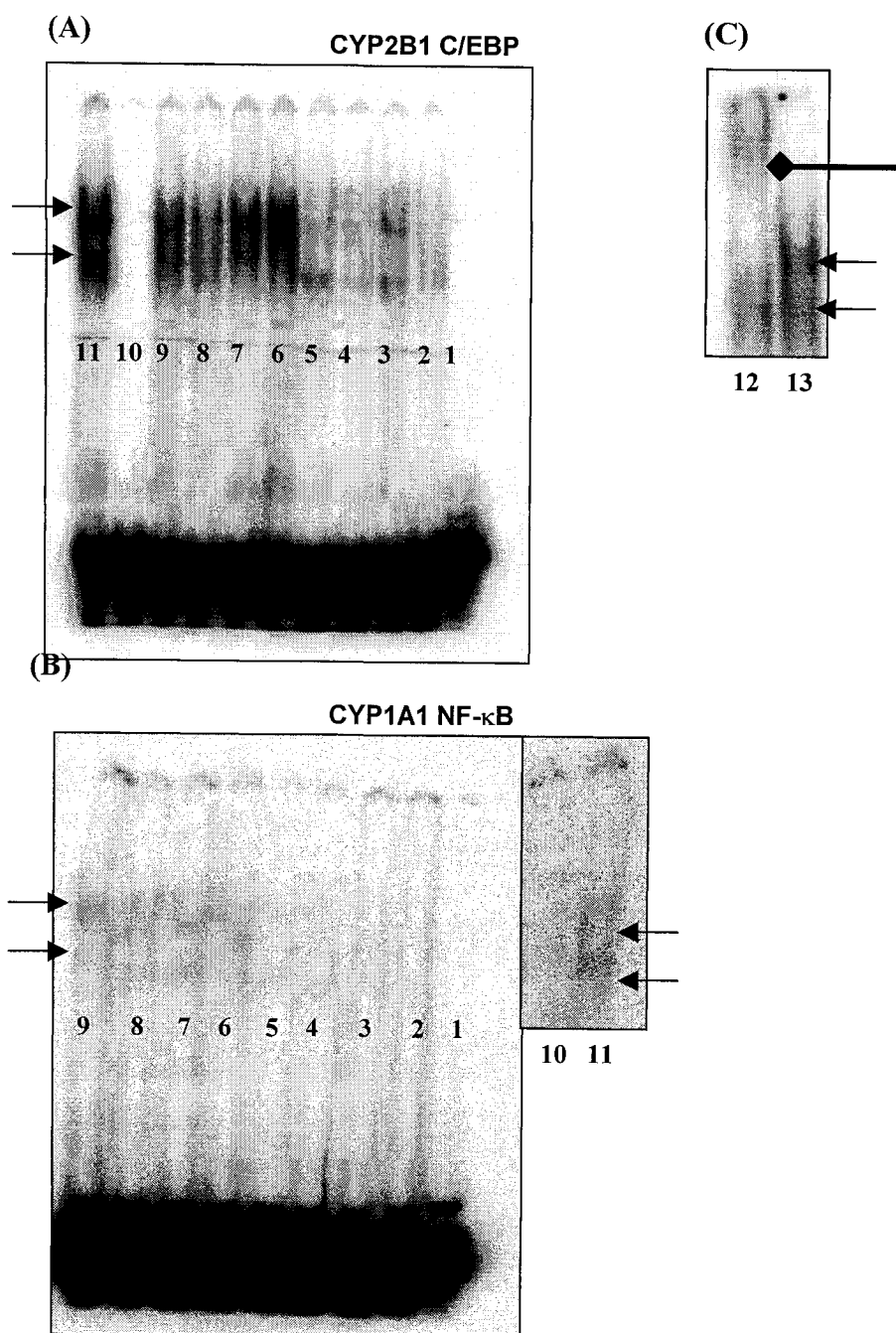
Figure 3.7.

observed to the CREB response element on the promoter region of CYP1A1 (identified

using MacVector®) (Figure 3.8).

3.4.4 The peripheral effects on hepatic CYP expression observed following the i.c.v. administration of LPS can not be completely accounted for by cytokines

The above results indicate that several important intra-hepatic biochemical changes are

occurring during this rodent model of LPS-induced CNS inflammation. We examined

several pathways to explain the mechanisms by which the i.c.v. administration of LPS is

causing the peripheral effects on hepatic CYPs and inflammatory mediator expression. It

is known that total cytochrome P450 levels are downregulated in response to the i.c.v.

administration of LPS [75]. Thus we chose to examine the effects of cytokines

administered centrally and cytokine inhibitors on total cytochrome P450 levels 24 hours

following the i.c.v. administration of LPS. When rats were administered a cytokine

cocktail i.c.v., we observed no change in total cytochrome P450 levels (Figure 3.9A). Co-

administration of Enbrel™ (TNFα soluble antibody) either i.c.v. or i.p. with LPS i.c.v.

could not prevent the LPS-induced downregulation in total cytochrome P450 levels

(Figure 3.9B and C). YVAD, the IL-1 inhibitor, was also not able to prevent the LPS-

induced downregulation in total cytochrome P450 levels when both agents were

administered i.c.v. (Figure 3.9D). Similar results were obtained when EROD activity

was examined (Figre 3.10).

3.4.5 LPS levels are detected in the serum of animals given 25 μg of LPS by i.c.v. or i.p. injection

Since the distribution of LPS following its administration i.c.v. to rats has not been

previously characterized, we determined whether LPS transfer to the periphery might

CYP1A1 CREB
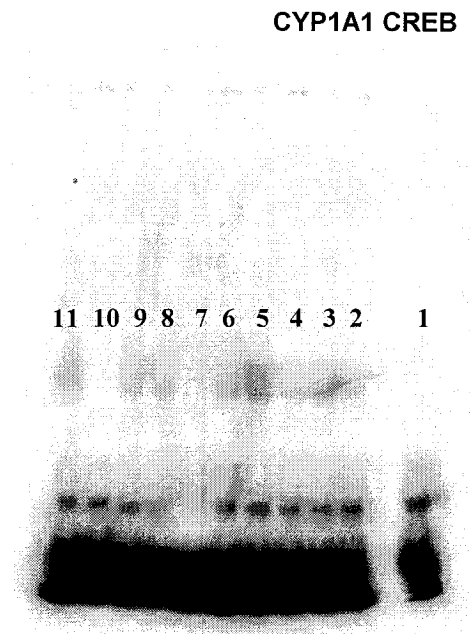
Figure 3.8. CREB does not play a role in the regulation of CYP1A1. Rats were injected with either 25 µg of LPS or 5 µl of saline i.c.v., and liver nuclear fractions were isolated 3 hours later. EMSA binding reactions were performed using single stranded oligonucleotides (Table 1) that were annealed according to a standard annealing procedure. The binding of CREB to a CREB responsive region on the promoter of CYP1A1 is shown. Specific competitions (Spec comp) and non-specific competitions (Non-spec comp) indicate competitions performed with excess non-radioactive specific oligonucleotide and non-radioactive non-specific oligonucleotide, respectively, as described in the Methods section. Each blot shows the results from 4 saline and 4 LPS treated rats. Lane 1 refers to probe only, while lanes 2 – 5 and 6 – 9 represent nuclear fractions obtained from saline and LPS treated animals, respectively. Lanes 10 and 11 represent specific and non-specific competition, respectively. Lanes 12 and 13 refers to an LPS sample and a super-shifted sample, respectively.

Figure 3.9. The non-involvement of several pathways in mediating the effects of LPS i.c.v. on hepatic CYP isoforms. Rats were administered a cytokine cocktail consisting of TNFα, IL-1β, IL-1α, IL-6, and IFNγ, and total cytochrome P450 levels were measured 24 hours later (A). In a separate set of experiments, rats were injected with 25 μg of LPS i.c.v. in addition to etanercept (Enbrel™) given either as a dose of 40 μg i.c.v. (B) or 2.5 mg/kg i.p. (C) or the IL-1 inhibitor YVAD administered as a dose of 0.63 μg i.c.v. (D), and total P450 levels were measured 24 hours later as described in the Methods section. "*" is statistically different compared to respective saline treated animals (p < 0.05, 2-WAY ANOVA performed for panels B, C, and D, t-test performed for panel A).

Figure 3.9.

(A)

(B)

(C)

(D)

(E)
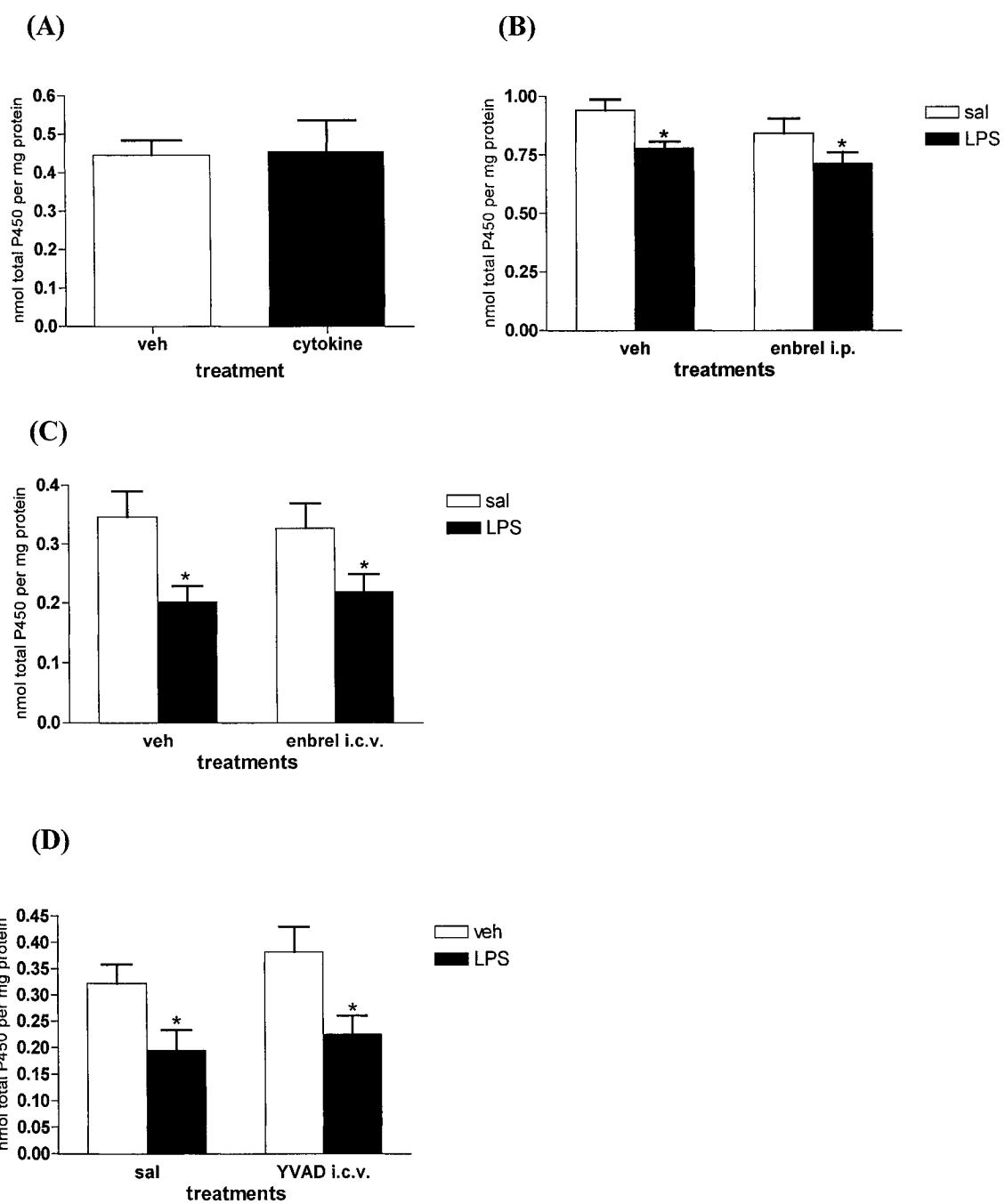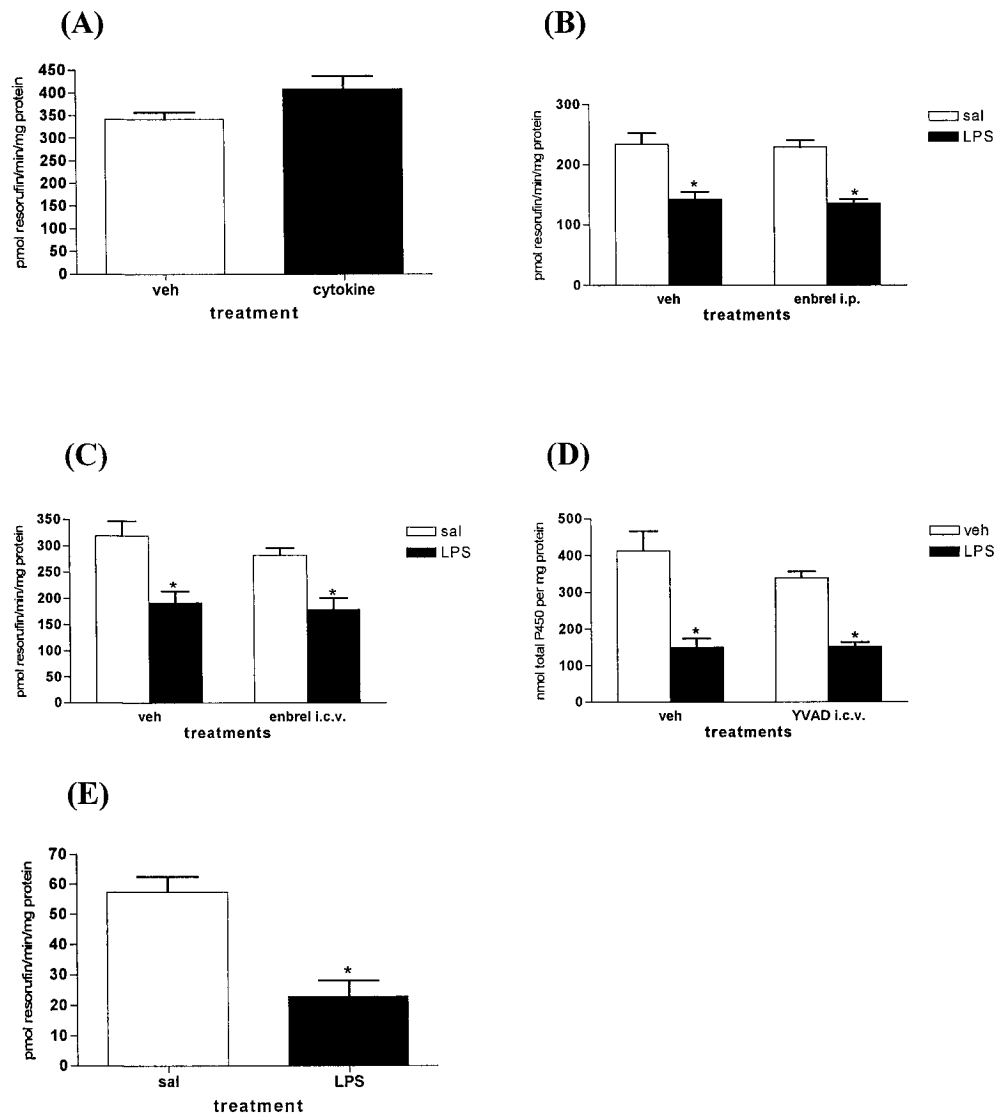
Figure 3.10. The non-involvement of several pathways in mediating the effects of LPS i.c.v. on hepatic CYP isoforms. Rats were administered a cytokine cocktail consisting of TNFα, IL-1β, IL-1α, IL-6, and IFNγ, and EROD activity was measured 24 hours later (A). In a separate set of experiments, rats were injected with 25 μg of LPS i.c.v. in addition to etanercept (Enbrel^{TM}) given either as a dose of 40 μg i.c.v. (B) or 2.5 mg/kg i.p. (C) or the IL-1 inhibitor YVAD administered as a dose of 0.63 μg i.c.v. (D), and EROD activity was measured 24 hours later as described in the Methods section. Finally, the effect of LPS administration on EROD activity in hypophesectimized rats is shown in (E). "*" is statistically different compared to respective saline treated animals (p < 0.05, 2-WAY ANOVA performed for panels B, C, and D, t-test performed for panel A).

contribute to the observed changes in hepatic CYPs. We measured the amounts of LPS

(in pg/mL) in the serum of animals administered 25 μg of LPS either

intracerebroventricularly or intraperitoneally. Following the i.c.v. administration of LPS,

the serum endotoxin levels were a 100 fold greater than the amounts detected in the

serum following the i.p. administration of the same dose of LPS (Figure 3.11). We have

previously shown that the administration of 25 μg LPS i.p. does not affect liver CYP

activity [75]. Minimal LPS was detected in control rats that did not receive LPS.

We then examined the effects on hepatic CYP levels if the entire amount of 25 μg of LPS

we normally inject i.c.v. was present in the bloodstream. We chose to examine the

expression of CYP2D1/5, CYP2B1/2, CYP1A1, TNFα, and IκBα at 3 and 6 hours

following the intravenous (i.v.) administration of LPS since these genes were

differentially regulated at these time points following the i.c.v. administration of LPS. We

observed a significant reduction in CYP2D1/5, CYP2B1/2, and CYP1A1 expression at 6

hours following the i.v. administration of LPS (22 %, 54 %, and 93 % less than the

respective saline groups, respectively) (Table 3.2). In addition, we observed a significant

increase in TNFα expression at 3 hours following the i.v. administration of LPS (328 %

increase compared to respective saline group) and a significant increase in IκBα

expression at 3 and 6 hours following the i.v. administration of LPS (10 fold and 3.3 fold

increase compared to respective saline group, respectively) (Table 3.2). These results

indicate that the effects of administering LPS i.v. on the expression of CYPs and

inflammatory mediators is similar to the effects observed following the i.c.v.

administration of LPS. We have previously shown that at 24 hours following the

administration of 25 μg of LPS i.c.v., a downregulation in total cytochrome P450 levels,
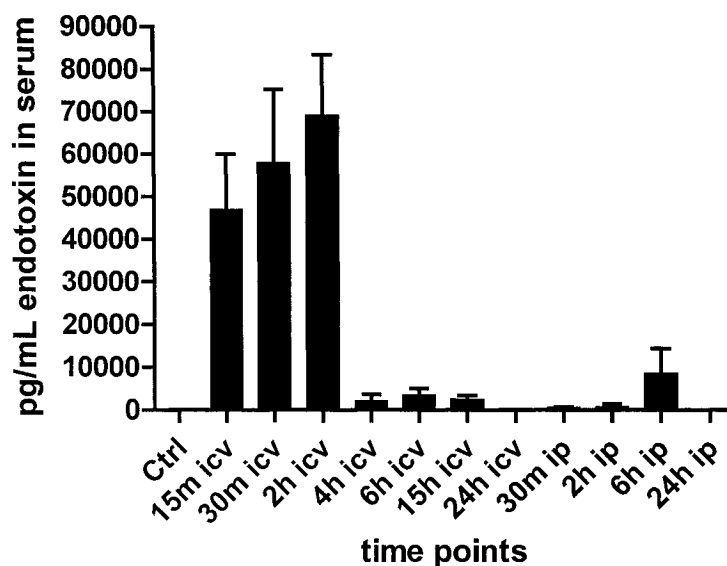
Figure 3.11. The levels of endotoxin detected in the serum of animals injected with 25 μg LPS i.p. or i.c.v. Animals were injected with 25 μg of LPS either i.p. or i.c.v. and serum was obtained at 15 minutes (15m), 30 minutes (30m), 2 hours (2h), 4 hours (4h), 6 hours (6h), 15 hours (15h), and 24 hours (24h) following injection. Endotoxin levels were measured according to a commercially available kinetic assay kit. The graph shown represents the results from 3 animals. In the 30 minute i.p. and the 2 hour i.p. groups, the presence of endotoxin was detected in only 2 out of the three animals. Non-injected rats served as control (ctrl) animals for the experiment.

100

CYP1A catalyzed EROD activity, and CYP2B catalyzed PROD activity occurs [75].

Examination of these endpoints revealed that the administration of 25 μg LPS i.v. was

able to cause a significant decrease in total cytochrome P450 levels (30% less than saline

treated rats), CYP1A catalyzed EROD activity (42% less than saline treated rats), and

CYP2B catalyzed PROD activity (48 % less compared to saline treated rats) following

the i.v. administration of LPS (Table 3.2).

Table 3.2 – The effects of 25 μg LPS administered i.v. on the activity and expression of hepatic P450 isoforms and inflammatory mediators

Assays were performed either 3, 6, or 24 hours following the i.v. injection of LPS. The values are presented as the pooled results from 4 different animals, and * is statistically different compared to corresponding saline treated animals ($p < 0.05$).

Assay description	Saline	25 μg LPS i.v.
CYP1A1 expression in liver relative to GAPDH (6 hour time point)	1.00 ± 0.39	0.069 ± 0.03*
CYP2B1/2 expression in liver relative to GAPDH (6 hour time point)	2.54 ± 0.63	1.18 ± 0.17*
TNFα expression in liver relative to GAPDH (3 hour time point)	0.38 ± 0.05	1.25 ± 0.37*
CYP2D1/5 expression in liver relative to GAPDH (6 hour time point)	87.80 ± 8.58	68.67 ± 2.07*
IκBα expression in liver relative to GAPDH (3 hour time point)	0.35 ± 0.13	3.50 ± 0.88*
IκBα expression in liver relative to GAPDH (6 hour time point)	0.72 ± 0.28	2.36 ± 0.26*
Total cytochrome P450 in nmol/mg protein (24 hour time point)	0.578 ± 0.043	0.400 ± 0.083*
CYP1A1/2 activity in pmol/mg protein/minute as measured by EROD assay (24 hour time point)	123.84 ± 40.22	71.58 ± 12.52*
CYP2B1/2 activity in pmol/mg protein/minute as measured by PROD assay (24 hour time point)	8.62 ± 3.61	4.51 ± 0.50*

3.5 Discussion

Inflammatory mediators such as cytokines, prostaglandins, and reactive oxygen species are known to be released from activated microglia, the resident macrophages of the brain, during conditions of CNS inflammation [91]. Our current results indicate that an inflammatory response occurs in the brain and in the peripheral tissues following the administration of LPS i.c.v. manifested by increases in the levels of pro-inflammatory cytokines in rat brain and blood [75] and increases in the mRNA expression of the acute-phase response genes TNFα, IκBα, and MAPKK in rat liver, as outlined in Figure 3.12. Changes in CYP gene regulation are well documented during inflammation responses occuring *in vitro* [51, 133]. It is likely that the regulation of hepatic CYPs observed *in vivo* [75, 114] also occurs as a result of changes in gene expression. We tested this idea by examining the regulation of hepatic CYP2D1/5, CYP2B1/2, and CYP1A1 using a well utilized model of CNS inflammation induced by the i.c.v. injection of LPS. These particular isoforms were selected since they are known to play a significant role in the metabolism of many clinically relevant drugs [85]. Our results indicate a significant reduction in the mRNA expression of CYP2D1/5, CYP2B1/2, and CYP1A1 in the liver following the i.c.v. administration of LPS, which is in agreement with the loss in enzymatic activity and/or protein levels previously reported for these isoforms [75].

NF-κB, AP-1, and CREB are important transcription factors that regulate a number of genes in the liver during the acute phase response [81, 82, 130]. Our current results indicate an increase in the binding of NF-κB, AP-1, and CREB in hepatic nuclear fractions obtained 3 hours following the i.c.v. administration of LPS, indicating a potential role for these acute phase proteins in the downregulation of hepatic CYPs

astrocyte
microglia

(2)

TNFα   ? NF-κB
IL-1β   ? AP-1

(1)   TLR

LPS

BBB   (3)

LPS

immune cell

Transcription
factor and
immune
cell activation

(4)

(5)   TLR

(5)   TNFα
IL-1β, IL-6

TLR

MAPK

?

NF-κB

JunFos

P450

(6)

hepatocyte
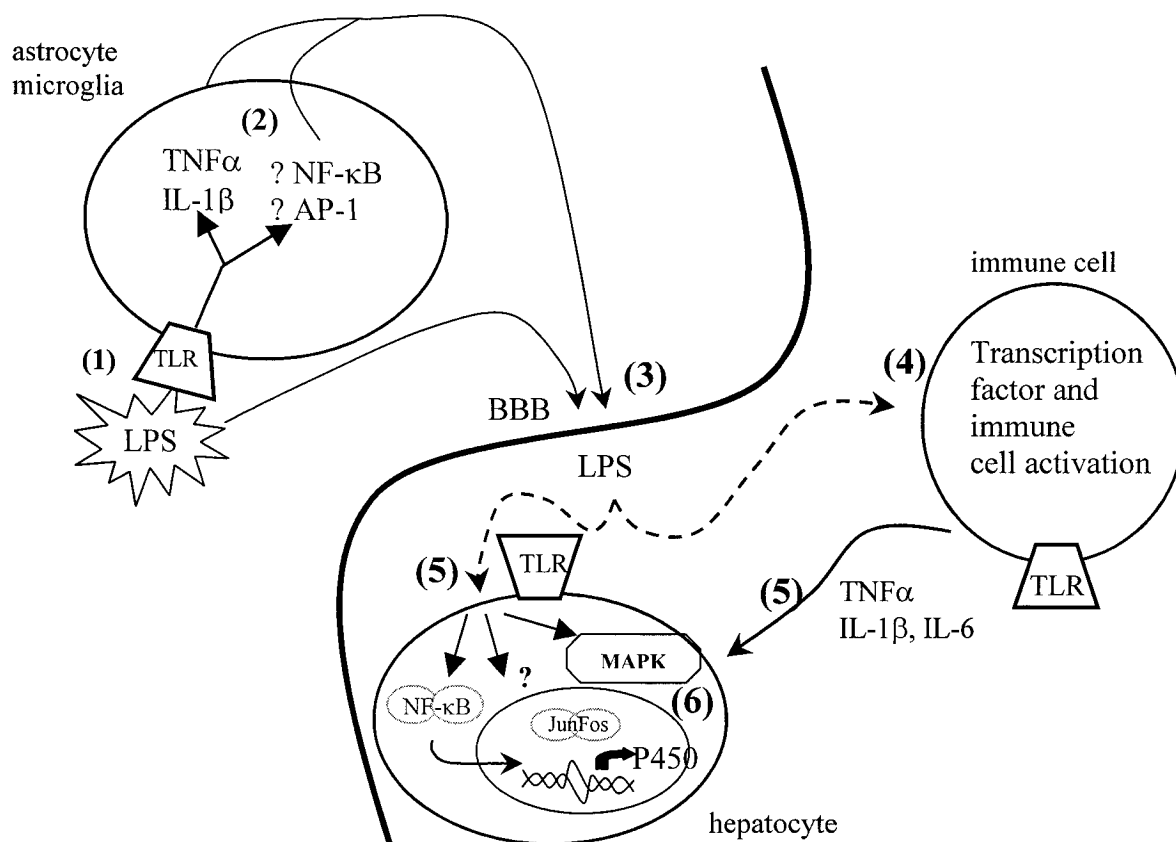
Figure 3.12. A proposed mechanism by which LPS regulates hepatic cytochrome P450 following its administration into the lateral cerebral ventricle. (1) The i.c.v. injection of LPS into the lateral cerebral ventricles of rats is thought to activate Toll-like receptor 4 (TLR4). (2) Activation of TLR4, normally present on microglia and astrocytes in the brain, would lead to the upregulation of cytokine and transcription factors in the brain. (3) The rapid "leakage" of LPS from the CNS into the periphery plays a role in downregulation of hepatic CYPs. Although cytokines are elevated in the CNS during this model of LPS-induced CNS inflammation, it appears from our results that centrally produced cytokines are not important for the regulation of hepatic CYPs. (4) The presence of LPS in the periphery induces a peripheral inflammatory response characterized by the production of cytokines (from immune cells such as macrophages) and the induction of an acute-phase response in the liver. (5) Cytokines from peripheral sources, in addition to LPS present in the serum, act on the hepatocyte to differentially regulate CYPs. (6) Some of the intra-hepatic mechanisms by which CYP regulation occurs involve upregulation of various transcription factors such as NF-κB, AP-1, and C/EBP. These transcription factors can then bind to the promoter regions on specific CYP isoforms, leading to changes in the transcription of these CYPs.

104

during LPS-induced CNS inflammation. In support of this, we have observed an increased production of both TNFα and IκBα in the liver, known target genes upregulated through the NF-κB pathway. The acute phase response in the liver characterized by cytokine production and transcription factor upregulation could be an intrahepatic mechanism responsible for the repression in CYP2D1/5, CYP2B1/2, and CYP1A1 expression in the liver following the i.c.v. administration of LPS. To test the hypothesis, we examined the effects of the i.c.v. administration of LPS to the binding of NF-κB to the promoter regions of specific CYP isoforms. Our results indicate that hepatic NF-κB is likely to play an important role in the regulation of CYP2B1, CYP1A1, and CYP2D5 during CNS inflammation through binding to NF-κB response elements on the promoters of these genes. In support of this finding, Ke *et al* has also demonstrated a role for this transcription factor in the regulation of CYP1A1 in an in vitro model of CNS inflammation. Furthermore, Morgan and co-workers have shown that NF-κB is responsible for the LPS-mediated downregulation in CYP2C11 [69, 83]. Figure 3.12 outlines the role of these acute phase proteins in the regulation of hepatic CYPs following the i.c.v. administration of LPS. We also observed using rat liver nuclear fractions that the i.c.v. administration of LPS caused an upregulation in the binding to a C/EBP region on the CYP2B1 promoter [131]. Although the importance of this C/EBP region in the regulation of CYP2B1 in the liver is not completely understood [81], these results are consistent with it playing some role in the regulation of CYP2B1 during inflammatory conditions. It has been shown CYP2B1/2 isoforms can be regulated at the post-translational level [134], and therefore it is possible that in our model of LPS-induced CNS inflammation, the downregulation in CYP2B1/2 activity observed at 24 hours

following the induction of CNS inflammation [75] may be occurring post-translationally or through enhanced proteolytic degradation of CYP2B proteins [135, 136].

Previous studies have suggested that a signalling pathway must exist between the brain and liver to account for the loss in hepatic CYPs during conditions of LPS-induced CNS inflammation [71, 72, 74, 75]. TNFα, IL-1β, and IL-6 have all been shown to regulate several CYP isoforms at the level of the enzyme and mRNA in both peripheral and CNS models of inflammation [51, 64, 76, 87]. We observed no effects on total cytochrome P450 levels following the i.c.v. administration of a cytokine cocktail (TNFα, IL-1α, IL-1β, IFNγ, and IL-6). In addition the central and peripheral blockade of the TNFα pathway (using the TNFα soluble antibody etanercept or Enbrel^{TM}) and the IL-1 signal transduction pathway (using the IL-1 inhibitor YVAD) could not prevent the downregulation in total cytochrome P450 levels induced by the i.c.v. administration of LPS. Similar results were observed when we examined the effects of the cytokine cocktail and cytokine inhibitors on CYP1A EROD catalyzed activity. Shimamoto *et al* demonstrated that adrenalectomy did not block the loss in hepatic CYPs in response to the i.c.v. administration of LPS [71, 72]. In support of these results, we observed that hypophesectimized rats maintained the response to the i.c.v. administration of LPS, indicating the lack of involvement of the hypothalamic-pituitary axis in the downregulation of hepatic CYPs during CNS inflammation. All these results support the idea that hepatic CYP regulation during the i.c.v. administration of LPS is occurring at an intrahepatic level with various acute phase proteins such as NF-κB playing a dominant role in this regulation.

The injection of LPS i.c.v. is a commonly used model to produce CNS

inflammation, however it has not been determined whether endotoxin leakage into the

periphery plays a role in the effects on hepatic CYPs observed by us and others [71, 72,

74, 75]. To test whether endotoxin leakage from the CNS might account for the effects

observed on hepatic CYPs in LPS treated rats, we measured endotoxin levels in serum

obtained from animals administered LPS directly into the lateral cerebral ventricle. We

were able to detect significant amounts of LPS in the serum of rats as early as 15 minutes

and for up to 2 hours following the i.c.v. administration of LPS. An energy mediated

transport mechanism or bulk re-absorption of the cerebrospinal fluid likely accounts for

the extremely rapid transfer of LPS from the CNS into the periphery. When animals were

treated with the same dose of LPS (25 μg) given by the i.p. route, only small amounts of

LPS were detected in the serum following LPS administration. Based on these results, the

bioavailability of LPS from its i.p. administration is relatively small compared to the

bioavailability which occurs from i.c.v. administration. This difference in bioavailability

could explain previous results by our laboratory and Shimamoto *et al* where the

administration of LPS by the i.p. route did not cause the downregulation in hepatic CYPs

that is observed by administering the same dose directly into the lateral cerebral ventricle

[71, 72, 75]. It is likely that the rapid transfer of LPS from the CNS into the periphery in

significant amounts is what accounts for the observed effects of i.c.v. LPS on hepatic

CYPs (as shown in Figure 3.12). In support of this idea, we have observed that the

administration of 25 μg of LPS by the intravenous route also causes a significant

downregulation in CYP2B1/2, CYP2D1/5, and CYP1A1 expression and a significant

upregulation in the expression of TNFα and IκBα at 3 – 6 hours.

In summary, we propose a signal transduction mechanism to explain the differential regulation of cytochrome P450 intrahepatically following a well-utilized LPS-induced model of CNS inflammation and provide insight into some of the molecular mechanisms by which rapid regulation of cytochrome P450 occurs in this model. Our results indicate that CYP regulation following the i.c.v. administration of LPS occurs at an intrahepatic level, with proteins such as NF-κB and C/EBP playing a dominant role in this regulation. We also show that the regulation of hepatic CYPs during LPS-mediated CNS inflammation results by a novel mechanism through which rapid transfer of LPS from the CNS into the periphery occurs following its i.c.v. administration.

CHAPTER 4

THE REGULATION OF HEPATIC CYP2D5 DURING LPS-INDUCED

PERIPHERAL AND CNS INFLAMMATION IN THE RAT

4.1 Abstract

Rat CYP2D1/5 is thought to share some enzymatic similarity to human CYP2D6 and is expressed in the liver and extra-hepatic tissues. Understanding the mechanisms regulating CYP2D1/5 during LPS induced inflammation is essential due to the important role of this isoform in the metabolism of some key xenobiotics. We have previously shown that CYP2D1/5 expression is downregulated during LPS-induced CNS inflammation, with the transcription factor NF-κB likely playing a role in this downregulation [79]. We now show that CYP2D1/5 mRNA expression is also downregulated during LPS-induced peripheral inflammation, and that this downregulation is associated with reduced binding at the NF-κB site on the promoter region of CYP2D5. Examination of the activity of a luciferase reporter plasmid spanning the NF-κB site on the CYP2D5 promoter revealed no changes in promoter activity in response to either TNFα treatment or transfection with the p65 subunit of NF-κB. When two base pair mutations were introduced in the putative NF-κB site on the CYP2D5 promoter, we observed a 70% reduction in luciferase reporter activity. Comparison of the mutated NF-κB site with the wildtype site revealed the presence of a GA binding protein (GABP) binding site overlapping the putative NF-κB site on the CYP2D5 promoter. The results obtained from the use of GABP proteins in transfection assays outline a possible role for this transcription factor in the regulation of the rat CYP2D5 gene.

4.2 Introduction

Cytochrome P450 2D (CYP2D) isoforms are present in several mammalian species and

are involved in the hepatic metabolism of a wide variety of chemicals such as

antidepressants, β-blockers, antiarrhythmics, antihypertensives, analgesics, and

neuroleptics, as well as neurotoxins such as MPTP [60, 137, 138]. CYP2D isoforms are

also thought to play a role in the metabolism of endogenous neurochemicals such as

tyramine and tryptamine [138]. The only CYP2D isoform identified in humans is

CYP2D6, which is expressed in a wide variety of tissues such as the liver, CNS, kidney,

lung, and breast [60]. In contrast, six CYP2D isoforms have been identified in rat:

CYP2D1, CYP2D2, CYP2D3, CYP2D4, CYP2D5, and CYP2D18 [60, 137]. The mRNA

and proteins of the rat CYP2D isoforms are expressed in a wide variety of tissues similar

to human CYP2D6, however each isoform is thought to show a specific tissue

distribution [60, 139]. The rat CYP2D isoforms also share a high sequence homology

among each other [60]. Although it is not known which rat isoform functionally

corresponds to the human CYP2D6 isoform, CYP2D1, which shares over 95% homology

in amino acid sequence to CYP2D5, exhibits the closest enzymatic relationship with

human CYP2D6 [137, 139].

4.2.1 Regulation of CYP2D isoforms

The regulation of rat CYP2D isoforms has not been extensively examined, since it is not

known which isoform is functionally similar to human CYP2D6. Using *in vitro* cell

cultures, it has been shown that various transcription factors are important for the

regulation of human CYP2D6. The use of "humanized" CYP2D6 mice with a conditional

knockout of HNF4 showed a 50% reduction in the catalytic activity of debrisoquine (a

substrate for CYP2D6), indicating a possible role for this transcription factor in regulating CYP2D6 [58]. The re-expression of C/EBPα in HepG2 human hepatoma cells (which normally express low levels of C/EBPα) caused an upregulation in the mRNA expression of CYP2D6, indicating a role for C/EBPα in the constitutive regulation of CYP2D6 [140]. A role for steroid hormones in rat CYP2D regulation in the brain has been proposed: the administration of testosterone to female rats was shown increase CYP2D expression, whereas the administration of progesterone caused a decrease in CYP2D expression [141].

4.2.2 GA binding proteins and CYP2D regulation

GABP belongs to the Ets family of transcription factors that regulate a wide variety of viral and cellular genes in cooperation with other transcription factors and co-factors through binding to an evolutionary-conserved purine-rich GGAA/T core DNA sequence [142]. It is unique among the Ets family in that it can not function unless it is in a tetrameric form, where the two proteins GABPα and GABPβ form an $\alpha_2\beta_2$ complex [143]. Within this complex, GABPα contains the DNA binding domain that binds to the target gene whereas GABPβ contains the transcriptional activation domain [143]. Using human hepG2 cells, Yokomori *et al* showed that GABP proteins transcriptionally regulate the male-specific mouse cyp2d9 gene [144, 145].

The Ets family of transcription factors regulate a variety of biological responses ranging from cell proliferation, development, and apoptosis [146]. Many genes are regulated by the Ets family of transcription factors, including the prolactin and the oxytocin receptor gene [146, 147]. GABP is thought to interact with other proteins to regulate the interleukin-2, interleukin-7, β_2 leukocyte integrin, and TNFα genes [148-

151]. GABP has also been shown to play a role in the regulation of cytochrome oxidase, an essential enzyme in regulating cellular energy production [152]. Among the drug metabolizing enzymes, both human sulfotransferase 1A1 (SULT1A1) and mouse cyp2d9 are under the control of GABP [153].

4.2.3 Regulation of CYP2D isoforms during inflammation

It is well documented that inflammation and infectious conditions affect the catalytic activity and expression of P450 [64, 66, 79], however information regarding the regulation of CYP2D during conditions of inflammation is limited. We have previously shown that the mRNA expression of CYP2D1/5 is downregulated following the i.c.v. administration of LPS in a model of CNS inflammation, and that the protein levels of CYP2D are downregulated 48 hours following the i.c.v. administration of LPS [75, 79]. The administration of nitric oxide to HepG2 cells causes downregulation of the expression of CYP2D6 through effects on the HNF4 site on the promoter region of the gene [154].

4.2.4 Objective

Since CYP2D isoforms play an important role in the metabolism of various endogenous substrates and xenobiotics, and their regulation during inflammation remains largely unknown, the objective of this work was to examine the potential role of NF-κB in the regulation of rat CYP2D1/5 during LPS-induced inflammation.

4.3 Materials and methods

4.3.1 Reagents

All laboratory reagents were purchased from Sigma (St. Louis, MO) with the exceptions noted in the text. Gel purified *Escherichia coli* lipopolysaccharide (LPS) of sereotype 0127:B8 was utilized in experiments as outlined below.

4.3.2 Animals and treatment

Male Sprague-Dawley rats (125 – 150 grams) were obtained from Charles River Laboratories (Quebec, Canada) and were housed on corncob bedding for a period of 5 days on a 12-hour light/dark cycle. All animal procedures were performed according to the Dalhousie University Committee on Laboratory Animals following the guidelines established by the Canadian Council on Animal Care. Rats were allowed *ad-libitum* access to food and water prior to and following the experimental procedure. Intracerebroventricular (i.c.v.) injections into the lateral ventricle were performed using a KOPF sterotaxic instrument. The coordinates utilized relative to bregma were 1.7 mm lateral and 4.7 mm below the skull surface. On the day of the experiment, rats were anaesthetized using enflurane and maintained on a 4% level of the anaesthetic during the surgery. A dose of 25 μg LPS was dissolved in pyrogen-free saline and injected in a volume of 5 μL. In a separate set of experiments, animals were injected intraperitoneally with a dose of LPS of 5 mg kg^{-1} (in 100 μL saline). This dose has been previously shown to cause a downregulation in P450 levels [155]. Liver samples (~100 mg) were obtained for RNA isolation at 2, 4, 6, 9, and 24 hours following the i.c.v. injection of LPS and at 2 and 24 hours following the i.p. injection of LPS. All experiments utilized 4 – 6 male rats per treatment.

4.3.3 Plasmids and constructs

The 851 base pair fragment from −796 until +55 of the rat CYP2D5 promoter was amplified from genomic rat liver DNA using Platinum® *Pfu* DNA polymerase (InVitrogen, Ontario, Canada) according to manufacturer's instructions. This fragment contained the putative NF-κB binding site (−673 5′ AGG GAC TTC CCA 3′ −659). The primers used are outlined in Table 4.1. The cycle parameters were as follows: denaturation step at 94°C for 2 minutes followed by two loops as follows: the initial loop consisted of 10 cycles with 10 seconds at 94°C, 30 seconds at 63°C, and 60 seconds at 68°C and the second loop consisted of 25 cycles with 10 seconds at 94°C, 30 seconds at 63°C, and a ramp from 60 seconds to 150 seconds at 68°C. The final extension was at 68°C for 7 minutes. The fragment was then directionally ligated into pGL3-basic vector (using *MluI* and *NheI* restriction enzyme sites) using T4 DNA Ligase (New England BioLabs, Ontario, Canada) according to manufacturer's instructions. The plasmid will be referred to as pCYP2D5–NFκB–Luc (clone1) throughout this thesis. To create the plasmid pCYP2D5–mutNFκB–Luc (mut7), two point mutations were inserted in the putative NF-κB site on the CYP2D5 promoter using site the QuikChange II site-directed mutagenesis kit (Stratagene, generous gift from Dr. Sinal) following manufacturer's instructions. The sequence of the mutated NF-κB region (−673 5′ AGG TAC CTC CCA 3′ −659; point mutations are underlined) was designed to contain a novel *KpnI* restriction enzyme site. To construct the plasmid p5×κB–Luc, five repeats of the oligonucleotide TGG GGA CTT TCC GC were constructed to contain directional MluI and NheI sticky fragments and ligated into pGL3-promoter vector using T4 DNA Ligase (New England BioLabs, Ontario, Canada) according to manufacturer's instructions. The 1670 base pair

fragment encoding mouse p65 was amplified using mouse liver cDNA using Takara *Ex Taq*™ Polymerase (Takara, WI, USA; generous gift of Dr. Pasmurathi) according to manufacturer's instructions. The primers used are outlined in Table 4.1. The cycle parameters were as follows: denaturation step at 94°C for 2 minutes followed by two initial loops as follows: the initial loop consisted of 10 cycles with 20 seconds at 94°C, 30 seconds at 60°C, and 60 seconds at 72°C and the second loop consisted of 25 cycles with 20 seconds at 94°C, 30 seconds at 60°C, and a ramp from 2 minutes to 5 minutes at 72°C. The final extension was at 68°C for 5 minutes. The amplified product was ligated into pSG5 plasmid using *EcoR1* insertion sites and T4 DNA Ligase (New England BioLabs, Ontario, Canada) according to manufacturer's instructions. The plasmids encoding the alpha and beta subunits of mouse GA binding protein were obtained from Dr. Masahiko Negishi (National Institute of Environmental Health Sciences, NIH, North Carolina, USA).

4.3.4 RNA extraction and northern blot analysis

Total liver RNA was extracted using the TriZol® method according to manufacturer's instructions and quality was determined using 260/280 nm ratios. 10 µg of total RNA was electrophoresed on a 1.1% formaldehyde gel and transferred onto an immobolin–NY+ membrane (Millipore Corporation, MA, USA) overnight and fixed to the membrane by UV cross linking and heating for 1 hour at 65°C. Blots were prehybridized for 1 hour in 10mL of Sigma Perfecthyb™ Plus (Sigma, St Lois, MS) after which the [^{32}P]dCTP (Perkin and Elmer, Canada) labelled probes (RmT Random Primer Labelling kit,

Table 4.1 – A description of the primers utilized for plasmid construction.

The location of the oligonucleotide on the gene is indicating for each primer. Underlined portions of the oligonucleotide indicate sites where site-directed mutagenesis was perfromed.

Description	Oligonucleotide
Rat CYP2D5 forward primer for construction of pCYP2D5–NFκB–Luc	–952 5′ AAG GAC AAG GCC TGC ACT GTC AC 3′ –929
Rat CYP2D5 reverse primer for construction of pCYP2D5–NFκB–Luc	+33 5′ GGT CAT TGG TCT TTG GGA GCC TG 3′ +55
Mouse p65 forward primer for construction of p65-SG5 (p65)	+210 5′ TAT AAA TGC GAG GGG CGC TCA GC 3′ +234
Mouse p65 reverse primer for construction of p65-SG5 (p65)	+1745 5′ ATC AGC TCC TAA GGT GCT GAC AGC 3′ +1768
Rat mutant CYP2D5 forward primer used for site-directed mutagenesis	–685 5′ CGG GGC CAA CTG AGG TAC CTC CCA AGA TCC TCA G 3′ –648
Rat mutant CYP2D5 reverse primer used for site-directed mutagenesis	–648 5′ CTG AGG ATC TTG GGA GGT ACC TAC GTT GGC CCC G 3′ –685

117

Stratagene, USA) were added to a specific activity of 1×10^7 cpm. Blots were exposed to a storage phosphor screen (Amersham Biosciences, NJ, USA) for 16 – 24 hours and scanned using a phospher imager (Amersham Biosciences, NJ, USA). Bands were quantified using ImageQuant 5.2™ software (Amersham Biosciences, NJ, USA). A CYP2D1/5 [127] probe was constructed from forward and reverse primers (sequences in Table 4.2) using a TOPO TA Cloning® kit (Invitrogen, Ontario, Canada) according to manufacturer's instructions. The human GAPDH probe was a generous gift from Dr. C. J. Sinal (Dalhousie University, Canada).

4.3.5 Real-time quantitative PCR

A total of 5 μg of liver RNA was reverse transcribed in a 25 μL reaction containing 62.5 nM random primers, 20 Units of RNaseOUT (Invitrogen, Ontario, Canada), 1× StrataScript® RT-buffer and 12.5 Units of StrataScript® Reverse Transcriptase (both Stratagene, California, USA) according to the instructions provided with the Reverse Transcriptase enzyme. Real-time quantitative PCR was performed using an MX3000P™ instrument (Stratagene, California, USA) in a total volume of 20 μL. Reactions contained 10 μL of 2× Brilliant® SYBR® Green QPCR mix (Stratagene, California, USA), 62.5 ng of both forward and reverse primers, and 25 nM of reference dye. Cycle parameters consisted of an initial 10 minute denaturation step at 95°C followed by 42 cycles for both GABPα and GABPβ as follows: 15 second denaturation at 94°C, 30 seconds annealing at 60°C, and 30 seconds extension at 72°C. Dissociation curves were also performed to verify the amplicon being amplified. Primers specific for GABPα, GABPβ, and GAPDH were specifically designed using the published sequences for rat GABPα (Accession number XP_344003.1), rat GABPβ (Accession number XP_227439.2), and rat GAPDH

Table 4.2 – A description of the primers utilized for northern blot probe synthesis and for QPCR analyses

Description	Oligonucleotide
Rat CYP2D1/5 forward primer for northern blot probe	5' CTG ATT GGC TGC GCA CCC TGC 3'
Rat CYP2D1/5 reverse primer for northern blot probe	5' GAA CAG GTC GGC CAC AGT CAC 3'
Rat GABPα forward primer for quantitative PCR	5' CCT TCT GCT ACG CCG ACT AC 3'
Rat GABPα reverse primer for quantitative PCR	5' GCT TGA ATT CCC CTT CAT CA 3'
Rat GABPβ forward primer for quantitative PCR	5' CGC CAA AGA CAT GCT ACA GA 3'
Rat GABPβ reverse primer for quantitative PCR	5' TCT CGG GGT TAG TGT TCA CC 3'
Rat GAPDH forward primer for quantitative PCR	5' AGA CAG CCG CAT CTT CTT GT 3'
Rat GAPDH reverse primer for quantitative PCR	5' CTT GCC GTG GGT AGA GTC AT 3'

(Accession number X02231) and are described in Table 4.2. The sizes of the amplified

fragments (amplicons) were as follows: 215 base pairs for GABPα, 220 base pairs for

GABPβ, and 207 base pairs for GAPDH. Data was analysed using the $2^{-\Delta\Delta C_T}$ method

[128], where the cycle threshold (C_T) values for GABPα, GABPβ, and GAPDH were ~

32, ~27, and ~19, respectively.

4.3.6 Liver nuclear fraction isolation

Liver nuclear fractions were isolated from rats 1 and 3 hours following the i.c.v.

administration of 25 μg LPS or the i.p. administration of 5 mg kg^{-1} of LPS according to a

previously described method [129]. Briefly, animals were decapitated and livers were

homogenized in 20 mL of Homogenization Buffer (100 mM HEPES, pH 7.4, containing

25 mM KCl, 0.15 mM spermine, 0.5 mM spermidine, 1 mM EDTA, 2 M sucrose, 10%

glycerol, 5 μg mL^{-1} pepstatin A, and 5 μg mL^{-1} leupeptin) and centrifuged at 17,000 rpm

for a period of 20 minutes at 4°C. The nuclear pellet was resuspended in 10 mL of

Nuclear Lysis Buffer (100 mM HEPES, pH 7.4, containing 100 mM KCl, 3 mM $MgCl_2$,

0.1 mM EDTA, 1 mM DTT, 0.1 mM PMSF, 10% glycerol, 5 μg mL^{-1} pepstatin A, and 5

μg mL^{-1} leupeptin) and homogenized using a Dounce homogenizer. The extraction was

initialized by the addition of $(NH_4)_2SO_4$ to the nuclear lysate in drop-wise fashion to a

final concentration of 0.4 M. The viscous lysates were incubated for period of 30 minutes

on ice with constant shaking, after which they were ultra-centrifuged at 35,000 rpm for a

period of 60 minutes at 4°C. Solid $(NH_4)_2SO_4$ was added to the supernatants at a

concentration of 0.3 g mL^{-1}. The solutions were inverted several times and incubated on

ice for a period of 20 minutes until all the $(NH_4)_2SO_4$ had dissolved. The solutions were

then further centrifuged at 35,000 rpm for a period of 25 minutes at 4°C and the pellets

were re-suspended in Suspension Buffer (25 mM HEPES, pH 7.6, containing 40 mM KCl, 0.1 mM EDTA, 1 mM DTT, 10% glycerol, 5 μg mL^{-1} pepstatin A, and 5 μg mL^{-1} leupeptin) and stored at –80°C until usage. Total protein concentrations were determined according to a modified Lowry protocol [105].

4.3.7 In vitro translation

All in vitro translation (IVT) reactions were carried out initially in the presence of ^{35}S-methionine (Perkin and Elmer, Canada, generously obtained from Dr. Chris MacMaster and Dr. Paola Marignini, Dalhousie University, Halifax, N.S.) to verify efficient translation of the GABPα and GABPβ plasmids into protein. The labeling reactions were carried out in a volume of 25 μL using a T$_N$T® Quick coupled transcription/translation system (Promega, Madison, WI, USA) according to the manufacturer's instructions. Proteins labelled with ^{35}S-methionine were run on a 7.5 % ready-made BioRad gel (BioRad, Ontario, Canada), after which the gels were dried using a Bio-Rad gel dryer (Bio-Rad, Ontario, Canada) operating under vacuum and set at 80°C for 105 minutes. The gels were then exposed to a low-energy storage screen and scanned following an overnight incubation (Figure 4.1A). Since multiple bands of equal intensity were observed for the GABPα IVT product, the IVT reactions were separated on a 7.5 % ready-made BioRad gel and transferred onto an Immobilon-P membrane (Millipore Corporation) using a wet transfer apparatus (Bio-Rad, Ontario, Canada) running over night at 22 V. GABPα was detected using a specific super-shift antibody (Santa Cruz) coupled with an anti-rabbit secondary antibody conjugated to peroxidase (30 μg of GABPα primary antibody and 1/25,000 dilution for secondary antibody). Bands were visualized using enhanced chemiluminescence+ (ECL$^+$) substrate (Amersham
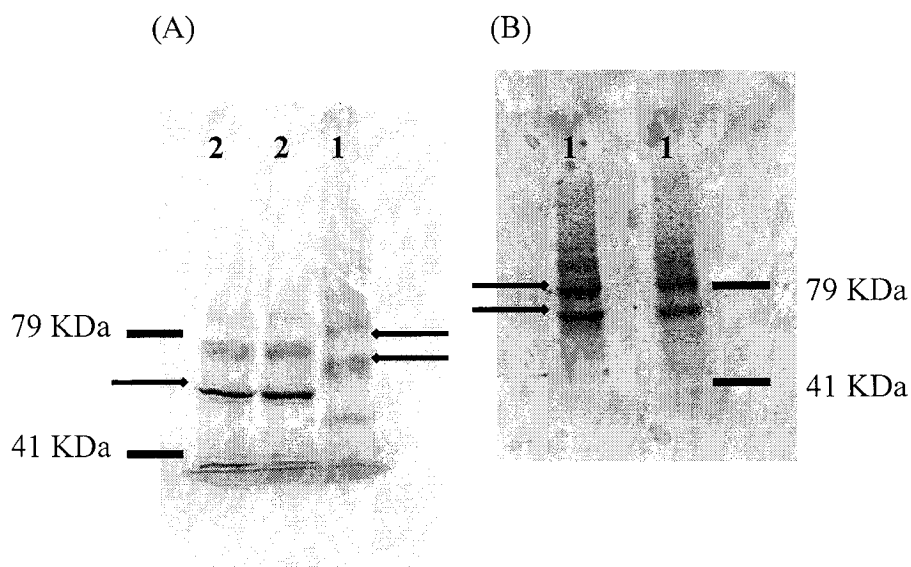
Figure 4.1. Identification of IVT translated product for GABPα and GABPβ using 35-sulpher methionine. The IVT reactions were performed as described in the methods section. A Kaleidoscope protein ladder (Bio-Rad) was run with the samples to determine approximate size. The expected molecular weights for GABPα and GABPβ are 62 and 50 KDa. The diamond-head arrows indicate bands consistent with mouse GABPα and GABPβ. Panel A consists of a scan of the gel with the radioactive IVT reactions and panel B represents the results of a western blot performed using the radioactive GABPα IVT reactions coupled with a GABPα antibody for detection of GABPα (see methods section for more details). In both panels, lane 1 refers to mouse GABPα IVT and lane 2 refers to mouse GABPβ IVT.

Biosciences). Band densities were detected using a phosphor imager (Amersham).

Following verification of the translated product, non-radioactive IVT reactions were performed using non-radiolabeled methionine and the newly translated proteins were then used in electromobility shift assays as described below.

4.3.8 Electromobility shift assays

Reactions were carried out in a total volume of 20 μL and contained 5 μg of protein, 50000 cpm of $[^{32}P]$-labeled probes, Binding Buffer (50 mM Tris-HcL, pH 7.9 containing 5 mM MgCl2, 2.5 mM EDTA, 2.5 mM DTT, 250 mM NaCl, and 20% glycerol), and 2 μg of polydIdC. Reactions were pre-incubated with the polydIdC for a period of 15 – 20 minutes after which the radiolabeled probe was added to initiate the reaction. In cases of competition, a 20× in excess non-radioactive oligonucleotide (either specific or non-specific) was utilized and was included in the reaction mixture. Reactions were incubated at room temperature for a period of 30 minutes and separated on a 5% TBE-acrylamide gel at a voltage of 170 V. The gels were then dried using a Bio-Rad gel dryer (Bio-Rad, Ontario, Canada) operating under vacuum and set at 80°C for 105 minutes. Gels were then exposed to a phospher-storage screen for a period of 16 – 24 hours and scanned using a phospher imager (Amersham Biosciences, NJ, USA). Bands were quantified using ImageQuant 5.2™ software (Amersham Biosciences, NJ, USA). The probes (described in Table 4.3) were either obtained commercially from Santa Cruz or as single-stranded oligonucleotides from Sigma Genosys (Sigma-Aldrich, Ontario, Canada) and annealed according to a standard protocol. Briefly, 300 pmoles of each oligonucleotide were incubated in Annealing Buffer (100 mM Tris, pH 7.9 and 50 mM $MgCl_2$) for 10 minutes at 95°C and allowed to gradually cool down to 25°C. For electromobility shift

Table 4.3 – A list of the primers used for EMSA studies.

The underlined portion in the last two oligonucleotides refers to the putative NF-κB or

mutant NF-κB binding site.

Description	Oligonucleotide	Source
NF-κB	5' AGT TGA GGG GAC TTT CCC AGG 3'	Santa Cruz
Ets consensus	5' GGG CTG CTT GAG GAA GTA TAA GAA T 3'	Santa Cruz
CYP2D5 NF-κB	–654 5' CCA ACG T<u>AG</u> <u>GGA CTT CCC A</u>AG ATC CT 3' –680	Single Stranded oligonucleotides annealed according to standard procedure
Mutant CYP2D5 NF-κB	–654 5' CCA ACG T<u>AG</u> <u>GTA CCT CCC A</u>AG ATC CT 3' –680	Single Stranded oligonucleotides annealed according to standard procedure

assays that required the use of IVT products, 1.5 μL of both GABPα and GABPβ or 3

μL of a luciferase positive control IVT product was incubated with the polydIdC for 20

minutes instead of nuclear fraction proteins. The binding buffer for the EMSA assays

requiring IVT products consisted of the following: 10% glycerol, 25 mM Tris-HCl (pH

7.4), 0.5 mM MgCl$_2$, 40 mM KCl, 0.1 mM EDTA, and 5 mM DTT. Everything else was

carried out as described in this section.

4.3.9 Transient transfection assays

The Fao rat hepatoma (generous gift from Dr. Mark Nachtigal, Dalhousie University,

Halifax, N.S.) and the cos7 cells (generous gift from Dr. Chris Sinal, Dalhousie

University, Halifax, N.S.) were maintained on 5% fetal bovine serum DMEM media

supplemented with 1% antibiotic/antimycotic. Transient transfections were achieved

using Lipofectamine2000^{TM} (InVitrogen, Ontario, Canada) in a total of 500 - 750 ng of

DNA in 24-well plate format according to manufacturer's instructions. All transfections

were terminated either 18 hours or 22 hours following the addition of the plasmids. The

22 hour transfections included a 4 hour treatment with TNFα at a dose of 20 ng mL^{-1}.

Tranfections were terminated by aspiration of the media and the addition of 150 μL of 1×

Reporter Lysis Buffer (Promega). The plates containing the lysed cells was left on a

shaker for 15 minutes at room temperature, and then stored in the −80°C for 15 minutes

to allow cellular lysis. Following this, the plates were spun at a speed of 4000 rpm for 10

minutes, and 50 μL and 20 μL of the lysate was assayed for β-galactosidase or luciferase

activity, respectively. For the β-galactosidase assay, 50 μL of a 2× β- galactosidase assay

(200 mM sodium phosphate buffer, pH 7.3, 2 mM MgCl$_2$, 100 mM β-mercaptoethanol,

1.33 mg mL^{-1} ONPG) was added and color was detected at 420 nm. Luciferase activities

were obtained using the luciferase assay system (Promega, Madison, WI, USA) and read

using a luminomenter (Luminoskan Ascent, Thermo Labsystems). Light unit values were

then standardized relative to β-galactosidase readings and are presented in both relative

light units (RLU) and fold induction.

4.3.10 Statistical analysis

All data are reported as the mean ± the standard error of the mean. For the *in vivo* work

and applicable EMSA gels, an unpaired Students t-test was utilized to compare saline

versus LPS groups, where $p < 0.05$ determined statistical significance. For the

transfection data, a one-way analysis of variance (1-WAY ANOVA) was used.

4.4 Results

4.4.1 CYP2D5 mRNA is downregulated following the i.p. administration of LPS

In the previous chapter CYP2D1/5 mRNA expression was shown to be downregulated at 6 and 9 hours following the i.c.v. administration of LPS [79]. The mRNA expression of CYP2D1/5 was significantly decreased by 40% and 60% at 3 and 24 hours, respectively, following i.p. administration of LPS (Figure 4.2 A). These results indicate that both i.c.v. and i.p. administration of LPS causes a significant decrease in the mRNA expression of CYP2D1/5. Examination of the binding activity of NF-κB on the CYP2D5 promoter using electromobility shift assays revealed an increase in binding of this transcription factor 3 hours following the i.p. administration of LPS (Figure 4.2 B). The binding of NF-κB was confirmed using specific and non-specific competitions and was supershifted using a p65 antibody (Figure 4.2 B).

4.4.2 Loss of CYP2D5 promoter activity following mutation of the NF-κB site

Two cell types (the Fao rat liver hepatoma cells and the African green monkey cos-7 kidney cells) were utilized to examine the effects of TNFα treatment and co-transfection of p65 subunit on the luciferase driven activity of the pCYP2D5–NFκB–Luc plasmid. This was carried out to examine whether the NF-κB fragment identified on the rat CYP2D5 promoter is active in the control of CYP2D5 gene expression. We observed higher levels of pCYP2D5–NFκB–Luc activity relative to pGL3-basic plasmid in both cell types examined. When cos-7 cells were transfected with the plasmid pCYP2D5–NFκB–Luc (clone1), a slight but not significant reduction in the promoter activity was observed in response to treatment with 20 ng mL^{-1} mouse TNFα compared to vehicle

Figure 4.2 – The effects of peripherally administered LPS on hepatic CYP2D1/5 mRNA expression and NF-κB binding. (A) For this panel, rat liver mRNA was isolated following the i.p. administration of either 5 mg kg^{-1} of LPS or saline and northern blot analyses using a rat CYP2D1/5 and a human GAPDH probe were performed as described in the methods section. LPS treated animals were compared to the respective group of saline treated animals at each time point, with each bar showing the mean results from 4 rats. The ratio of intensity of CYP2D1/5 to GAPDH was obtained for each band and the results are plotted as % control of the respective saline groups. The average absolute values for CYP2D1/5 expression (relative to GAPDH) was 8.2 arbitrary units for the 3 hour saline group and 10.9 arbitrary units for the 24 hour saline group. * CYP expression is lower compared to respective saline treated animals using an un-paired t-test (p < 0.05). (B) For this panel, rats were injected with either 5 mg kg^{-1} of LPS or saline i.p. and liver nuclear fractions were isolated 3 hours later and used in electromobility shift assays using a ^{32}-P labelled oligonucleotide containing the NF-κB region on the rat CYP2D5 promoter (see Table 4.3 for sequence). An upregulation in NF-κB binding to this region is shown, where the solid arrow indicates specific binding and the dashed arrow indicates non-specific binding. Specific and non-specific competitions indicate competitions performed with excess non-radioactive specific oligonucleotide and non-radioactive non-specific oligonucleotide, respectively. The binding of NF-κB was confirmed using supershift assays, where the diamond-head arrow indicates a supershift observed following incubation with a p65 antibody. The blot shows the results from 4 saline and 4 LPS treated rats. Lane 1 refers to probe only, while lanes 2 – 5 and 6 – 9 represent nuclear fractions obtained from saline and LPS treated animals, respectively. Lanes 10 and 11 represent specific and non-specific competitions, respectively. Lanes 12 and 13 refers to an LPS sample and a super-shifted sample, respectively.

(A)

(B)

Figure 4.2.

129
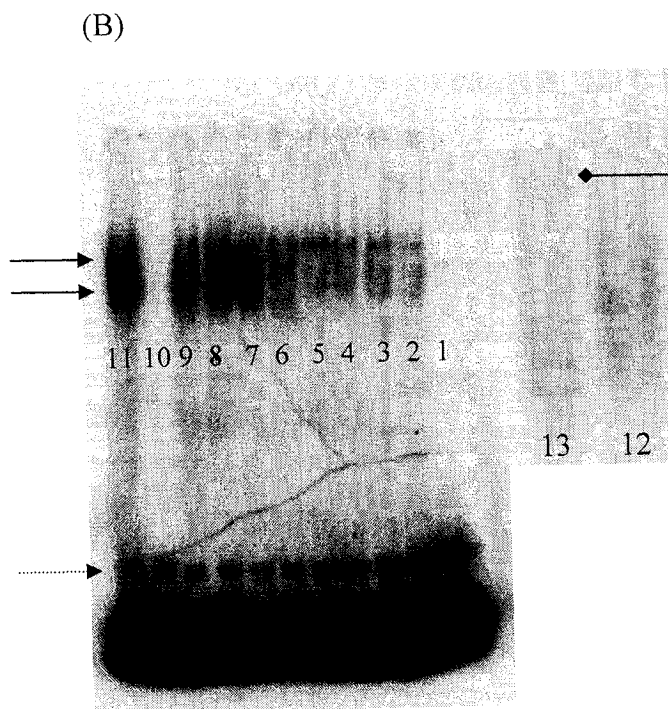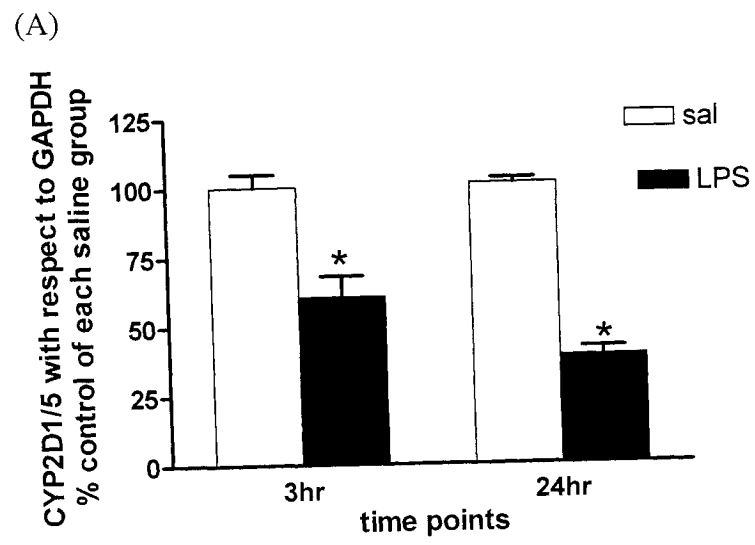
treated cells in the pSG5 group only (Figure 4.3 A and B). No effect of TNFα treatment

or p65 transfection was observed in Fao cells (Figure 4.3 C and D). Upon co-transfection

of cells with pCYP2D5–NFκB–Luc and p65, no change was observed in the promoter

activity in both the Fao cells and the cos-7 cells under both vehicle and TNFα treatment

(Figure 4.3 A – D). To determine the constitutive activity of NF-κB in both cell types, we

used the plasmid p5×κB–Luc as a positive control to determined the effects of p65 co-

transfection and TNFα treatment on luciferase activity. Using cos-7 cells, we observed

that TNFα increased the luciferase driven activity of p5×κB–Luc (p5X) in the pSG5

group, and that the co-transfection with p65 caused an augmentation in the activity of

p5×κB–Luc in both vehicle and TNFα treatments (Figure 4.4 A and B). On the other

hand, the Fao cells exhibited a high constitutive activity of NF-κB activation indicated by

the activation of p5×κB–Luc in the absence of TNFα treatment in the pSG5 group

(Figure 4.4 C and D). The co-transfection with p65 had no effect on p5×κB–Luc activity

in these cells (Figure 4.4 C and D). When the pCYP2D5–mutNFκB–Luc (mut7) was

transfected in both the cos-7 cells (Figure 4.5 A) and Fao cells (Figure 4.5 B), a 70 %

reduction in pCYP2D5–mutNFκB–Luc promoter activity compared to pCYP2D5–

NFκB–Luc promoter activity was observed.

4.4.3 GA binding protein increases the basal luciferase activity of CYP2D5 promoter

Based on the observed loss in pCYP2D5–mutNFκB–Luc promoter activity, we used the

MacVector program to compare the effects of the two base pair mutations on the NF-κB
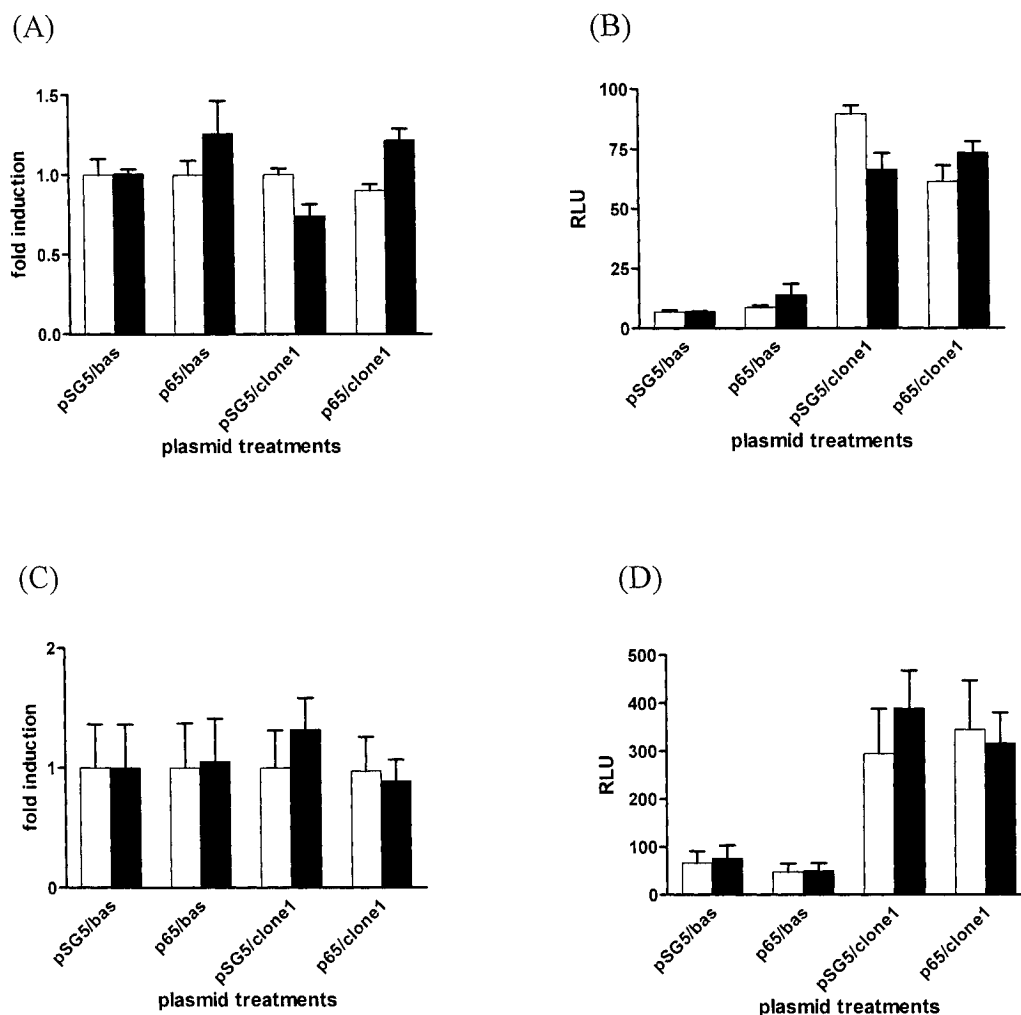
Figure 4.3 – The effects of TNFα treatment and p65 co-transfection on pCYP2D5–NFκB–Luc in cos-7 cells and Fao cells. Cells were transiently transfected with either pGL3-basic (bas) or clone1 (pCYP2D5–NFκB–Luc) in the presence of either pSG5 or p65 using Lipofectamine2000™ reagent as described in the methods section. The white bars represents results obtained from vehicle (0.1 % BSA in PBS) treated cells and the black bars represent results obtained from cells treated with 20 ng mL⁻¹ of TNFα for 4 hours following an 18 hour initial transfection (see methods section for details). The results are presented as the average of 3 experiments performed in duplicate in either relative light units (RLU) or fold induction over each representative vehicle treatment. Panels A and B represent the results obtained from cos-7 cells and panels C and D represent results obtained from Fao cells.

Figure 4.4 – The effects of TNFα treatment and p65 co-transfection on p5×κB–Luc in cos-7 cells and Fao cells. Cells were transfected with either pGL3-promoter (prom) or p5× (p5×κB–Luc) in the presence of either pSG5 or p65 using Lipofectamine2000™ reagent as described in the methods section. The white bars represents results obtained from vehicle (0.1 % BSA in PBS) treated cells and the black bars represent results obtained from cells treated with 20 ng mL^{-1} of TNFα for 4 hours following an 18 hour initial transfection (see methods section for details). The results are presented as the average of 3 experiments performed in duplicate in either relative light units (RLU) or fold induction over each representative vehicle treatment. Panels A and B represent the results obtained from cos-7 cells and panels C and D represent results obtained from Fao cells. Statistical analysis was performed using a one-way ANOVA coupled with Bonferroni post-hoc analysis, where * refers to statistical significance ($p < 0.05$) compared to vehicle treatment in the pSG5/p5X group.

132
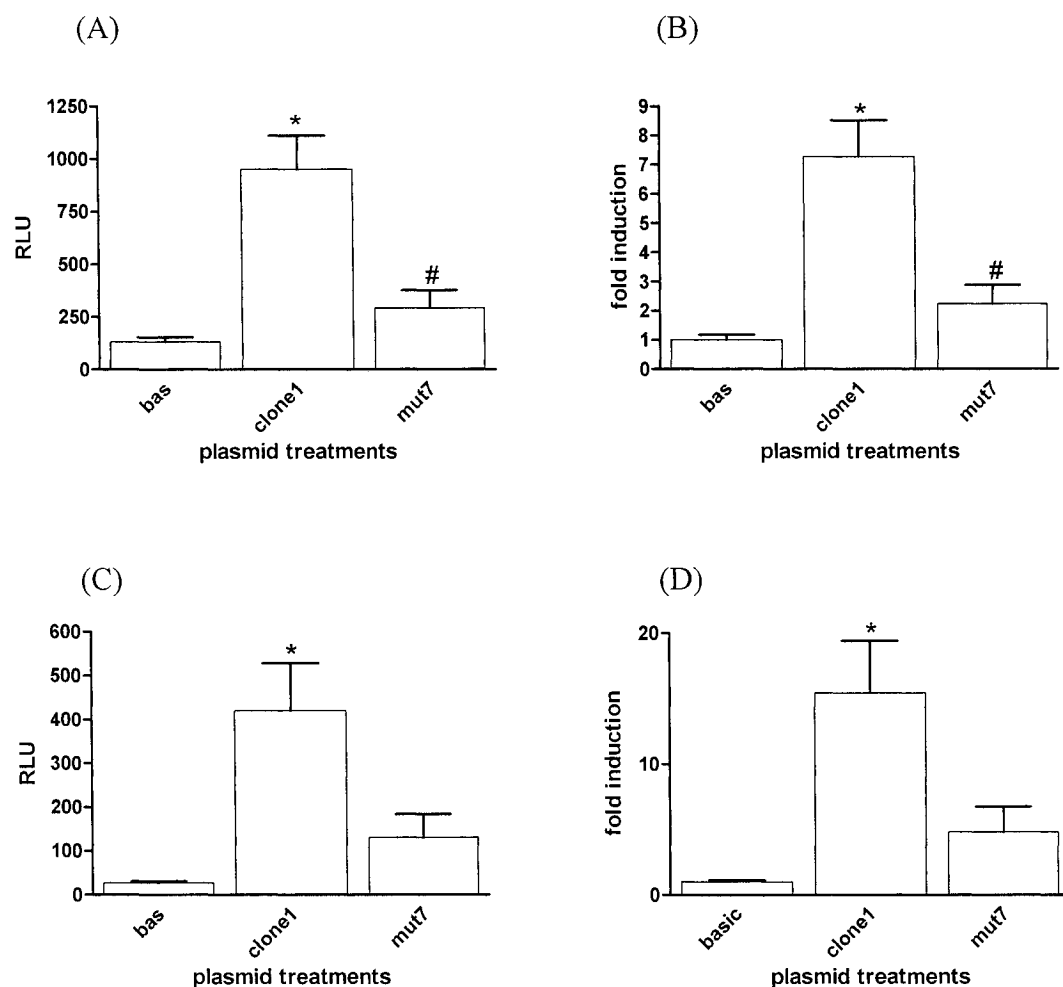
Figure 4.5 – The reduction in pCYP2D5–mutNFκB–Luc compared to pCYP2D5–
NFκB–Luc activity in cos-7 cells and Fao cells. Cells were transfected with either
pGL3-basic (bas), clone1 (pCYP2D5–NFκB–Luc), or mut7 (pCYP2D5–mutNFκB–Luc)
using Lipofectamine2000™ reagent as described in the methods section. No TNFα
treatments were utilized for these experiments. Luciferase and β-galactosidase activity
was assayed 18 hours following transfection. The results are presented as the average of 3
experiments performed in duplicate in either relative light units (RLU) or fold induction
over each representative vehicle treatment. Panels A and B represent the results obtained
from cos-7 cells and panels C and D represent results obtained from Fao cells. Statistical
analysis was performed using a one-way ANOVA coupled with Bonferroni post-hoc
analysis, where * refers to statistical significance ($p < 0.05$) compared to basic only
transfected cells, and # refers to statistical significance ($p < 0.05$) compared to clone1
only transfected cells.

putative site on the rat CYP2D5 promoter. It was determined that these two base pair point mutations leads to the loss of a binding site for GA binding protein (GABP) in addition to a disruption in the NF-κB binding site, and therefore we wanted to examine whether GABP has any control on the promoter activity of CYP2D5. Both cos-7 cells and Fao cells were transfected with increasing amounts of GABPα and GABPβ and the effects on pCYP2D5–NFκB–Luc and pCYP2D5–mutNFκB–Luc were monitored. In the cos-7 cells, the presence of GABPα and GABPβ caused a slight upregulation in the promoter activity of pCYP2D5–NFκB–Luc with increasing amounts, however this upregulatory effect was also observed on the basic plasmid, thereby making the overall effect of the GABP proteins minimal (Figure 4.6 A and B). GABPα and GABPβ had no effect on the basic plasmid when examined in the Fao cells, and an increase in promoter activity of pCYP2D5–NFκB–Luc with increasing doses of GABP proteins was observed (Figure 4.6 C and D). This effect was specific to the pCYP2D5–NFκB–Luc plasmid, since GABPα and GABPβ had no effect on the pCYP2D5–mutNFκB–Luc plasmid (Figure 4.6 C and D).

4.4.4 GA BP binding is decreased during peripheral inflammation induced by LPS

To observe whether GABP protein binding is affected in the liver during conditions of LPS-induced inflammation, we examined binding to a commercially available Ets oligonucleotide site following both the i.c.v. and i.p. administration of LPS. Our results indicated a decrease in binding to the Ets site when nuclear fractions obtained at 3 hours following the i.p. administration of LPS were used (Figure 4.7 A). Minimal Ets binding was observed in liver nuclear fractions obtained 3 hours following the i.c.v. administration of LPS (Figure 4.7 B). We then examined whether the use of a GABP

134

(A)

(B)

(C)

(D)
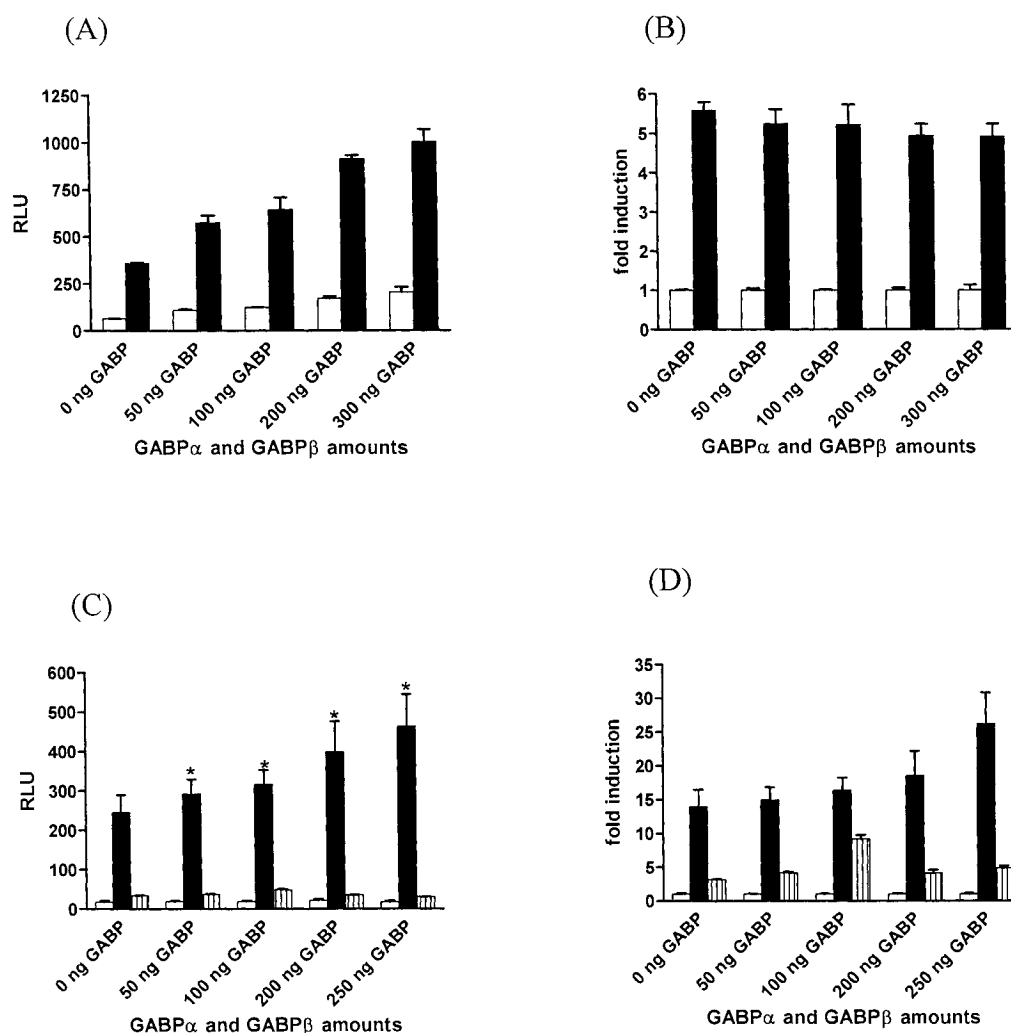
Figure 4.6 – The effects of GABPα and GABPβ on pCYP2D5–NFκB–Luc and pCYP2D5–mutNFκB–Luc in cos-7 and Fao cells. Cells were transfected with either pGL3-basic (bas), clone1 (pCYP2D5–NFκB–Luc), or mut7 (pCYP2D5–mutNFκB–Luc) using Lipofectamine2000™ reagent as described in the methods section. The white bars represent results obtained cells transfected with basic, the black bars represent results obtained from cells transfected with clone1, and the dotted bars represent results obtained from cells transfected with mut7. The results are presented as the average of 3 experiments performed in duplicate in either relative light units (RLU) or fold induction over each representative basic transfection. Panels A and B represent the results obtained from cos-7 cells and panels C and D represent results obtained from Fao cells

135

Figure 4.7 – The effects of administering LPS i.p. and i.c.v. on Ets binding in rat liver. Rats were injected with either 25 μg of LPS i.c.v. or 5 mg kg^{-1} of LPS i.p. (for details see methods section) and liver nuclear fractions were isolated 3 hours later and used in electromobility shift assays along with a ^{32}-P labelled Ets consensus oligonucleotide (see Table 4.3 for sequence). The effects on Ets binding following the i.p. administration of LPS (A) and the i.c.v. administration of LPS (B) are shown. The solid arrow indicates specific binding. Specific and non-specific competitions indicate competitions performed with excess non-radioactive specific oligonucleotide and non-radioactive non-specific oligonucleotide, respectively. The blot shows the results from 3 – 4 saline and 3 – 4 LPS treated rats. Lane 1 refers to probe only, while lanes 2 – 5 and 6 – 9 represent nuclear fractions obtained from saline and LPS treated animals, respectively. Lanes 10 and 11 represent specific and non-specific competitions, respectively.

136

(A)

(B)
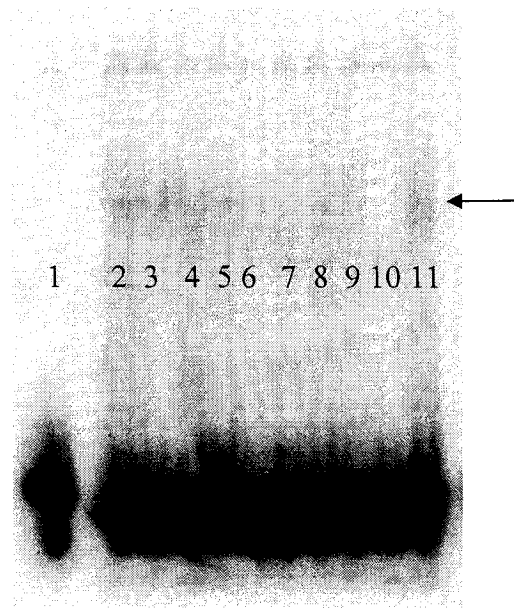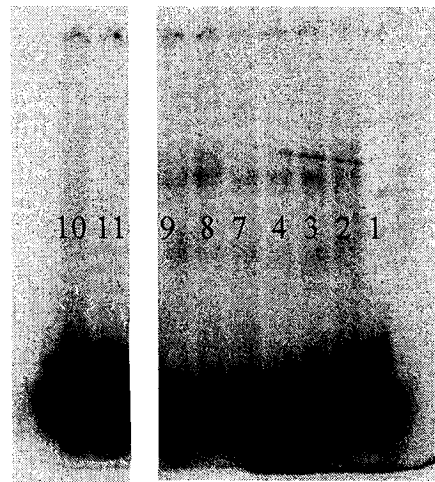
Figure 4.7.

137

supershift antibody would aid in determining whether GABP binds to the putative NF-κB

site identified on the CYP2D5 promoter. Using a GABPα specific supershift antibody

(Santa Cruz) at various incubation schedules (indicated in the legend of Figure 4.8) site

identified on the CYP2D5 promoter. Using a GABPα specific supershift antibody (Santa

Cruz) at various incubation schedules (indicated in the legend of Figure 4.8) revealed no

supershift complexes (Figure 4.8). In vitro translation was used (T_NT® Quick Coupled

transcription/translation systems, Promega, Madison, USA) to translate the GABPα and

GABPβ proteins and perform electromobility shift assays to determine whether these

proteins bind directly to the putative NF-κB region on the CYP2D5 promoter. IVT was

used because it provides a controlled situation whereby each reaction is known to contain

GABPα and GABPβ protein. We observed a high level of non-specific binding

evidenced by the presence of binding complexes in the experimental positive control

where luciferase protein (made through the IVT kit) was incubated with the ^{32}-P labeled

probes (Figure 4.9). Therefore we were unable to verify GABP binding to the CYP2D5

putative NF-κB region using the current techniques.

Finally, we were interested in examining if the i.c.v. and i.p. administration of

LPS had any effect on GABPα and GABPβ mRNA expression. Using quantitative PCR,

we observed an upregulation in GABPα mRNA expression at 2 and 24 hours following

the i.c.v. administration of LPS (Figure 4.10 A). GABPβ mRNA appeared to be increased

at 6 hours and was significantly upregulated at 24 hours following the i.c.v.

administration of LPS (Figure 4.10 B). An increase in GABPα mRNA was observed at 3

hours following the i.p. administration of LPS (Figure 4.11 A). GABPβ mRNA

138
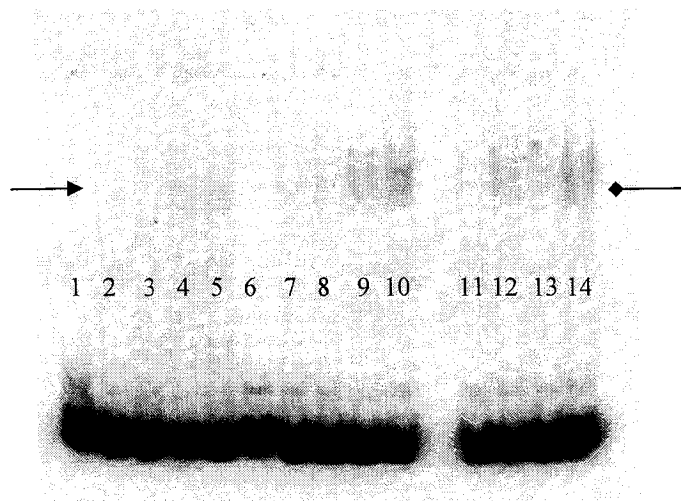
Lane #	1	2	3	4	5	6	7	8	9	10	11	12	13	14
Saline treatment	-	+	+	+	+	-	+	+	-	-	+	-	+	-
LPS treatment	-	-	-	-	-	-	-	-	+	+	-	+	-	+
CYP2D5 NF-κB	-	-	-	-	-	+	+	+	+	+	+	+	+	+
Ets consensus	+	+	+	+	+	-	-	-	-	-	-	-	-	-
GABPα Ab	-	-	-	+	+	-	+	+	+	+	+	+	+	+

Figure 4.8. No GABPα supershifts are observed on the Ets consensus or CYP2D5 NF-κB promoter. Rats were injected with either 5 mg kg^{-1} of LPS or saline i.p. and liver nuclear fractions were isolated 3 hours later and used in electromobility shift assays using a ^{32}-P labelled oligonucleotide for either the NF-κB region on the rat CYP2D5 promoter or the Ets consensus region (see Table 4.3 for sequence). The table underneath the gel indicates the presence (+) or absence (-) of the listed components. For Lanes 4, 11, and 12, the incubation with 5 µg of the GABPα supershift antibody occurred 1 hour prior to the addition of the ^{32}-P labelled probe at room temperature. For Lanes 7 – 10 the incubation with 5 µg of the GABPα supershift antibody occurred 1 hour prior to the addition of the ^{32}-P labelled probe at 4^0C. For lanes 5, 13, and 14, the incubation with 5 µg of the GABPα supershift antibody occurred 30 – 45 minutes after the addition of the ^{32}-P labelled probe at room temperature. The regular head arrow indicates binding of GABP to the Ets consensus sequence and the diamond-head arrow indicates binding of NF-κB to the CYP2D5 promoter. No GABPα supershifts were observed.

139
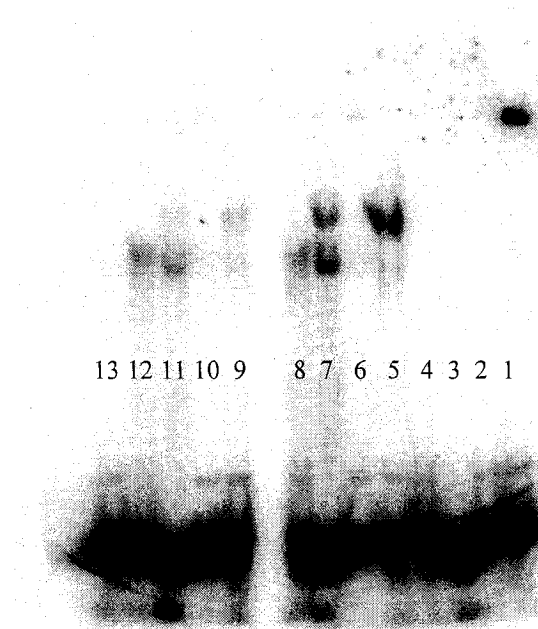
Lane #	1	2	3	4	5	6	7	8	9	10	11	12	13
CYP2D5 NF-κB	+	-	-	-	+	-	-	-	+	-	-	-	+
CYP2D5 mutNF-κB	-	+	-	-	-	+	-	-	-	+	-	-	-
Ets consensus	-	-	+	-	-	-	+	-	-	-	+	-	-
Regular NF-κB	-	-	-	+	-	-	-	+	-	-	-	+	-
Luc IVT	-	-	-	-	+	+	+	+	-	-	-	-	-
GABPα IVT	-	-	-	-	-	-	-	-	+	+	+	+	+
GABPβ IVT	-	-	-	-	-	-	-	-	+	+	+	+	+
Specific comp	-	-	-	-	-	-	-	-	-	-	-	-	+

Figure 4.9 – Inability to determine whether GABPα and GABPβ proteins obtained through IVT reactions can bind directly to the putative NF-κB region on rat CYP2D5 promoter. IVT reactions for GABPα and GABPβ were performed and used for EMSA assays as described in the methods section. The oligonucleotides used are described in Table 4.3. The table underneath the gel indicates the presence (+) or absence (-) of the listed components. No results could be deduced from the gel due to the high level of non-specific binding observed in lanes 5 – 8.

140

(A)

(B)
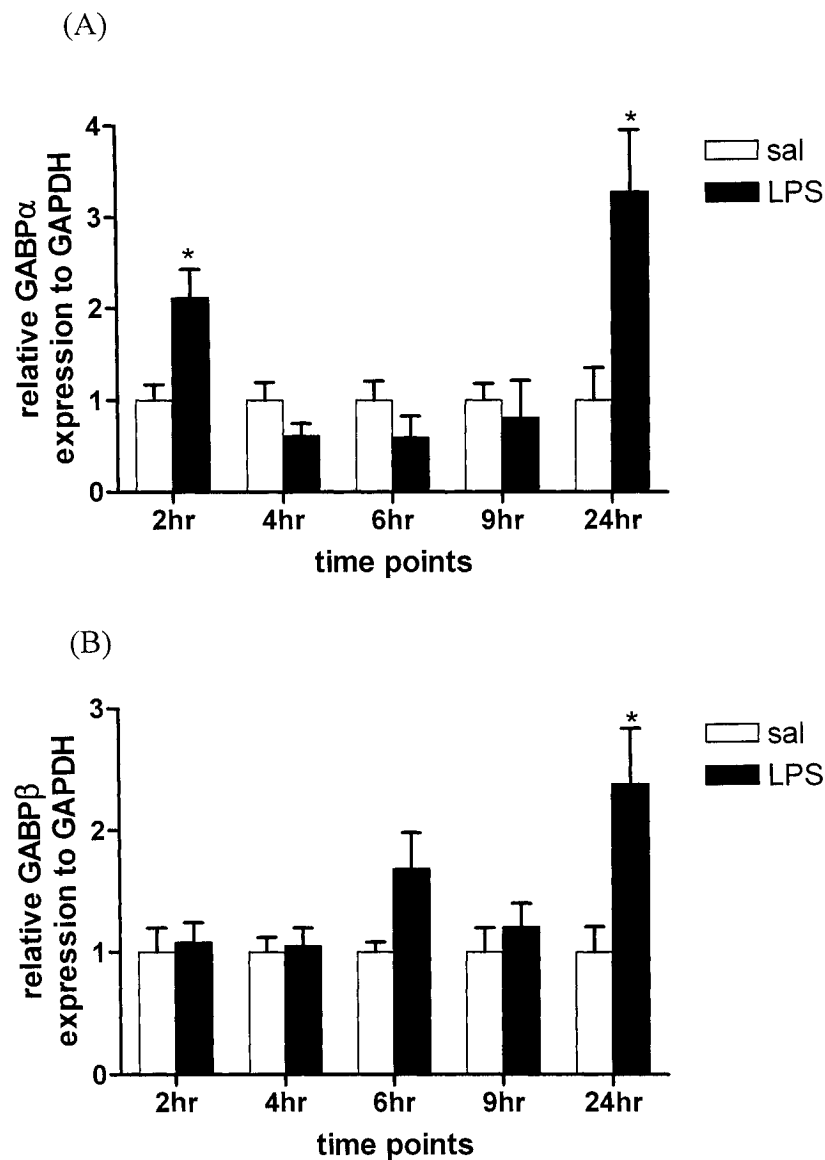
Figure 4.10. The effects of the i.c.v. administration of LPS on hepatic GABPα and GABPβ mRNA expression. Animals were administered either 25 μg of LPS or 5 μL of saline i.c.v., and liver RNA was isolated at the indicated time points. Specific primers for rat GABPα (A) and rat GABPβ (B) were utilized for quantitative PCR. LPS treated animals were compared to the respective group of saline treated animals at each time point, with each bar showing the mean results from 4 rats. The $2^{-\Delta\Delta C_T}$ method was used to obtain the fold change in GABPα and GABPβ at each time point compared to its respective saline treated group. .* GABP expression is lower compared to respective saline treated animals using an un-paired t-test (p < 0.05).

(A)

relative GABPα expression to GAPDH

10.0

7.5

5.0

2.5

0.0

*

☐ sal
■ LPS

3hr   24hr

time points

(B)

relative GABPβ expression to GAPDH

3

2

1

0

☐ sal
■ LPS

3hr   24hr
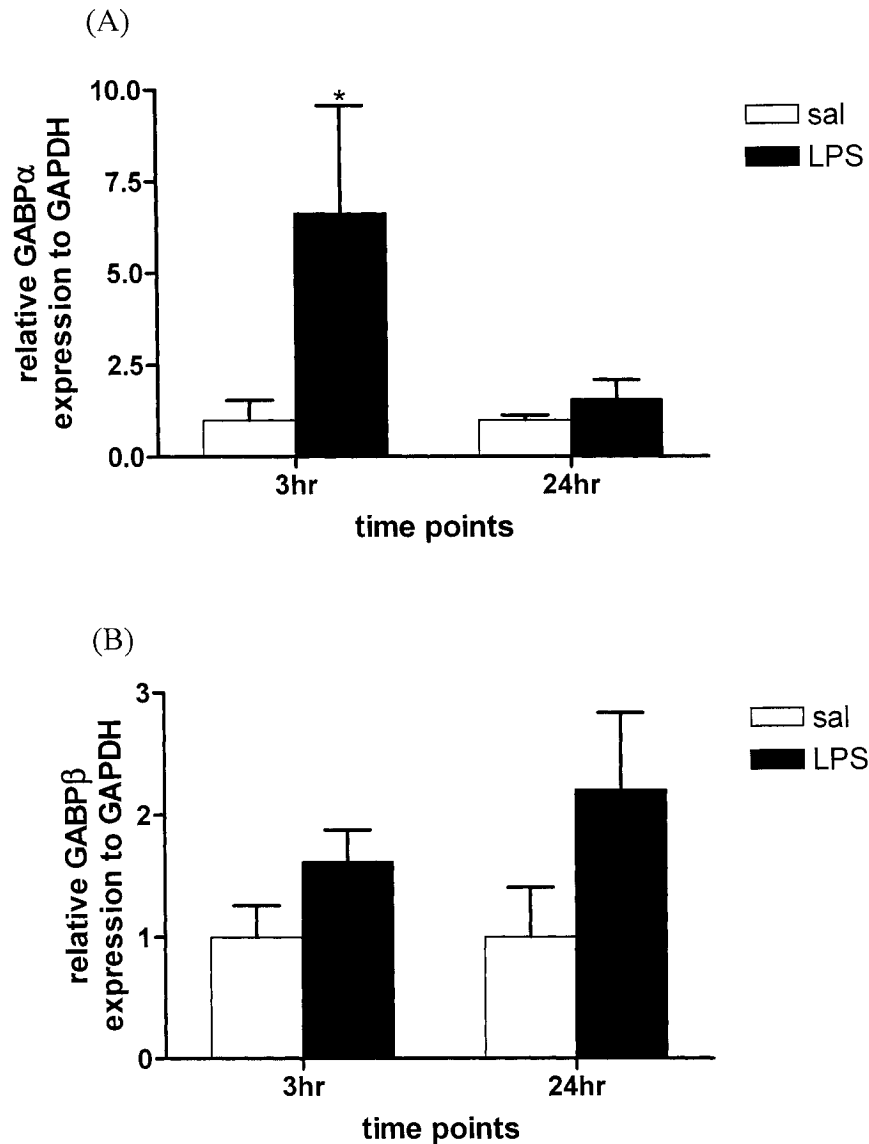
time points

Figure 4.11. The effects of the i.p. administration of LPS on hepatic GABPα and GABPβ mRNA expression. Animals were administered either 5 mg kg^{-1} LPS or saline i.p., and liver RNA was isolated at the indicated time points. Specific primers for rat GABPα (A) and rat GABPβ (B) were utilized for quantitative PCR. LPS treated animals were compared to the respective group of saline treated animals at each time point, with each bar showing the mean results from 4 rats. The $2^{-\Delta\Delta C_T}$ method was used to obtain the fold change in GABPα and GABPβ at each time point compared to its respective saline treated group. .* GABP expression is lower compared to respective saline treated animals using an un-paired t-test (p < 0.05).

expression levels were unchanged at 3 and 24 hours following the i.p. administration of LPS (Figure 4.11 B).

4.5 Discussion

In the previous chapter, we examined the potential mechanisms involved in cytochrome P450 regulation in the liver following the i.c.v. administration of LPS. We showed that LPS transfers into the serum following its administration into the lateral cerebral ventricle thereby contributing to the regulation of liver P450 through various intra-hepatic mechanisms [79]. Prominent among the intra-hepatic transcription factors, NF-κB was observed to play an important role in the regulation of various cytochrome P450 isoforms in the liver. Many studies have revealed a role for this transcription factor in the regulation of cytochrome P450; it is known to regulate the activity of CYP1A1 and CYP2C11 during inflammation [51, 83]. We have also shown that binding to a putative NF-κB site on the rat CYP2D5 promoter is increased following the i.c.v. administration of LPS [79]. The objective of the current study was to outline and provide further clarification to the role of NF-κB in the transcriptional control of rat CYP2D1/5.

CYP2D isoforms are known to play an essential role in the metabolism of a wide myriad of endogenous substrates and xenobiotics [139], and therefore understanding their regulation would be of valuable clinical importance. Rat CYP2D1, which is known to share a 95% amino acid homology with CYP2D5, is thought to exhibit the closest enzymatic similarity to human CYP2D6 [137, 139]. Our current results show that CYP2D1/5 mRNA expression is significantly downregulated at 3 and 24 hours following the i.p. administration of LPS. In addition, we observed an increase in protein binding to

143

the putative NF-κB region identified on the rat CYP2D5 promoter ([79]) using liver

nuclear fractions obtained 3 hours following the administration of 5 mg kg^{-1} LPS to rats.

Based on the effects of LPS on CYP2D1/5 mRNA expression and binding to the

NF-κB site on CYP2D5 promoter, we constructed a plasmid containing 851 base pairs of

the CYP2D5 promoter region driving luciferase activity (pCYP2D5–NFκB–Luc) to test

if the putative NF-κB region controls the transcriptional activity of CYP2D5. Initially, we

utilized the stimulation of TNFα as a mechanism to induce NF-κB activiation in both

cos-7 and Fao cells but only observed a minor effect on pCYP2D5–NFκB–Luc in cos-7

cells and no effect in the Fao cells. The use of the NF-κB p65 subunit in this *in vitro*

system also did not allow us to observe any effects on pCYP2D5–NFκB–Luc activity in

both cell types. NF-κB normally resides in an inactive state in the cytoplasm, and

translocates into the nucleus upon stimulation by an appropriate stimulus [16]. It is

known to play a role in normal and physiological conditions [16], which could be one

reason explaining the difficulty in ascertaining its role in the activity of pCYP2D5–

NFκB–Luc observed in our *in vitro* system. If the level of NF-κB activation were

saturated in either the cos-7 or Fao cells, then it would be difficult to examine if

additional stimulation by TNFα has an effect on luciferase driven activity of pCYP2D5–

NFκB–Luc. In line with this, we observed a high level of constitutive NF-κB activation

in the Fao cells even under non-stimulated conditions, indicating a possibility that there is

already existing inhibition of pCYP2D5–NFκB–Luc activity even in the absence of

stimulation. Ke *et al* were able to show that NF-κB can downregulate CYP1A1 activity

using hepa1c1c7 cells, a mouse hepatoma cell line [51]. However, the system used by

their investigations involved looking at interactions between that transcription factor and

AhR mediated induction of the cyp1a1 gene, allowing them to have a high enough basal level of cyp1a1 promoter activity to consider the effects of LPS. Iber *et al* examined the effects of NF-κB on the cyp2c11 using primary cultured rat hepatocytes [83]. It is known that hepatoma cells lines such as the hepa1c1c7 and the Fao cells are functionally different compared to primary cultured hepatocytes [156], and therefore this is could account for our inability to observe any effects of NF-κB on pCYP2D5–NFκB–Luc activity. Finally, it is possible that NF-κB plays little role in the control of the CYP2D5 gene, or that its control is on CYP2D1.

Upon examination of the effects of introducing mutations in pCYP2D5–NFκB–Luc, we were surprised to observe a 70% reduction in the activity of pCYP2D5–mutNFκB–Luc plasmid in both the cos-7 and the Fao cells. The two base pairs chosen for the mutation in the putative NF-κB site were selected based on known site required for NF-κB activity [157, 158]. Utilizing the program MacVector, we were able to determine that the point mutations used to create pCYP2D5–mutNFκB–Luc abolished a binding site for GA-binding protein (GABP), a protein belonging to the Ets family of transcription factors found in diverse species and playing a role in various critical cellular functions [143]. The idea that GABP may control a drug-metabolizing enzyme is not unique; these transcription factors have been shown to be critical in the regulation of mouse male specific cyp2d9 and human sulfonyltransferase SULT1A1 gene [144, 153]. By using increasing amounts of GABPα and GABPβ, we were able to observe a modest increase in activity of pCYP2D5–NFκB–Luc but not pCYP2D5–mutNFκB–Luc in the Fao cells only. GABPα and GABPβ had non-specific effects on the basic plasmid in cos-7 cells, thereby obliterating the overall effect on pCYP2D5–NFκB–Luc. The non-specific effects

145

of the GABP proteins we observed on pGL3-basic plasmid in cos-7 cells were also made

by others [144]. Therefore it is possible that GABP proteins exhibit some level of control

on the transcriptional activity of CYP2D5. On the other hand, it is also possible that NF-

κB is important in maintaining basal activity of the promoter based on our results of

mutating the binding site for this transcription factor.

Finally, we were interested in examining the effects of inflammation on GABP

binding and whether NF-κB interacts with either GABPα or GABPβ to control CYP2D5

transcription. Our results indicate that LPS-induced peripheral and systemic inflammation

causes an upregulation in the mRNA expression of GABPα and GABPβ. It could be

possible that the downregulation in CYP2D1/5 initiates a positive feedback loop that

causes the upregulation of GABPα and/or GABPβ, which have been shown to be

positive regulaters of CYP2D1/5 expression in this work. In terms of changes in binding,

we were able to observe a downregulation in the binding to a consensus Ets sequence

(known to bind to both GABP isoforms, Santa Cruz) only in liver nuclear fractions

obtained 3 hours following the i.p. administration of LPS. The fact that this binding was

not observed in liver nuclear fractions obtained from administering rats LPS i.c.v. is

intriguing, especially since we have previously shown that upon i.c.v. administration,

LPS is rapidly detected in the serum [79]. It is possible that the amount of LPS that is

bioavailable to cause an effect on GABP binding is higher during the i.p. route of

administration in comparison to the i.c.v. route. Our attempts to supershift GABP from

binding to either the Ets consensus site or the rat CYP2D5 putative NF-κB site were

unsuccessful. In addition, the utilization of IVT reactions containing GABP proteins did

not provide us with any useful results due to the high degree of non-specific binding we

146

obtained from these experiments. Therefore, it yet remains to be examined whether NF-κB interacts with GABP to control the transcriptional activity of rat CYP2D5. GABP proteins are known to interact with a wide variety of proteins such as Sp-1, AP-1, and CREB [147, 153, 159], however, whether NF-κB can be added to the list of proteins that can possibly interact with GABP is yet to be determined.

In summary, we were not able to show a role for NF-κB in the transcriptional control of CYP2D5, however we show that GABPα and GABPβ increases the transcriptional activity of CYP2D5 both through transfection assays with GABP isoforms and through site-directed mutagensis of the NF-κB site on the CYP2D5 promoter. We have not been able to show that NF-κB interacts with either GABP isoform.

CHAPTER 5

THE DIFFERENTIAL REGULATION OF HEPATIC CYP2E1 DURING LPS-

INDUCED PERIPHERAL AND CNS INFLAMMATION IN THE RAT

Portions of this chapter will appear in the following publication:

Abdulla D and Renton KW. (In preparation for submission) *The regulation of*

cytochrome P450 2E1 during LPS-induced inflammation in the rat.

5.1 Abstract

It is well known that inflammatory and infectious conditions differentially regulate cytochrome P450 (P450) mediated drug metabolism in the liver. We have previously outlined a potential pathway by which the intracerebroventricular (i.c.v.) administration of lipopolysaccharide (LPS) causes a downregulation in hepatic cytochrome P450 [79]. The purpose of this study was to outline the effects of LPS-induced peripheral and central nervous system inflammation on hepatic cytochrome P450 2E1 (CYP2E1), an enzyme that plays an important role in various physiological and pathological states. We report an increase in hepatic mRNA expression of CYP2E1 occurring as early as 2 – 3 hours following either the intraperitoneal (i.p.) injection of 5 mg/kg LPS or i.c.v. administration of 25 μg of LPS. This increase in CYP2E1 mRNA expression was sustained until 24 hours following LPS administration by either route. In sharp contrast to the increase in hepatic CYP2E1 mRNA, we observed a reduction in the catalytic activity of this enzyme 24 hours following either the i.c.v. or i.p. administration of LPS. The administration of LPS along with either cycloheximide or antinomycin-D did not change the LPS-mediated downregulation in hepatic CYP2E1 catalytic activity. These results support the idea that LPS acts at two different levels to regulate hepatic CYP2E1: a transcriptional level to increase CYP2E1 mRNA expression and a post-transcriptional level to regulate CYP2E1 protein and activity.

5.2 Introduction

5.2.1 CYP2E1

CYP2E1 is constitutively expressed in the liver, but can also be found extra-hepatically in organs such as the kidneys and the central nervous system (CNS) [133, 160]. Under constitutive and inducible conditions, hepatic CYP2E1 is found in the centrilobular region [161]. This hepatic localization is important because substrates of CYP2E1 such as carbon tetrachloride and acetaminophen primarily cause damage to cells in that region of the liver [161]. Most of the substrates of CYP2E1 are small and hydrophobic and include substances such as organic solvents, acetaminophen, volatile anesthetics, dimethylnitrosamine, ethanol, and acetaldehydes [162]. Some of the substrates of CYP2E1 are potent pro-carcinogenic and pro-mutagenic substances [163, 164].

CYP2E1 was initially purified from rabbits, and was subsequently identified and isolated from rats [165]. Hepatic CYP2E1 can not be detected immediately after birth, but a dramatic increase in the enzyme occurs within one week following birth due to activation of the gene [165]. CYP2E1 mRNA remains relatively constant in the livers of rats from a few days old until adult [166]. Determining the amino-acid sequence of this protein allowed its allocation to the P450 2 gene subfamily [165, 167]. The mouse CYP2E1 gene is located on chromosome 7 and contains 9 exons [165].

CYP2E1 plays an important toxicological role in various physiological disease-induced states such as alcohol induced liver injury, diabetes, and non-alcoholic steatohepatitis [89, 168, 169]. CYP2E1 induction can increase the risk of developing cancer due to its role in the production of reactive oxygen species [169]. CYP2E1 also acts as an acetone/acetal hydroxylase since the levels of acetone are 10 fold higher in

fasting CYP2E1 knockout mice compared to wildtype [57]. In addition, low levels of

CYP2E1 over-expression have been shown to cause lipid-peroxidation mediated

apoptosis [57]. CYP2E1 has pronounced oxidase activity that is usually balanced through

cellular anti-oxidants mechanisms [57]. This generation of reactive oxygen species and

other radical intermediates by CYP2E1 is thought to be a cause of apoptotic injury to

glial cells and hepatocytes, both of which contain the enzyme [57, 161]. There is a

possibility that CYP2E1 mediated toxicities are not restricted to liver cells only [57].

5.2.2 CYP2E1 Regulation

CYP2E1 regulation is thought to occur at many cellular levels. At birth and during

conditions of starvation, a rapid induction in the expression and protein levels of the

enzyme occurs [162]. CYP2E1 can also be regulated at the level of the protein, where

substrates are known to bind to the heme group of the enzyme and prevent its

proteosomal degradation [57].

5.2.2.1 Ethanol regulation of CYP2E1

It is well known that the chronic administration of ethanol causes a sharp induction in

CYP2E1 protein [163, 170]. It has been shown now that this induction occurs at the post-

translational level, since chronic ethanol administration for 21 days in rats causes an

increase in CYP2E1 protein levels without affecting the mRNA of this isoform [163].

Roberts *et al* propose that the induction of CYP2E1 by ethanol can occur through a

decrease in ubiquitin conjugation which normally targets proteins for rapid proteolysis

and destruction upon binding [170]. They propose that the decrease in ubiquitin binding

can occur either by substrate binding to prevent ubiquitin targeting or through allosteric

modification of the enzyme through ethanol binding [170].

5.2.2.2 CYP2E1 during conditions of inflammation

It is well known that the cytochrome P450 family of enzymes are differentially regulated during conditions of inflammation and infection [66, 69]. The administration of lipopolysaccharide (LPS) in the rat induces a potent acute phase response (APR) characterized by an increased production in pro-inflammatory cytokines such as TNFα, IL-1β, and IL-6 [75, 160]. The effects of inflammatory and infectious states on CYP2E1 have been examined, however little is known regarding the mechanisms of regulation of this isoform during such conditions. It has been shown that the expression and catalytic activity of CYP2E1 is downregulated in a rat hepatoma cell line following the administration of the pro-inflammatory cytokines IL-1β, TNFα and IL-6 [156]. When cytokines and/or LPS are administered to rats i.p., a downregulation in the activity and protein levels of CYP2E1 is observed [75]. IL-4 has been shown to cause an upregulation in the protein and mRNA levels of the enzyme in a human hepatoma cell line [164]. This indicates that cytokines differentially regulate CYP2E1 during conditions of inflammation. In the CNS, it has been shown that CYP2E1 is upregulated both *in vitro* and *in vivo* in the brain following LPS administration [56]. The upregulation of CYP2E1 in the CNS has been shown to occur through an increase in mRNA, which is an unusual method of induction for this isoform [133].

5.2.2.3 Role of transcription factors in CYP2E1 regulation

It is thought that the majority of CYP2E1 regulation occurs at the level of the protein [161], however regulation at the transcriptional level does occur [156]. Starvation and IL-4 administration are both documented examples of transcriptional mediated induction of CYP2E1, however the exact mechanism by which an increase in CYP2E1 occurs is still

unclear [156]. It has been postulated that an AP-1 site found on the CYP2E1 promoter may be responsible for the upregulation in mRNA observed in response to IL-4 treatment [160, 171]. One of the main liver enriched transcription factors known to play a role in the transcriptional control of constitutive CYP2E1 expression in the liver is hepatocyte nuclear factor-1 (HNF-1) [156, 166]. HNF-1 is also thought to play a role in the regulation of CYP2E1 during endotoxin treatment [160]. Tindberg *et al* recently identified a repressor jun-binding site on intron 2 segment of CYP2E1 responsible for the downregulation of the enzyme during LPS administration using primary cortical glial cells [57]. Pan *et al* used STAT1 (signal transducers and activators of transcription proteins) knockout mice to show that this transcription factor may play a role in the post-transcriptional regulation of CYP2E1.

5.2.3 Objective

The objective of this section was to examine the mechanisms that regulate CYP2E1 during LPS-mediated peripheral and CNS inflammatory models. We observed an increase in mRNA expression of CYP2E1 and a decrease in enzyme activity following either the i.c.v. or i.p. administration of LPS. Using inhibitors of transcription and translation to examine the LPS-mediated effects on hepatic CYP2E1, we present evidence that hepatic CYP2E1 regulation during conditions of LPS-induced inflammation in the rat occurs mainly at the post-transcriptional level.

153

5.3 Materials and methods

5.3.1 Reagents

All laboratory reagents were purchased from Sigma (St. Louis, MO) with the exceptions noted in the text. Gel purified *Escherichia coli* lipopolysaccharide (LPS) of sereotype 0127:B8 (Sigma, St Louis, USA) was utilized in the experiments as outlined below.

5.3.2 Animals and treatment

Male Sprague-Dawley rats (125 – 150 grams) were obtained from Charles River Laboratories (Quebec, Canada) and were housed on corncob bedding for a period of 5 days on a 12-hour light/dark cycle. All animal procedures were performed according to the Dalhousie University Committee on Laboratory Animals following the guidelines established by the Canadian Council on Animal Care. Rats were allowed *ad-libitum* access to food and water prior to and following the experimental procedure. Intracerebroventricular (i.c.v.) injections into the lateral ventricle were performed using a KOPF® sterotaxic instrument. The coordinates utilized relative to bregma were 1.7 mm lateral and 4.7 mm below the skull surface. On the day of the experiment, rats were anaesthetized using enflurane and maintained on a 4% level of the anaesthetic during the surgery. A dose of 25 µg LPS was dissolved in pyrogen-free saline and injected in a volume of 5 µL. To induce systemic inflammation, animals were injected intraperitoneally with a dose of 5 mg kg^{-1} LPS (in 100 µL saline). This dose has been previously shown to cause a downregulation in P450 levels [155]. Figure 5.1 illustrates the dosing schedule for the experiments utilizing cycloheximide (CHX) or actinomycin-D (AD) at the doses of 10 mg kg^{-1} for CHX and 7 mg kg^{-1} for AD. These doses were chosen based upon previous reports outlining that the use of these antibiotics at the specified

154
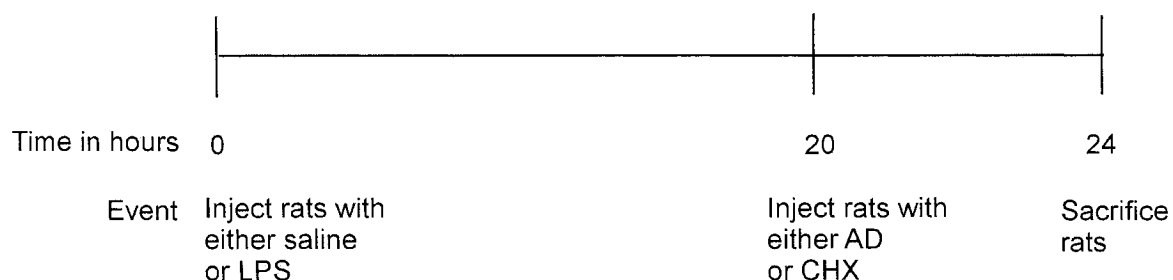
Figure 5.1. Schematic indicating the dose schedules for the administration of cycloheximide and actinomycin-D. The time of the three events indicated (rats were injected with saline or LPS by either the i.c.v. or i.p. route, rats injected with either CHX or AD i.p., animal sacrifice) is given in hours beginning from time 0. The doses for CHX and AD were 10 mg kg^{-1} and 7 mg kg^{-1}, respectively.

doses for 6 hours was sufficient to cause an inhibition in the P450 isoform CYP3A [172]. The results for the CHX and AD experiments were obtained 24 hours following LPS administration by either route because both the upregulation in CYP2E1 mRNA and the downregulation in CYP2E1 activity can be observed at this time point. All experiments utilized 4 – 6 rats per treatment.

5.3.3 Microsomal fraction preparation and CYP2E1 metabolism assay

Liver microsomes were isolated at 2 and 24 hours following i.c.v. and i.p. injections as described previously [75] and suspended in a glycerol-phosphate buffer (50 mM KH_2PO_4 buffer, pH 7.4, containing 20% glycerol and 0.4% KCl). Liver microsomal fractions were stored at $-80^{\circ}C$ until usage. Protein concentrations were determined according to a modified Lowry protocol [105].

The formation of 6-hydroxychlorzoxazone (6-OH CZX) from chlorzoxazone (CZX) was used as a specific marker for rat CYP2E1 activity [173]. Incubation mixtures containing 1 mg of total microsomal protein were incubated with 100 μM of CZX in 50 mM of KH_2PO_4 buffer, pH 7.4. The reaction mixtures were pre-incubated in a $37^{\circ}C$ water bath with a shaker set at 100 oscillations/minute for a period of 2 minutes. Reactions were initiated by the addition of the cofactor NADPH (1 mM) and incubated at $37^{\circ}C$ for a period of 10 minutes. Reactions were terminated by the addition of 5 mL of dichloromethane at which point 2000 ng of the internal standard pentoxifylline was added to each sample. The samples were centrifuged at 2700 rpm for a period of 10 minutes, and the lower organic phase containing the metabolites and internal standard was transferred into a clean glass tube and evaporated to dryness using a nitrogen evaporator. The metabolite and internal standard residues were then reconstituted in 125 μl of HPLC

mobile phase (22% acetonitrile in 0.5% H_3PO_4, v/v), and 50 µl was separated on a reverse phase C-18 (25 cm × 4.5 mm I.D.) analytical column (Beckman Coulter, Fullerton, CA, USA) attached to a Waters 2690 Separations Module. The mobile phase flow rate for separation was set at 1.0 ml min^{-1}, with detection by UV absorption at 287 nm (Waters 2487 Dual λ absorption unit). The approximate retention times were 6.7 minutes for 6-OH CZX, 7.8 minutes for pentoxifylline, and 21.5 minutes for CZX.

5.3.4 Western blot analysis

A total of 25 µg of microsomal protein was separated by electrophoresis on a 7.5 % ready-made gel (Bio-Rad, Canada) and transferred on to an Immobilon P membrane using a Bio-RAD wet transfer apparatus running overnight at 90 mA (Bio-Rad, Canada). CYP2E1 was detected using a polyclonal anti-rat CYP2E1 antibody (1/1000 dilution) (Gentest) and an anti-goat secondary IgG antibody conjugated to peroxidase (1/100,000). Proteins bands were visualized using a Storm scanner (Amersham Biosciences, NJ, USA) and enhanced chemiluminescence plus (ECL$^+$; Amersham Biosciences, NJ, USA). Bands were quantified using ImageQuant 5.2™ software (Amersham Biosciences, NJ, USA). Amido black staining was utilised to ascertain equal protein loading.

5.3.5 RNA extraction and northern blot analysis

Liver samples (~100 mg) were obtained for RNA isolation at 2, 4, 6, 9, and 24 hours following the i.c.v. injection of 25 µg of LPS and at 3 and 24 hours following the i.p. injection of 5 mg kg^{-1} LPS. Total liver RNA was extracted using the TriZol® method according to manufacturer's instructions and quality was determined using 260/280 nm ratios. 10 µg of total RNA was electrophoresed on a 1.1% formaldehyde gel and transferred onto an immobolin–NY+ membrane (Millipore Corporation, MA, USA)

overnight and fixed to the membrane by UV cross linking and heating for 1 hour at 65°C.

Blots were prehybridized for 1 hour in 10mL of Sigma Perfecthyb™ Plus (Sigma, St

Lois, MS) after which the $[^{32}P]dCTP$ (Perkin and Elmer, Canada) labelled probes (RmT

Random Primer Labelling kit, Stratagene, USA) were added to a specific activity of 1 ×

10^7 cpm. Blots were exposed to a storage phosphor screen (Amersham Biosciences, NJ,

USA) for 16 – 24 hours and scanned using a phospher imager (Amersham Biosciences,

NJ, USA). Bands were quantified using ImageQuant 5.2™ software (Amersham

Biosciences, NJ, USA). A CYP2E1 [174] probe was constructed from forward and

reverse primers (CYP2E1 FWD 5′ CTG ATT GGC TGC GCA CCC TGC 3′, CYP2E1

REV 5′ GAA CAG GTC GGC CAC AGT CAC 3′, primer sequences verified using an

NCBI BLAST search) using a TOPO TA Cloning® kit (Invitrogen, Ontario, Canada)

according to manufacturer's instructions. The human GAPDH probe was a generous gift

from Dr. C. J. Sinal (Dalhousie University, Canada).

5.3.6 Liver nuclear fraction isolation

Liver nuclear fractions were isolated from rats 3 hours following either the i.c.v.

administration of 25 µg LPS or the i.p. administration of 5 mg kg^{-1} of LPS according to a

previously described method [129]. Briefly, animals were decapitated and livers were

homogenized in 20 mL of Homogenization Buffer (100 mM HEPES, pH 7.4, containing

25 mM KCl, 0.15 mM spermine, 0.5 mM spermidine, 1 mM EDTA, 2 M sucrose, 10%

glycerol, 5 µg mL^{-1} pepstatin A, and 5 µg mL^{-1} leupeptin) and centrifuged at 17,000 rpm

for a period of 20 minutes at 4°C. The nuclear pellet was resuspended in 10 mL of

Nuclear Lysis Buffer (100 mM HEPES, pH 7.4, containing 100 mM KCl, 3 mM MgCl$_2$,

0.1 mM EDTA, 1 mM DTT, 0.1 mM PMSF, 10% glycerol, 5 µg mL^{-1} pepstatin A, and 5

μg mL^{-1} leupeptin) and homogenized using a Dounce homogenizer. The extraction was initialized by the addition of $(NH_4)_2SO_4$ to the nuclear lysate in drop-wise fashion to a final concentration of 0.4 M. The viscous lysates were incubated for period of 30 minutes on ice with constant shaking, after which they were ultra-centrifuged at 35,000 rpm for a period of 60 minutes at 4°C. Solid $(NH_4)_2SO_4$ was added to the supernatants at a concentration of 0.3 g mL^{-1}. The solutions were inverted several times and incubated on ice for a period of 20 minutes until all the $(NH_4)_2SO_4$ had dissolved. The solutions were then further centrifuged at 35,000 rpm for a period of 25 minutes at 4°C and the pellets were re-suspended in Suspension Buffer (25 mM HEPES, pH 7.6, containing 40 mM KCl, 0.1 mM EDTA, 1 mM DTT, 10% glycerol, 5 μg mL^{-1} pepstatin A, and 5 μg mL^{-1} leupeptin) and stored at −80°C until usage. Protein concentrations were determined according to a modified Lowry protocol [105].

5.3.7 Electromobility shift assays

Reactions were carried out in a total volume of 20 μL and contained 5 μg of protein, 50000 cpm of [^{32}P]-labeled probes, 1× Binding Buffer (50 mM Tris-HcL, pH 7.9 containing 5 mM MgCl$_2$, 2.5 mM EDTA, 2.5 mM DTT, 250 mM NaCl, and 20% glycerol), and 2 μg of polydIdC. Reactions were pre-incubated with the polydIdC for a period of 15 minutes after which the radiolabeled probe was added to initiate the reaction. In the case of non-specific competitions, a 20× excess amount of non-radioactive non-self oligonucleotide was utilized in the reaction mixture. In cases of specific competitions, a 20× excess amount of non-radioactive self-oligonucleotide was utilized and was included in the reaction mixture. Reactions were incubated at room temperature for a period of 30 minutes and run on a 5% TBE-acrylamide gel at a voltage of 170 V. The gels were then

dried using a Bio-Rad gel dryer (Bio-Rad, Ontario, Canada) operating under vacuum and set at 80°C for 105 minutes. Gels were then exposed to a phospher-storage screen for a period of 16 – 24 hours and scanned using a phospher imager (Amersham Biosciences, NJ, USA). Bands were quantified using ImageQuant 5.2™ software (Amersham Biosciences, NJ, USA). The probes (described in Table 5.1) were obtained as single-stranded oligonucleotides from Sigma Genosys (Sigma-Aldrich, Ontario, Canada) and annealed according to a standard protocol. Briefly, 300 pmoles of each oligonucleotide were incubated in Annealing Buffer (100 mM Tris, pH 7.9 and 50 mM $MgCl_2$) for 10 minutes at 95°C and allowed to gradually cool down to 25°C.

5.3.8 Statistical analysis

All data are reported as the mean ± the standard error of the mean. An unpaired t-test was utilized to compare saline versus LPS groups in the time response experiments, where $p < 0.05$ determined statistical significance. Unpaired t-tests were performed in the time response experiments because they utilized animals injected on separate days, and were performed because the main interest of this work was to outline differences at each time point being studied. Data is presented in one graph for all time points for convenience. A two-way analysis of variance was used to analyze the CHX and AD experiments coupled with Bonferroni post-hoc tests.

Table 5.1 – List of the EMSA oligonucleotides.

Description	Oligonucleotide	Source
CYP2E1 AP-1	5' CTG ACC GTG ATT CAC CAG AAT 3'	Single stranded oligonucleotides annealed according to standard procedure
CYP2E1 MKK3	5' TTC TGC TCT CAT TTT CCA AAC AGG C 3'	Single stranded oligonucleotides annealed according to standard procedure
CYP2E1 HNF1α	5' TGA AAT GAT AGC CAA CTG CAG CTA ATA ATA AAC CAG TAC 3'	Single stranded oligonucleotides annealed according to standard procedure

5.4 Results

5.4.1 Hepatic CYP2E1 mRNA levels are upregulated in response to the i.c.v. or i.p. administration of LPS

It has previously been shown that the central or peripheral injection of LPS causes a downregulation in hepatic cytochrome P450 expression and catalytic activity [75, 155]. To examine the effects of the i.c.v. or i.p. administration of LPS on hepatic CYP2E1, the mRNA expression of this isoform was examined in the liver using northern blotting at various time points following LPS administration by either route. We observed a significant increase in the mRNA levels of hepatic CYP2E1 occurring as early as 2 hours and this persisted up to 24 hours following the i.c.v. administration of 25 μg of LPS compared to saline treatment (Figure 5.2 A and B). Similarly, a significant upregulation in the expression of hepatic CYP2E1 mRNA was observed at 3 and 24 hours following the i.p. administration of 5 mg kg^{-1} LPS compared to saline treated animals (Figure 5.2 C).

We then examined the role of several transcription factors as potential mediators of the upregulation in hepatic CYP2E1 expression following the i.c.v. or i.p. administration of LPS. We utilized an HNF-1α sequence previously identified by Ueno *et al* for the constitutive activation of CYP2E1 ([166]) to determine whether this transcription factor plays a role in the changes in CYP2E1 mRNA observed in this study. Our results indicate that the binding to HNF-1α is slightly increased following the i.c.v. administration of LPS, whereas the effects of the i.p. administration of LPS is to decrease HNF-1α binding (Figure 5.3). The binding of HNF-1α was not affected by the presence of 20× excess nonself non-radioactive oligonucleotide, and was completely abolished in

(A)

(C)

(B)
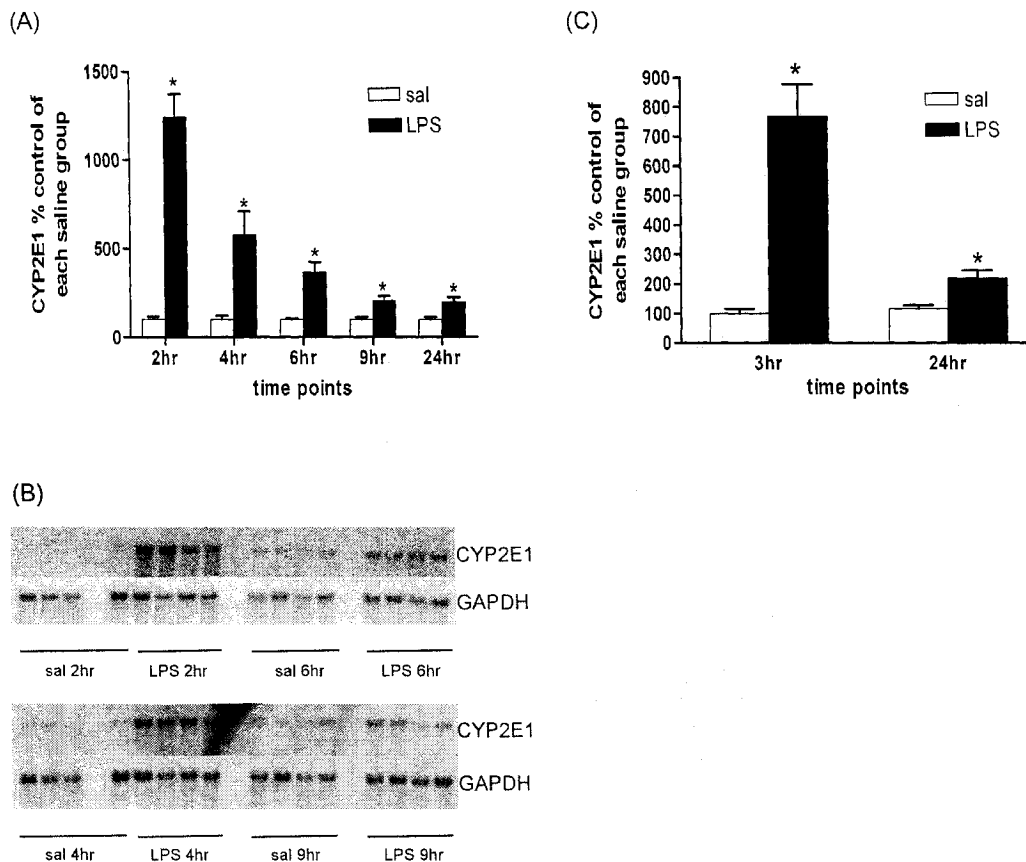
Figure 5.2. CYP2E1 mRNA is upregulated in response to the i.c.v. and i.p. administration of LPS. Total liver mRNA was extracted and northern blotting was performed as outlined in the Methods section. The effects of the i.c.v. administration of 25 μg of LPS on CYP2E1 mRNA relative to GAPDH is shown in panel (A), with representative blots shown in panel (B). The effects of the i.p. administration of 5 mg kg^{-1} LPS on CYP2E1 mRNA relative to GAPDH is shown in panel (C). Each bar represents the average results from 4 animals ± S.E.M. The average absolute values for CYP2E1 expression (with respect to GAPDH) following the i.c.v. administration of LPS was 0.051 for the 2 hour saline samples, 0.049 for the 4 hour saline samples, 0.108 for the 6 hour saline samples, 0.079 for the 9 hour saline samples, and 0.091 for the 24 hour saline samples. The average absolute values for CYP2E1 expression (with respect to GAPDH) following the i.p. administration of LPS was 0.12 for the 3 hour saline samples and 0.22 for the 24 hour saline samples. * CYP2E1 expression higher compared to respective saline treated animals using a non-paired t-test (p < 0.05).

163

the presence of 20× excess self non-radioactive oligonucleotide (Figure 5.3). Using the published sequence for CYP2E1 [166], we identified a putative activator protein-1 (AP-1) binding region using MacVector on intron segment 1 of the CYP2E1 gene. Examining the binding activity of this AP-1 region using EMSA assays revealed an increase in binding to nuclear fractions isolated 3 hours following either the i.c.v. administration of 25 µg LPS (Figure 5.4 A) or the i.p. administration of 5 mg kg^{-1} LPS (Figure 5.4 B). The binding of AP-1 was not affected by the presence of 20× excess non-self non-radioactive oligonucleotide, and was completely abolished in the presence of 20× excess self non-radioactive oligonucleotide. Examination of a map kinase kinase-3 (MKK3)/CAAT-enhancer binding protein (C/EBP) region [133] using hepatic nuclear fractions obtained 3 hours following the administration of 5 mg kg^{-1} LPS i.p. indicated that no binding occurred for this transcription factor on the CYP2E1 promoter (Figure 5.4 C).

5.4.2 CYP2E1 catalytic activity and protein is downregulated in response to the i.c.v. or i.p. administration of LPS

The effects of administering 25 µg of LPS i.c.v. or 5 mg kg^{-1} LPS i.p. on hepatic CYP2E1 catalytic activity and protein levels are shown in Figures 5.5 and 5.6. A significant decrease in the catalytic activity of hepatic CYP2E1 occurred 24 hours following either the i.c.v. or i.p. administration of LPS (Figure 5.5 A and B). CYP2E1 activity in the liver was not affected at 2 hours following i.c.v. or i.p. administration of LPS (Figure 5.5A and B). To examine whether changes in protein levels contribute to the downregulation in hepatic CYP2E1 catalytic activity, we examined the effects of the i.c.v. or i.p. administration of LPS on CYP2E1 protein levels in the liver using western
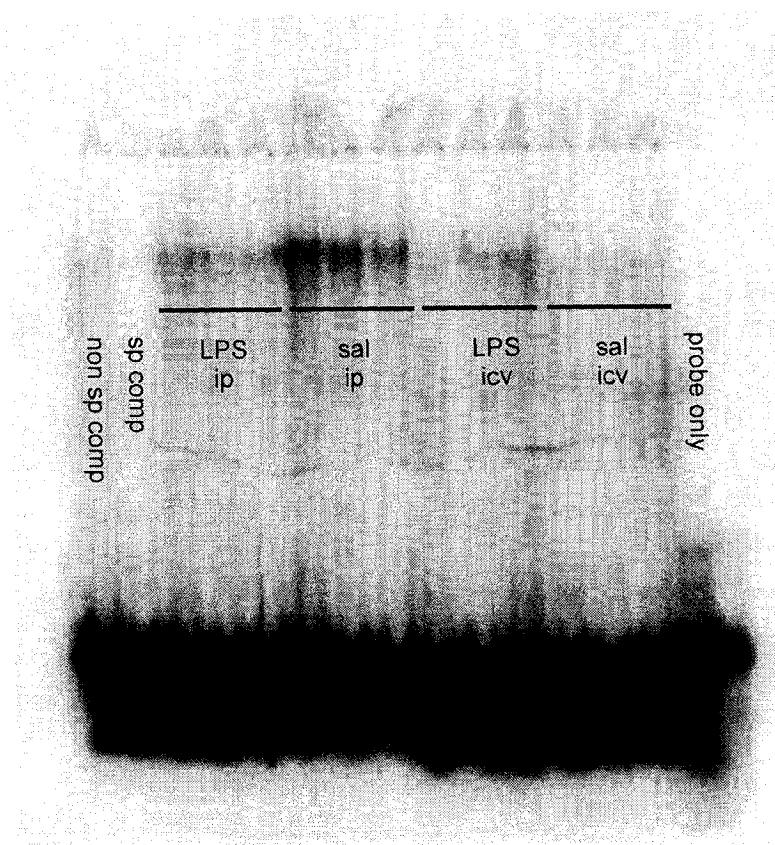
Figure 5.3 – The effects of LPS on HNF-1α binding on CYP2E1 promoter. The binding of HNF-1α to a region on CYP2E1 promoter known to bind to this transcription factor (see [166]) was examined. Liver nuclear fractions were isolated at 3 hours following either the i.c.v. or i.p. administration of LPS and EMSA assays were performed as described in the methods section. Lanes are as indicated on the gel. Specific competitions (spec comp) and non-specific competitions (non-spec comp) indicate competitions performed with excess non-radioactive specific oligonucleotide and non-radioactive non-specific oligonucleotide, respectively, as described in the Methods section.

(A)

(B)

(C)
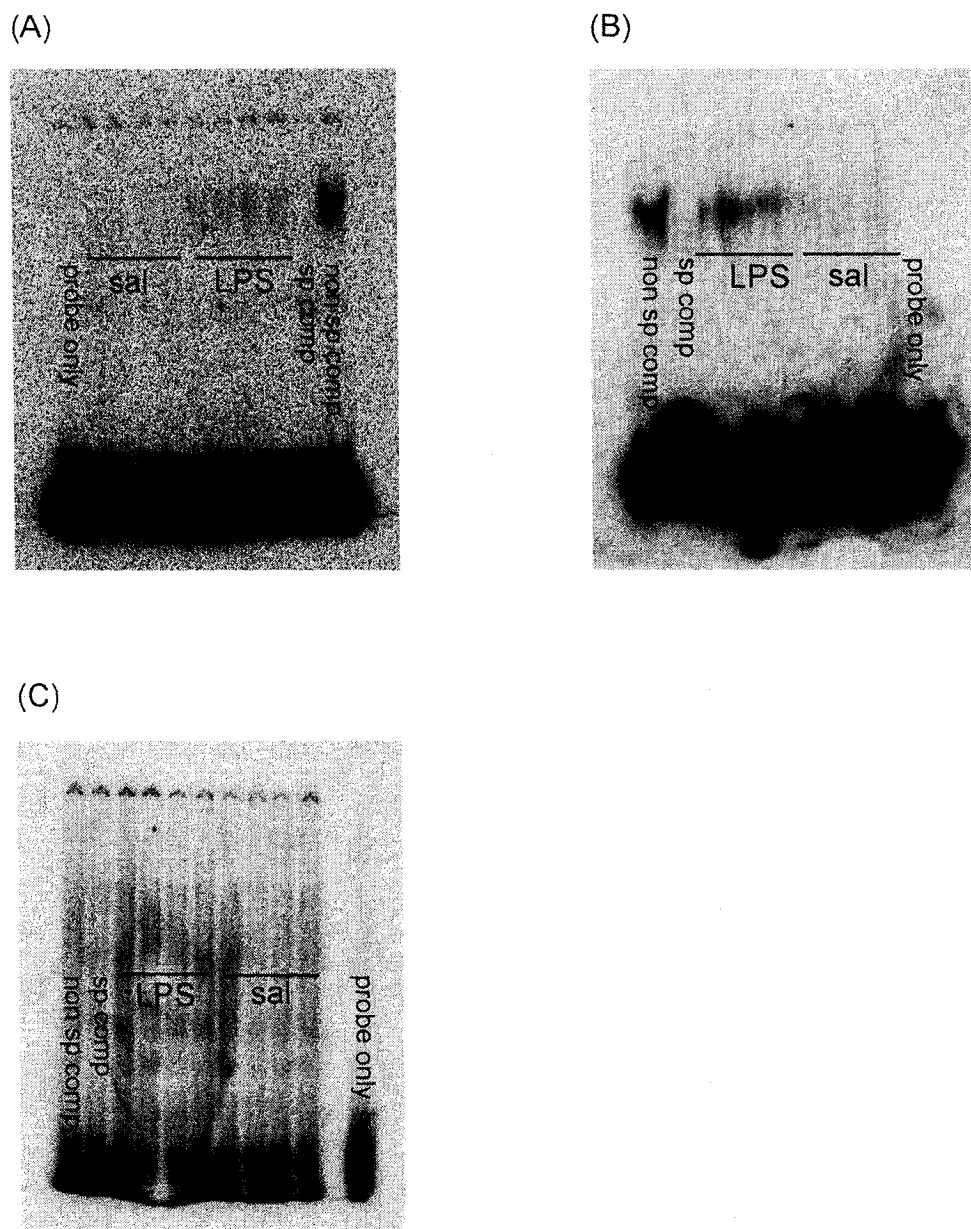
Figure 5.4 – The effects of LPS on AP-1 and MKK3 binding on CYP2E1 promoter.
The binding of AP-1 to liver nuclear fractions obtained 3 hours following the i.p. (A) and
i.c.v. (B) administration of LPS to rats is shown. The effects of the administration of 25
μg of LPS i.c.v. to rats on MKK3 binding is is shown in (C). Specific competitions (spec
comp) and non-specific competitions (non-spec comp) indicate competitions performed
with excess non-radioactive specific oligonucleotide and non-radioactive non-specific
oligonucleotide, respectively, as described in the Methods section.

166

(A)

(B)
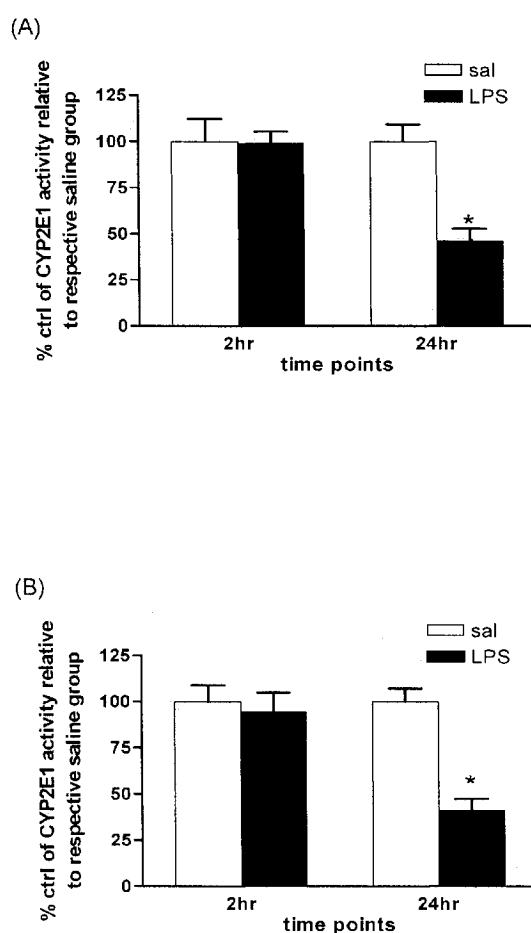
Figure 5.5. CYP2E1 catalytic activity is downregulated in response to the i.c.v. and i.p. administration of LPS. Rat liver microsomes were prepared at 2 and 24 hours using animals injected with either 25 μg of LPS i.c.v. or 5 mg kg^{-1} LPS i.p. and CYP2E1 catalytic activity was determined using the hydroxylation of the substrate CZX. The results from the i.c.v. administration of LPS are shown in (A) and the results from the i.p. administration of LPS are shown in (B). The results are plotted as % control of the respective saline groups, with each bar representing the average results from 4 animals ± S.E.M. * CYP2E1 expression lower compared to respective saline treated animals using a non-paired t-test (p < 0.05). The absolute value for the saline 2 hour time point (LPS given i.c.v.) is 85.7 ng 6OH CZX/mg protein/min and for the saline 24 hour time point (LPS given i.c.v.) is 118.3 ng 6OH CZX/mg protein/min. The absolute value for the saline 2 hour time point (LPS given i.p.) is 131.6 ng 6OH CZX/mg protein/min and for the saline 24 hour time point (LPS given i.p.) is 98.1 ng 6OH CZX/mg protein/min.

blotting. We observed a significant downregulation in hepatic CYP2E1 protein at 24

hours following the administration of 25 μg LPS i.c.v., and no change in the protein

levels at all other time points examined (Figure 5.6 A and B).

5.4.3 Cycloheximide and actinomycin-D have no effect on the LPS-induced

downregulation in catalytic CYP2E1 activity

Since we observed a reduction in the catalytic activity of hepatic CYP2E1 combined with

an increase in mRNA expression following the i.c.v. or i.p. administration of LPS, we

examined the effects of actinomycin-D (AD, an inhibitor of transcription) and

cycloheximide (CHX, an inhibitor of translation) on the LPS-induced effects on hepatic

CYP2E1. As expected, the administration of LPS by both routes was still able to cause a

2-fold increase in CYP2E1 mRNA in animal groups treated with vehicle only. AD was

able to prevent the LPS-induced upregulation in CYP2E1 mRNA following both routes

of LPS administration (Figure 5.7 A and B and Table 5.2). In contrast, CHX injection

caused a significant augmentation in the LPS-induced upregulation of CYP2E1 mRNA

(Figure 5.8 A and B and Table 5.2). On examination of CYP2E1 activity, we observed a

significant downregulation in catalytic activity caused by LPS in both vehicle groups

(Figures 5.7 C, 5.7 D, 5.8 C, and 5.8 D). Actinomycin-D treatment did not prevent the

LPS-induced downregulation in CYP2E1 activity (Figure 5.7 C and D). LPS was able to

significantly downregulate CYP2E1 catalytic activity in the presence of CHX only in the

i.p. group (Figure 5.8 C and D).

(A)

% ctrl of CYP2E1 arbitrary units
relative to respective saline group

□ sal
■ LPS

150
100
50
0

*

2hr   24hr
time points

(B)

% ctrl of CYP2E1 arbitrary units
relative to respective saline group

□ sal
■ LPS

200
100
0

2hr   24hr
time points
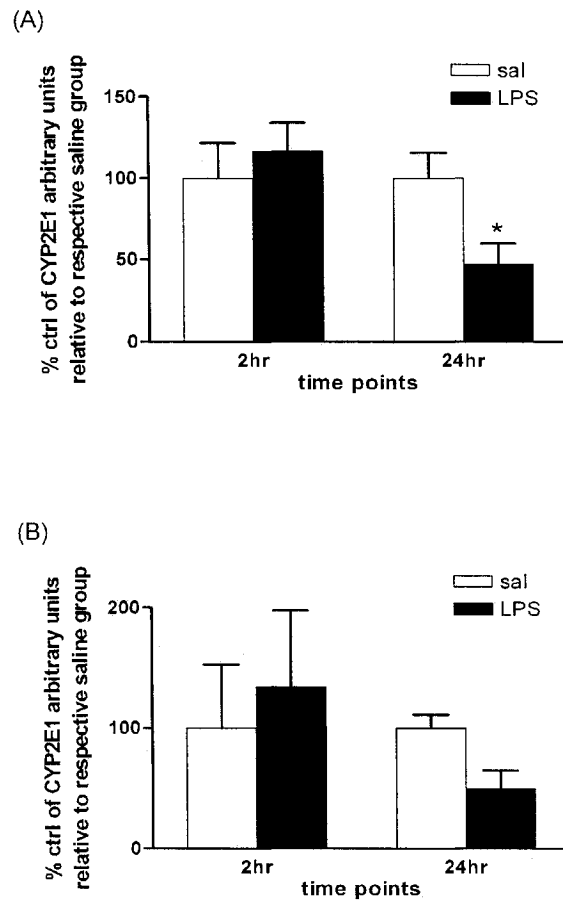
Figure 5.6. CYP2E1 protein level is downregulated in response to the i.c.v. administration of LPS. Rat liver microsomes obtained from animals injected either with 25 µg LPS i.c.v. or 5 mg kg^{-1} LPS i.p. were subjected to electrophoresis and CYP2E1 protein was detected using a polyclonal antibody directed towards this isoform. The effects of the i.c.v. administration of LPS is shown in (A) and the effects of the i.p. administration of LPS is shown in (B). The results are plotted as % control of the respective saline groups, with each bar representing the average results from 4 animals ± S.E.M. * CYP2E1 expression lower compared to respective saline treated animals using a non-paired t-test (p < 0.05). The absolute value for the saline 2 hour time point (LPS given i.c.v.) is 3.64 × 10^5 arbitrary units and for the saline 24 hour time point (LPS given i.c.v.) is 5.01 × 10^5 arbitrary units. The absolute value for the saline 2 hour time point (LPS given i.p.) is 1.34 × 10^6 arbitrary units and for the saline 24 hour time point (LPS given i.p.) is 3.79 × 10^6 arbitrary units.
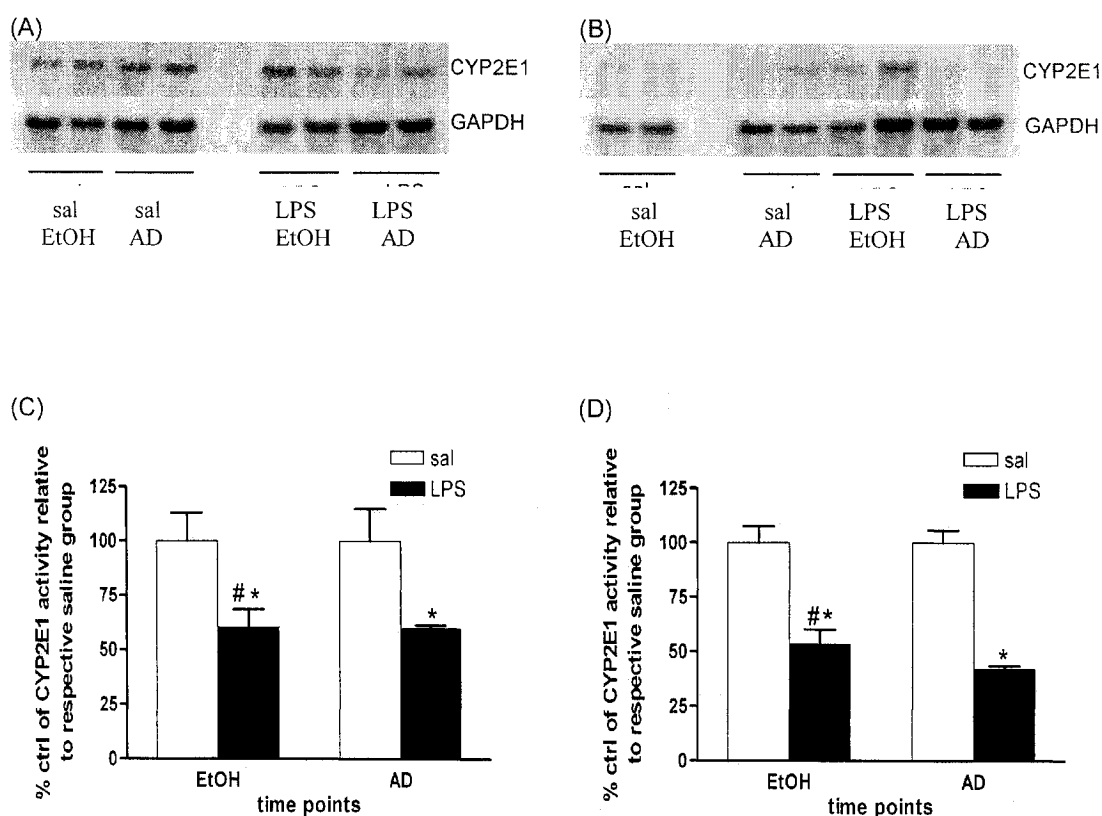
Figure 5.7. The administration of actinomycin-D has no effect on LPS-induced effects on hepatic CYP2E1. AD was administered i.p. at a dose of 7 mg kg^{-1} to rats 4 hours prior to sacrifice in the presence of either saline or LPS. Representative blots for the effects of AD on CYP2E1 mRNA is shown in the case of administering 25 µg of LPS i.c.v. (A) and in the case of administering 5 mg kg^{-1} LPS i.p. (B). The effects of administering AD on CYP2E1 activity is shown for the i.c.v. (C) and i.p. (D) administration of LPS. The results for panels C and D are plotted as % control of the respective saline groups, with each bar representing the average average results from 4 animals ± S.E.M. * represents statistical significance compared to saline treated animals in the vehicle group using a 2-WAY ANOVA coupled with Bonferroni post-hoc tests (p < 0.05). # represents statistical significance compared to saline treated animals in the AD group using a 2-WAY ANOVA coupled with Bonferroni post-hoc tests (p < 0.05). The absolute value for the saline-ethanol group (LPS given i.c.v.) is 71.3 ng 6OH CZX/mg protein/min and for the saline-AD group (LPS given i.c.v.) is 71.8 ng 6OH CZX/mg protein/min. The absolute value for the saline-ethanol group (LPS given i.p.) is 78.9 ng 6OH CZX/mg protein/min and for the saline-AD group (LPS given i.p.) is 83.5 ng 6OH CZX/mg protein/min.
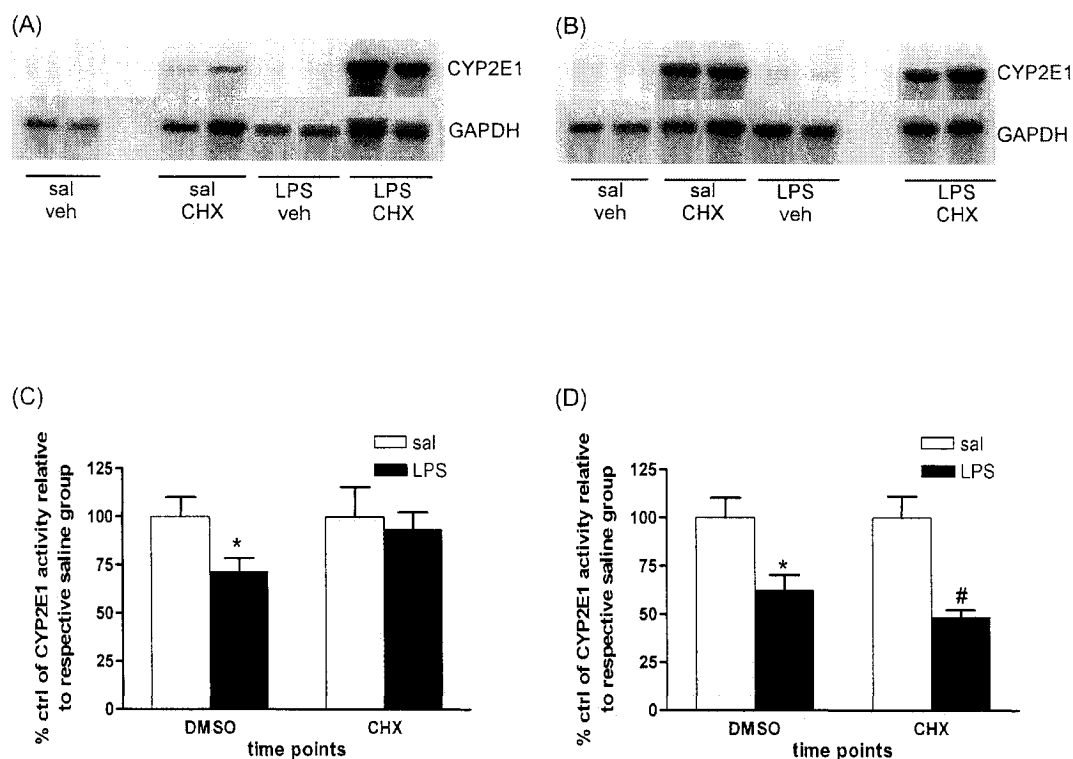
Figure 5.8. The administration of cycloheximide has no effect on LPS-induced effects on hepatic CYP2E1. CHX was administered i.p. at a dose of 10 mg kg^{-1} to rats 4 hours prior to sacrifice in the presence of either saline or LPS. Representative blots for the effects of CHX on CYP2E1 mRNA is shown in the case of administering 25 µg of LPS i.c.v. (A) and in the case of administering 5 mg kg^{-1} LPS i.p. (B). The effects of administering CHX on CYP2E1 activity is shown for the i.c.v. (C) and i.p. (D) administration of LPS. The results for panels C and D are plotted as % control of the respective saline groups, with each bar representing the average results from 4 animals ± S.E.M. * represents statistical significance compared to saline treated animals in the vehicle group using a 2-WAY ANOVA coupled with Bonferroni post-hoc tests (p < 0.05). # represents statistical significance compared to saline treated animals in the AD group using a 2-WAY ANOVA coupled with Bonferroni post-hoc tests (p < 0.05). The absolute value for the saline-DMSO group (LPS given i.c.v.) is 121.6 ng 6OH CZX/mg protein/min and for the saline-CHX group (LPS given i.c.v.) is 82.2 ng 6OH CZX/mg protein/min. The absolute value for the saline-DMSO group (LPS given i.p.) is 89.8 ng 6OH CZX/mg protein/min and for the saline-CHX group (LPS given i.p.) is 104.9 ng 6OH CZX/mg protein/min.

Table 5.2 – The effects of cycloheximide and actinomycin-D on the mRNA expression levels of CYP2E1 following either the i.c.v. or i.p. administration of LPS. The dosing schedule for CHX and AD administration is shown in Figure 1. The doses for CHX and AD were 10 mg kg^{-1} and 7 mg kg^{-1}, respectively. Statistical significance is indicated underneath each respective group and was performed using a 2-WAY ANOVA coupled with a Bonferroni post-hoc analysis test.

Route of administration	Treatment	Value
i.c.v.	Saline – DMSO	0.049 ± 0.009
i.c.v.	LPS – DMSO	0.090 ± 0.01 [@]
i.c.v.	Saline – cycloheximide	0.858 ± 0.53 [@]
i.c.v.	LPS – cycloheximide	2.339 ± 0.57 [*]
* represents statistical significance with respect to the saline – ethanol group **@ represents statistical significance with respect to LPS – cycloheximide group**		
i.p.	Saline – DMSO	0.062 ± 0.025
i.p.	LPS – DMSO	0.090 ± 0.038
i.p.	Saline – cycloheximide	1.405 ± 0.29 [@]
i.p.	LPS – cycloheximide	2.941 ± 1.77 [*]
* represents statistical significance with respect to the saline – ethanol group **@ represents statistical significance with respect to LPS – cycloheximide group**		
i.c.v.	Saline – ethanol	0.035 ± 0.013
i.c.v.	LPS – ethanol	0.056 ± 0.019 [#]
i.c.v.	Saline – actinomycin-D	0.032 ± 0.017

	i.c.v.	LPS – actinomycin-D	0.016 ± 0.004
# represents statistical significance with respect saline – DMSO group			
	i.p.	Saline – ethanol	0.026 ± 0.007
	i.p.	LPS – ethanol	0.045 ± 0.008 [#]
	i.p.	Saline – actinomycin-D	0.038 ± 0.027
	i.p.	LPS – actinomycin-D	0.018 ± 0.01
# represents statistical significance with respect to saline – DMSO group			

173

5.5 Discussion

LPS and various pro-inflammatory cytokines have been shown to modulate the expression, protein levels, and activity of various CYP isoforms both *in vivo* and *in vitro* [64, 77, 79, 114, 121, 156, 175]. CYP2E1 is known to play an important role in various physiological and pathological situations, thereby making it essential to understand its regulation during conditions of inflammation [57, 169]. We therefore chose to examine the *in vivo* regulation of hepatic CYP2E1 during conditions of LPS-mediated inflammation. We have previously shown that the injection of 25 μg LPS i.c.v. is associated with a leakage of endotoxin from the cerebral fluid into the serum as early as 15 minutes following its administration [79]. Therefore, we would expect that the regulation of CYP2E1 following the administration of 25 μg LPS i.c.v. would be consistent with its regulation following the i.p. administration of 5 mg kg^{-1} LPS. Our results indicate that the mRNA expression of CYP2E1 is upregulated at various time points following either the i.c.v. or i.p. administration of LPS, which is in sharp contrast to the observed downregulation in the protein and activity levels of this isoform at 24 hours.

The sharp increase in hepatic CYP2E1 mRNA occurred as early as 2 hours following the administration of LPS either i.c.v. or i.p., and the magnitude of this increase in mRNA gradually decreased with time. To our knowledge, this is the first time an upregulation in hepatic CYP2E1 mRNA expression has been observed *in vivo* following LPS administration. In an attempt to explain the mechanism by which LPS upregulates hepatic CYP2E1 mRNA, we examined the effects of both the i.c.v. and i.p. administration of LPS on the binding of several transcription factors to the promoter

174

region of CYP2E1. We observed a differential effect of i.c.v. and i.p. administered LPS

on HNF-1α binding, with the binding slightly increased following the i.c.v.

administration of LPS and decreased following the i.p. administration of LPS. Our results

are in agreement with a previous report which showed that the i.p. administration of LPS

to rats causes a decrease in binding to a consensus HNF-1α sequence [160]. However,

since LPS causes a similar upregulation in mRNA expression regardless of its effects on

HNF-1α, one can speculate that the increase in mRNA expression occurs independent of

changes in the binding to HNF-1α. We observed an increase in binding to an AP-1

(activator protein-1) region located in intron 1 of the CYP2E1 gene, which may play a

role in the upregulation of this isoform in the liver following the i.c.v. or i.p.

administration of LPS. AP-1 has been identified as possibly playing a role in the

regulation of CYP2E1 [160], and therefore may likely play a role in the regulation of

hepatic CYP2E1 in LPS-mediated models of CNS and peripheral inflammation. In a

study to examine the effects of STAT1 (signal transducer and activator of transcription-1)

protein deficiency on hepatic cytochrome P450 expression in the mouse following the

peripheral administration of LPS, Pan *et al* showed that CYP2E1 mRNA is slightly but

not significantly upregulated 24 hours following the administration of LPS in wildtype

mice [176]. In addition, their results revealed that STAT1 may possibly play a role in the

post-transcriptional modulation of CYP2E1 following the i.p. administration of LPS

[176]. Other reports have indicated increases in the mRNA of CYP2E1 in the brain

following administration of LPS, but this induction of expression was associated with an

increased activity of the enzyme [56, 133].

In the present study, we show a downregulation in hepatic CYP2E1 activity and protein levels 24 hours following either the i.c.v. administration of 25 μg of LPS or the i.p. administration of 5 mg kg^{-1} LPS, which is a similar finding to that reported previously [75]. The loss in CYP2E1 protein and activity is surprising in light of the observation that the mRNA expression of this isoform is upregulated in the liver 2 – 9 hours following either the i.c.v. or i.p. administration of LPS. The mechanisms delineating the downregulation in hepatic CYP2E1 *in vivo* following LPS administration have not been explored.

When AD was utilised to inhibit transcription, no induction in hepatic CYP2E1 mRNA was observed in response to LPS, indicating that the increase in mRNA observed in this study results from an increase in transcription. AD treatment had no effect on the LPS-mediated loss in catalytic activity of CYP2E1, indicating that changes in the mRNA expression of CYP2E1 have no effect on the downregulation in catalytic activity of this isoform during LPS-induced conditions of central and peripheral inflammation. CHX caused a significant induction in CYP2E1 mRNA on its own, and this induction was further enhanced in the presence of LPS. Since CHX is an inhibitor of translation, it is possible that the lack of newly synthesized CYP2E1 protein in the hepatocyte causes a positive feedback mechanism that activates further CYP2E1 mRNA production. The LPS-mediated downregulation in hepatic CYP2E1 catalytic activity was not affected in the presence of CHX in rats administered 5 mg kg^{-1} LPS i.p., indicating that changes in the transcription and translation of the CYP2E1 gene have no effect on the regulation of this isoform during conditions of inflammation. Collectively, the AD and CHX results indicate that LPS mediates a downregulation in CYP2E1 catalytic activity irrespective of

176

changes in the mRNA of this isoform, and acts mainly at a post-transcriptional level. It is likely that CYP2E1 downregulation observed *in vivo* following the administration of 25 µg of LPS i.c.v. or 5 mg kg^{-1} LPS i.p. is caused by changes to the stability of CYP2E1 protein already present in the hepatocyte, which has been observed previously by others [170]. Ubiquitin conjugation and subsequent proteolysis of hepatic CYP2E1 may play a role during LPS-induced conditions of inflammation, similar to the effect of ethanol withdrawal on CYP2E1 [170]. In contrast to our current results, Hakkola *et al* showed that pro-inflammatory cytokines inhibit CYP2E1 activity *in vitro* at the level of the gene through control of hepatocyte nuclear factor-1 alpha (HNF-1α) function and other transcription factors on the CYP2E1 promoter [156]. The predominant post-transcriptional regulation of hepatic CYP2E1 *in vivo* we observed in this study is in contrast to the regulation of other hepatic CYP isoforms such as CYP1A, CYP2D, and CYP3A during conditions of inflammation, where we and others have shown that the regulation occurs mainly at the level of the gene [51, 79, 83, 89, 177, 178].

In summary, we have shown an upregulation in CYP2E1 mRNA occurring as early as 2 hours following either the i.c.v. administration of 25 µg of LPS or the i.p. administration of 5 mg kg^{-1} LPS, indicating that LPS is acting at a transcriptional level to causes changes in the mRNA expression of CYP2E1. In sharp contrast, CYP2E1 catalytic activity was downregulated following the i.c.v. or i.p. injection of LPS. Using AD and CHX to shed some light on the mechanism of CYP2E1 regulation, we were able to show that the regulation of hepatic CYP2E1 activity during conditions of LPS-mediated inflammation occurs predominantly at the post-transcriptional level.

CHAPTER 6

CONCLUSION

6.1 Summary

It is evident from the results of this thesis that there are numerous mechanisms by which inflammatory and infectious conditions can affect the regulation of hepatic and extra-hepatic P450. It is important to be aware of the complexities involved in the various levels of regulation, since the P450 family of enzymes have many diverse functions ranging from the metabolism and synthesis of endogeneous substances to the biotransformation and elimination of foreign chemicals and xenobiotics [44, 64, 65]. The utilization of a simplified *in vitro* model of CNS inflammation allowed us to examine potential protective agents against the downregulation in CYP1A observed in cultured astrocytes following LPS administration. In addition, by using available molecular biology techniques, we have been able to delineate some of the potential mechanisms of P450 regulation during conditions of LPS-induced CNS and peripheral inflammation.

We have previously observed a downregulation in the enzymatic activity of CYP1A in astrocytes in response to the administration of LPS and cytokines [76, 77]. The treatment of cultured astrocytes with LPS represents a simplified model of CNS inflammation, allowing us to examine the effects on drug metabolizing enzymes present in astrocytes in the absence of the complications of organ or whole body inflammatory responses [76, 77]. The results presented in chapter 2 of this thesis show that isoproterenol, a general β-adrenergic agonist, and clenbuterol, a specific β_2-adrenergic agonist, can both protect against the LPS-induced downregulation in CYP1A activity in astrocytes. We were able to show that this protection is mediated through cAMP and TNFα expression. The β-adrenergic modulation of the LPS-induced downregulation in CYP1A activity was not dependent on changes in NF-κB levels. The clinical importance

of this observation would be that the stimulation of β-adrenergic receptors in patients

with a CNS inflammatory disease could potentially prevent the downregulation in

CYP1A activity.

The i.c.v. administration of LPS to induce CNS inflammation is a widely used and

accepted model, and is associated with a downregulation in hepatic and brain cytochrome

P450 [65, 66]. In chapters 3 –5, we were interested in examining the potential pathways

by which hepatic P450 isoforms are regulated during conditions of LPS-induced CNS

inflammation. Our results indicate that the transfer of LPS across the BBB into the

peripheral circulation occurs in the rat as early as 15 minutes following the administration

of LPS [79]. Similarly, when mice are given 2.5 µg of LPS i.c.v., endotoxin is detected in

the serum of the animals at 15 minutes – 2 hours following endotoxin administration

[178]. These results go against the central idea or dogma that a pathway must exist

between the CNS and the periphery to mediate the peripheral inflammatory response and

subsequent downregulation in hepatic P450 following the i.c.v. administration of LPS

[71, 72, 74, 75]. Our results clearly indicate that the leakage of LPS from the ventricles

into the serum is likely wholly responsible for the inflammatory reponse and change

P450 regulation observed following the i.c.v. administration of endotoxin [79, 178]. Of

interest is the fact that the bioavailablity of LPS following its i.c.v. administration is

different in the mouse and rat [79, 178]. The administration of 25 µg of LPS i.p. in rats

was associated with minimum endotoxin detection in the serum, whereas the

administration of 2.5 µg of LPS i.c.v or i.p. to mice was associated with the detection of

about equal amounts of LPS in the serum of mice. These results are of importance since it

indicates an important difference between the mouse and rat in terms of the effects of LPS on BBB permeability.

Our results indicate that regulation of P450 following LPS-induced peripheral or CNS inflammation occurs intrahepatically, with transcription factors such as NF-κB playing an important role. We show that NF-κB plays a role in the regulation of CYP1A, CYP2B, and CYP2D following the i.c.v. administration of LPS. We also show that various other inflammatory mediators are upregulated in the liver following the i.c.v. administration of LPS, likely contributing to the downregulation in P450. By using the mouse as a model to examine the effects of LPS-induced CNS inflammation on P450, various knockout mouse strains can be used to determine the specific involvement of proteins/receptors in the downregulation of P450. The administration of LPS i.c.v. to TLR-4 deficient mice indicated that LPS signals the downregulation in CYP3A11 in the mouse by signaling through TLR-4 [178].

We were also interested in further examining and outlining the intra-hepatic mechanisms governing the regulation of CYP2D1/5 and CYP2E1 during LPS-induced peripheral and CNS inflammation, since both isoforms are known to play an important role in toxicology and drug metabolism. The results of this thesis indicate that "unconventional" proteins such as GABP are involved in the transcriptional control of CYP2D5, which indicates the complexity of cytochrome P450 regulation during basal and inflammatory conditions. The changes in CYP2E1 regulation during LPS-induced conditions of inflammation also indicate the role of multiple mechanisms in cytochrome P450 regulation, since in contrast to the other isoforms, changes in CYP2E1 regulation occur predominantly at the post-transcriptional level.

6.2 Significance

Understanding the mechanisms that cause changes in the regulation of cytochrome P450 during conditions of inflammation and infection are essential, since they would allow for the development of specific strategies to prevent undesired adverse drug reactions in therapeutics. In addition, many xenobiotics are administered as prodrugs and require bioactivation by P450 to deliver therapeutic benefits to the patients, therefore changes in the P450 enzymes during inflammation and infectious conditions may cause less active drug to be available. This establishes an immense clinical demand to explain how LPS and other pro-inflamamtory cytokines affect P450 in the liver and other extra-hepatic tissues.

Outlining the various transcription factors involved in causing changes to basal P450 expression during conditions of inflammation allows us to appreciate the complexities associated with the regulation of this family of drug metabolizing enzymes. The results of this thesis reveal that many evolutionary conserved proteins such as NF-κB, GABPα, and GABPβ are involved in either the basal transcriptional expression of P450 or changes in the regulation of P450 during inflammation, indicating that this is a process that has probably been occurring for millions of years. One of the strengths of this thesis is the examination of such levels of regulation in whole animal models rather than confining the studies to cell culture systems, allowing them a certain degree of relevance to human therapeutics. By detailing the molecular aspects of P450 regulation, one might be able to predict newer and more specific theraupeutic agents that could be used as targets to prevent the differential regulation of P450 during inflammation.

Many systems interact with each other during inflammatory conditions to change P450 regulation [66, 69]. One of the main aspects highlighted in this current work is the fact that the stimulation of the adrenergic system is not only anti-inflammatory, but can also protect against the LPS-induced downregulation of CYP1A activity in primary cultured astrocytes. This indicates an important interaction between the immune and the nervous systems. Much study over the previous two decades has indicated a role for the CNS in the regulation of immune cell function, with the sympathetic nervous system playing a vital role in this regulatory pathway [99]. In addition, the endocrine system can also interact with the CNS to regulate immune function [179]. Cytokines released by LPS stimulation can signal the nervous system to release hormones such as adrenocorticotropic hormone, eventually leading to glucocorticoid release and anti-inflammatory effects [179]. Many immune cells have been shown to express adrenergic and purinergic (stimulated by adenosine) receptors whose stimulation by the appropriate ligands regulates the release of important pro-inflammatory molecules [99]. The fact that CYP1A activity can be regulated through β-adrenergic receptor stimulation is therefore not surprising [78], and adds the drug metabolizing system in the circuit of CNS and immune system interactions.

The use of the mouse to stimulate and study inflammation allows us to examine the role of various receptors and proteins and their roles in changes to the regulation of P450 during infection and inflammation. It has been shown that changes in the regulation of specific P450 isoforms such as CYP2D9 and CYP2E1 in response to LPS treatment is differentially regulated by TNFα binding to its receptor with the use of mice lacking specific components of the TNFα receptor [180]. In addition, it has been determined

using STAT1 knockout mice that the regulation of CYP2E1 during LPS-induced inflammation may be dependent on STAT1 protein [176]. We show that changes in the regulation of liver P450 in response to the i.c.v. administration of LPS depends on the presence of TLR4 by utilizing mice known to contain a mutation in the *tlr-4* gene, rendering it inactive [178]. Endotoxin resistant mice have been previously characterized, however it has only been a recent observation that a deficiency in TLR-4 is the cause of the phenotype of these mice [181].

Finally, a major observation made in this work relates to changes in the permeability of the BBB following the i.c.v. administration of LPS. We observe an extremely rapid "transfer" of LPS from the lateral cerebral ventricle into the blood stream as early as 15 minutes following the i.c.v. administration in both rats and mice [79, 178]. The implications of this observation are immense, since it indicates that changes to the BBB permeability during conditions of LPS-induced inflammation occur rapidly, which is in contrast to the belief that these changes require 18 – 24 hours to be manifested [26]. Since endotoxin is being detected at an early time point following its i.c.v. administration, it is possible that changes in the bulk-flow of the cerebral spinal fluid may contribute to transfer of LPS into the blood. This has been shown to be the case for leptin (a protein important in the regulation of body weight and metabolism) following its i.c.v. administration into the CNS [182, 183]. The fact that LPS is transferred into the periphery following its i.c.v. administration sheds light on the many studies that administer various drugs and compounds into the cerebral ventricle and examine peripheral effects without examining the possibilty that the observed effects could be due to direct transfer of the compound to the periphery. It is therefore plausible that in

184

bacterial infections of the CNS in humans, a similar transfer of bacterial-derived protein causes the usually observed reduction in P450 in peripheral systems.

6.3 Future work

6.3.1 Examination of potential mechanisms and pathways to protect against the LPS-induced downregulation in CYP1A activity

We have attempted to delineate some of the pathways by which β-adrenergic receptor stimulation can prevent against the LPS-induced downregulation in CYP1A activity *in vitro* [78]. We show that the protection is dependent on β-adrenergic receptor stimulation, and that cyclic AMP likely plays a role while NF-κB plays a minimal role [78]. It would be interesting to examine other intracellular pathways involved in normal signaling during β-adrenergic receptor stimulation to determine if they are involved in the protection against the LPS-induced downregulation in CYP1A activity in primary cultured astrocytes. This would include examination of whether changes in protein kinase A (PKA) activation and intracellular calcium stores plays a role in the protective effect [184]. In addition, it would be interesting to examine whether β-adrenergic receptor stimulation is protective against the LPS-induced downregulation in CYP1A activity *in vivo*. It has been shown that stimulation of the vagus nerve can attenuate the effects of LPS on pro-inflammatory cytokine production *in vivo* [185], and therefore the stimulation of this pathway might protect against the LPS-induced downregulation in CYP1A activity both *in vitro* and *in vivo*.

6.3.2 Determining the kinetics of LPS following its i.c.v. administration and determining the mechanisms by which it causes changes in the regulation of hepatic P450

The fact that LPS is detected in the serum as early as 15 minutes following its i.c.v. administration opens up the avenue to explore the kinetics of LPS following its administration by various routes (i.p., i.v., and i.c.v.). This would include examination of the bioavailability of LPS following the administration of 25 μg both i.c.v. and i.p., since we have previously shown that administration of the same dose i.p. has no effect on hepatic P450 [75]. This would then be compared to the bioavailability of LPS following the administration of 5 mg kg^{-1} i.p., a dose known to cause an effect on hepatic P450 [155]. The mechanisms involved in LPS transfer from the lateral cerebral ventricle into the serum woud be a potential area of research. This could involve performing studies looking at BBB permeability at various time points following the i.c.v. adminstration of LPS and examining the possibility that LPS leakage could be occurring through bulk-flow of the cerebrospinal fluid.

We have shown that the hepatic downregulation in CYP3A11 in the mouse following the administration of LPS is dependent on the presence of TLR4 [178]. Other pathways involved in LPS signaling that could be responsible for hepatic P450 regulation. One example would be the use of MyD-88 knockout mice (described in [15]) to determine whether this protein is required intracellularly to mediate the effects of LPS on hepatic P450. Similarly, knockout mice for other intracellular proteins known to play a role in TLR4 signal transduction would aid in determining the role of these proteins in the changes to P450 regulation in the liver following LPS administration. If a conditional knockout mouse existed such that TLR4 or any of its intracellular signaling proteins were missing in the hepatocyte, this would aid in determining whether regulation of hepatic

P450 occurs directly at the level of the hepatocyte or through other immune mediated cells.

6.3.3 Understanding the role of GABP and whether it interacts with NF-κB in the regulation of CYP2D1/5

It is essential to establish whether the putative NF-κB site identified on CYP2D5 promoter plays a role in the transcriptional regulation of CYP2D5. We have not been able to obtain a definitive result demonstrating downregulation of CYP2D5 transcription by NF-κB and GABP mediated pathways in our transfection assays. This may have been due to the high constitutive activity for this transcription factor present even in un-stimulated cases. The search for other appropriate cell types could aid in determining whether CYP2D5 promoter is under the transcriptional control of NF-κB. In addition, it could be possible that the rat CYP2D isoform responsible for the downregulation in CYP2D mRNA expression observed in our studies is CYP2D1 (and not CYP2D5), and therefore it would be essential to search the rat CYP2D1 promoter for potential NF-κB sites and determine whether NF-κB can regulate the transcription of this isoform.

We also describe a potential importance for GABP in the control of CYP2D5 transcription. This transcription factor belongs to the Ets family of transcription factor proteins and was originally discovered in studies of viral gene transcription [143]. Recent observations however have indicated a role for this transcription factor in the regulation of many eukaryotic cellular functions [143]. Since it is has been shown that GABP can interact with diverse transcription factors and proteins, it would be interesting to examine whether GABP interacts with some of the NF-κB subunits. We have not been able to show such an interaction in the work presented in this thesis, which is likely due to the

lack of an appropriate GABPα or GABPβ supershift antibody in the setup of the EMSA assays described in this work. Other assays such as a yeast-two hybrid system would allow for the establishment of such an interaction.

6.3.4 Further elucidation of hepatic CYP2E1 regulation during LPS-induced inflammation

The upregulation in CYP2E1 mRNA expression following either the i.c.v. or i.p. administration of LPS is a novel finding of this thesis. In chapter 5, we have attempted to describe whether it is transcriptional or post-transcriptional mechanisms that are important in the regulation of CYP2E1 during LPS-induced inflammation. The importance of CYP2E1 mRNA regulation following LPS administration and the mechanisms by which it occurs still remain to be determined. The utilization of an assay to detect the formation of hnRNA (heterogeneous nuclear RNA) would aid in determining whether the increase in CYP2E1 mRNA we observe is due to newly synthesized mRNA (mRNA half-life study). If this is not the case, then LPS signal transduction pathways may cause an intracellular mechanism to stabilize already existing CYP2E1 mRNA in the hepatocyte, thereby allowing us to observe upregulation in mRNA expression. It would also be valuable to perform a DNA footprinting assay to determine the changes induced by LPS on protein binding sites on the CYP2E1 promoter *in vivo*. The *in vivo* aspect of these experiments would be critical, since most of the work explaining the changes in the regulation of CYP2E1 during inflammation has been performed using *in vitro* inflammatory models in various hepatoma cell lines that may or may not resemble what is happening *in vivo* in the actual hepatocyte.

Appendix A

This appendix consists of the following manuscript:

Goralski KB, Abdulla D, Sinal CJ, Arsenault A, Renton KW. (2005). *Toll-like receptor-4 regulation of hepatic Cyp3a11 metabolism in a mouse model of LPS-induced CNS inflammation.* American Journal of Physiology: Gastrointestinal and Liver Physiology. 289(3):G434-43. Epub 2005 May 5

PhD candidate contributed to half of the work performed in this manuscript, however due to the fact that it is a co-authored manuscript, the advisory committee felt it more appropriate to include as an appendix, since it has been referenced and used as a discussion point throughout the thesis.

ACKNOWLEDGEMENTS

ABSTRACT

Central nervous system infection/inflammation severely reduces the capacity of cytochrome P450 metabolism in the liver. We have developed a mouse model to examine the effect of CNS inflammation on hepatic cytochrome P450 metabolism. FVB, C57/Bl/6 or C3H/HeouJ mice were given *E.coli* LPS (2.5 µg) by intracranial ventricular injection (i.c.v.). The CNS inflammatory response was confirmed by the elevation of TNFα and/or IL-1β proteins in the brain. In all mouse strains, LPS produced a 60-70% loss in hepatic Cyp3a11 expression and activity compared to saline-injected controls. Adrenalectomy did not prevent the loss in Cyp3a11 expression/activity, thereby precluding the involvement of the HPA axis. Endotoxin was detectable (1-10 ng ml^{-1}) in serum between 15 and 120 min after i.c.v. dosing of 2.5 µg of LPS. Peripheral administration of 2.5 µg of LPS by i.p. injection produced similar serum endotoxin levels and a similar loss (60%) in Cyp3a11 expression and activity in the liver. The loss of Cyp3a11 in response to centrally or peripherally administered LPS could not be evoked in TLR4 mutant (C3H/HeJ) mice indicating that TLR4 receptor-signaling pathways are directly involved in the enzyme loss. In summary, it is concluded that LPS is transferred from the brain to the circulation in significant quantities in a model of CNS infection/inflammation. Subsequently, LPS that has reached the circulation stimulates a TLR4 receptor-dependent mechanism in the periphery that evokes a reduction in Cyp3a11 expression and metabolism in the liver.

Key Words: Lipopolysaccharide, cytochrome P450, drug metabolism

Introduction

The cytochromes P450 (P450) are a gene superfamily of heme containing enzymes that contribute to the metabolism and elimination of exogenous and endogenous substances [44, 85]. The highest amounts of drug metabolizing P450s are found in the liver and intestine with lower amounts in other organs including the kidney, lung and brain. In rodents and humans, enzymes of the CYP3A subfamily comprise the majority of cytochrome P450 in the liver (30-50%) and metabolize 50-60% of clinically used drugs [85].

It is well known that cytochrome P450s are modulated during inflammatory responses and/or infectious diseases [64, 114]. In general, acute systemic inflammatory responses trigger reductions in hepatic cytochrome P450 enzyme expression and activity with the consequence of reduced drug metabolism during episodes of inflammation. Bacterial LPS is the major stimulus for inflammatory responses in the CNS caused by gram-negative meningeal pathogens [186]. Inflammatory responses in the brain caused by the administration of *E. coli* lipopolysaccharide (LPS) into the lateral ventricle of rats reduce hepatic CYP1A1/2, CYP2B1/2, CYP2D1, CYP2E1 and CYP3A1/2 enzyme activity and/or protein level [72, 75, 92, 114, 187, 188]. The signaling mechanisms that produce peripheral responses during CNS infection have been proposed to include peripheral inflammatory cytokines, the hypothalamic-adrenal pituitary axis, the sympathetic nervous system and reactive oxygen species [70, 74, 189]. Due to the complex nature of these signaling mechanisms it has been difficult to determine which pathways are most important for the loss in hepatic drug metabolism *in vivo*. Mice with disruptions of genes contributing to inflammatory signaling pathways (TNFα receptor, Il-

6, STAT1 and nitric oxide synthase-2 null mice) have been used as a tool to delineate the factors that are important for decreasing hepatic drug metabolism during peripheral inflammatory responses [176, 180, 190, 191]. The availability of mice with genetic alterations in immune signaling pathways will allow a more precise mechanistic examination of the biochemical links between CNS infection/inflammation and drug metabolism and disposition *in vivo*.

TLR4 has been identified as the transmembrane receptor that specifically recognizes LPS and initiates intracellular signal transduction and an immune response to that bacterial cell wall component [5, 192]. LPS signaling during conditions of systemic inflammation involves the binding of LPS to the serum protein LPS-binding protein (LBP), followed by association with CD14, a receptor found in either the membrane or in soluble form. The complex is then thought to translocate to TLR4 to initiate intracellular signal transduction pathways that include NF-κB activation and inflammatory cytokine production [5, 13]. A similar process occurs in the regions of the brain (choroid plexus, leptomeninges and circumventricular organs) that co-express the CD14 and TLR4 components of LPS signal transduction pathway [14, 124]. Despite the importance of the TLR4 receptor in LPS signaling, it has received minimal attention with regard to regulation of drug metabolism by inflammatory processes. C3H/HeJ mice contain a single point mutation at amino acid 712 that renders the TLR4 receptor ineffective and the mice unresponsive to stimulation by LPS [181, 192]. Thus, the C3H/HeJ mouse strain represents a useful model to examine whether changes in hepatic cytochrome P450 expression during LPS exposure can be specifically attributed to activation of TLR4 receptor signaling pathways.

The aim of this study was to examine the signaling mechanisms responsible for the loss in hepatic cytochrome P450 3A in a model of gram-negative bacterial infection/inflammation of the mouse brain. Our novel findings indicated that in this experimental model, the flux of LPS from brain to blood and the activation of a peripheral TLR4 receptor mediated immune response leads to a reduction Cyp3a11 drug metabolism in the liver.

Materials and Methods

Mice and production of CNS inflammation. FVB and C57/Bl/6 mouse strains were used initially in the study to develop methodology and to characterize the effects of CNS infection/inflammation on mouse cytochrome P450 metabolism. Subsequently, the C3H/HeJ and closely related C3H/HeouJ strains were used to specifically address the role of TLR4 receptor in mediating changes in hepatic P450 expression and activity. Adult male mice (FVB strain) and adrenalectomized FVB mice were obtained from Taconic Laboratories (Germantown, NY). Male mice (6-8 weeks old) containing either a spontaneous mutation in TLR 4 gene (C3H/HeJ) and age-matched LPS-responsive (C3H/HeouJ) mice were obtained from Jackson laboratories (Bar Harbor, Maine, USA). C57/Bl/6 mice were obtained from our in house breeding colony. The mice were housed in cages lined with corncob bedding and had free access to water and Purina mouse chow. Drinking water for adrenalectomized mice was supplemented with 5% glucose. Mice were kept on a 12-hour day/night cycle and were allowed to acclimatize in the animal holding facilities for a period of 1 week prior to experimentation. On the day of the experiments, mice were anaesthetized with enflurane (3.0% – 4.0%) and were given an infusion of either endotoxin free saline (2.5 μl) or gel-purified *E.coli* LPS (serotype 0127:B8; 2.5 μg in 2.5 μl) into the lateral cerebral ventricle (i.c.v.) using a Harvard Apparatus syringe pump. The solutions were injected at a rate of 2.5 μl min^{-1}. The coordinates for the sterotaxic injections in mm were –2.5 dorsal/ventral, –1.5 lateral, and –0.2 anterior/posterior from bregma [193]. For the i.p. experiments, mice were injected intraperitoneally (i.p.) either a low (2.5 μg) or high (125 μg) dose of purified *E.coli* LPS suspended in 100 μl 0.9% endotoxin free saline. Control mice were injected with 100 μl

195

of the saline vehicle. Phenol extracted LPS, but not the gel purified LPS contain μM

levels of biologically active contaminants including glutamate and adenosine [194],

which could precipitate non-specific responses in our model. For those reasons

chromatographically purified LPS is the preferred preparation for *in vivo* studies of this

nature. To assess blood-brain barrier permeability changes, a tracer amount (4 nmol) of

D-[1-^{14}C]-mannitol was administered peripherally to control mice and 0, 1, 4 and 24 hr

after 2.5 μg of LPS was administered into the lateral ventricle. Brain levels of total

radioactivity (DPM) were measured by scintillation counting 1 hr after the ^{14}C-mannitol

injection. For the TNFα experiment 50 ng of recombinant mouse TNFα (R&D systems)

or vehicle containing sterile filtered PBS and 0.1% BSA was administered into the lateral

ventricle in a total volume of 2.5 μl.

Tissue and microsome preparation. Mice were killed 4 or 24 hours after the i.c.v.

administration of either LPS or saline, at which point liver and brain samples were

obtained. Whole brain was homogenized in 1.5 mL of phosphate buffer saline (PBS; pH

7.4) and spun at 13,000 rpm for 10 minutes. Brain supernatants were stored at – 80°C

until utilized for cytokine measurements. One hundred mg samples were obtained from

the liver and frozen in liquid nitrogen for total RNA isolations. The remaining liver was

removed and used to prepare microsomes according to previously published methods

[195]. The liver tissue was homogenized in ice-cold 1.15% KCl for 15-20 sec using a

polytron homogenizer. The homogenates were centrifuged at 10,000xg for 10 minutes at

4°C and the supernatants were re-centrifuged at 110,000xg for 40 minutes. The resulting

microsomal pellets were resuspended in 0.8 ml of glycerol buffer (pH 7.5) that contained

50 mM KH_2PO_4, 20% glycerol, 0.40 % KCl. Samples were stored at -80°C until

196

enzymatic assays were performed. Microsomal protein content was determined by the method of Lowry *et al* using bovine serum albumin as a standard [105].

Cyp3a11 enzyme assays. The formation of α-hydroxytriazolam from triazolam was used as a specific indicator for mouse Cyp3a11 activity [196]. Incubation mixtures (performed in duplicate) contained 500 μg of total microsomal protein, 20 μM triazolam, in and 1 mM NADPH in 100 mM phosphate buffer (pH 7.4). The reaction mixtures (1 ml final volume) were incubated in a 37°C water bath with a shaker set at 100 oscillations/minute. After 15 minutes, the reactions were stopped by the addition of 5 mL of dichloromethane and 2000 ng of phenacetin was added to each sample as an internal standard. The samples were then centrifuged at 2700 rpm for a period of 10 minutes, and the lower organic phase containing the metabolites and internal standard was transferred into a clean glass tube and evaporated to dryness using a nitrogen evaporator followed by reconstitution in 200 μl of HPLC mobile phase. The HPLC mobile phase consisted of acetonitrile (20% v/v) and methanol (35% v/v) in 0.01 M potassium phosphate buffer (45% v/v) buffered to pH 7.4 with NaOH. Reconstituted samples (50 μl) were separated on a reverse phase C-8 column (25 cm × 4.5 mm I.D) analytical column (Beckman Coulter, Fullerton, CA, USA) attached to a Waters 2690 Separations Module. The mobile phase flow rate for separations was set at 1.0 ml min^{-1}. The approximate retention times were 5.0 minutes for α-hydroxytriazolam, 8.0 minutes for phenacetin, and 12.0 for triazolam and were detected by UV absorption at 220 nm (Waters 2487 Dual λ absorption unit).

RNA isolation and northern analyses. Total liver RNA was isolated using TriZol^{TM} reagent (Invitrogen. Carlsbad, CA) according to the manufacturer's instructions. Quality

of the RNA was determined spectrally by measuring the 260/280 absorbance ratio and was typically between 1.8-2.0. For northern analyses, 10 μg of total RNA was resolved on a 1.1% agarose formaldehyde denaturing gel. RNA was transferred overnight to a nylon membrane (Immobilon NY$^+$; Millipore Corporation, Bedford, MA, USA) and was fixed to the membrane by UV cross-linking and heating for 1 hr at 65 °C. ^{32}P-CTP probes for mouse *Cyp3a11 and Gapdh* mRNA were generated from the corresponding cDNAs using the RmT Random Primer Labeling Kit according to manufacturers instructions (Stratagene). Blots were prehybridized for 1 hr at 65°C in 10 ml of Sigma Perfecthyb^{TM} Plus (Sigma, St. Louis, MS) followed by overnight hybridization with ^{32}P-CTP labeled probes. Blots were exposed to storage phosphor screen (Amersham Biosciences, Piscataway, NJ, USA) for 16-24 hours and scanned using a phosphor imager (Amersham Biosciences, Piscataway, NJ, USA). Quantification was performed using ImageQuant 5.2^{TM} software (Amersham Biosciences, Piscataway, NJ, USA).

Quantitative real-time PCR Real-Time PCR. Total RNA (5 μg) was reverse transcribed using Stratacript^{TM} Reverse Transcriptase (Stratagene, Cedar Creek, TX) with 12.5 ng/ul random hexamers pd(N)$_6$ and 1.0 mM dNTPs according to the supplier's instructions. 1 μl of the cDNA product was amplified by quantitative-PCR using 125 nM of gene specific primers in a total volume of 20 μl with Brillant SYBR Green QPCR Master Mix using the Stratagene MX3000p thermocycler. For TNFα a 61 base pair product was generated with the forward 5′ ccc tca cac tca gat cat ctt ct 3′ and reverse 5′ gct acg acg tgg gct aca g 3′ primers (Genbank Accession# NM_013693). For Gapdh a 245 base pair amplicon was generated with the forward 5′ aag gtc ggt gtg aac gga ttt gg 3′ and reverse 5′ ttg atg tta gtg ggg tct cgc tcc 3′ primers (Genbank Accession# NM_008084). The

amplification protocol consisted of a 10 min hot start at 94°C, followed by 40 cycles of denaturation at 94°C for 15 s, annealing at 60°C for 18 s, and elongation at 72°C for 30 s. Melting curves followed by separation of PCR products on a 2.5% agarose gel were used to ensure the formation of a single product at the appropriate size. The threshold cycle (C_T) values for TNFα and control gene GAPDH were obtained with a threshold of 3 standard deviations above background. Relative TNFα expression normalized to Gapdh was calculated using the $\Delta\Delta C_T$ method [128].

Cytokine measurements. The levels of TNFα and IL-1β were measured in brain homogenates and serum 2 or 4 hours after LPS administration i.c.v. using a murine sandwich ELISA prepared as previously described [197]. The results are expressed as ng of cytokine per g of brain wet weight or ng of cytokine per ml of serum.

Serum LPS measurements. LPS (2.5 μg) was administered by the i.c.v. or i.p. route to endotoxin responsive C3H/HeouJ mice. Mice were killed 15 min, 30 min, 2 hr or 24 hr later and trunk blood was collected. All groups were compared to non-injected control mice. Serum LPS levels were measured using the kinetic chromogenic Limulus Ameboctye Lysate assay as per manufacturer's instructions (Associates of Cape Cod, MA, USA). The assay was linear from 0.395 pg mL^{-1} to 100 ng mL^{-1} of LPS. Area under the curve (AUC $_{0.25-2hr}$) was calculated from the mean serum LPS concentrations using the trapezoidal method.

Data Analysis. Data are expressed as mean ± s.e. mean of 3-4 separate animals. An unpaired t-test was used to compare means between two groups. Analysis of variance (ANOVA) was used for multiple comparison procedures. A Tukey's test was used for

post-hoc analysis of the significant ANOVA. A difference in mean values with a value

of $p \leq 0.05$ was considered to be significant.

Chemicals. Purified *E.coli* LPS (serotype 0127:B8), phenacetin and α-hydroxytriazolam,

ethoxyresorufin, resorufin, NADPH and dichloromethane were obtained from Sigma (St

Louis, MI). ^{32}P-dCTP was obtained from Perkin Elmer (Boston, MA). Triazolam was

obtained from Roche Pharmaceuticals. All other reagents were of the finest grade

available and were purchased from commercial suppliers.

Results

Administration of LPS into the lateral ventricle reduces hepatic Cyp3a11 expression and activity. The initial experiments carried out in the two mouse strains (FVB and C57/Bl/6) were required to develop a mouse model of CNS infection/inflammation and to determine if this model exhibited reductions in Cyp3a11 expression and activity. The dose of LPS was based on our previous studies that demonstrated 0.1 µg kg^{-1} of LPS administered i.c.v. was required for significant down-regulation of hepatic cytochrome P450 enzymes in rat [75, 114, 187]. The expression of Cyp3a11 and Gapdh mRNA was measured in the liver by northern blot analyses 4 and 24 hours following the administration of E.coli LPS into the left lateral cerebral ventricle (**Fig. 1A**). Cyp3a11 mRNA was unchanged at 4 hr and was decreased by 60% 24 hr after LPS treatment compared to the respective saline controls (**Fig. 1B,D**). Liver Gapdh expression was not altered by LPS treatment. Consistent with mRNA expression, the rate of α-hydroxylation of triazolam (Cyp3a11 activity) was unchanged at 4 hr but was decreased by 60% at 24 hr by LPS treatment as compared to the respective saline control (**Fig. 1C, E**). LPS (2.5 µg) administered i.c.v. to C57/Bl/6 mice produced a similar reduction in Cyp3a11 mRNA (80%) and α-hydroxylation of triazolam (60%) and indicated that the effect of LPS was not restricted to the FVB strain of mice (**Fig. 2**).

Administration of LPS into the lateral cerebral ventricle produces CNS inflammation. Two hours after LPS was administered into the lateral ventricle of FVB mice, TNFα and Il-1β levels were significantly increased (2-fold) compared to the saline controls (**Fig. 3A, B**). The increased level of TNF-α and Il-1β are consistent with the production of CNS inflammation in response to LPS. A parallel increase (2-fold) in

201
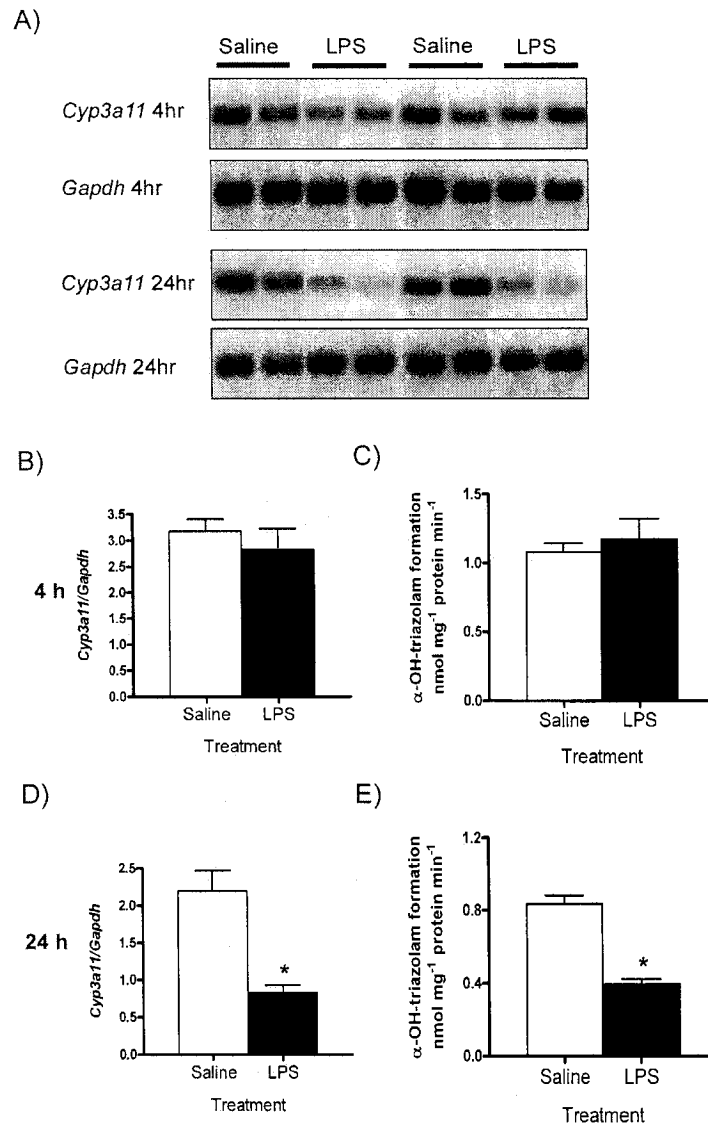
Fig 1. Hepatic Cyp3a11 mRNA and activity were down-regulated 24 hr following i.c.v. administration of LPS (2.5 μg) to male FVB mice. (**A**) Representative northern blots of *Cyp3a11* and *Gapdh* at 4 and 24 hr following the i.c.v. administration of LPS or saline. Band intensities were determined by densitometry and hepatic *Cyp3a11* (**B, D**) mRNA was normalized to *Gapdh* mRNA. Cyp3a11 activity was measured 4 hr (**C**) and 24 hr (**E**) after LPS or saline administration by monitoring the formation of α-hydroxytriazolam from triazolam in liver microsomal fractions. Each bar represents the mean ± s.e. mean of 4 mice. * *Cyp3a11* mRNA and activity was lower compared to the respective saline treated mice, $p < 0.05$, unpaired t-test.
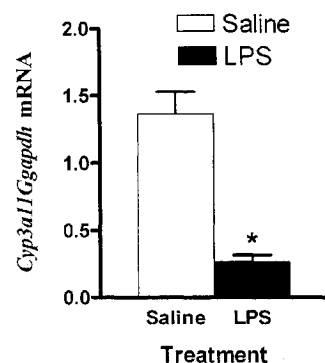
A)   B)
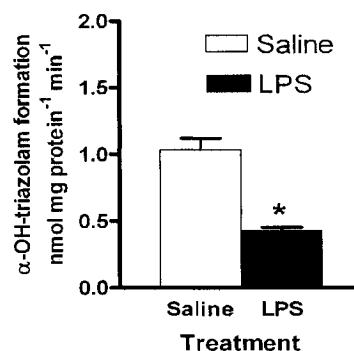
Fig 2. Hepatic Cyp3a11 mRNA and activity were down-regulated 24 hr following i.c.v. administration of LPS (2.5 μg) to male C57/Bl/6 mice. (A) Hepatic *Cyp3a11* mRNA expression normalized to *Gapdh* expression as determined by northern analysis. Band intensities were determined by densitometry. Cyp3a11 activity was measured by monitoring the formation of α-hydroxytriazolam from triazolam in liver microsomal fractions. Each bar represents the mean ± s.e. mean of 4 mice. * $p < 0.05$, compared to the respective saline treated mice, unpaired t-test.

A)

B)

C)

D)
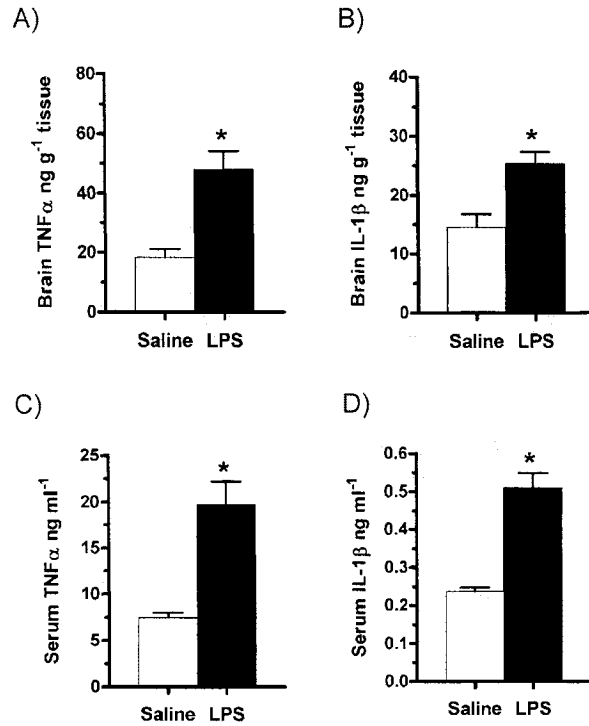
Fig 3. Brain and serum inflammatory cytokines were elevated after i.c.v. administration of LPS. Male FVB mice were injected with 2.5 μg of LPS or 2.5 μl of saline into the lateral cerebral ventricle. The levels of TNFα and IL-1β proteins in brain (**A, B**) and serum (**C, D**) were measured 2 hours following the i.c.v. administration of LPS or saline. Each bar represents the mean ± s.e. mean of 4 mice. * Mean cytokine levels were higher compared to the respective saline treated control, $p < 0.05$, unpaired t-test.

TNFα and IL-1β in serum indicated a systemic response to i.c.v. administered LPS (**Fig. 3C, D**).

The HPA axis does not mediate hepatic Cyp3a11 down-regulation following the i.c.v. administration of LPS. The release of inflammatory cytokines after LPS injection into the brain is known to activate the HPA axis and increase circulating corticosteroids, which can affect the acute phase response and gene transcription in the liver [74, 198, 199]. Thus, it was important to determine the relevance of the HPA axis in contributing to the down-regulation of Cyp3a11 mRNA and enzyme activity in our model (**Fig. 4**). Adrenalectomized and control FVB mice were left untreated or were injected with 2.5 μg of LPS or saline i.c.v. LPS reduced Cyp3a11 expression and activity to the same degree (70%) in both control and adrenalectomized mice (**Fig. 4A, B, C**). In control mice and adrenalectomized mice, saline administration had no effect on hepatic Cyp3a11 mRNA or triazolam metabolism compared to the respective untreated animals. Similarily, basal Cyp3a11 expression and triazolam hydroxylation in adrenalectomized mice was not significantly different from controls. LPS injection i.c.v. in control mice, significantly increased serum corticosterone compared to saline-treated or untreated control mice indicating activation of the HPA axis (**Fig. 4D**). Adrenalectomy completely prevented the elevation in serum corticosterone after i.c.v. administration of LPS.

TLR4 receptor signaling regulates hepatic Cyp3a11 expression. TLR4-expressing (C3H/HeouJ) and TLR4 mutant (C3H/HeJ) mice were utilized to determine if the down-regulation of hepatic Cyp3a11 by LPS was mediated through stimulation of the TLR4 receptor. Twenty-four hours after LPS (2.5 μg) administration to C3H/HeouJ mice, Cyp3a11 mRNA was decreased by 70% compared to the saline control (**Fig. 5A, B**). In

205

A)

B)

C)

D)
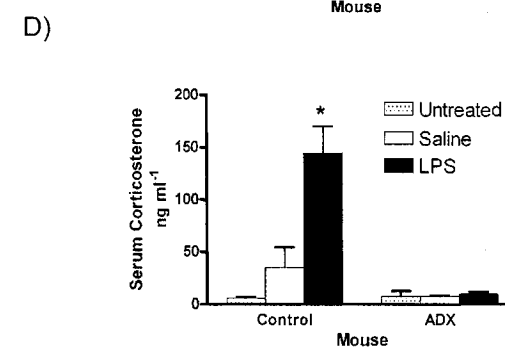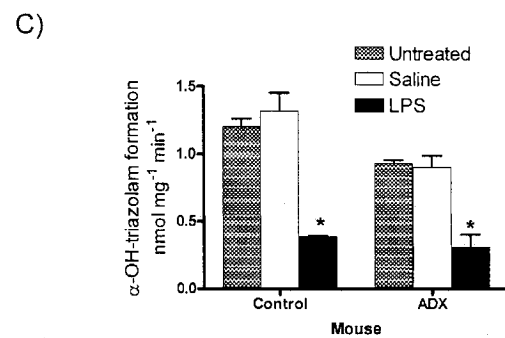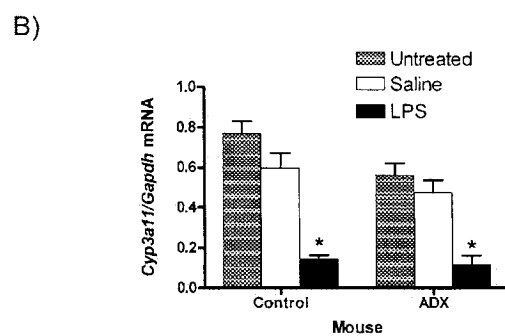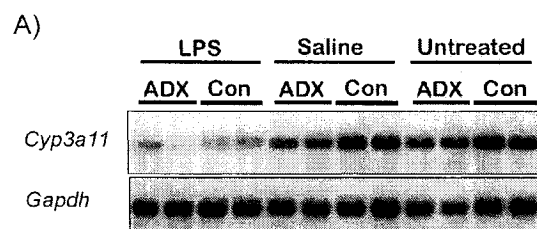
Figure 4 (legend appears on following page).

Fig 4. The HPA axis does not contribute to hepatic Cyp3a11 down-regulation after i.c.v. administration of LPS. The experiment was performed two weeks after adrenalectomy. Control mice and adrenalectomized mice were injected with 2.5 μg of LPS or 2.5 μl of saline into the lateral cerebral ventricle. Analyses were performed 24 hr after the i.c.v. injections. (**A**) Representative northern blots for hepatic *Cyp3a11* and *Gapdh*, (**B**) hepatic *Cyp3a11/Gapdh* expression as determined by densitometry, (**C**) hepatic Cyp3a11 activity (α-OH-triazolam formation) and (**D**) serum corticosterone level. For the corticosterone measurement, the LPS-ADX (adrenalectomy) bar represents the average of 2 mice. All other bars represent the mean ± s.e. mean of 3-4 mice. Different compared to the respective saline-treated control or the untreated control,* $p < 0.05$, ANOVA followed by Tukey's *post hoc* test. Statistical comparison of serum corticosterone in the ADX mice was not performed because of insufficient sample size (n=2) in the LPS-ADX group.
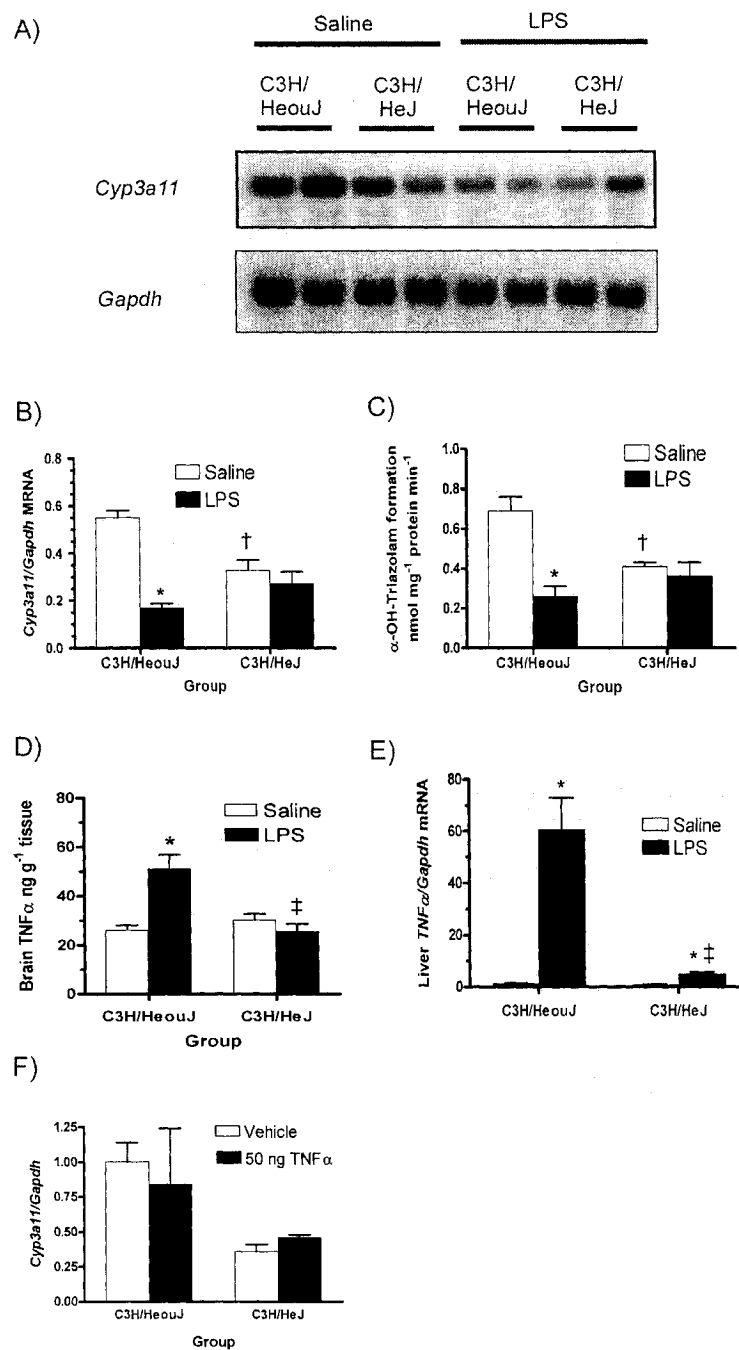
Figure 5 (legend appears on following page).

Fig 5. TLR4 mutant (C3H/HeJ) mice are resistant to down-regulation of Cyp3a11 mRNA and activity following i.c.v. administration of LPS. TLR4 mutant (C3H/HeJ) and wild-type (C3H/HeouJ) were injected with 2.5 μg of LPS or 2.5 μl of saline into the lateral cerebral ventricle. (**A**) Representative northern blots of *Cyp3a11*, and *Gapdh*, (**B**) hepatic *Cyp3a11/ Gapdh* mRNA expression as determined by densitometry, and (**C**) Cyp3a11 enzyme activity (α-OH-triazolam formation) 24 hr following treatment. (**D**) TNFα protein was measured by ELISA in brain homogenates 4 hr after the i.c.v. injection of LPS as a marker of the CNS inflammatory response (**E**) TNFα mRNA was measured in liver 4 hr after the i.c.v. injection of LPS as a marker of an inflammatory response in that organ. (**F**) The effect of i.c.v. administration of 50 ng of TNFα on hepatic *Cyp3a11* expression. Each bar represents the mean ± s.e. mean of 4 mice. * Different in LPS-treated compared to the respective saline-treated mice, $p < 0.05$; [†] *Cyp3a11* mRNA and activity was lower in saline-treated C3H/HeJ mice compared to the saline-treated C3H/HeouJ mice and [‡] TNFα was lower compared to LPS-treated C3H/HeouJ mice, $p < 0.05$, ANOVA followed by Tukey's *post hoc* test.

sharp contrast, no loss in Cyp3a11 mRNA was evoked 24 hr after LPS was administered

directly into the lateral cerebral ventricle the TLR4 mutant (C3H/HeJ) mice. Liver

Gapdh expression was similar in both mouse strains and was not altered by LPS

treatment. Correspondingly, triazolam metabolism to α-hydroxytriazolam was reduced

by 60% in the C3H/HeouJ (wild-type) mice but was unchanged in the C3H/HeJ (TLR4

mutant) mice compared to the respective saline controls (**Fig. 5C**). Basal Cyp3a11

mRNA and triazolam hydroxylation were 40% lower in saline-treated C3H/HeJ versus

C3H/HeouJ mice. After 4 hr, LPS increased brain TNFα protein in the C3H/HeouJ mice

but not in the C3H/HeJ mice compared to the respective saline controls (**Fig. 5D**). Liver

TNFα mRNA expression was increased 60-fold in the C3H/HeouJ mice but only 5-fold

in the C3H/HeJ mice 4 hr after LPS treatment compare to the respective saline controls

(**Fig. 5E**). These results demonstrate an inhibition of the brain and liver inflammatory

responses to LPS in the TLR4 mutant C3H/HeJ mice and indicate that the reduction in

hepatic Cyp3a11 expression and activity are linked to stimulation of the TLR4 receptor

by LPS. Recombinant TNFα (50 ng) administered i.c.v. to the C3H/HeouJ and C3H/HeJ

mice did not produce a loss in cyp3a11 expression in either mouse strain 24 hr after

dosing (**Fig. 5F**). The dose of TNFα was chosen to approximate the TNFα level detected

in the brain 2-4 hours after LPS dosing.

LPS is rapidly transferred from the CNS to the periphery after administration into

the lateral cerebral ventricle. During a CNS infection the leakage of endotoxin into the

periphery could play a role in reducing hepatic cytochrome P450 metabolism; however,

the systemic distribution of LPS after its administration i.c.v. has not been previously

characterized. LPS (2.5 µg) administered by the i.c.v. route was detected in the serum

210

(1000-10000 pg ml^{-1} range) between 15 min and 2 hr after dosing. LPS was not

detectable in the serum 24 hr after i.c.v. administration or in untreated control mice (**Fig**

6A). When 2.5μg of LPS was administered via the intraperitoneal (i.p.) route, the levels

of endotoxin detected were very similar to those obtained following administration of

LPS by the i.c.v. route (**Fig 6B**). The i.p. administration of 2.5 μg of LPS also produced

a 60 % reduction in hepatic Cyp3a11 mRNA and triazolam metabolism (**Fig. 6C, D, E**).

The AUC$_{0.25-2 \text{ hr}}$ calculated for the serum LPS data was 11817 pg ml^{-1} hr^{-1} and 8847 pg

ml^{-1} hr^{-1} after i.c.v. and i.p. injection of LPS, respectively. This result directly supports

the idea that a peripheral inflammatory response produced by LPS reaching the

circulation after i.c.v. injection is sufficient to produce reductions in hepatic P450

metabolism. The uptake of peripherally administered ^{14}C-mannitol was used as a marker

of changes in blood brain permeability induced by LPS administration i.c.v. (**Fig. 6F**).

Increased blood-brain permeability was suggested by the significant increase in total

brain ^{14}C-mannitol 5 hr and 24 hr after LPS administration as compared to control mice.

The systemic administration of LPS mediates a reduction in hepatic Cyp3a11

expression and activity through TLR4 receptor signaling. The importance of TLR4

receptor in mediating hepatic Cyp3a11 down-regulation following the administration of

LPS by the i.p. route was examined using the TLR4-expressing and TLR4 mutant mice.

In the C3H/HeouJ mice, a high dose (5 mg kg^{-1}) of LPS produced a 90% reduction in

Cyp3a11 mRNA and corresponding 60% loss of α-OH-triazolam formation (**Fig. 7**). In

contrast, the TLR4 mutant (C3H/HeJ) mice were completely resistant to the loss in

Cyp3a11 mRNA and activity produced by the high dose of LPS administered by the i.p.

route. These data identify that peripheral TLR4 receptor stimulation is a requirement for
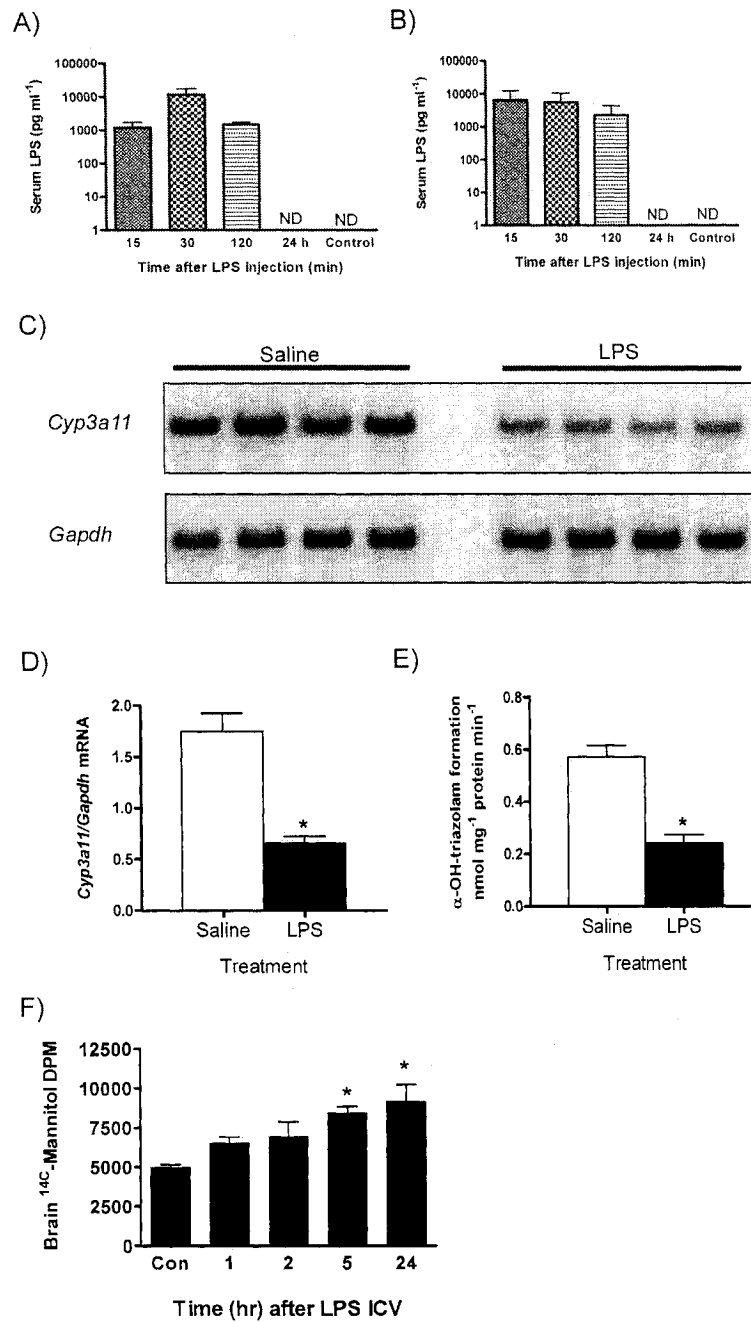
Figure 6 (legend appears on following page).

212

Fig 6. After i.c.v. administration, LPS is transferred from the brain to the periphery. Serum endotoxin levels were measured by the kinetic chromogenic Limulus Ameboctye Lysate assay in non-injected mice or at various times after 2.5 μg of LPS were administered i.c.v. (**A**) or i.p. (**B**) to C3H/HeouJ mice. (**C**) Northern blots for hepatic *Cyp3a11* and *Gapdh* mRNA, (**D**) hepatic *Cyp3a11/Gapdh* mRNA expression determined by densitometry and (**E**) hepatic microsomal Cyp3a11 activity (α-OH-triazolam formation) 24 hr after 2.5 μg of LPS or saline was administered i.p. to C3H/HeouJ mice. (**F**) The brain accumulation of peripherally administered ^{14}C-mannitol (4 nmol) was used as marker of blood-brain solute permeability changes at various times after 2.5 μg of LPS was administered by i.c.v. injection. Each bar represents the mean ± s.e. mean of 3-4 mice. Panel C-D, * *Cyp3a11* mRNA or enzyme activity was lower compared to the saline treated control, $p < 0.05$, unpaired t-test . Panel E, * P <0.05 compared to control, ANOVA followed by Tukey's HSD test.

213

A)

B)
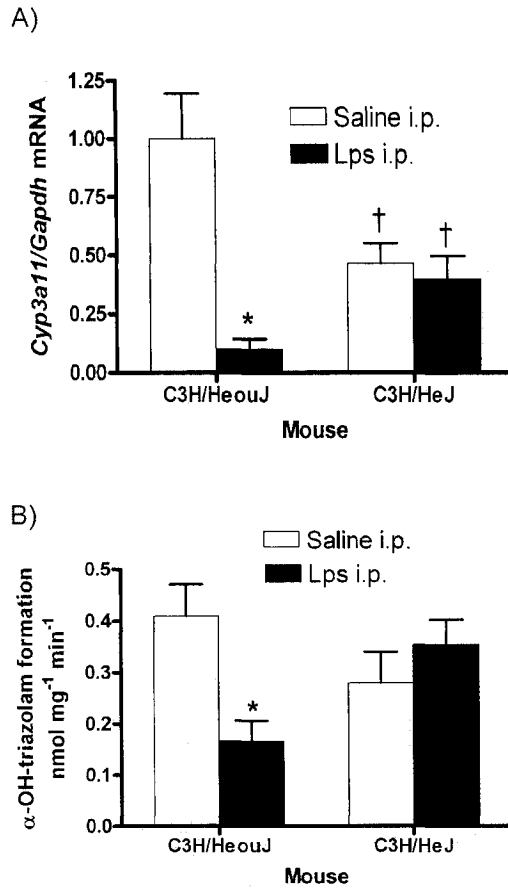
Fig 7. Regulation of hepatic Cyp3a11 metabolism by systemic LPS is mediated via TLR4 receptor signaling pathways. TLR4 mutant (C3H/HeJ) and wild-type (C3H/HeouJ) were injected with 125 μg (5 mg kg^{-1}) of LPS or saline into the peritoneal cavity. (**A**) Hepatic *Cyp3a11/ Gapdh* mRNA expression as measured by densitometry and (**B**) Cyp3a11 enzyme activity 24 hr after the injection of LPS i.p.. Each bar represents the mean ± s.e. mean of 4 mice. * Cyp3a11 expression or activity was lower compared to the saline-treated C3H/HeouJ mice, $p < 0.05$ and † *Cyp3a11* expression in the C3H/HeJ mice was different compared to the respective saline-treated or LPS-treated C3H/HeouJ mice, $p < 0.05$, ANOVA followed by Tukey's *post hoc* test.

214

the down-regulation of the major drug-metabolizing hepatic cytochrome P450 enzyme by

systemic *E.coli* LPS.

Discussion

In experimental models of CNS infection/inflammation, the central administration of LPS

produces an inflammatory response in the brain characterized by the activation of

microglia, astrocytes and proinflammatory cytokine pathways, the release of

inflammatory cytokines (TNFα, IL-1β and IL-6), and leukocyte infiltration [40, 124].

The CNS inflammatory response in our mouse model was confirmed by the presence of

elevated inflammatory cytokines (TNFα and IL-1β) in the brains of LPS-treated FVB or

C3H/HeouJ mice. We have observed a significant down-regulation of expression and

metabolic activity of hepatic Cyp3a11 in FVB, C57/Bl/6 and C3H/HeouJ but not

C3H/HeJ mice. A large reduction in hepatic CYP3A metabolism produced by an

inflammatory response would have implications for drug toxicity as that P450 subfamily

metabolizes a large percentage of clinically used drugs in humans [85]. The present

results were not restricted to *Cyp3a11* expression as similar losses in hepatic *Cyp1a1*

expression were generated by the imposed experimental conditions (**Fig. 8**). The extent

(50%-70%) of hepatic cytochrome P450 down-regulation in the mouse was similar to the

loss in hepatic cytochrome P450s that occurred in our previously established rat model of

CNS infection/inflammation [75, 114, 187].

The existence of a pathway to activate a peripheral acute phase response during

infections of the CNS was supported by the previous observations that inflammatory

cytokine levels in the periphery were elevated and the hepatic acute phase response was

stimulated [70, 74, 189, 200]. This undetermined signaling pathway has been proposed

to regulate drug metabolism in the liver during CNS infections or inflammation [72, 73,

75]. The HPA axis is activated by cytokines during the acute phase response and may
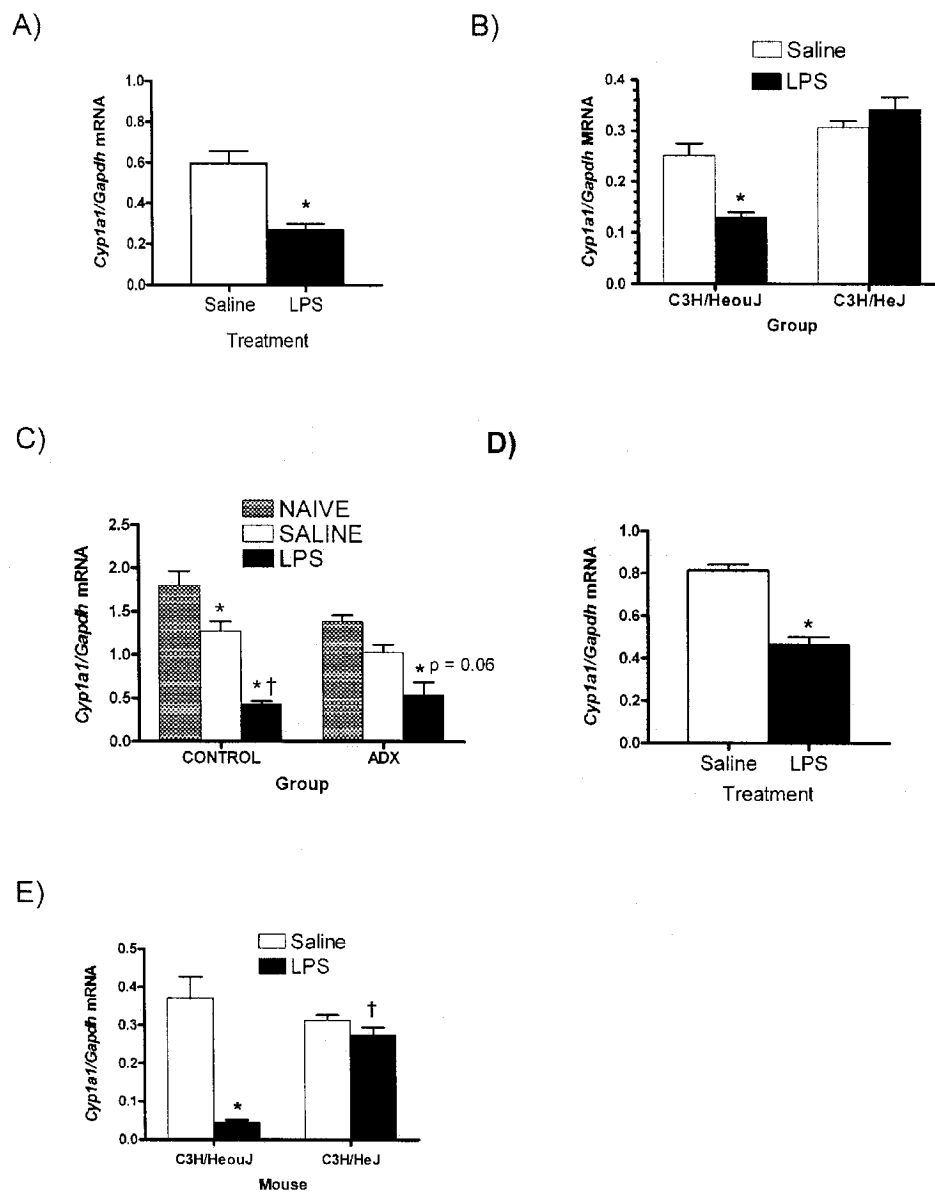
Figure 8 (legend appears on following page.)

Fig 8. Regulation of hepatic *Cyp1a1* mRNA expression by *E. coli* LPS. In panels **A-C** mice received an i.c.v. injection of LPS (2.5 µg) or 2.5 µl of saline. Hepatic *Cyp1a1* levels were measured 24 hr following treatment. **A)** I.c.v. treatment with LPS decreased hepatic *Cyp1a1* mRNA: (**A**) in male FVB mice, (**B**) in TLR4-expressing (C3H/HeouJ) but not TLR4 mutant (C3H/HeJ) mice and (**C**) in control and adrenalectomized FVB mice as compared to the relative saline controls and/or naïve mice. **D**) Hepatic *Cyp1a1* mRNA was decreased (45 %) 24 hr following the i.p. administration of LPS (2.5 µg) to C3H/HeouJ mice as compared to the saline injected control. **E)** Hepatic *Cyp1a1* mRNA was decreased (85%) 24 hr following the i.p. administration of 125 µg of LPS to TLR4-expressing (C3H/HeouJ) but not TLR4 mutant (C3H/HeJ) mice as compared to the respective saline controls. Each bar represents the mean ± s.e. mean of 3 to 4 samples. An unpaired t-test was used for statistical comparison in panel **A** and **D**. An ANOVA was used for statistical comparison in panels **B**, **C** and **E**. * $p < 0.05$, compared to the respective saline treated mice. † $p < 0.05$ compared to the respective naïve mice (**C**). ‡ $p <$ 0.05 compared to the LPS treated C3H/HeouJ mice (**B** and **E**). The mean *Cyp1a1* mRNA level in LPS-treated adrenalectomized mice approached statistical significance as compared to the saline control $p = 0.06$.

have a suppressive role against the reduction of ethoxyresorufin O-deethylase (Cyp1a), pentoxyresorufin O-depentylase (Cyp2b), imipramine N-demethylase (Cyp2d) and erythromycin N-demethylase (Cyp3a) metabolism after i.c.v. injection of LPS to rats [73, 74, 199]. In the present study, adrenalectomy prevented the elevation of plasma corticosterone but did not protect or enhance the LPS-evoked depression in hepatic Cyp3a11 expression and activity after LPS administration. This confirms that the HPA axis plays no role in hepatic cyp3a11 down-regulation in the mouse model of CNS infection/inflammation. Others have examined the stimulation of the sympathetic nervous system or transduction of TNFα, Il-1β and IFNγ from the brain to the periphery but neither of these pathways could explain the link between CNS infection/inflammation and the loss in hepatic cytochrome P450 enzyme activity in rats [72, 114]. Consistent with the findings of Nicholson et al. [114] in the present study, centrally administered TNFα did not reduce cyp3a11 expression in C3H/HeouJ or C3H/HeJ mice suggested that CNS derived TNFα is not the major factor involved in down-regulating hepatic cyp3a11 after the i.c.v. injection of LPS. IL-6 could also contribute to cyp3a11 down-regulation. However, LPS decreased hepatic cyp3a11 expression by 80% in both IL-6- expressing and IL-6-null mice and suggested against a major role for that cytokine for the down-regulation of cyp3a11 expression by LPS [191].

LPS has been identified as a specific ligand of the TLR4 receptor [5, 192]. Signaling through the LPS receptor (TLR4) is an additional pathway that could initiate the reduction in hepatic drug metabolism in the model of CNS inflammation. We observed that the TLR 4 mutants (C3H/HeJ mice) were totally resistant to the LPS-mediated loss in hepatic Cyp3a11 expression and activity that was observed mice that

express functional TLR4. Basal levels of *Cyp3a11* mRNA expression and triazolam

hydroxylation were reduced in the C3H/HeJ mice. Based on that data, C3H/HeJ mice

behaved phenotypically as slow metabolizers of triazolam whereas the C3H/HeouJ mice

were fast metabolizers of the drug. The LPS effect in the C3H/HeouJ mice was

functionally significant as it was able to change the metabolic phenotype of the

C3H/HeouJ mice from that of a fast metabolizer to that of a slow metabolizer of

triazolam. Several of our findings also support that C3H/HeJ mice are resistant to LPS-

mediated reductions in *Cyp3a11* expression and activity because of inhibition of signal

transduction through the TLR4 receptor and not because of reduced basal expression of

that cytochrome P450 gene. First, it was clear from the peripheral inflammation study

that LPS could reduce *cyp3a11* mRNA and triazolam hydroxylation in C3H/HeouJ mice

below basal levels in the C3H/HeJ mice. Second, basal Cyp1a1 expression was similar in

C3H/HeouJ and C3H/HeJ (**Fig. 8**) mice but was only depressed by LPS in the

C3H/HeouJ mice. Finally, hypo-responsiveness to LPS in the TLR4 mutant mice was

confirmed by the lack of a TNFα response in the brain and liver.

The lack of the TNFα response in C3H/HeJ mice after the i.c.v. administration of

LPS indicated the absence of a CNS inflammatory response. However, we could not

conclude that blockade of the CNS inflammatory response was the only factor that

protected the TLR4 mutant mice from the loss in hepatic Cyp3a11 because TLR4

receptors are also present on peripheral macrophages and hepatocytes and could still

elicit an immune response to *E.coli* LPS [13, 201]. This idea of a peripheral

inflammatory response is supported by the observation that liver *TNFα* mRNA and

serum levels of TNFα and IL-1β were elevated by i.c.v. administered LPS. If LPS was

220

secreted into the blood from the cerebral spinal fluid then a resulting peripheral inflammatory response could explain the decrease in hepatic Cyp3a11 metabolism.

Several studies have suggested that LPS was restricted to the CNS when it was injected into the lateral ventricle of the brain [72, 75]. In contrast, the present observations provide convincing evidence that LPS is not restricted to the CNS after central administration and is transferred to the blood in significant quantities. Similar quantities of LPS were detected in serum and a similar loss in hepatic Cyp3a11 expression and activity was observed following the administration of LPS (2.5 µg) via the i.p. route. The systemic bioavalability, as approximated by AUC, was similar after both routes of administration. These results indicated that after i.c.v. administration, the amount of LPS reaching the systemic circulation is large enough to alter hepatic cytochrome P450 solely by actions in peripheral tissues. Thus, a transfer of LPS from the CNS may have lead to the previous observation of reduced hepatic cytochrome P450 after i.c.v. administration of LPS to rats [72, 75].

E. coli LPS (0127:B8, 200 µg) injected i.c.v. to rats increased blood-brain barrier permeability between 4-16 hr after the injection [202]. Changes in blood-brain barrier permeability could result in LPS leakage into the peripheral circulation. However, our experimental results suggested that peak LPS transfer (between 1-2 hr) from the ventricles occured on a time scale that preceded the opening of the blood-brain barrier. The majority of cerebral spinal fluid is resorbed by bulk flow into the systemic circulation via transfer from the subarchnoid villi into the superior sagital venous sinus [182]. The bulk flow mechanism begins to return other blood-brain barrier impermeable substances (albumin and leptin) to the systemic circulation within minutes of their

221

injection by the i.c.v. route [182, 183]. Thus, the bulk flow reabsorption of cerebral spinal fluid is likely the more important mechanism for LPS transfer to the peripheral circulation as opposed to passage across the blood-brain barrier.

The decrease in hepatic Cyp3a11 expression and activity in response to circulating levels of LPS also appears to involve TLR4 receptors as the administration of LPS by i.p. injection had no effect in TLR4 mutant mice. Others have shown that C3H/HeJ mice were resistant to LPS down-regulation of hepatic ethoxycoumarin dealkylase (Cyp2a) and ethoxyresorufin dealkylase (Cyp1a/2) enzyme activities 24 hr after LPS was administered i.p. but this work was prior to the identification of TLR4 as a critical component of the LPS signal transduction pathway, [203, 204]. Also, in a model of indomethacin induced intestinal injury, TLR4 receptor activation by LPS released from intestinal flora may contribute to down-regulation of hepatic Cyp3a11, Cyp1a1/2 and Cyp2d9 enzyme activities [205]. Taken together, these results directly support the idea that peripheral TLR4 receptors are involved in the regulation of hepatic cytochrome P450 enzymes by peripheral administered LPS. TLR4-mediated signaling occurs through two intracellular pathways [206]. The MyD88-dependent pathway results in the direct induction of inflammatory cytokines (e.g. TNF, IL-1β and IL-6). The MyD88-independent pathway activates NF-κB with delayed kinetics as well as the interferon response factor-3 (IRF-3), which up-regulates the expression of interferon-inducible genes. Although not determined in the present study, experiments in MyD88-deficient and IRF-3 deficient mice should reveal which of these two pathways is most important for *cyp3a11* down-regulation by LPS.

Our findings have led to a putative model of how CNS infection could lead to the loss of cytochrome P450 expression and activity in the liver as shown in **Fig. 9**. LPS injected within the lateral ventricle produces TLR4-dependent CNS inflammation. The localized inflammation is likely important for the loss in P450 that occurs in the brain [75] but is not the major factor that depresses cytochrome P450 metabolism in the liver. We propose that centrally administered LPS is rapidly transferred from the cerebral spinal fluid to the blood. Through a TLR4 dependent mechanism, circulating LPS then reduces hepatic *Cyp3a11* mRNA expression and enzyme activity. The loss of hepatic P450 produced by systemic LPS could occur indirectly through the action of circulating cytokines such as TNFα, IL-1β and IL-6 that are released from a peripheral source (e.g. macrophages or kupffer cells)[64, 114, 203, 204]. Those cytokines activate nuclear transcription factors within the hepatocyte which regulate P450 expression in the liver [69, 83, 84, 198, 207-209]. Despite the direct link between cytokines and cytochrome P450 expression, large doses of LPS (1-5 mg kg^{-1}) were able to mediate hepatic Cyp3a11 down regulation *in vivo* in mice with targeted disruptions in IL-6 and the TNFα receptor [180, 191]. This could be explained by the observations that LPS stimulates NF-κB signalling in isolated hepatocytes through TLR4 receptors that are present on those cells [201, 210]. Thus, the direct action of LPS on the hepatocyte represents a potential mechanism for *cyp3a11* down-regulation in the liver.

In summary, in the presence of a CNS infection the transfer of endotoxin from the brain to the periphery could stimulate a peripheral immune response that produces a loss in P450 mediated drug metabolism in the liver. We have also identified that stimulation of the TLR4 receptor is responsible for linking the immune response to *E.coli* endotoxin

Brain CSF

Microglia +
Astrocytes

LPS i.c.v. ⟹ TLR4 Inflammatory Response ⟹ (-) Brain P450s

Macrophages

LPS ⟹ TLR4 (+) ⟹ Cytokines TNFα, IL1β, IL6

TLR4 (+) ⟹ TFs, e.g. NF-κB (+) ⟸ Cyt R

(-) P450 mRNA And activity **Liver**

Peripheral Circulation
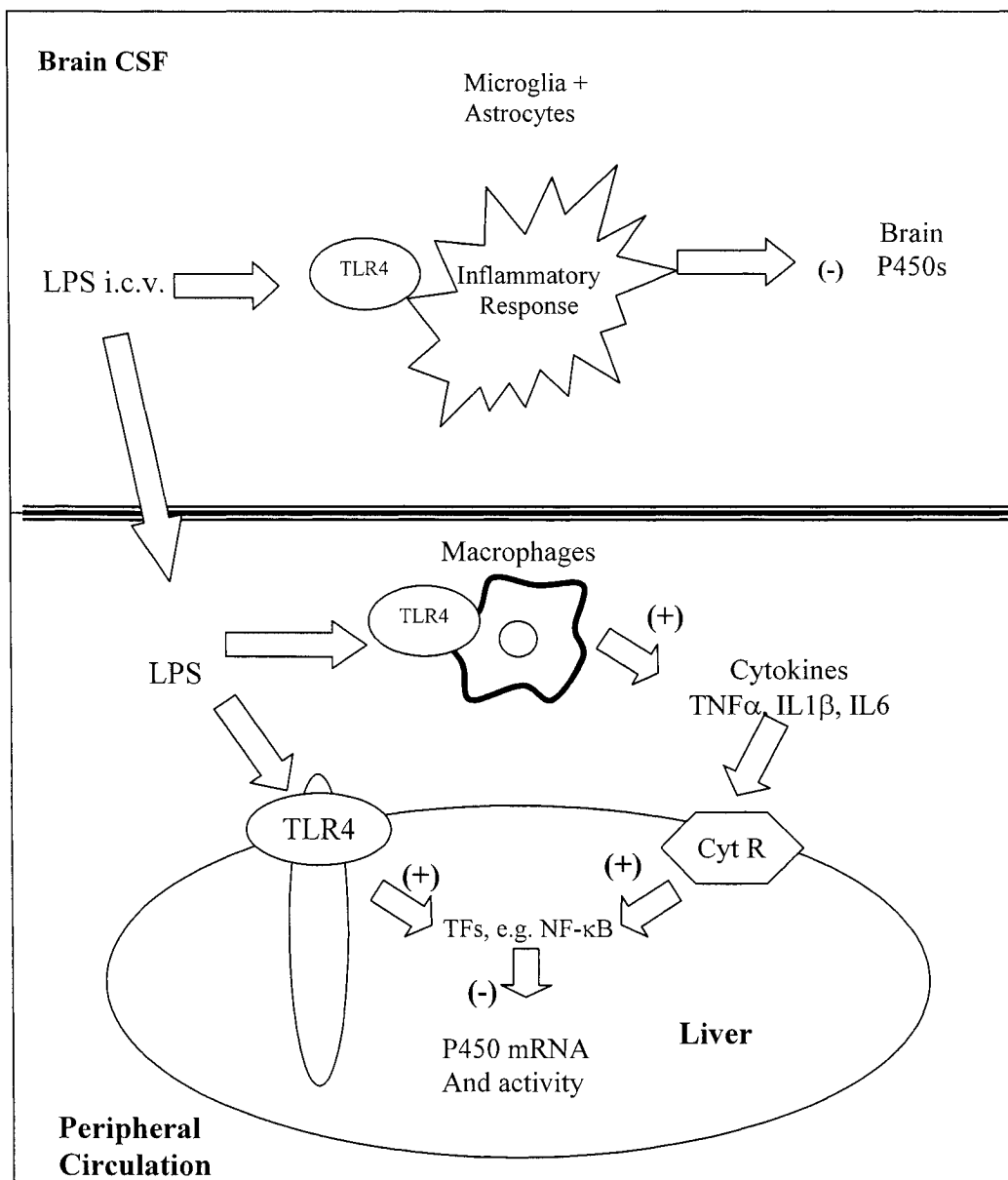
Figure 9 (legend appears on following page).

Fig 9. Down regulating hepatic cytochrome P450 metabolism in a model of gram-negative bacterial infection of the CNS. LPS injected within the lateral ventricle produces TLR4-dependent CNS inflammation, which may be important for decreased P450 activity in the brain but is not likely the major factor that reduces hepatic P450 metabolism. We demonstrate an alternative mechanism where centrally administered LPS is rapidly transferred from the cerebral spinal fluid to the blood. Peripheral LPS activates TLR4 dependent inflammatory pathways in peripheral immune cells (e.g. macrophages), which lead to an elevation in circulating inflammatory cytokines (e.g.TNFα, IL-1β and IL-6). It is well known that those inflammatory cytokines activate signal transduction pathways within the hepatocyte and the expression/activation hepatic transcription factors (e.g. NF-κB), which inhibit expression of cytochrome P450 expression. Additionally, direct LPS stimulation of TLR4 receptor signaling pathways in the hepatocyte represents a potential pathway that could trigger the intracellular events that lead to Cyp3a11 down-regulation. TF, transcription factor; CytR, cytokine receptor; The (+) signs indicate activation and (-) signs inhibition or down regulation.

with a major drug metabolizing P450 in the mouse liver. The reduction in P450 enzymes during inflammatory responses or infections of the CNS may reduce the metabolism and elimination of several clinically used drugs and increases the potential for adverse drug interactions.

Appendix B

COPYRIGHT PERMISSION FORMS

Dear Dalya Abdulla

We hereby grant you permission to reproduce the material detailed below at no charge **in your thesis** subject to the following conditions:

1.   If any part of the material to be used (for example, figures) has appeared in our publication with credit or acknowledgement to another source, permission must also be sought from that source. If such permission is not obtained then that material may not be included in your publication/copies.

2.   Suitable acknowledgment to the source must be made, either as a footnote or in a reference list at the end of your publication, as follows:

> "Reprinted from Publication title, Vol number, Author(s), Title of article, Pages No., Copyright (Year), with permission from Elsevier".

3.   Reproduction of this material is confined to the purpose for which permission is hereby given.

4.   This permission is granted for non-exclusive world **English** rights only. For other languages please reapply separately for each one required. Permission excludes use in an electronic form. Should you have a specific electronic project in mind please reapply for permission.

5.   This includes permission for the National Library of Canada to supply single copies, on demand, of the complete thesis. Should your thesis be published commercially, please reapply for permission.

Yours sincerely

Jennifer Jones
Rights Assistant

Your future requests will be handled more quickly if you complete the online form at www.elsevier.com/permissions

Dear Sir or Madam

Please find a copyright requst form attached to this email. I require
one of

those forms to include one of my publications in my PhD thesis which is
being

prepared for submission to the Faculty of Graduate Studies, Dalhoousie

University, Halifax, Nova Scotia. The publication is:

Beta-adrenergic receptor modulation of the LPS-mediated depression in
CYP1A

activity in astrocytes. Abdulla D., Renton K.W. Biochem Pharmacol. 2005
Mar

1;69(5):741-50. Epub 2005 Jan 13.

I would greatly appreciate it if you could fill the form out and fax it
back to

me as soon as it is convenient for you. My fax number is 1-902-494-
1388.

Thank you

Dalya Abdulla

November 24, 2005

Biochemical Pharmacology,

Elsevier Publishing

Science & Technology Rights Department

Elsevier Ltd

PO Box 800

Oxford OX5 1DX

UK

I am preparing my PhD thesis for submission to the Faculty of Graduate
Studies at Dalhousie University, Halifax, Nova Scotia, Canada. I am
seeking your permission to include a manuscript version of the
following paper as a chapter in the thesis:

Beta-adrenergic receptor modulation of the LPS-mediated depression in
CYP1A activity in astrocytes. Abdulla D., Renton K.W. Biochem
Pharmacol. 2005 Mar 1;69(5):741-50. Epub 2005 Jan 13.

Canadian graduate theses are reproduced by the Library and Archives of
Canada (formerly National Library of Medicine) through a non-exclusive,
world-wide license to reproduce, loan, distribute, or sell thesis. I am
also seeking your permission for the material described above to be
reproduced and distributed by LAC(NLC). Further details about the
LAC(NLC) thesis program are available on the LAC(NLC) website (www.nlc-
bnc.ca).

Full publication details and a copy of this permission letter will be
included in the thesis.

Yours sincerely,

Dalya Abdulla

Permission is granted for:

a)   the inclusion of the material described above in my thesis

b)   the material described above to be included in the copy of my
thesis that is sent to the Library and Archives of Canada (formerly
National Library of Medicine) for reproduction and distribution

Name: Title:

Signature: Date:

⊛ ASPET

AMERICAN SOCIETY FOR PHARMACOLOGY AND EXPERIMENTAL THERAPEUTICS

November 18, 2005

Dalya Abdulla
Faculty of Graduate Studies
Dalhoousie University
Halifax, Nova Scotia
Canada

Fax: 902-494-1388

Dear Dalya Abdulla:

This is to grant you permission to reproduce the following article in your dissertation for the Faculty of Graduate Studies at Dalhoousie University:

> Dalya Abdulla, Kerry B. Goralski, Elena Garcia Del Busto Cano, and Kenneth W. Renton, "The Signal Transduction Pathways Involved In Hepatic Cytochrome P450 Regulation In The Rat During A Lipopolysaccharide-Induced Model Of Central Nervous System Inflammation", *Drug Metabolism and Disposition*, vol. 33, no. 12, pp. 1521-1531, December 2005
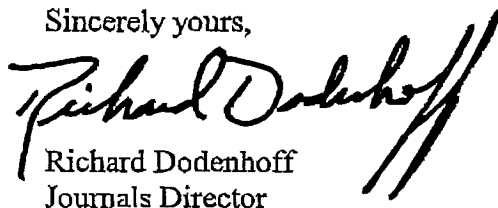
On the first page of each copy of the article, please add the following:

> Reprinted with permission of the American Society for Pharmacology and Experimental Therapeutics. All rights reserved.

In addition, the original copyright line published with the paper must be shown on the copies included with your dissertation.

The article may be included in the copy of your dissertation that is sent to the Library and Archives of Canada for reproduction and distribution.

Sincerely yours,

Richard Dodenhoff
Journals Director

Granted

November 24, 2005

Penny Ripka
Publications Office
American Physiological Society
9650 Rockville Pike
Bethesda, MD 20814-3991

I am preparing my PhD thesis for submission to the Faculty of Graduate Studies at Dalhousie University, Halifax, Nova Scotia, Canada. I am seeking your permission to include a manuscript version of the following paper as a chapter in the thesis:

Toll-like receptor-4 regulation of hepatic Cyp3a11 metabolism in a mouse model of LPS-induced CNS inflammation. Goralski K.B., Abdulla D., Sinal C.J., Arsenault A., Renton K.W. Am J Physiol Gastrointest Liver Physiol. 2005 Sep;289(3):G434-43. Epub 2005 May 5.

Canadian graduate theses are reproduced by the Library and Archives of Canada (formerly National Library of Medicine) through a non-exclusive, world-wide license to reproduce, loan, distribute, or sell thesis. I am also seeking your permission for the material described above to be reproduced and distributed by LAC(NLC). Further details about the LAC(NLC) thesis program are available on the LAC(NLC) website (www.nlc-bnc.ca).

Full publication details and a copy of this permission letter will be included in the thesis.

Yours sincerely,

Dalya Abdulla

_____

Permission is granted for:

a)   the inclusion of the material described above in my thesis
b)   the material described above to be included in the copy of my thesis that is sent to the Library and Archives of Canada (formerly National Library of Medicine) for reproduction and distribution

Name: _____   Title: _____

THE AMERICAN PHYSIOLOGICAL SOCIETY
9650 Rockville Pike -- Bethesda, MD 20814-3991

Signature: _____   Date: _____

Permission is granted for use of the material specified above provided the publication is credited as the source, including the words "used with permission."

F: 1-902-494-1388   11-28-05   *A. Ripka*
                                      Date   Publ Mgr & Exec Editor

References cited:

1. Matyszak, M.K., *Inflammation in the CNS: balance between immunological privilege and immune responses.* Prog Neurobiol, 1998. **56**(1): p. 19-35.

2. Goldsby, R.A., T.J. Kindt, B.A. Osbourne, and J. Kuby, *Kuby immunology.* 4th ed. 1999, New York: W.H. Freeman. xxv, 670.

3. Miller, S.I., R.K. Ernst, and M.W. Bader, *LPS, TLR4 and infectious disease diversity.* Nat Rev Microbiol, 2005. **3**(1): p. 36-46.

4. Prescott, L.M., J.P. Harley, and D.A. Klein, *Microbiology.* 5th ed. 2002, Boston: McGraw-Hill. 1 v. (various pagings).

5. Chow, J.C., D.W. Young, D.T. Golenbock, W.J. Christ, and F. Gusovsky, *Toll-like receptor-4 mediates lipopolysaccharide-induced signal transduction.* J Biol Chem, 1999. **274**(16): p. 10689-92.

6. Triantafilou, M. and K. Triantafilou, *The dynamics of LPS recognition: complex orchestration of multiple receptors.* J Endotoxin Res, 2005. **11**(1): p. 5-11.

7. Petty, M.A. and E.H. Lo, *Junctional complexes of the blood-brain barrier: permeability changes in neuroinflammation.* Prog Neurobiol, 2002. **68**(5): p. 311-23.

8. Sanna, P.P., F. Weiss, M.E. Samson, F.E. Bloom, and E.M. Pich, *Rapid induction of tumor necrosis factor alpha in the cerebrospinal fluid after intracerebroventricular injection of lipopolysaccharide revealed by a sensitive capture immuno-PCR assay.* Proc Natl Acad Sci U S A, 1995. **92**(1): p. 272-5.

9. Fitzgerald, K.A., E.M. Palsson-McDermott, A.G. Bowie, C.A. Jefferies, A.S. Mansell, G. Brady, E. Brint, A. Dunne, P. Gray, M.T. Harte, D. McMurray, D.E.

Smith, J.E. Sims, T.A. Bird, and L.A. O'Neill, *Mal (MyD88-adapter-like) is required for Toll-like receptor-4 signal transduction.* Nature, 2001. **413**(6851): p. 78-83.

10. Cohen, J., *The immunopathogenesis of sepsis.* Nature, 2002. **420**(6917): p. 885-91.

11. Takeda, K. and S. Akira, *Toll-like receptors in innate immunity.* Int Immunol, 2005. **17**(1): p. 1-14.

12. Bottcher, T., M. von Mering, S. Ebert, U. Meyding-Lamade, U. Kuhnt, J. Gerber, and R. Nau, *Differential regulation of Toll-like receptor mRNAs in experimental murine central nervous system infections.* Neurosci Lett, 2003. **344**(1): p. 17-20.

13. Beutler, B., K. Hoebe, X. Du, and R.J. Ulevitch, *How we detect microbes and respond to them: the Toll-like receptors and their transducers.* J Leukoc Biol, 2003. **74**(4): p. 479-85.

14. Laflamme, N. and S. Rivest, *Toll-like receptor 4: the missing link of the cerebral innate immune response triggered by circulating gram-negative bacterial cell wall components.* Faseb J, 2001. **15**(1): p. 155-163.

15. Kawai, T., O. Adachi, T. Ogawa, K. Takeda, and S. Akira, *Unresponsiveness of MyD88-deficient mice to endotoxin.* Immunity, 1999. **11**(1): p. 115-22.

16. Hayden, M.S. and S. Ghosh, *Signaling to NF-kappaB.* Genes Dev, 2004. **18**(18): p. 2195-224.

17. Fitzgerald, K.A., D.C. Rowe, and D.T. Golenbock, *Endotoxin recognition and signal transduction by the TLR4/MD2-complex.* Microbes Infect, 2004. **6**(15): p. 1361-7.

18.   Opal, S.M. and T. Gluck, *Endotoxin as a drug target.* Crit Care Med, 2003. **31**(1 Suppl): p. S57-64.

19.   Rivest, S., *How circulating cytokines trigger the neural circuits that control the hypothalamic-pituitary-adrenal axis.* Psychoneuroendocrinology, 2001. **26**(8): p. 761-88.

20.   Li, X. and J. Qin, *Modulation of Toll-interleukin 1 receptor mediated signaling.* J Mol Med, 2005. **83**(4): p. 258-66.

21.   Bendayan, R., G. Lee, and M. Bendayan, *Functional expression and localization of P-glycoprotein at the blood brain barrier.* Microsc Res Tech, 2002. **57**(5): p. 365-80.

22.   Bonizzi, G. and M. Karin, *The two NF-kappaB activation pathways and their role in innate and adaptive immunity.* Trends Immunol, 2004. **25**(6): p. 280-8.

23.   Abbott, N.J., *Evidence for bulk flow of brain interstitial fluid: significance for physiology and pathology.* Neurochem Int, 2004. **45**(4): p. 545-52.

24.   de Vries, H.E., J. Kuiper, A.G. de Boer, T.J. Van Berkel, and D.D. Breimer, *The blood-brain barrier in neuroinflammatory diseases.* Pharmacol Rev, 1997. **49**(2): p. 143-55.

25.   Rubin, L.L. and J.M. Staddon, *The cell biology of the blood-brain barrier.* Annu Rev Neurosci, 1999. **22**: p. 11-28.

26.   Kim, K.S., C.A. Wass, and A.S. Cross, *Blood-brain barrier permeability during the development of experimental bacterial meningitis in the rat.* Exp Neurol, 1997. **145**(1): p. 253-7.

27.   Peterson, P.K. and J.S. Remington, *In defense of the brain : current concepts in the immunopathogenesis and clinical aspects of CNS infections.* 1997, Malden, Mass.: Blackwell Science. xi, 355.

28.   Xiao, B.G. and H. Link, *Immune regulation within the central nervous system.* J Neurol Sci, 1998. **157**(1): p. 1-12.

29.   Huber, J.D., R.D. Egleton, and T.P. Davis, *Molecular physiology and pathophysiology of tight junctions in the blood-brain barrier.* Trends Neurosci, 2001. **24**(12): p. 719-25.

30.   Abbott, N.J., *Astrocyte-endothelial interactions and blood-brain barrier permeability.* J Anat, 2002. **200**(6): p. 629-38.

31.   Duffy, K.R. and W.M. Pardridge, *Blood-brain barrier transcytosis of insulin in developing rabbits.* Brain Res, 1987. **420**(1): p. 32-8.

32.   Franke, H., H. Galla, and C.T. Beuckmann, *Primary cultures of brain microvessel endothelial cells: a valid and flexible model to study drug transport through the blood-brain barrier in vitro.* Brain Res Brain Res Protoc, 2000. **5**(3): p. 248-56.

33.   Pan, W. and A.J. Kastin, *TNFalpha transport across the blood-brain barrier is abolished in receptor knockout mice.* Exp Neurol, 2002. **174**(2): p. 193-200.

34.   Osburg, B., C. Peiser, D. Domling, L. Schomburg, Y.T. Ko, K. Voigt, and U. Bickel, *Effect of endotoxin on expression of TNF receptors and transport of TNF-alpha at the blood-brain barrier of the rat.* Am J Physiol Endocrinol Metab, 2002. **283**(5): p. E899-908.

35.   Davidson, J., H.T. Abul, A.S. Milton, and D. Rotondo, *Cytokines and cytokine inducers stimulate prostaglandin E2 entry into the brain.* Pflugers Arch, 2001. **442**(4): p. 526-33.

36.   Mark, K.S., W.J. Trickler, and D.W. Miller, *Tumor necrosis factor-alpha induces cyclooxygenase-2 expression and prostaglandin release in brain microvessel endothelial cells.* J Pharmacol Exp Ther, 2001. **297**(3): p. 1051-8.

37.   Andersson, P.B., V.H. Perry, and S. Gordon, *The acute inflammatory response to lipopolysaccharide in CNS parenchyma differs from that in other body tissues.* Neuroscience, 1992. **48**(1): p. 169-86.

38.   Perry, V.H., D.C. Anthony, S.J. Bolton, and H.C. Brown, *The blood-brain barrier and the inflammatory response.* Mol Med Today, 1997. **3**(8): p. 335-41.

39.   Vilhardt, F., *Microglia: phagocyte and glia cell.* Int J Biochem Cell Biol, 2005. **37**(1): p. 17-21.

40.   Perry, V.H., P.B. Andersson, and S. Gordon, *Macrophages and inflammation in the central nervous system.* Trends Neurosci, 1993. **16**(7): p. 268-73.

41.   Lehnardt, S., C. Lachance, S. Patrizi, S. Lefebvre, P.L. Follett, F.E. Jensen, P.A. Rosenberg, J.J. Volpe, and T. Vartanian, *The toll-like receptor TLR4 is necessary for lipopolysaccharide-induced oligodendrocyte injury in the CNS.* J Neurosci, 2002. **22**(7): p. 2478-86.

42.   Bowman, C.C., A. Rasley, S.L. Tranguch, and I. Marriott, *Cultured astrocytes express toll-like receptors for bacterial products.* Glia, 2003. **43**(3): p. 281-91.

43.   Meunier, B., S.P. de Visser, and S. Shaik, *Mechanism of oxidation reactions catalyzed by cytochrome p450 enzymes.* Chem Rev, 2004. **104**(9): p. 3947-80.

44.   Chang, G.W.M. and P.C.A. Kam, *The physiological and pharmacological roles of cytochrome P450 isoenzymes.* Anaesthesia, 1999. **54**: p. 42-50.

45.   Guengerich, F.P., *Human cytochrome P-450 enzymes.* Life Sci, 1992. **50**(20): p. 1471-8.

46.   Coon, M.J., X.X. Ding, S.J. Pernecky, and A.D. Vaz, *Cytochrome P450: progress and predictions.* Faseb J, 1992. **6**(2): p. 669-73.

47.   van der Weide, J. and L.S. Steijns, *Cytochrome P450 enzyme system: genetic polymorphisms and impact on clinical pharmacology.* Ann Clin Biochem, 1999. **36 (Pt 6)**: p. 722-9.

48.   Gonzalez, F.J., *Molecular genetics of the P-450 superfamily.* Pharmacol Ther, 1990. **45**(1): p. 1-38.

49.   Dai, R., M.R. Pincus, and F.K. Friedman, *Molecular modeling of mammalian cytochrome P450s.* Cell Mol Life Sci, 2000. **57**(3): p. 487-99.

50.   Nebert, D.W., M. Adesnik, M.J. Coon, R.W. Estabrook, F.J. Gonzalez, F.P. Guengerich, I.C. Gunsalus, E.F. Johnson, B. Kemper, W. Levin, and et al., *The P450 gene superfamily: recommended nomenclature.* DNA, 1987. **6**(1): p. 1-11.

51.   Ke, S., A.B. Rabson, J.F. Germino, M.A. Gallo, and Y. Tian, *Mechanism of suppression of cytochrome P-450 1A1 expression by tumor necrosis factor-alpha and lipopolysaccharide.* J Biol Chem, 2001. **276**(43): p. 39638-44.

52.   Honkakoski, P. and M. Negishi, *Regulation of cytochrome P450 (CYP) genes by nuclear receptors.* Biochem J, 2000. **347**(Pt 2): p. 321-37.

53.   Bertilsson, P.M., P. Olsson, and K.E. Magnusson, *Cytokines influence mRNA expression of cytochrome P450 3A4 and MDRI in intestinal cells.* J Pharm Sci, 2001. **90**(5): p. 638-46.

54.   Drocourt, L., J.C. Ourlin, J.M. Pascussi, P. Maurel, and M.J. Vilarem, *Expression of CYP3A4, CYP2B6, and CYP2C9 is regulated by the vitamin D receptor pathway in primary human hepatocytes.* J Biol Chem, 2002. **277**(28): p. 25125-32.

55.   Cholerton, S., A.K. Daly, and J.R. Idle, *The role of individual human cytochromes P450 in drug metabolism and clinical response.* Trends Pharmacol Sci, 1992. **13**(12): p. 434-9.

56.   Tindberg, N., H.A. Baldwin, A.J. Cross, and M. Ingelman-Sundberg, *Induction of cytochrome P450 2E1 expression in rat and gerbil astrocytes by inflammatory factors and ischemic injury.* Mol Pharmacol, 1996. **50**(5): p. 1065-72.

57.   Tindberg, N., I. Bengtsson, and Y. Hu, *A novel lipopolysaccharide-modulated Jun binding repressor in intron 2 of CYP2E1.* J Neurochem, 2004. **89**(6): p. 1336-46.

58.   Corchero, J., C.P. Granvil, T.E. Akiyama, G.P. Hayhurst, S. Pimprale, L. Feigenbaum, J.R. Idle, and F.J. Gonzalez, *The CYP2D6 humanized mouse: effect of the human CYP2D6 transgene and HNF4alpha on the disposition of debrisoquine in the mouse.* Mol Pharmacol, 2001. **60**(6): p. 1260-7.

59.   Gibson, G.G. and P. Skett, *Introduction to drug metabolism.* 3rd ed. 2001, Cheltenham ;: Nelson Thornes Publishers. viii, 256.

60.   Hiroi, T., T. Chow, S. Imaoka, and Y. Funae, *Catalytic specificity of CYP2D isoforms in rat and human.* Drug Metab Dispos, 2002. **30**(9): p. 970-6.

61. Tirona, R.G., W. Lee, B.F. Leake, L.B. Lan, C.B. Cline, V. Lamba, F. Parviz, S.A. Duncan, Y. Inoue, F.J. Gonzalez, E.G. Schuetz, and R.B. Kim, *The orphan nuclear receptor HNF4alpha determines PXR- and CAR-mediated xenobiotic induction of CYP3A4.* Nat Med, 2003. **9**(2): p. 220-4.

62. Goodsell, D.S., *The molecular perspective: cytochrome P450.* Stem Cells, 2001. **19**(3): p. 263-4.

63. Poulos, T.L. and R. Raag, *Cytochrome P450cam: crystallography, oxygen activation, and electron transfer.* Faseb J, 1992. **6**(2): p. 674-9.

64. Morgan, E.T., *Regulation of cytochrome p450 by inflammatory mediators: why and how?* Drug Metab Dispos, 2001. **29**(3): p. 207-12.

65. Renton, K.W., *Cytochrome P450 regulation and drug biotransformation during inflammation and infection.* Curr Drug Metab, 2004. **5**(3): p. 235-43.

66. Renton, K.W., *Alteration of drug biotransformation and elimination during infection and inflammation.* Pharmacology & Therapeutics, 2001. **92**: p. 147-163.

67. Shedlofsky, S.I., B.C. Israel, C.J. McClain, D.B. Hill, and R.A. Blouin, *Endotoxin administration to humans inhibits hepatic cytochrome P450-mediated drug metabolism.* J Clin Invest, 1994. **94**(6): p. 2209-14.

68. Shedlofsky, S.I., B.C. Israel, R. Tosheva, and R.A. Blouin, *Endotoxin depresses hepatic cytochrome P450-mediated drug metabolism in women.* Br J Clin Pharmacol, 1997. **43**(6): p. 627-32.

69. Morgan, E.T., T. Li-Masters, and P.Y. Cheng, *Mechanisms of cytochrome P450 regulation by inflammatory mediators.* Toxicology, 2002. **181-182**: p. 207-10.

70. Gottschall, P.E., G. Komaki, and A. Arimura, *Increased circulating interleukin-1 and interleukin-6 after intracerebroventricular injection of lipopolysaccharide.* Neuroendocrinology, 1992. **56**(6): p. 935-8.

71. Shimamoto, Y., H. Kitamura, H. Hoshi, A. Kazusaka, Y. Funae, S. Imaoka, M. Saito, and S. Fujita, *Differential alterations in levels of hepatic microsomal cytochrome P450 isozymes following intracerebroventricular injection of bacterial lipopolysaccharide in rats.* Arch Toxicol, 1998. **72**(8): p. 492-8.

72. Shimamoto, Y., H. Kitamura, M. Iwai, M. Saito, A. Kazusaka, and S. Fujita, *Mechanism of decrease in levels of hepatic P450 isozymes induced by intracerebral endotoxin: independence from sympathetic nervous and adrenocortical systems.* Arch Toxicol, 1999. **73**(1): p. 41-9.

73. Shimamoto, Y., T. Tasaki, H. Kitamura, K. Hirose, A. Kazusaka, and S. Fujita, *Decrease in hepatic CYP2C11 mRNA and increase in heme oxygenase activity after intracerebroventricular injection of bacterial endotoxin.* J Vet Med Sci, 1999. **61**(6): p. 609-13.

74. Terrazzino, S., C. Perego, A. De Luigi, and M.G. De Simoni, *Interleukin-6, tumor necrosis factor and corticosterone induction by central lipopolysaccharide in aged rats.* Life Sci, 1997. **61**(7): p. 695-701.

75. Renton, K.W. and T.E. Nicholson, *Hepatic and central nervous system cytochrome P450 are down-regulated during lipopolysaccharide-evoked localized inflammation in brain.* J Pharmacol Exp Ther, 2000. **294**(2): p. 524-30.

76.   Nicholson, T.E. and K.W. Renton, *The role of cytokines in the depression of CYP1A activity using cultured astrocytes as an in vitro model of inflammation in the central nervous system.* Drug Metab Dispos, 2002. **30**(1): p. 42-6.

77.   Nicholson, T.E. and K.W. Renton, *Modulation of cytochrome P450 by inflammation in astrocytes.* Brain Res, 1999. **827**(1-2): p. 12-8.

78.   Abdulla, D. and K.W. Renton, *Beta-adrenergic receptor modulation of the LPS-mediated depression in CYP1A activity in astrocytes.* Biochem Pharmacol, 2005. **69**(5): p. 741-50.

79.   Abdulla, D., K.B. Goralski, E. Garcia Del Busto Cano, and K.W. Renton, *The signal transduction pathways involved in hepatic cytochrome P450 regulation in the rat during an LPS-induced model of CNS inflammation.* Drug Metab Dispos, 2005.

80.   Fang, C., S. Yoon, N. Tindberg, H.A. Jarvelainen, K.O. Lindros, and M. Ingelman-Sundberg, *Hepatic expression of multiple acute phase proteins and down-regulation of nuclear receptors after acute endotoxin exposure.* Biochem Pharmacol, 2004. **67**(7): p. 1389-97.

81.   Akiyama, T.E. and F.J. Gonzalez, *Regulation of P450 genes by liver-enriched transcription factors and nuclear receptors.* Biochim Biophys Acta, 2003. **1619**(3): p. 223-34.

82.   Ruminy, P., C. Gangneux, S. Claeyssens, M. Scotte, M. Daveau, and J.P. Salier, *Gene transcription in hepatocytes during the acute phase of a systemic inflammation: from transcription factors to target genes.* Inflamm Res, 2001. **50**(8): p. 383-90.

83. Iber, H., Q. Chen, P.Y. Cheng, and E.T. Morgan, *Suppression of CYP2C11 gene transcription by interleukin-1 mediated by NF-kappaB binding at the transcription start site.* Arch Biochem Biophys, 2000. **377**(1): p. 187-94.

84. Jover, R., R. Bort, M.J. Gomez-Lechon, and J.V. Castell, *Down-regulation of human CYP3A4 by the inflammatory signal interleukin-6: molecular mechanism and transcription factors involved.* Faseb J, 2002. **16**: p. 1799 - 1801.

85. Anzenbacher, P. and E. Anzenbacherova, *Cytochromes P450 and metabolism of xenobiotics.* Cell Mol Life Sci, 2001. **58**(5-6): p. 737-47.

86. Strobel, H.W., C.M. Thompson, and L. Antonovic, *Cytochromes P450 in brain: function and significance.* Curr Drug Metab, 2001. **2**(2): p. 199-214.

87. Barker, C.W., J.B. Fagan, and D.S. Pasco, *Interleukin-1 beta suppresses the induction of P4501A1 and P4501A2 mRNAs in isolated hepatocytes.* J Biol Chem, 1992. **267**(12): p. 8050-5.

88. Iba, M.M., A. Storch, A. Ghosal, S. Bennett, K.R. Reuhl, and H.E. Lowndes, *Constitutive and inducible levels of CYP1A1 and CYP1A2 in rat cerebral cortex and cerebellum.* Arch Toxicol, 2003. **77**(10): p. 547-54.

89. Xu, C. and D.S. Pasco, *Suppression of CYP1A1 transcription by H2O2 is mediated by xenobiotic-response element.* Arch Biochem Biophys, 1998. **356**(2): p. 142-50.

90. Gavrilyuk, V., C. Dello Russo, M.T. Heneka, D. Pelligrino, G. Weinberg, and D.L. Feinstein, *Norepinephrine increases I kappa B alpha expression in astrocytes.* J Biol Chem, 2002. **277**(33): p. 29662-8.

91.   Rivest, S., *Molecular insights on the cerebral innate immune system*. Brain Behav
       Immun, 2003. **17**(1): p. 13-9.

92.   Monshouwer, M. and R.F. Witkamp, *Cytochromes and cytokines: changes in
       drug disposition in animals during an acute phase response: a mini-review*. Vet
       Q, 2000. **22**(1): p. 17-20.

93.   Goralski, K.B. and K.W. Renton, *Brain inflammation enhances 1-methyl-4-
       phenylpyridinium-evoked neurotoxicity in rats*. Toxicol Appl Pharmacol, 2004.
       196(3): p. 381-9.

94.   Brady, A.E. and L.E. Limbird, *G protein-coupled receptor interacting proteins:
       emerging roles in localization and signal transduction*. Cell Signal, 2002. **14**(4):
       p. 297-309.

95.   Alberts, B., *Molecular biology of the cell*. 3rd ed. 1994, New York: Garland Pub.
       xliii, 1294, [67].

96.   Ma, Y.C. and X.Y. Huang, *Novel signaling pathway through the beta-adrenergic
       receptor*. Trends Cardiovasc Med, 2002. **12**(1): p. 46-9.

97.   Zinyama, R.B., G.J. Bancroft, and L.B. Sigola, *Adrenaline suppression of the
       macrophage nitric oxide response to lipopolysaccharide is associated with
       differential regulation of tumour necrosis factor-alpha and interleukin-10*.
       Immunology, 2001. **104**(4): p. 439-46.

98.   Feinstein, D.L., *Suppression of astroglial nitric oxide synthase expression by
       norepinephrine results from decreased NOS-2 promoter activity*. J Neurochem,
       1998. **70**(4): p. 1484-96.

99. Hasko, G., *Receptor-mediated interaction between the sympathetic nervous system and immune system in inflammation.* Neurochem Res, 2001. **26**(8-9): p. 1039-44.

100. Hasko, G., Z.H. Nemeth, C. Szabo, G. Zsilla, A.L. Salzman, and E.S. Vizi, *Isoproterenol inhibits Il-10, TNF-alpha, and nitric oxide production in RAW 264.7 macrophages.* Brain Res Bull, 1998. **45**(2): p. 183-7.

101. Hasko, G., T.P. Shanley, G. Egnaczyk, Z.H. Nemeth, A.L. Salzman, E.S. Vizi, and C. Szabo, *Exogenous and endogenous catecholamines inhibit the production of macrophage inflammatory protein (MIP) 1 alpha via a beta adrenoceptor mediated mechanism.* Br J Pharmacol, 1998. **125**(6): p. 1297-303.

102. Junker, V., A. Becker, R. Huhne, M. Zembatov, A. Ravati, C. Culmsee, and J. Krieglstein, *Stimulation of beta-adrenoceptors activates astrocytes and provides neuroprotection.* Eur J Pharmacol, 2002. **446**(1-3): p. 25-36.

103. Szabo, C., G. Hasko, B. Zingarelli, Z.H. Nemeth, A.L. Salzman, V. Kvetan, S.M. Pastores, and E.S. Vizi, *Isoproterenol regulates tumour necrosis factor, interleukin-10, interleukin-6 and nitric oxide production and protects against the development of vascular hyporeactivity in endotoxaemia.* Immunology, 1997. **90**(1): p. 95-100.

104. Izeboud, C.A., M. Monshouwer, A.S. van Miert, and R.F. Witkamp, *The beta-adrenoceptor agonist clenbuterol is a potent inhibitor of the LPS-induced production of TNF-alpha and IL-6 in vitro and in vivo.* Inflamm Res, 1999. **48**(9): p. 497-502.

105.   Lowry, O.H., N.J. Rosebrough, A.L. Farr, and R.J. Randall, *Protein measurement with folin phenol reagent.* J Biol Chem, 1951. **193**: p. 265-275.

106.   Dignam, J.D., R.M. Lebovitz, and R.G. Roeder, *Accurate transcription initiation by RNA polymerase II in a soluble extract from isolated mammalian nuclei.* Nucleic Acids Res, 1983. **11**(5): p. 1475-89.

107.   Cearley, C., L. Churchill, and J.M. Krueger, *Time of day differences in IL1beta and TNFalpha mRNA levels in specific regions of the rat brain.* Neurosci Lett, 2003. **352**(1): p. 61-3.

108.   Gerlier, D. and N. Thomasset, *Use of MTT colorimetric assay to measure cell activation.* J Immunol Methods, 1986. **94**(1-2): p. 57-63.

109.   Pahan, K., A.M. Namboodiri, F.G. Sheikh, B.T. Smith, and I. Singh, *Increasing cAMP attenuates induction of inducible nitric-oxide synthase in rat primary astrocytes.* J Biol Chem, 1997. **272**(12): p. 7786-91.

110.   Hansson, E. and L. Ronnback, *Glial neuronal signaling in the central nervous system.* Faseb J, 2003. **17**(3): p. 341-8.

111.   Wanaka, A., H. Kiyama, T. Murakami, M. Matsumoto, T. Kamada, C.C. Malbon, and M. Tohyama, *Immunocytochemical localization of beta-adrenergic receptors in the rat brain.* Brain Res, 1989. **485**(1): p. 125-40.

112.   Tasken, K. and E.M. Aandahl, *Localized effects of cAMP mediated by distinct routes of protein kinase A.* Physiol Rev, 2004. **84**(1): p. 137-67.

113.   Monshouwer, M., R.A. McLellan, E. Delaporte, R.F. Witkamp, A.S. van Miert, and K.W. Renton, *Differential effect of pentoxifylline on lipopolysaccharide-*

246

induced downregulation of cytochrome P450. Biochem Pharmacol, 1996. **52**(8): p. 1195-200.

114. Nicholson, T.E. and K.W. Renton, *Role of cytokines in the lipopolysaccharide-evoked depression of cytochrome P450 in the brain and liver.* Biochem Pharmacol, 2001. **62**(12): p. 1709-17.

115. Klotz, L., M. Sastre, A. Kreutz, V. Gavrilyuk, T. Klockgether, D.L. Feinstein, and M.T. Heneka, *Noradrenaline induces expression of peroxisome proliferator activated receptor gamma (PPARgamma) in murine primary astrocytes and neurons.* J Neurochem, 2003. **86**(4): p. 907-16.

116. Jiang, C., A.T. Ting, and B. Seed, *PPAR-gamma agonists inhibit production of monocyte inflammatory cytokines.* Nature, 1998. **391**(6662): p. 82-6.

117. Diab, A., R.Z. Hussain, A.E. Lovett-Racke, J.A. Chavis, P.D. Drew, and M.K. Racke, *Ligands for the peroxisome proliferator-activated receptor-gamma and the retinoid X receptor exert additive anti-inflammatory effects on experimental autoimmune encephalomyelitis.* J Neuroimmunol, 2004. **148**(1-2): p. 116-26.

118. Simeonidis, S., I. Castagliuolo, A. Pan, J. Liu, C.C. Wang, A. Mykoniatis, A. Pasha, L. Valenick, S. Sougioultzis, D. Zhao, and C. Pothoulakis, *Regulation of the NK-1 receptor gene expression in human macrophage cells via an NF-kappa B site on its promoter.* Proc Natl Acad Sci U S A, 2003. **100**(5): p. 2957-62.

119. Vermeulen, L., G. De Wilde, S. Notebaert, W. Vanden Berghe, and G. Haegeman, *Regulation of the transcriptional activity of the nuclear factor-kappaB p65 subunit.* Biochem Pharmacol, 2002. **64**(5-6): p. 963-70.

120. Gavrilyuk, V., P. Horvath, G. Weinberg, and D.L. Feinstein, *A 27-bp region of the inducible nitric oxide synthase promoter regulates expression in glial cells.* J Neurochem, 2001. **78**(1): p. 129-40.

121. Pan, J., Q. Xiang, and S. Ball, *Use of a novel real-time quantitative reverse transcription-polymerase chain reaction method to study the effects of cytokines on cytochrome P450 mRNA expression in mouse liver.* Drug Metab Dispos, 2000. **28**(6): p. 709-13.

122. Barker, C.W., J.B. Fagan, and D.S. Pasco, *Down-regulation of P4501A1 and P4501A2 mRNA expression in isolated hepatocytes by oxidative stress.* J Biol Chem, 1994. **269**(6): p. 3985-90.

123. Garcia Del Busto Cano, E. and K.W. Renton, *Modulation of hepatic cytochrome P450 during Listeria monocytogenes infection of the brain.* J Pharm Sci, 2003. **92**(9): p. 1860-8.

124. Nadeau, S. and S. Rivest, *Endotoxemia prevents the cerebral inflammatory wave induced by intraparenchymal lipopolysaccharide injection: role of glucocorticoids and CD14.* J Immunol, 2002. **169**(6): p. 3370-81.

125. Burke, M.D., S. Thompson, C.R. Elcombe, J. Halpert, T. Haaparanta, and R.T. Mayer, *Ethoxy-, pentoxy- and benzyloxyphenoxazones and homologues: a series of substrates to distinguish between different induced cytochromes P-450.* Biochem Pharmacol, 1985. **34**(18): p. 3337-45.

126. Omura, T. and R. Sato, *The Carbon Monoxide-Binding Pigment of Liver Microsomes. I. Evidence for Its Hemoprotein Nature.* J Biol Chem, 1964. **239**: p. 2370-8.

127. Chow, T., S. Imaoka, T. Hiroi, and Y. Funae, *Developmental changes in the catalytic activity and expression of CYP2D isoforms in the rat liver.* Drug Metab Dispos, 1999. **27**(2): p. 188-92.

128. Livak, K.J. and T.D. Schmittgen, *Analysis of relative gene expression data using real-time quantitative PCR and the 2(-Delta Delta C(T)) Method.* Methods, 2001. **25**(4): p. 402-8.

129. Gorski, K., M. Carneiro, and U. Schibler, *Tissue-specific in vitro transcription from the mouse albumin promoter.* Cell, 1986. **47**(5): p. 767-76.

130. Della Fazia, M.A., G. Servillo, and P. Sassone-Corsi, *Cyclic AMP signalling and cellular proliferation: regulation of CREB and CREM.* FEBS Lett, 1997. **410**(1): p. 22-4.

131. Park, Y. and B. Kemper, *The CYP2B1 proximal promoter contains a functional C/EBP regulatory element.* DNA Cell Biol, 1996. **15**(8): p. 693-701.

132. Shaw, P.M., M. Edigkaufer, J. Doehmer, and M. Adesnik, *Sequence of the rat PB-inducible CYP2B1 promoter.* Biochim Biophys Acta, 1996. **1305**(1-2): p. 54-8.

133. Kelicen, P. and N. Tindberg, *Lipopolysaccharide induces CYP2E1 in astrocytes through MAP kinase kinase-3 and C/EBPbeta and -delta.* J Biol Chem, 2004. **279**(16): p. 15734-42.

134. Agrawal, A.K. and B.H. Shapiro, *Phenobarbital induction of hepatic CYP2B1 and CYP2B2: pretranscriptional and post-transcriptional effects of gender, adult age, and phenobarbital dose.* Mol Pharmacol, 1996. **49**(3): p. 523-31.

135. Han, X., G. Lee, C. Hefner, J.J. Maher, and M.A. Correia, *HEME-REVERSIBLE IMPAIRMENT OF CYP2B1/2 INDUCTION IN HEME DEPLETED RAT HEPATOCYTES IN PRIMARY CULTURE : TRANSLATIONAL CONTROL BY A HEPATIC eIF2{alpha} KINASE?* J Pharmacol Exp Ther, 2005.

136. Lee, S.H. and S.M. Lee, *Suppression of hepatic cytochrome p450-mediated drug metabolism during the late stage of sepsis in rats.* Shock, 2005. **23**(2): p. 144-9.

137. Funae, Y., W. Kishimoto, T. Cho, T. Niwa, and T. Hiroi, *CYP2D in the brain.* Drug Metab Pharmacokinet, 2003. **18**(6): p. 337-49.

138. Daniel, W.A., A. Haduch, and J. Wojcikowski, *Inhibition and possible induction of rat CYP2D after short- and long-term treatment with antidepressants.* J Pharm Pharmacol, 2002. **54**(11): p. 1545-52.

139. Hiroi, T., S. Imaoka, T. Chow, and Y. Funae, *Tissue distributions of CYP2D1, 2D2, 2D3 and 2D4 mRNA in rats detected by RT-PCR.* Biochim Biophys Acta, 1998. **1380**(3): p. 305-12.

140. Jover, R., R. Bort, M.J. Gomez-Lechon, and J.V. Castell, *Re-expression of C/EBP alpha induces CYP2B6, CYP2C9 and CYP2D6 genes in HepG2 cells.* FEBS Lett, 1998. **431**(2): p. 227-30.

141. Baum, L.O. and H.W. Strobel, *Regulation of expression of cytochrome P-450 2D mRNA in rat brain with steroid hormones.* Brain Res, 1997. **765**(1): p. 67-73.

142. Oikawa, T. and T. Yamada, *Molecular biology of the Ets family of transcription factors.* Gene, 2003. **303**: p. 11-34.

143. Rosmarin, A.G., K.K. Resendes, Z. Yang, J.N. McMillan, and S.L. Fleming, *GA-binding protein transcription factor: a review of GABP as an integrator of*

intracellular signaling and protein-protein interactions. Blood Cells Mol Dis, 2004. **32**(1): p. 143-54.

144.   Yokomori, N., R. Kobayashi, R. Moore, T. Sueyoshi, and M. Negishi, *A DNA methylation site in the male-specific P450 (Cyp 2d-9) promoter and binding of the heteromeric transcription factor GABP.* Mol Cell Biol, 1995. **15**(10): p. 5355-62.

145.   Gonzalez, F.J. and Y.H. Lee, *Constitutive expression of hepatic cytochrome P450 genes.* Faseb J, 1996. **10**(10): p. 1112-7.

146.   Schweppe, R.E. and A. Gutierrez-Hartmann, *Pituitary Ets-1 and GABP bind to the growth factor regulatory sites of the rat prolactin promoter.* Nucleic Acids Res, 2001. **29**(5): p. 1251-60.

147.   Hoare, S., J.A. Copland, T.G. Wood, Y.J. Jeng, M.G. Izban, and M.S. Soloff, *Identification of a GABP alpha/beta binding site involved in the induction of oxytocin receptor gene expression in human breast cells, potentiation by c-Fos/c-Jun.* Endocrinology, 1999. **140**(5): p. 2268-79.

148.   Tomaras, G.D., D.A. Foster, C.M. Burrer, and S.M. Taffet, *ETS transcription factors regulate an enhancer activity in the third intron of TNF-alpha.* J Leukoc Biol, 1999. **66**(1): p. 183-93.

149.   Xue, H.H., J. Bollenbacher, V. Rovella, R. Tripuraneni, Y.B. Du, C.Y. Liu, A. Williams, J.P. McCoy, and W.J. Leonard, *GA binding protein regulates interleukin 7 receptor alpha-chain gene expression in T cells.* Nat Immunol, 2004. **5**(10): p. 1036-44.

150.   Hoffmeyer, A., A. Avots, E. Flory, C.K. Weber, E. Serfling, and U.R. Rapp, *The GABP-responsive element of the interleukin-2 enhancer is regulated by*

JNK/SAPK-activating pathways in T lymphocytes. J Biol Chem, 1998. **273**(17): p. 10112-9.

151. Rosmarin, A.G., D.G. Caprio, D.G. Kirsch, H. Handa, and C.P. Simkevich, *GABP and PU.1 compete for binding, yet cooperate to increase CD18 (beta 2 leukocyte integrin) transcription.* J Biol Chem, 1995. **270**(40): p. 23627-33.

152. Zhang, C. and M.T. Wong-Riley, *Depolarizing stimulation upregulates GA-binding protein in neurons: a transcription factor involved in the bigenomic expression of cytochrome oxidase subunits.* Eur J Neurosci, 2000. **12**(3): p. 1013-23.

153. Hempel, N., H. Wang, E.L. LeCluyse, M.E. McManus, and M. Negishi, *The human sulfotransferase SULT1A1 gene is regulated in a synergistic manner by Sp1 and GA binding protein.* Mol Pharmacol, 2004. **66**(6): p. 1690-701.

154. Hara, H. and T. Adachi, *Contribution of hepatocyte nuclear factor-4 to down-regulation of CYP2D6 gene expression by nitric oxide.* Mol Pharmacol, 2002. **61**(1): p. 194-200.

155. Rockich, K. and R. Blouin, *Effect of the acute-phase response on the pharmacokinetics of chlorzoxazone and cytochrome P-450 2E1 in vitro activity in rats.* Drug Metab Dispos, 1999. **27**(9): p. 1074-7.

156. Hakkola, J., Y. Hu, and M. Ingelman-Sundberg, *Mechanisms of down-regulation of CYP2E1 expression by inflammatory cytokines in rat hepatoma cells.* J Pharmacol Exp Ther, 2003. **304**(3): p. 1048-54.

157. Leung, T.H., A. Hoffmann, and D. Baltimore, *One nucleotide in a kappaB site can determine cofactor specificity for NF-kappaB dimers.* Cell, 2004. **118**(4): p. 453-64.

158. Huang, D.B., C.B. Phelps, A.J. Fusco, and G. Ghosh, *Crystal structure of a free kappaB DNA: insights into DNA recognition by transcription factor NF-kappaB.* J Mol Biol, 2005. **346**(1): p. 147-60.

159. Sawada, J., N. Simizu, F. Suzuki, C. Sawa, M. Goto, M. Hasegawa, T. Imai, H. Watanabe, and H. Handa, *Synergistic transcriptional activation by hGABP and select members of the activation transcription factor/cAMP response element-binding protein family.* J Biol Chem, 1999. **274**(50): p. 35475-82.

160. Roe, A.L., S.M. Poloyac, G. Howard, S.I. Shedlofsky, and R.A. Blouin, *The effect of endotoxin on hepatocyte nuclear factor 1 nuclear protein binding: potential implications on CYP2E1 expression in the rat.* J Pharm Pharmacol, 2001. **53**(10): p. 1365-71.

161. Hu, Y., M. Ingelman-Sundberg, and K.O. Lindros, *Induction mechanisms of cytochrome P450 2E1 in liver: interplay between ethanol treatment and starvation.* Biochem Pharmacol, 1995. **50**(2): p. 155-61.

162. Simi, A. and M. Ingelman-Sundberg, *Post-translational inhibition of cytochrome P-450 2E1 expression by chlomethiazole in Fao hepatoma cells.* J Pharmacol Exp Ther, 1999. **289**(2): p. 847-52.

163. Roberts, B.J., S.E. Shoaf, K.S. Jeong, and B.J. Song, *Induction of CYP2E1 in liver, kidney, brain and intestine during chronic ethanol administration and*

withdrawal: evidence that CYP2E1 possesses a rapid phase half-life of 6 hours or less. Biochem Biophys Res Commun, 1994. **205**(2): p. 1064-71.

164.   Lagadic-Gossmann, D., C. Lerche, M. Rissel, F. Joannard, M. Galisteo, A. Guillouzo, and L. Corcos, *The induction of the human hepatic CYP2E1 gene by interleukin 4 is transcriptional and regulated by protein kinase C.* Cell Biol Toxicol, 2000. **16**(4): p. 221-33.

165.   Umeno, M., B.J. Song, C. Kozak, H.V. Gelboin, and F.J. Gonzalez, *The rat P450IIE1 gene: complete intron and exon sequence, chromosome mapping, and correlation of developmental expression with specific 5' cytosine demethylation.* J Biol Chem, 1988. **263**(10): p. 4956-62.

166.   Ueno, T. and F.J. Gonzalez, *Transcriptional control of the rat hepatic CYP2E1 gene.* Mol Cell Biol, 1990. **10**(9): p. 4495-505.

167.   Khani, S.C., P.G. Zaphiropoulos, V.S. Fujita, T.D. Porter, D.R. Koop, and M.J. Coon, *cDNA and derived amino acid sequence of ethanol-inducible rabbit liver cytochrome P-450 isozyme 3a (P-450ALC).* Proc Natl Acad Sci U S A, 1987. **84**(3): p. 638-42.

168.   Leclercq, I.A., G.C. Farrell, J. Field, D.R. Bell, F.J. Gonzalez, and G.R. Robertson, *CYP2E1 and CYP4A as microsomal catalysts of lipid peroxides in murine nonalcoholic steatohepatitis.* J Clin Invest, 2000. **105**(8): p. 1067-75.

169.   Caro, A.A. and A.I. Cederbaum, *Oxidative stress, toxicology, and pharmacology of CYP2E1.* Annu Rev Pharmacol Toxicol, 2004. **44**: p. 27-42.

170. Roberts, B.J., B.J. Song, Y. Soh, S.S. Park, and S.E. Shoaf, *Ethanol induces CYP2E1 by protein stabilization. Role of ubiquitin conjugation in the rapid degradation of CYP2E1.* J Biol Chem, 1995. **270**(50): p. 29632-5.

171. Langouet, S., L. Corcos, Z. Abdel-Razzak, P. Loyer, B. Ketterer, and A. Guillouzo, *Up-regulation of glutathione S-transferases alpha by interleukin 4 in human hepatocytes in primary culture.* Biochem Biophys Res Commun, 1995. **216**(3): p. 793-800.

172. Kim, H., D.A. Putt, R.C. Zangar, C.R. Wolf, F.P. Guengerich, R.J. Edwards, P.F. Hollenberg, and R.F. Novak, *Differential induction of rat hepatic cytochromes P450 3A1, 3A2, 2B1, 2B2, and 2E1 in response to pyridine treatment.* Drug Metab Dispos, 2001. **29**(3): p. 353-60.

173. Kharasch, E.D. and K.E. Thummel, *Identification of cytochrome P450 2E1 as the predominant enzyme catalyzing human liver microsomal defluorination of sevoflurane, isoflurane, and methoxyflurane.* Anesthesiology, 1993. **79**(4): p. 795-807.

174. Hellmold, H., J.G. Lamb, A. Wyss, J.A. Gustafsson, and M. Warner, *Developmental and endocrine regulation of P450 isoforms in rat breast.* Mol Pharmacol, 1995. **48**(4): p. 630-8.

175. Morgan, E.T., *Regulation of cytochromes P450 during inflammation and infection.* Drug Metab Rev, 1997. **29**(4): p. 1129-88.

176. Pan, J., Q. Xiang, S. Ball, J. Scatina, J. Kao, and J.Y. Hong, *Lipopolysaccharide-mediated modulation of cytochromes P450 in Stat1 null mice.* Drug Metab Dispos, 2003. **31**(4): p. 392-7.

177. Luc, P.V., M. Adesnik, S. Ganguly, and P.M. Shaw, *Transcriptional regulation of the CYP2B1 and CYP2B2 genes by C/EBP-related proteins.* Biochem Pharmacol, 1996. **51**(3): p. 345-56.

178. Goralski, K.B., D. Abdulla, C.J. Sinal, A. Arsenault, and K.W. Renton, *Toll-like receptor-4 regulation of hepatic Cyp3a11 metabolism in a mouse model of LPS induced CNS inflammation.* Am J Physiol Gastrointest Liver Physiol, 2005.

179. Mastronardi, C.A., W.H. Yu, and S.M. McCann, *Lipopolysaccharide-induced tumor necrosis factor-alpha release is controlled by the central nervous system.* Neuroimmunomodulation, 2001. **9**: p. 148-156.

180. Warren, G.W., S.M. Poloyac, D.S. Gary, M.P. Mattson, and R.A. Blouin, *Hepatic cytochrome P-450 expression in tumor necrosis factor-alpha receptor (p55/p75) knockout mice after endotoxin administration.* J Pharmacol Exp Ther, 1999. **288**(3): p. 945-50.

181. Qureshi, S.T., L. Lariviere, G. Leveque, S. Clermont, K.J. Moore, P. Gros, and D. Malo, *Endotoxin-tolerant mice have mutations in Toll-like receptor 4 (Tlr4).* J Exp Med, 1999. **189**(4): p. 615-25.

182. Davson, H., K. Welch, and M.B. Segal, *Physiology and pathophysiology of the cerebrospinal fluid.* 1987, Edinburgh ; New York: Churchill Livingstone. 1013.

183. Maness, L.M., A.J. Kastin, C.L. Farrell, and W.A. Banks, *Fate of leptin after intracerebroventricular injection into the mouse brain.* Endocrinology, 1998. **139**(11): p. 4556-62.

184. Johnson, M., *The beta-adrenoceptor.* Am J Respir Crit Care Med, 1998. **158**(5 Pt 3): p. S146-53.

185.	Borovikova, L.V., S. Ivanova, M. Zhang, H. Yang, G.I. Botchkina, L.R. Watkins, H. Wang, N. Abumrad, J.W. Eaton, and K.J. Tracey, *Vagus nerve stimulation attenuates the systemic inflammatory response to endotoxin.* Nature, 2000. **405**(6785): p. 458-62.

186.	Scheld, W.M., U. Koedel, B. Nathan, and H.W. Pfister, *Pathophysiology of bacterial meningitis: mechanism(s) of neuronal injury.* J Infect Dis, 2002. **186 Suppl 2**: p. S225-33.

187.	Goralski, K.B., G. Hartmann, M. Piquette-Miller, and K.W. Renton, *Downregulation of mdr1a expression in the brain and liver during CNS inflammation alters the in vivo disposition of digoxin.* Br J Pharmacol, 2003. **139**(1): p. 35-48.

188.	Renton, K.W., S. Dibb, and T.L. Levatte, *Lipopolysaccharide evokes the modulation of brain cytochrome P4501A in the rat.* Brain Res, 1999. **842**(1): p. 139-47.

189.	De Simoni, M.G., R. Del Bo, A. De Luigi, S. Simard, and G. Forloni, *Central endotoxin induces different patterns of interleukin (IL)-1 beta and IL-6 messenger ribonucleic acid expression and IL-6 secretion in the brain and periphery.* Endocrinology, 1995. **136**(3): p. 897-902.

190.	Sewer, M.B., T.B. Barclay, and E.T. Morgan, *Down-regulation of cytochrome P450 mRNAs and proteins in mice lacking a functional NOS2 gene.* Mol Pharmacol, 1998. **54**(2): p. 273-9.

191. Siewert, E., R. Bort, R. Kluge, P.C. Heinrich, J. Castell, and R. Jover, *Hepatic cytochrome P450 down-regulation during aseptic inflammation in the mouse is interleukin 6 dependent.* Hepatology, 2000. **32**(1): p. 49-55.

192. Poltorak, A., X. He, I. Smirnova, M.Y. Liu, C. Van Huffel, X. Du, D. Birdwell, E. Alejos, M. Silva, C. Galanos, M. Freudenberg, P. Ricciardi-Castagnoli, B. Layton, and B. Beutler, *Defective LPS signaling in C3H/HeJ and C57BL/10ScCr mice: mutations in Tlr4 gene.* Science, 1998. **282**(5396): p. 2085-8.

193. Franklin, K.B.J. and G. Paxinos, *The mouse brain in stereotaxic coordinates.* 1997, San Diego: Academic Press. xxii , [186] of plates.

194. Hardy, K.W. and T.D. White, *Some commercial preparations of Escherichia coli bacterial endotoxin lipopolysaccaride (LPS) are contaminated with biologically active substances.* J Neurochem, 2001. **78**(5): p. 1183-4.

195. el-Masry, S.e.-D., G.M. Cohen, and G.J. Mannering, *Sex-dependent differences in drug metabolism in the rat. I. Temporal changes in microsomal drug-metabolizing system of the liver during sexual maturation.* Drug Metab Dispos, 1974. **2**(3): p. 267-78.

196. Perloff, M.D., L.L. von Moltke, M.H. Court, T. Kotegawa, R.I. Shader, and D.J. Greenblatt, *Midazolam and triazolam biotransformation in mouse and human liver microsomes: relative contribution of CYP3A and CYP2C isoforms.* J Pharmacol Exp Ther, 2000. **292**(2): p. 618-28.

197. McCurdy, J.D., T.J. Lin, and J.S. Marshall, *Toll-like receptor 4-mediated activation of murine mast cells.* J Leukoc Biol, 2001. **70**(6): p. 977-84.

258

198.   Baumann, H. and J. Gauldie, *The acute phase response.* Immunol Today, 1994. **15**(2): p. 74-80.

199.   Del Rey, A. and H.O. Besedovsky, *Metabolic and neuroendocrine effects of pro-inflammatory cytokines.* Eur J Clin Invest, 1992. **22 Suppl 1**: p. 10-5.

200.   Wilcockson, D.C., S.J. Campbell, D.C. Anthony, and V.H. Perry, *The systemic and local acute phase response following acute brain injury.* J Cereb Blood Flow Metab, 2002. **22**(3): p. 318-26.

201.   Liu, S., D.J. Gallo, A.M. Green, D.L. Williams, X. Gong, R.A. Shapiro, A.A. Gambotto, E.L. Humphris, Y. Vodovotz, and T.R. Billiar, *Role of toll-like receptors in changes in gene expression and NF-kappa B activation in mouse hepatocytes stimulated with lipopolysaccharide.* Infect Immun, 2002. **70**(7): p. 3433-42.

202.   Jaworowicz, D.J., Jr., P.J. Korytko, S. Singh Lakhman, and K.M. Boje, *Nitric oxide and prostaglandin E2 formation parallels blood-brain barrier disruption in an experimental rat model of bacterial meningitis.* Brain Res Bull, 1998. **46**(6): p. 541-6.

203.   Ghezzi, P., B. Saccardo, and M. Bianchi, *Recombinant tumor necrosis factor depresses cytochrome P450-dependent microsomal drug metabolism in mice.* Biochem Biophys Res Commun, 1986. **136**(1): p. 316-21.

204.   Shedlofsky, S.I., A.T. Swim, J.M. Robinson, V.S. Gallicchio, D.A. Cohen, and C.J. McClain, *Interleukin-1 (IL-1) depresses cytochrome P450 levels and activities in mice.* Life Sci, 1987. **40**(24): p. 2331-6.

205. Masubuchi, Y. and T. Horie, *Resistance to indomethacin-induced down-regulation of hepatic cytochrome P450 enzymes in the mice with non-functional Toll-like receptor 4.* J Hepatol, 2003. **39**(3): p. 349-56.

206. Takeda, K. and S. Akira, *TLR signaling pathways.* Semin Immunol, 2004. **16**(1): p. 3-9.

207. Ramadori, G. and B. Christ, *Cytokines and the hepatic acute-phase response.* Semin Liver Dis, 1999. **19**(2): p. 141-55.

208. Pascussi, J.M., S. Gerbal-Chaloin, L. Pichard-Garcia, M. Daujat, J.M. Fabre, P. Maurel, and M.J. Vilarem, *Interleukin-6 negatively regulates the expression of pregnane X receptor and constitutively activated receptor in primary human hepatocytes.* Biochem Biophys Res Commun, 2000. **274**(3): p. 707-13.

209. Beigneux, A.P., A.H. Moser, J.K. Shigenaga, C. Grunfeld, and K.R. Feingold, *Reduction in cytochrome P-450 enzyme expression is associated with repression of CAR (constitutive androstane receptor) and PXR (pregnane X receptor) in mouse liver during the acute phase response.* Biochem Biophys Res Commun, 2002. **293**(1): p. 145-9.

210. Wang, X., W. Li, J. Lu, N. Li, and J. Li, *Lipopolysaccharide suppresses albumin expression by activating NF-kappaB in rat hepatocytes.* J Surg Res, 2004. **122**(2): p. 274-9.